

The RASopathies
Molecular Genetics and Genotype-Phenotype Correlations

Dissertation

zur Erlangung des akademischen Grades

doctor rerum naturalium

(Dr. rer. nat.)

genehmigt durch die Fakultät für Naturwissenschaften

der Otto-von-Guericke-Universität Magdeburg

von M. Sc. Christina Antonia Lißewski

geboren am 05 April 1983 in Wilhelmshaven

Gutachter: Prof. Dr. med Martin Zenker

Prof. Dr. rer nat. Andreas Winterpacht

eingereicht am: 22. Oktober 2017

verteidigt am: 28. März 2018

TABLE OF CONTENTS

ABSTRACT	V
ZUSAMMENFASSUNG	VI
1. INTRODUCTION	1
1.1. The RASopathies	1
1.2. The RAS/MAPK pathway	3
1.3. Molecular causes of RASopathies	4
1.4. Clinical diagnosis criteria and clinical signs of RASopathies	9
1.5. Molecular diagnosis of RASopathies	13
1.6. Aims.....	14
2. METHODS	15
2.1. Genotyping	15
2.1.1. Patient samples and ethical issues	15
2.1.2. DNA Preparation	15
2.1.3. Sanger sequencing.....	16
2.1.4. Verification of parentage	20
2.1.5. High Resolution Melting (HRM) analysis	20
2.1.5.1. ESTABLISHMENT OF EXPERIMENTAL METHOD	22
2.1.5.2. VALIDATION OF THE METHOD	23
2.1.5.3. ANALYSIS METHOD.....	23
2.1.5.4. STANDARD PROTOCOL.....	26
2.1.6. Next Generation Sequencing.....	27
2.1.6.1. SELECTION PROCESS.....	27
2.1.6.2. NEXTERA RAPID CAPTURE ENRICHMENT.....	28
2.1.6.3. SEQUENCING BY SYNTHESIS.....	28
2.1.6.4. SEQUENCE ANALYSIS.....	28
2.1.6.5. EXPERIMENTAL PROCEDURE	29
2.1.6.6. VALIDATION OF VARIANTS.....	31
2.1.7. Classification of variants	31
2.2. Database.....	32
2.2.1. Consensus process.....	33
2.2.2. Structure	34
2.2.2.1. DATA SUBMISSION	35
2.2.2.2. DATA BROWSER.....	37
2.2.3. Ethical issues	38
2.2.4. Data entry and analysis	38
2.3. Statistics.....	50
3. RESULTS	51

3.1.	Genotyping.....	51
3.1.1.	HRM.....	51
3.1.1.1.	VALIDATION OF THE METHOD.....	51
3.1.1.2.	HRM RESULTS AND FALSE-POSITIVES.....	55
3.1.1.3.	SEQUENCE-SPECIFICITY OF HRM.....	58
3.1.1.4.	MUTATION DISTRIBUTION.....	60
3.1.2.	Sanger sequencing.....	61
3.1.3.	Next Generation Sequencing.....	62
3.1.4.	Novel or rarely described variants.....	67
3.2.	Database.....	70
3.2.1.	SHOC2.....	79
3.2.2.	RIT1.....	81
3.2.3.	NRAS.....	83
3.3.	CBL.....	89
3.4.	HRAS.....	91
3.5.	Copy number changes containing RAS-MAPK genes.....	92
3.6.	Novel genes for RASopathies.....	94
4.	DISCUSSION.....	98
4.1.	Detection and prevalence of mutations.....	98
4.2.	The NSEuroNet database and its uses.....	101
4.2.1.	SHOC2 mutations and Mazzanti syndrome.....	103
4.2.2.	Genotype phenotype correlations with germline RIT1 mutations.....	106
4.2.3.	Genotype phenotype correlations with germline NRAS mutations.....	112
4.3.	Prenatal symptoms in CBL syndrome.....	117
4.4.	Copy number changes containing RAS-MAPK genes.....	120
4.5.	Novel RASopathy genes.....	123
4.6.	Conclusion and outlook.....	132
5.	REFERENCES.....	134
5.1.	Online Resources.....	144
6.	SUPPLEMENTS.....	145
6.1.	Clinical tables.....	145
6.1.1.	SHOC2.....	145
6.1.2.	RIT1.....	152
6.1.3.	NRAS.....	156
6.1.4.	SOS2.....	158
6.2.	List of primers.....	159
6.3.	List of genes analyzed on the NGS panel.....	161
6.4.	Patient list.....	162

6.5.	List of Abbreviations.....	172
6.6.	Funding sources	174
6.7.	Publications	175
6.8.	Erklärung	178

ABSTRACT

The RASopathies are a group of developmental disorders caused by mutations in genes coding for components or modulators of the RAS/MAPK pathway. The pathway is known to be involved in a variety of physiological processes including differentiation, proliferation, survival, and apoptosis. The most common entities among the RASopathies are Neurofibromatosis type 1 and Noonan syndrome. All syndromes associated with mutations in this pathway have some symptoms in common, others differ, and some may be variable in severity. Patients with Noonan syndrome are usually short in stature, have congenital heart defects and developmental delays along with a typical facial gestalt. Cardio-facio-cutaneous and Costello syndromes are much rarer entities with particular risk of neurodevelopmental issues and tumor development, respectively.

This PhD thesis was aimed at expanding the spectrum of mutations causing RASopathies, including the identification of novel mutations in already known genes as well as novel genes, and delineating genotype-phenotypes correlations. To achieve this, an online database (NSEuroNet database) was developed. This allowed the aggregation of detailed and standardized clinical and related genotype data from a large number of patients with a variety of mutations, including all published cases (with a limited set of clinical data) and patients whose underlying mutation was identified during this project. To identify the underlying genetic cause in a large study cohort of patients with various RASopathies and RASopathy-like phenotypes, different methods for mutation screening of previously established and novel RASopathy genes were utilized and compared. High resolution melting (HRM) technology was established and utilized early in this thesis project for faster and cost-efficient pre-screening of samples and was complemented by conventional Sanger sequencing. With the advent and availability of Next generation sequencing (NGS) the analysis of a multi-gene panel was introduced and established a method for a comprehensive mutation screening.

A total of 606 patients were investigated molecularly by varying combinations of these technologies. HRM proved to be a useful and sensitive screening method in 325 individuals screened by this method. However, with the steady increase in number of genes involved in RASopathies and the advantages of NGS-based mutation screening, this method evolved as a primary screening tool during this thesis work and was eventually utilized in 144 cases. In total, a pathogenic or likely pathogenic variant was identified in 330 (54%) of this clinically heterogeneous cohort. Several novel mutations were identified, thereby leading to a significant expansion of the mutation spectrum of several genes including the identification of novel mutation hotspots.

Genotype-phenotype studies were carried out with the help of the data aggregated in the database and were particularly focused on the genes identified shortly before the start of this thesis (*NRAS*, *SHOC2*, *CBL*) or during it (*RIT1*). Thereby the clinical phenotype and molecular spectrum was further delineated for patients with mutations in these genes and compared to the phenotype in patients carrying mutations in the more commonly mutated genes *PTPN11* and *SOS1*.

Finally, another aspect addressed by this thesis was regarding the significance of copy number variations containing RAS-MAPK pathway genes, particularly duplications, as a cause of a RASopathy phenotype. Careful review of literature cases and new patients from two families revealed that there is so far insufficient evidence for such CNVs being a cause of a RASopathy phenotype.

In conclusion, this work could make a significant contribution to the understanding of genotype phenotype correlations of RASopathies and created a valuable resource for ongoing and future genotype-phenotype studies with the NSEuroNet database.

ZUSAMMENFASSUNG

Die RASopathien sind eine Gruppe kongenitaler genetischer Störungen, die durch Keimbahnmutationen in Genen, die für Komponenten oder Modulatoren des RAS/MAPK Signalweges kodieren, hervorgerufen werden. Dieser Signalweg ist in eine Vielzahl von physiologischen Prozessen involviert, einschließlich Differenzierung, Proliferation und Apoptose. Die häufigsten Erkrankungen unter den RASopathien sind Noonan-Syndrom und Neurofibromatose Typ 1. Alle Syndrome, die mit Mutationen in diesem Signalweg assoziiert sind, zeigen gewisse Überlappungen in ihrer phänotypischen Ausprägung, können aber besonders in ihrem Schweregrad variieren. Das Noonan-Syndrom ist geprägt durch proportionierten Kleinwuchs, kongenitale Herzfehler, eine Entwicklungsverzögerung und typische faziale Dysmorphien. Cardio-fazio-cutanes und Costello-Syndrom sind seltenere Krankheitsbilder mit Mutationen des gleichen Signalweges, heben sich aber durch ein besonderes Risiko für neurologische Entwicklungsstörungen beziehungsweise Tumorentwicklung ab.

Das Ziel dieser Doktorarbeit war es, das für RASopathien ursächliche Mutationsspektrum zu erweitern. Dazu gehörte die Identifizierung von neuen Mutationen sowohl in bereits bekannten Genen als auch in bisher nicht mit RASopathien assoziierten Genen. Ein weiteres Ziel war, Genotyp-Phänotyp-Korrelationen näher zu untersuchen, wofür eine online Datenbank (NSEuroNet) entwickelt wurde. So konnten detaillierte und standardisierte klinische Informationen sowie die dazugehörigen Genotyp-Daten großer Kohorten gesammelt und analysiert werden. Die in die Datenbank eingegebenen Patienten stammten sowohl aus Publikationen (mit eingeschränkten klinischen Informationen) als auch aus unserer eigenen Kohorte, bei denen die zugrundeliegende Mutation in diesem Projekt nachgewiesen wurde. Die Identifizierung der kausalen Mutationen, in bekannten und neuen Genen, unserer Patientenkohorte mit einer RASopathie oder einem RASopathie-ähnlichen Phänotyp erforderte die Etablierung verschiedener Methoden. Dafür wurde die High Resolution Melting (HRM) Technologie im Rahmen dieser Arbeit etabliert und zu Beginn der Arbeit genutzt. Mit Hilfe der HRM konnten Patientenproben schnell und kosteneffizient voruntersucht werden. Diese Methode wurde durch konventionelle Sanger-Sequenzierung vervollständigt und validiert. Durch die Einführung und Verfügbarkeit der Next Generation Sequencing Technologie (NGS) wurde auch diese Methode für eine umfassende molekulargenetische Analyse mit einem Multi-Gen-Panel etabliert und genutzt.

Insgesamt wurden 606 Patienten aus unserer klinisch heterogenen Kohorte molekulargenetisch mit einer variablen Kombination dieser Technologien untersucht. Es wurden 325 Patienten mit der HRM untersucht, wobei gezeigt werden konnte, dass diese Analyse eine nützliche und sensible Screening-Methode darstellt. Gleichzeitig zeigen sich immer mehr Vorteile der NGS-basierten Mutationsanalyse, da die Anzahl der Gene, die kausal für RASopathien sein sollen, weiter zunimmt, weshalb sich diese Methode als primäre Analysemethode durchgesetzt hat. Im Rahmen dieser Doktorarbeit wurden 144 Patienten mit einem NGS Multi-Gen-Panel untersucht. Insgesamt konnte in 330 Patienten (54%) aus unserem Patientenkollektiv eine pathogene oder wahrscheinlich pathogene Variante nachgewiesen werden. Außerdem wurden mehrere neue Mutationen identifiziert, die das Mutationsspektrum bereits bekannter Gene erheblich erweitern konnten. Darüber hinaus wurden neue Mutationshotspots identifiziert.

Mit Hilfe der gesammelten klinischen Daten aus der NSEuroNet Datenbank wurden außerdem Genotyp-Phänotyp-Korrelationsstudien für *NRAS*, *SHOC2*, *CBL* und *RIT1* durchgeführt. Mutationen in diesen Genen wurden erst kurz vor Beginn beziehungsweise während der Doktorarbeit als kausal für RASopathien identifiziert. So konnte das phänotypische und molekulare Spektrum von Patienten mit Mutationen in diesen Genen weiter differenziert und mit denen von Patienten mit Mutationen in häufiger mutierten Genen wie *PTPN11* oder *SOS1* verglichen werden.

Ein weiterer Aspekt, der in dieser Arbeit untersucht wurde, ist die Signifikanz von Kopiezahl-Veränderungen, insbesondere Duplikationen, in denen RAS/MAPK Signalweg Gene enthalten sind und als ursächlich für einen RASopathie-Phänotyp angesehen werden. Eine sorgfältige Analyse von Patienten aus der Literatur und neuen Patienten aus zwei Familien zeigte jedoch, dass es zurzeit nur unzureichende Beweise für Kopiezahlveränderungen als Ursache eines RASopathie Phänotyps gibt.

Diese Arbeit leistet einen erheblichen Beitrag zum Verständnis von Genotyp-Phänotyp-Korrelationen bei RASopathien. Ferner wurde mit der NSEuroNet Datenbank eine wertvolle Ressource geschaffen, die sowohl für laufende und zukünftige Genotyp-Phänotyp-Studien genutzt werden kann als auch für Ärzte und Wissenschaftler eine sinnvolle Übersicht über das bisher bekannte Mutationsspektrum bei RASopathien bietet.

1. INTRODUCTION

1.1. The RASopathies

The RASopathies constitute a group of developmental disorders characterized by craniofacial anomalies, cardiac defects, short stature, and variable developmental delay (Rauen 2013). At the beginning of this thesis, mutations in multiple genes encoding components or modulators of the RAS/MAPK pathway had been identified as being causative for Noonan syndrome (NS) and the other RASopathies (*BRAF*, *CBL*, *HRAS*, *KRAS*, *MEK1*, *MEK2*, *NF1*, *NRAS*, *PTPN11*, *RAF1*, *SPRED1*, *SHOC2* and *SOS1*) (Zenker 2011). Since then more genes have been identified, several of which will be discussed as part of this thesis and more genetic heterogeneity is expected.

Noonan syndrome (NS; OMIM 163950) is the most common condition within the group of RASopathies. It was first reported by Noonan and Ehmke who described patients with heart defects and similar facies. It was recognized that this syndrome represents a new entity, which can be present in both boys and girls with no apparent chromosomal abnormality (Noonan 1968, Noonan 1963). Other disorders in the group of RASopathies share many of the key features of NS and have overlapping craniofacial anomalies, but differ in the level of cognitive impairment, ectodermal features, tumor risk and other signs (Rauen 2013). They include Neurofibromatosis type 1 (NF1; OMIM 162200), Legius syndrome (LS; OMIM 611431), cardio-facio-cutaneous syndrome (CFCS; OMIM 115150), Costello syndrome (CS; OMIM 218040), as well as distinct variant types of NS such as Noonan syndrome with multiple lentiginos (NSML), formerly known as LEOPARD syndrome (OMIM 151100), and Noonan-like syndrome with loose anagen hair (NSLAH; OMIM 607721).

Similarly common to NS with an incidence of about 1 in 3000 individuals and first described even before NS was NF1 in 1882 (Brosius 2010, Uusitalo et al. 2015). NF1 is also a syndrome of the RAS/MAPK pathway, but with distinct symptoms. Patients with NF1 usually have pigmented lesions like café-au-lait spots or Lisch nodules, and many develop neurofibromas. They are also at risk for a number of benign neoplasms (Gutmann et al. 2017). A variant type of NF1 is LS. Affected individuals have café-au-lait spots, similar to those with NF1, but no NF1-associated tumors (Zenker 2011).

In 1985 Allanson and colleagues first described a combined phenotype of NS and NF1 in four patients with a typical facial appearance for NS, short stature (10th centile and under) as well as

symptoms of NF1 (Allanson, Hall and Van Allen 1985). They suggested that NS-NF may be another new disorder or a variant of either NS or NF1.

CFCS was first described by Reynolds et al in a cohort of eight patients with heart defects, ectodermal abnormalities, short stature (≤ -2.00 standard deviations (SD)) and common facial characteristics as well as developmental delay (Reynolds et al. 1986). Identifying features of CFCS are developmental delay that is usually more severe than in NS, and ectodermal abnormalities (Rauen 2013). These typically consist of sparse, curly scalp hair, sparse eyebrows and eyelashes, hyperkeratosis, keratosis pilaris, ichthyosis, eczema, and progressively forming melanocytic nevi. Cutaneous hemangioma may be present (Rauen 2013). Also failure to thrive together with gastrointestinal dysfunctions such as gastro-esophageal reflux, vomiting, oral aversion, and constipation can be frequently observed in patients with CFCS.

In 1977 Costello and colleagues described a new syndrome in two children with intellectual disability, nasal papillomata, short stature and similar facial features (Costello 1977). The most important features of CS are congenital heart defects, short stature, a typical craniofacial appearance, developmental delay, failure to thrive in early infancy and gastrointestinal dysfunctions often requiring gastrostomy tube feeding, ectodermal abnormalities, and connective tissue abnormalities including soft skin and deep palmar and plantar creases (Rauen 2013). Also a high risk of malignancies, particularly embryonal rhabdomyosarcoma, neuroblastoma, or bladder carcinoma, is associated with CS.

Noonan syndrome with multiple lentigines (NSML) was originally described as LEOPARD syndrome by Gorlin and colleagues in 1969 (Gorlin, Anderson and Blaw 1969). LEOPARD is an acronym for *L*entigines, *E*lectrocardiographic (ECG) conduction abnormalities, *O*cular hypertelorism, *P*ulmonic stenosis, *a*bnormal genitalia, *R*etardation of growth, and *D*eafness. Aside from multiple lentigines which occur rarely before childhood and may be quite variable in number, the overall phenotype and outcome of LEOPARD syndrome is not much different from NS. It is therefore regarded as a subtype of NS (NSML) (Zenker 2011).

In 2003 Mazzanti and colleagues first described three patients with short stature (height significantly below the 3rd centile), darkly pigmented skin, mild psychomotor delay and growth hormone deficiency (Mazzanti et al. 2003). Interestingly they also had sparse hair with a peculiar anomaly called “loose anagen hair”, which means it can easily be pulled from the scalp and a microscopic analysis of the hair showed that most of the hair is in the anagen phase and devoid of its sheath and no hair is in the telogen phase instead of the normal 15-20%

(Mazzanti et al. 2003). All three patients also had a similar facial appearance. NS and CFCS were considered in the differential diagnosis, but loose anagen hair had never been reported in either condition. Since this condition can be distinguished clinically from NS and other known conditions of the RASopathies, it is now named Noonan syndrome-like disorder with loose anagen hair (NSLAH) (Zenker 2011).

1.2. The RAS/MAPK pathway

The RAS/MAPK pathway controls many biological functions including proliferation, migration, survival, differentiation, and apoptosis (Tartaglia and Gelb 2010). It is expressed in a wide range of cells throughout development and in adults. Figure 1.1 depicts the canonical RAS/MAPK pathway and its components which may be mutated in RASopathies.

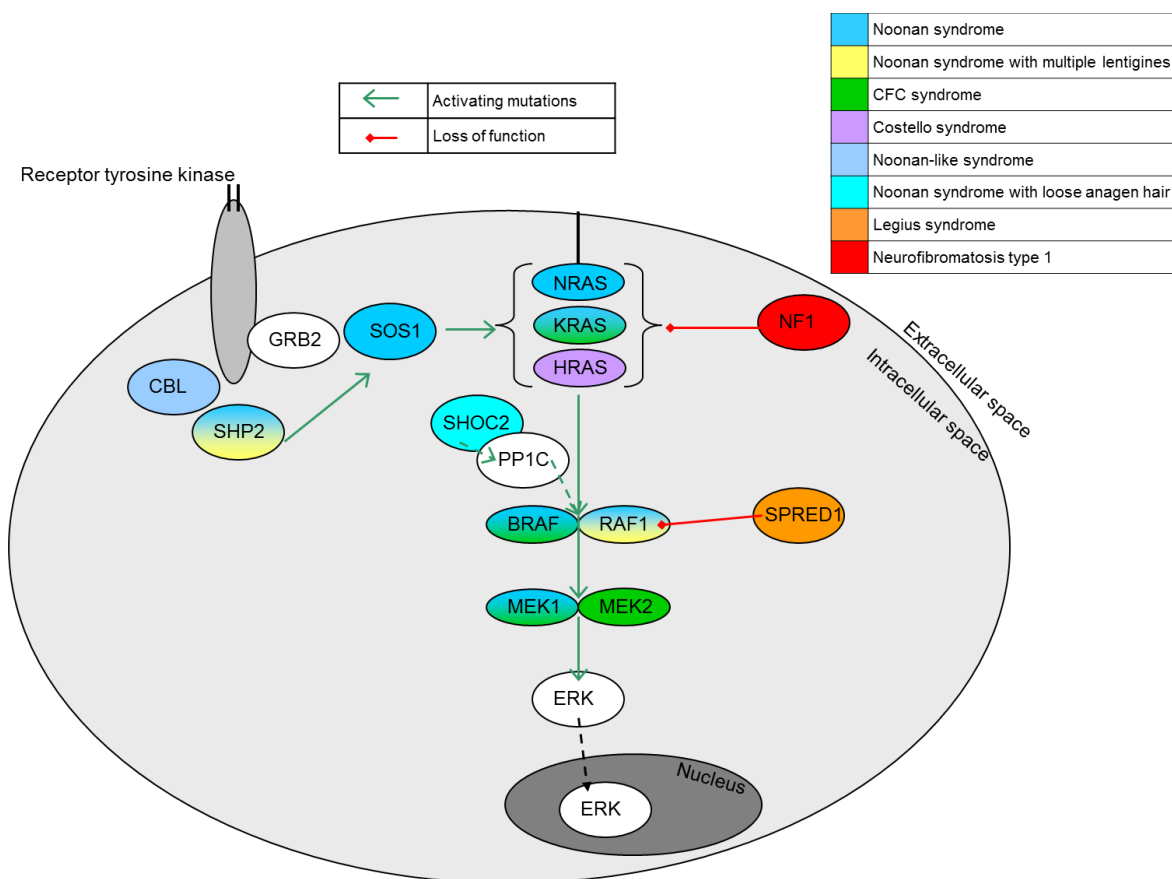


Figure 1.1: The RAS/MAPK pathway. This figure shows the RAS/MAPK signaling cascade. Proteins in which mutations are known to cause a certain RASopathy syndrome are depicted in a specific color for each syndrome as shown in the legend.

Activation of the RAS/MAPK pathway is possible by various signaling molecules such as EGF (epidermal growth factor), FGF (fibroblast growth factor) and HGF (hepatocyte growth factor), SRC family kinase and IL (interleukin)-1/TNF (tumor necrosis factor)-dependent NF-kappaB (nuclear factor kappa-light-chain-enhancer of activated B cells) activation (Tartaglia and Gelb 2005). RAS signaling is switched on upon any of these ligands binding to their respective cell surface receptor, which creates an intracellular docking site for further molecules. These recruit and activate guanine nucleotide exchange factors (GEFs), which will be further explained subsequently, setting the pathway in motion (Tartaglia and Gelb 2010).

The Ras molecules (KRAS, HRAS, NRAS and others) belong to the group of small GTPases. They have two switch regions (switch-I and switch-II) which undergo conformational changes between the GTP (guanosine triphosphate)-bound active form and the GDP (guanosine diphosphate)-bound inactive form (Simanshu, Nissley and McCormick 2017). Guanine nucleotide exchange factors (GEFs), such as SOS1 and 2, expedite the switch from GDP-bound to GTP-bound state by binding to RAS. This weakens the affinity of GDP which is then released. Due to the intracellular abundance of GTP it is more likely that GTP will be bound by Ras, thus activating the protein. For the conversion of the GTP-bound state back to the inactive GDP-bound state of Ras GTP hydrolysis is necessary. However, the intrinsic GTPase activity is too slow to self-inactivate making the interaction with a GTPase activating protein (GAP), such as neurofibromin (NF1), necessary (Simanshu et al. 2017). The GAP interacts with the switch-II region of Ras resulting in the GTP hydrolysis reaction. Another negative regulator of the RAS/MAPK pathway is Spred1. It has been shown to bind NF1 and recruit it to the cell membrane (Brems et al. 2007). Spred1 can also inhibit Ras-GTP in activating Raf. Normally the GTP-bound form of RAS allows binding of effectors such as the Raf kinases (RAF1, BRAF, CRAF), which in turn phosphorylate the mitogen-activated protein kinase kinase (MEK1 and MEK2) (Tartaglia and Gelb 2010). Phosphorylation of extracellular signal regulated kinases (ERK1 and ERK2) is done by MEKs acting as dual specificity kinases. In turn, ERKs function as serine/threonine protein kinases modulating cytoplasmic and nuclear substrates, including those responsible for gene expression (Tartaglia and Gelb 2010).

1.3. Molecular causes of RASopathies

By 2010, when this thesis was started, mutations in multiple genes encoding components or modulators of the RAS/MAPK pathway had been identified as being causative for NS and the other RASopathies (*BRAF*, *CBL*, *HRAS*, *KRAS*, *MEK1*, *MEK2*, *NF1*, *NRAS*, *PTPN11*,

RAF1, *SPRED1*, *SHOC2* and *SOS1*) (Zenker 2011). All RASopathies are inherited in an autosomal dominant manner with a high frequency of sporadic mutations.

In 1991 the gene responsible for NF1, which was accordingly called *NF1*, was identified (Gutmann, Wood and Collins 1991). The location was previously mapped to 17q11.2 and the gene was found through two patients with chromosome 17 translocations (Cawthon et al. 1990, Viskochil et al. 1990, Wallace et al. 1990). Following this the entire coding sequence and the gene product was identified (Gutmann et al. 1991, Marchuk et al. 1991). Mutations in *NF1* are loss-of-function mutations, which reduce the GTPase activity of Ras resulting in an increase of GTP-bound Ras thus resulting in an increase of downstream signaling (Rauen 2013). The mutation spectrum is more complex than is seen in the other RASopathies. Specifically the mutations can be missense, frameshift, splice site, or stop mutations (Messiaen et al. 2000). Rarer are intronic mutations, which affect splicing, microdeletions or insertions, and chromosomal abnormalities.

In 2001 Tartaglia et al discovered that mutations in the gene *PTPN11* cause NS (Tartaglia et al. 2001). Previous mapping studies had suggested that a gene for NS is on chromosome 12q24.1 between D12S84 and D12S79 (Brady et al. 1997, Jamieson et al. 1994, Legius et al. 1998). Overall 50% of patients tested were found to have a mutation in *PTPN11*. *PTPN11* encodes a protein tyrosine phosphatase, non-receptor type 11 (also known as SHP2). It is a cytoplasmic SH2 domain containing protein tyrosine phosphatase that is widely expressed in embryonic and adult tissues and required for many essential developmental processes (Tartaglia and Gelb 2005). The N-terminal (N-SH2) domain of the two SH2 domains present in SHP2 interacts with the PTP domain, blocking the catalytic site. While the phosphotyrosil containing target binds to another site the N-SH2 domain undergoes a conformational change and dissociated from the PTP domain, making the catalytic site available to substrate. Most mutations found in *PTPN11* are in the N-SH2/PTP interdomain binding network (Tartaglia and Gelb 2010). This network normally stabilizes SHP2 in its inactive conformation, while mutations impair the switch from inactive to active shifting the equilibrium toward an active conformation. Mutations in other domains increase the binding affinity or alter binding specificity for signaling partners thus upregulating SHP2's function (Rauen 2013).

In 2005 mutations in the harvey rat sarcoma viral oncogene homolog gene (*HRAS*) were found to cause CS using a candidate gene approach (Aoki et al. 2005). *HRAS* was chosen along with *NRAS*, *KRAS* and *ERAS* because of previous studies linking mutations in *PTPN11* to disrupted RAS/MAPK signaling. Aoki et al were able to identify *HRAS* mutations

in almost all individuals in the study with CS. These mutations had previously been described somatically in tumors (Aoki et al. 2005). Functional effects of mutations in *HRAS* result in a hyperactivation of the RAS/MAPK pathway by different means. The most common mutation at codon 12 probably prevents the GAPs interaction with Ras, thus preventing hydrolysis and keeping Ras GTP-bound, whereas mutations at codons 146 or 158 result in an abnormal accumulation of Ras-GTP by dissociating GDP more rapidly than normal (Simanshu et al. 2017).

In 2006 several more genes encoding components of the pathway were identified to cause NS and CFCS. Schubbert et al found that mutations in the Kirsten rat sarcoma viral oncogene homolog gene (*KRAS*) can cause NS and CFCS (Schubbert et al. 2006). The *KRAS* germline mutations found in these patients are not found somatically in tumors. Germline mutations in *KRAS* are functional hypomorphs compared to the cancer-associated somatic mutations and the authors suggest that these oncogenic mutations are lethal when present in the germline (Schubbert et al. 2006). Niihori et al specifically analyzed the DNA of patients with CFCS for mutations in the RAS genes and downstream molecules in the RAS/MAPK pathway (Niihori et al. 2006). They found mutations in *KRAS* and v-raf murine sarcoma viral oncogene homolog B (*BRAF*). Independently, Rodriguez-Viciana et al identified mutations in the genes *BRAF*, *MEK1* and *MEK2* to be causative for CFCS (Rodriguez-Viciana et al. 2006). The mutations in *BRAF*, which is also a proto-oncogene, often mutated in cancer cells, were (mainly) not on codons that are typically affected by somatic mutations in cancer. Niihori and colleagues as well as Rodriguez-Viciana and colleagues showed increased levels of MEK and ERK phosphorylation. Mutations in *MEK1* or *2* also showed a higher activation of phosphorylated ERK compared to wildtype *MEK1* or *2* (Niihori et al. 2006, Rodriguez-Viciana et al. 2006).

With these discoveries it was clear that NS, CS and CFCS do not only share phenotypic features but also have a common pathogenesis. Bentires-Alj et al proposed the term Neuro-Cardio-Facio-Cutaneous (NCFC) syndromes for these clinically and molecularly related syndromes, but the term never caught on (Bentires-Alj, Kontaridis and Neel 2006).

Just a year later mutations in two more members of the RAS/MAPK pathway were reported in connection with NS, namely *SOS1* (Roberts et al. 2007, Tartaglia et al. 2007) and v-raf-1 murine leukemia viral oncogene homolog 1 (*RAF1*) (Pandit et al. 2007, Razaque et al. 2007). Roberts et al recognized some phenotypic differences between *PTPN11*-positive and *SOS1*-positive individuals, possibly related to the level of hyperactivation of the pathway (Roberts et

al. 2007). Tartaglia et al noticed that individuals with mutations in the *SOS1* gene may exhibit ectodermal symptoms resembling those of patients with CFCS (Tartaglia et al. 2007). Razzaque and colleagues identified mutations in the *RAF1* gene to be the leading cause for hypertrophic cardiomyopathy (HCM) in NS (Razzaque et al. 2007). Mutations in *SOS1* are mostly in regions that contribute structurally to the maintenance of the catalytically autoinhibited conformation. This promotes gain-of-function and enhances RAS and ERK activation. *SOS1* is not typically mutated in cancers (Tartaglia and Gelb 2010).

Also in 2007 Brems and colleagues reported loss-of-function mutations in *SPRED1* in patients with a NF1-like phenotype (Brems et al. 2007). They identified five families in which the affected individuals had multiple café-au-lait spots, axillary freckling, and macrocephaly. Some patients additionally had NS-like features. Mutations and linkage to the *NF1* locus was excluded and, using a candidate gene approach, mutations in the *SPRED1* gene were identified. Similarly to NF1 and contrary to NS, *SPRED1* mutations are loss-of-function. Mutated *SPRED1* is unable to bind to neurofibromin and thus unable to transfer it to the cell membrane (Brems and Legius 2013).

Tidyman and Rauen introduced the term RASopathy as a collective term for the disorders associated with mutations in the RAS/MAPK pathway, which was then adopted by other researchers and has been used to collectively describe NS and Noonan like disorders, CFCS, CS, NF1, and LS (Tidyman and Rauen 2009).

In 2009 a unique mutation in the *SHOC2* gene (c.4A>G (p.(Ser2Gly))) was found to cause NSLAH (Cordeddu et al. 2009). The glycine at position 2 results in the protein being labelled for N-terminal myristoylation, a posttranslational modification. During this process a 14-carbon saturated fatty acid is bound to the N-terminal glycine residue after excision of the methionine at position 1. Without N-myristoylation the protein cannot anchor to the membrane and does not translocate to the nucleus. Cordeddu and colleagues showed that the expression of the mutant *SHOC2* protein in cells leads to increased MAPK activation (Cordeddu et al. 2009). The precise mechanism, however, by which *SHOC2* activates the pathway has remained elusive.

In 2010, neuroblastoma RAS viral (v-ras) oncogene homolog (*NRAS*) was reported to cause a small percentage of cases with NS (Cirstea et al. 2010). Through a candidate gene approach four out of 917 unrelated individuals with NS were found to carry a mutation in this gene. *NRAS* is also a Ras gene and is almost identical to *KRAS* and *HRAS*. A total number of 18 patients from 12 unrelated families with mutations in *NRAS* have been reported, by 2015

(Cirstea et al. 2010, Denayer et al. 2012, Digilio et al. 2011, Ekvall et al. 2015, Kraoua et al. 2012, Runtuwene et al. 2011). Similar to what had been observed for germline *KRAS* mutations, the reported *NRAS* mutations causing NS did not affect the oncogenic hotspots and appear to be functional hypomorphs compared to the cancer-associated somatic mutations (Cirstea et al. 2010, Denayer et al. 2012, Runtuwene et al. 2011). In contrast, *HRAS* mutations in CS typically occur at two well-known oncogenic hotspots (*i.e.*, p.Gly12, p.Gly13), which has been postulated to explain the high incidence of tumors in patients with this disorder (Estep et al. 2006).

In 2010 three reports of patients with germline mutations in the *CBL* gene were published. Martinelli and colleagues used a candidate gene approach and in a cohort of 365 patients with a diagnosis of NS, some not strictly fitting into diagnostic criteria, found a variant in four unrelated individuals (Martinelli et al. 2010). Overall six mutation carriers, the four index patients and two family members, were identified without typical heart defects for NS. One of the two fathers with the familial mutation only had minimal symptoms for a RASopathy, including a broad neck and Chiari type 1 malformation, but did not exhibit the typical facial dysmorphism or short stature. The latter was present in only one patient of the cohort, most had developmental delays, thorax anomalies, and a short neck. Hypermobile or hyperextensible joints were also common along with similar facial features to other patients with NS. Since the overall phenotype is not completely typical for NS the authors use the term “Noonan-like syndrome”. The second report established a connection between myeloproliferative disorders (particularly JMML) and homozygous *CBL* mutations (Perez et al. 2010). Perez and colleagues found three patients with heterozygous germline *CBL* mutations in a cohort of 65 patients with JMML (Perez et al. 2010). These patients also had developmental delays and a reminiscent gestalt of NS. In the DNA samples extracted from mononucleated hematopoietic cells loss of heterozygosity was confirmed. The third report investigated germline mutations in *CBL* in a cohort of patients with JMML (Niemeyer et al. 2010). In the leukemic blood samples of 21 patients with JMML they found homozygous *CBL* mutations. Normal tissues of 17 of these patients were analyzed and a heterozygous mutation identified. Additionally these patients also had developmental delays and short stature. The JMML resolved spontaneously in 5 of the 6 patients that were followed up for more than 7 years. In 17 out of the original 21 patients, other tissue was available for molecular testing and revealed heterozygous *CBL* mutations in all 17. The authors suggest that this may be a new syndrome with overlapping congenital anomalies as in NS or NF1 or LS and an increased risk for JMML (Niemeyer et al. 2010).

The mutations in the aforementioned genes identified to cause Noonan and related syndromes are almost exclusively missense mutations and a few small in-frame deletions or indels (Zenker 2009). Contrary to this, disease-causing mutations in *NF1* and *SPRED1*, antagonists of the RAS pathway, include also nonsense, frameshift or splicing mutations as well as larger deletions or indels and even whole gene or exon deletions have been reported (Bianchessi et al. 2015, Brems and Legius 2013, Mensink et al. 2006). It has consistently been shown that the consequences of mutations at either sites of this pathway, that are associated with RASopathies, is a dysregulation (mostly hyperactivation) of the RAS/MAPK pathway (Keilhack et al. 2005, Tartaglia et al. 2006). Few observations of duplications encompassing RAS pathway genes have been reported in the literature and have raised the hypothesis that increased gene dosage might also account for a RASopathy phenotype (Chen et al. 2014a, Graham et al. 2009, Luo et al. 2012, Shchelochkov et al. 2008).

1.4. Clinical diagnosis criteria and clinical signs of RASopathies

In 1994, before the identification of the first NS associated gene, van der Burgt et al developed a scoring system for a clinical diagnosis of NS, which was updated in 2007 (Table 1.1) (van der Burgt 2007).

Feature	A=Major	B=Minor
1 Facial	Typical face dysmorphology	Suggestive face dysmorphology
2 Cardiac	Pst, HOCM and/or ECG typical of NS	Other defect
3 Height	<P3	<P10
4 Chest wall	Pectus carinatum/excavatum	Broad thorax
5 Family	First degree relative with definite NS	First degree relative with suggestive NS
6 Other	Mental retardation, cryptorchidism and lymphatic dysplasia	One of mental retardation, cryptochdidism, lymphatic dysplasia

Table 1.1: Scoring system for a clinical diagnosis of NS. Definitive NS: 1 "A" plus one other major sign or two minor signs; 1 "B" plus two major signs or three minor signs. (adapted from (van der Burgt 2007))

The first major sign is “typical face dysmorphology”. The craniofacial appearance of individuals affected by RASopathies is recognizable especially in children and includes a wide forehead, hypertelorism, ptosis, a flat nasal bridge, low-set ears, and a broad neck (Figure 1.2). These features may become less obvious in adults with NS.



Figure 1.2: Facial features in NS. The facial features of individuals with NS change over time. This graphic depicts the same person (*PTPN11*: p.Met504Val) at 2 years old (A), 5 years old (B), 8 years old (C), 11 years old (D), 13 years old (E), and 18 years old (F). At 8 (C) and 11 (D) years old the often described triangular face can be seen. All pictures show hypertelorism, flat nasal bridge, and low set ears. This patient also has the striking blue irises often described in NS.

In the diagnostic criteria the significance of the craniofacial phenotype in RASopathies is highlighted (van der Burgt 2007, van der Burgt et al. 1994). According to this the recognition of a typical or at least a suggestive craniofacial phenotype is required for the clinical diagnosis. This implicates, of course, that one who is using this scoring system needs to be familiar with RASopathies, and a subjective bias cannot be excluded. The characteristic heart defects in RASopathies are pulmonary valve stenosis (Pst), hypertrophic cardiomyopathy (HCM) or a combination of both. Pst in RASopathies typically results from pulmonary valve dysplasia leading to thickened or fused valve leaflets (see Figure 1.3). HCM is an inappropriate thickening of the heart muscle, which may impair its proper function. It can be asymptomatic and is a common cause for sudden cardiac arrest in young people. In patients with NS it presents early in life with more than half diagnosed in the first 6 months of life (Gelb, Roberts and Tartaglia 2015). At diagnosis it is more likely that a patient with NS and HCM is in

congestive heart failure, compared to patients without NS. HCM with congestive heart failure is also the major contributor to mortality in NS. A variety of other cardiac anomalies may occur, for example septal defects, aortic coarctation, and valve anomalies other than pulmonary stenosis, but they all lack a particular specificity for RASopathies.

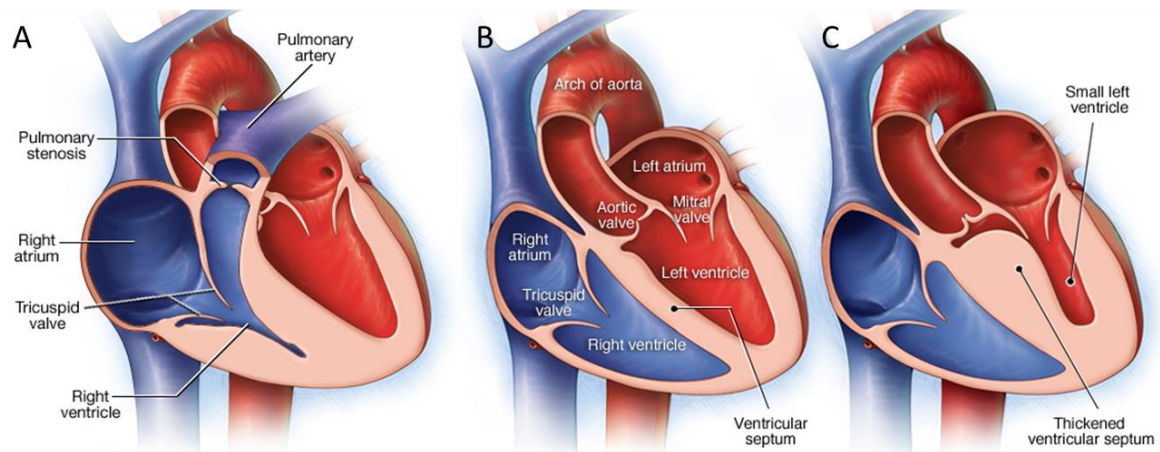


Figure 1.3: Common heart anomalies in RASopathies. Panel A depicts the heart with pulmonary valve stenosis. Also shown is a thickened right ventricle, which may be present due to the pumping against increased pressure. Panel B shows a normal heart in comparison to panel C, which shows HCM with thickened ventricular septum and a small left ventricle. (adapted from MayoClinic 2016, MayoClinic 2017)

Short stature (-2 SD) is proportionate and typically of postnatal onset (Zenker 2011). Also chest wall deformities are very common in individuals with NS; upper pectus carinatum and lower excavatum is the typical thorax anomaly (Figure 1.4).



Figure 1.4: Thorax anomalies in NS. Depicted here is the typical thorax anomaly seen in patients with NS (upper pectus carinatum and lower pectus excavatum).

Besides these phenotypic signs a positive family history has been added to the diagnostic criteria. Since NS is inherited in an autosomal dominant manner, individuals with NS have a 50% chance of passing it on to their children. There are additional features that are less

common in or less specific for patients with RASopathies. Developmental delays are usually mild, and some patients do not experience any intellectual disabilities (Pierpont et al. 2009), while they are more severe in CS and CFCS. Other symptoms of RASopathies include cryptorchidism (undescended testes), lymphatic abnormalities (manifesting as fetal nuchal edema or postnatal lymphedema), feeding difficulties and failure to thrive in infancy, bleeding diathesis, ectodermal signs (hyperkeratosis, curly hair), strabismus, refractive errors, macrocephaly, and an increased risk of malignancies (Rauen 2013, Zenker 2009).

In a considerable number of pregnancies with a fetus affected by a RASopathy prenatal abnormalities are recorded, but these are not exclusive to these disorders, but may also present in other syndromes (Baldassarre et al. 2011, Lee et al. 2009). Nuchal edema or cystic hygroma of the fetal neck as well as polyhydramnios are the most common prenatal abnormalities, not only in pregnancies where the fetus has a RASopathy but also with chromosomal abnormalities (Beke et al. 2009, Lee et al. 2009). Congenital chylothorax is rare (incidence 1/10,000-15,000 births), but the most common cause of pleural effusions in fetuses and newborns (Fernandez Alvarez, Kalache and Grauel 1999). It has been described with a number of syndromes including trisomy 21, Turner syndrome, NS, and Adams-Oliver syndrome (Chen et al. 2009, Farrell et al. 1993, Kabbani et al. 2005, Moerman et al. 1993, Prasad, Singh and Singh 2002). Fetal chylothorax is also common in patients with RASopathies and may be associated with or progress to hydrops fetalis (Baldassarre et al. 2011). While short stature is a frequent finding in RASopathies, affected individuals are usually of normal birth weight and length (Zenker 2011). Moreover, in patients with CS, macrosomia is often reported which may be due to lymphatic fluid accumulation (Rauen 2013).

Patients with NF1 usually show symptoms like café-au-lait macules, axillary freckling and neurofibromas (Rauen 2013). Clinical features in patients with NF1 develop over the course of life (Gutmann et al. 2017). In infancy café-au-lait macules may be present, along with plexiform neurofibromas, orbital dysplasia, tibial dysplasia, or pseudoarthritis. In early childhood learning deficits and developmental delays may be noticed, but also optic pathway glioma. In adolescence the children may develop freckling in the axillar and inguinal areas, Lisch nodules of the iris, and also scoliosis. A variety of neoplasms occur in NF1. Almost every patient develops dermal neurofibromas by mid adulthood which may be numerous. Paraspinal neurofibromas or brainstem glioma are among the common tumor manifestations. In adulthood other tumors may present, such as breast cancer, glioma, or malignant peripheral nerve sheath tumors (Gutmann et al. 2017). The diagnostic criteria for NF1 have been defined by the National Institutes of Health (NIH) and are shown in Table 1.2.

National Institutes of Health Diagnostic Criteria for NF1
Two or more of the following clinical features signify the presence of NF1 in a patient
Six or more café-au-lait macules (0.5 cm at largest diameter in prepubertal individuals or 1.5 cm in individuals past puberty)
Axillary freckling or freckling in inguinal regions
Two or more neurofibromas of any type or_1 plexiform neurofibroma
Two or more Lisch nodules (iris hamartomas)
A distinctive osseous lesion
A first-degree relative with NF1 diagnosed by using the above-listed criteria

Table 1.2: Diagnostic criteria for NF1 (1988, Williams et al. 2009)

Additionally to the typical NF1 symptoms described above, patients may have NS-like symptoms, such as facial gestalt, short stature, heart defects, and developmental delay (Zenker 2011). The term NS-NF was introduced for individuals fulfilling clinical criteria for NF1 and NS (1988).

1.5. Molecular diagnosis of RASopathies

Sanger sequencing has long been the method of choice for many laboratories to identify mutations causative for NS. Nowadays, since there are so many genes to be sequenced to have comprehensive molecular diagnostics, this method has become very expensive and is being replaced by multigene panel sequencing approaches using modern “next generation sequencing” (NGS) technologies. Genotype-phenotype correlations are known for some genes, but only rarely will this point to a specific gene to test. HCM is most commonly associated with the *RAF1* gene, which means that a patient with HCM and other symptoms for NS most likely has a mutation in the *RAF1* gene, but the causative mutation can also be in one of the other known genes. The phenotypic variability for a specific mutation and even intrafamilial is high. It has been shown repeatedly that parents only find out that they have NS, because they become parents of a more severely affected child. Alternative screening methods are available like dHPLC and high resolution melting (HRM) (Lo et al. 2009, Tartaglia et al. 2001). HRM has previously been used for mutation detection in the *PTPN11* gene (Lo et al. 2009). Lo et al. ran a series of tests with DNA from patients with known mutations and determined standardized settings for the analysis (Lo et al. 2009). Afterwards they screened 50 patients with NS for mutations in 5 exons of *PTPN11*. HRM is a useful tool to screen a large cohort for variants in small amplicons allowing a fast prescreening of many samples and thus requiring fewer sequencing reactions. Another alternative method is Next Generation Sequencing (NGS). Using this method, a collection of amplicons, so called panels, can be analyzed in one run for multiple patients. The technology has been used previously and

successfully and has shown that it provides high quality results in a shorter time and with lower costs compared to Sanger sequencing (Lepri et al. 2014).

1.6. Aims

The aim of this study was to further elucidate the molecular genetics and genotype-phenotype correlations of RASopathies. In a cohort of patients with a clinical diagnosis of a RASopathy syndrome the mutation spectrum was to be identified in established genes. Furthermore, this cohort was to be used to identify and evaluate novel genes with the NSEuroNet consortium. To facilitate this, new methods for the molecular analysis of RASopathy genes were to be established and evaluated, including HRM and NGS technologies.

For the collection of mutation information and detailed standardized clinical information a database was to be built. Genotype-phenotype correlations studies of large patient cohorts with mutations in the same gene were then possible based on the standardized information available from the database.

2. METHODS

2.1. Genotyping

2.1.1. Patient samples and ethical issues

DNA samples and patient data were received from multiple collaborators. Some patients were seen in the genetic outpatient clinic of our own department, but most patients were recruited from other doctors and hospitals throughout the world. All patients or their legal representatives gave their consent to genetic testing and scientific exploitation of anonymous clinical and associated genotype data. Photos are only shown of those patients where specific consent was given to publish photographs. This study was approved by the ethics committee of the University of Magdeburg (Aktenzeichen: 06/10).

2.1.2. DNA Preparation

DNA EXTRACTION

DNA samples from peripheral blood or saliva were either extracted in house or received as DNA. In the latter case the extraction method was unknown. The in house DNA extraction was performed by the laboratory technicians using standard procedures.

Venous blood samples were taken from some patients and DNA was extracted using the chemagic Magnetic Separation Module 1 (PerkinElmer chemagen; Baesweiler, Germany) according to manufacturer's instructions by the laboratory technicians. Another extraction method for blood samples was the QIAcube robotic workstation (QIAGEN; Hilden, Germany). Here the QIAamp DNA Blood kit (QIAGEN; Hilden, Germany) was used in an automated system. Where no blood samples were available, saliva was collected using Oragene-DNA collection kits (DNA Genotek Inc.; Kanata, ON, Canada) and manufacturer's instructions followed for extraction.

DNA QUALITY CONTROL AND QUANTIFICATION

All DNA samples were analyzed by agarose gel electrophoresis for quality control purposes. The bands were made visible using ethidium bromide, which intercalates with double stranded DNA. The 1% gels were prepared using 200 ml TBE buffer and 2 g Agarose (Invitrogen by Thermo Fisher Scientific; Waltham, MA, USA). The mixture was heated in a microwave (Sharp K. K.; Osaka, Japan) for 2 minutes or longer until the agarose was completely

dissolved. This was incubated at room temperature on a magnetic stir plate IKAMAG RCT (IKA Werke GmbH & Co. KG; Staufen, Germany) for 10 minutes. Ethidium Bromide (Carl Roth GmbH + Co. KG; Karlsruhe, Germany) was added to a final concentration of 1% (10 mg/ μ l). The agarose was poured into a gel tray put into a casting chamber (VWR International; Radnor, PA, USA) and combs were added to produce wells for the samples. The gel set after 20 minutes at room temperature. The gel on the tray was then transferred into the buffer chamber (VWR International; Radnor, PA, USA) and the samples were loaded into the wells using 5 μ l PCR product mixed with 3 μ l loading dye. A 1 kb marker (Invitrogen by Thermo Fisher Scientific; Waltham, MA, USA) was also loaded onto the gel. The gel was run at 50 V for 40 minutes. The gel was then transferred onto a UV transilluminator set in a DeVision D Box (Deacon Science Tec GmbH; Hohengandern, Germany) and analyzed under UV light. A band of high molecular weight was determined to be good quality and a smear of fragments of different sizes, including high molecular weight, was also deemed usable. Only very fragmented DNA or samples with no visible DNA on the gel were excluded.

Quantification of all DNA samples was done using the NanoDrop spectrophotometer 2000/2000c UV-Vis (Thermo Fisher Scientific Inc; Waltham, MA, USA). Samples were measured according to manufacturer's instructions using 1 μ l aliquots. The NanoDrop measured the absorbance at 230 nm, 260 nm and 280 nm and from that calculated the concentration and purity ratio. The ratio of absorbance at 260 nm and 280 nm was used to assess the purity of DNA and RNA. The 260/230 ratio was used as a secondary measure of nucleic acid purity. A ratio of \sim 1.8 (260/280) is generally accepted as "pure" for DNA. Expected 260/230 values are commonly in the range of 2.0-2.2. If either ratio is lower it may indicate contaminants, which absorb at 280 and 230 nm respectively.

2.1.3. Sanger sequencing

Sanger sequencing was performed on DNA samples from 443 patients. Of these 177 had previously been analyzed with HRM and the genes *PTPN11* exon 01 and *NRAS* exons 2 and 3, which were not included in the HRM, were analyzed using Sanger sequencing. Additional genes were analyzed for a small number of these patients. If the phenotype of the patient was compatible with CFCS or CS the genes for these disorders were analyzed. Additionally to those patients that had been analyzed using HRM, 266 DNA samples were also analyzed using Sanger sequencing. The extent of the genetic testing always depended on the phenotype of the patient and the previous analyses. Some patients had previous testing done in external laboratories, which was not repeated in the primary analysis.

STEP 1: POLYMERASE CHAIN REACTION

For target regions where new oligonucleotide primers needed to be designed it was done using the Primer3web 4.0.0 software (www.primer.ut.ee). The main criteria for these primers were: Specificity for the target sequence, no SNPs or long monomers in primer sequence, and products between 200 and 600 bp, leaving about 100 bp from the exon intron borders. Primers were ordered in HPLC-purified quality and dried from Thermo Fisher Scientific (Waltham, MA, USA). They were dissolved to a concentration of 500 M according to manufacturer's instructions. Then the solution was incubated overnight on a rolling incubator to ensure complete solution. A working dilution was made with a concentration of 2.5 pmol/ μ l for PCR and sequencing reactions. A list of all primers used can be found in supplemental Table 6.5.

Polymerase chain reaction (PCR) was used to amplify specific DNA fragments of interest. PCR reagents were used according to standard procedures in the lab according to the composition shown in Table 2.1.

Reagent	Amount
Template DNA (50 ng/ μ l)	0.7 μ l
Forward Primer (2,5 pmol/ μ l)	2.0 μ l
Reverse Primer (2,5 pmol/ μ l)	2.0 μ l
dNTPs (2 mM)	2.0 μ l
Buffer (10x)	2.0 μ l
MgCl ₂ (50 mmol)	0.6 μ l
DMSO (5%)	1.0 μ l
Betaine (5M)	4.0 μ l
Taq polymerase	0.1 μ l
H ₂ O	5.6 μ l
TOTAL	20 μ l

Table 2.1: Amount of reagents used in single PCR reaction

All reagents were supplied by Invitrogen by Thermo Fisher Scientific Inc (Waltham, MA, USA) except for the Dimethyl sulfoxide (DMSO, Merck KGaA; Darmstadt, Germany) and betaine (Sigma-Aldrich Corporation; St. Louis, MO, USA).

Except for the primer and template DNA the ingredients were prepared in a mastermix. After the addition of the mastermix to template DNA and primer, the mixture was vortexed, centrifuged and loaded into a thermal cycler. Here the DNA polymerase copies the DNA starting at the primer. In this case a standard touch-down PCR program was used as shown in Table 2.2 on a Manual Dual Cycler (VWR International; Radnor, PA, USA) or 2720 Thermal

Cycler (Applied Biosystems by Thermo Fisher Scientific Inc; Waltham, MA, USA). The touch-down program enabled the use of different primers, with different melting temperatures under the same cycling conditions.

Temperature	Time	Cycles
94°C	3 min	1
94°C	30 sec	2
65°C	45 sec	
72°C	45 sec	
94°C	30 sec	2
63°C	45 sec	
72°C	45 sec	
94°C	30 sec	2
61°C	45 sec	
72°C	45 sec	
94°C	30 sec	2
59°C	45 sec	
72°C	45 sec	
94°C	30 sec	2
57°C	45 sec	
72°C	45 sec	
94°C	30 sec	31
55°C	45 sec	
72°C	45 sec	
72°C	10 min	

Table 2.2: Standard touch down PCR Program

STEP 2: CONTROL OF PCR PRODUCTS

PCR products were checked on an agarose gel to ensure that the reaction was successful. The 2% gels were prepared using 200 ml TBE buffer (Tris base, boric acid, and EDTA) and 4 g Agarose (Invitrogen by Thermo Fisher Scientific Inc; Waltham, MA, USA) according to the instruction provided in section 2.1.2. Two different sizes of gel trays were used: Mini M and Mini L according to the number of samples. The PCR samples were loaded into the wells of the gel using 5 µl PCR product mixed with 3 µl loading dye. A 100 bp marker (Invitrogen by Thermo Fisher Scientific Inc; Waltham, MA, USA) was also loaded onto the gel. The Mini L gel was run at 100 V for 30 minutes, whereas the Mini M gel was run at 70 V for 20 minutes. The gel was then transferred onto a UV transilluminator set in a DeVision D Box (Deacon Science Tec GmbH; Hohengandern, Germany) and analyzed under UV light. If a band was present in the expected size the PCR product was used in the next reaction. If no band was visible in the gel, the PCR reaction was repeated with platinum taq (Invitrogen by Thermo

Fisher Scientific Inc; Waltham, MA, USA) to enhance specificity and yield. The platinum taq can be used in the same experimental setup as the regular taq.

STEP 3: PURIFICATION OF PCR PRODUCTS

After control of the PCR products the samples were purified. This is done to ensure that nothing but the PCR product remains in the sample and all contaminants, including left over dNTPs and other reagents, are removed, which may cause artifacts in the following reactions. Purification was done using AMPure XP magnetic beads (Agencourt, Beckman Coulter; Brea, CA, USA), which bind to the PCR product and everything else was washed away using 70% ethanol. This process was automated on the pipetting robot Biomek NX^P (Beckman Coulter; Brea, CA, USA).

STEP 4: SANGER SEQUENCING

The purified PCR products were then used in a sequencing reaction. The primers are the same as the ones used in the PCR reaction. All reagents were supplied by Thermo Fisher Scientific Inc (Waltham, MA, USA). The composition is shown in Table 2.3.

Reagent	Amount
Forward or Reverse Primer	0.6 μ l
PCR product	0.5 μ l
Big Dye Terminator v1.1	0.2 μ l
Buffer	1.0 μ l
H ₂ O	2.7 μ l
TOTAL	5.0 μ l

Table 2.3: Amount of reagents used in single sequencing reaction

The buffer and Big Dye Terminator, containing the dNTPs, ddNTPs, and polymerase, were prepared in a mastermix and added to the primer. The purified PCR product was added last and the samples were centrifuged. The cycler program used on a Veriti 96-Well Fast Thermal Cycler (Thermo Fisher Scientific Inc.; Waltham, MA, USA) is shown in Table 2.4.

Temperature	Time	Cycles
96°C	10 sec	26
55°C	10 sec	
60°C	1 min	

Table 2.4: Cycler program for sequencing reaction

STEP 5: PURIFICATION OF SEQUENCING REACTION

After the sequencing reaction the samples were purified again to remove any unbound fluorescent ddNTPs. This was done using CleanSEQ magnetic beads (Agencourt, Beckman Coulter; Brea, CA, USA). This process was automated on the pipetting robot Biomek NX^P (Beckman Coulter; Brea, CA, USA).

STEP 7: SEQUENCING RUN

The sequencing run was done on the 3500xL Genetic Analyzer (Applied Biosystems by Thermo Fisher Scientific Inc.; Waltham, MA, USA) using the program: RapidSeq50_POP7xl_1DyeE_BDT1.1.

STEP 8: SEQUENCING ANALYSIS

For the analysis of the sequencing data the program Sequence Pilot (JSI medical systems GmbH; Ettenheim, Germany) was used. This program allows comparison between reference sequences and the user generated sequences from patient samples. Sequence variants are annotated. Whether or not a variant is disease causing is determined by several criteria, which will be explained in chapter 2.1.7 of this thesis.

2.1.4. Verification of parentage

Genotyping of 15 highly polymorphic microsatellite makers on different chromosomes was carried out with the AmpF ℓ STR Identifiler SGM Plus PCR Amplification Kit (Applied Biosystems by Thermo Fisher Scientific Inc.; Waltham, MA, USA) to confirm the indicated relationships in cases of *de novo* mutations. The AmpF ℓ STR Identifiler kit is a short tandem repeat (STR) multiplex assay that includes 15 tetranucleotide loci as well as the Amelogenin marker to determine gender. The reaction was prepared according with the manufacturer's instructions and run on the 3500xL Genetic Analyzer (Applied Biosystems by Thermo Fisher Scientific Inc.; Waltham, MA, USA) using the program specified by the manufacturer. For analysis of the results the program GeneMapper (Applied Biosystems; Waltham, MA, USA) was used.

2.1.5. High Resolution Melting (HRM) analysis

HRM analysis was carried out on a LightCycler 480 II instrument (Roche; Mannheim, Germany). HRM is a rapid method to distinguish the melting behavior of PCR-derived short double-stranded DNA fragments (PCR amplicons of 150-300 bp length). Single nucleotide

changes affect the melting behavior and thus sequences with one or more variants can be distinguished from a reference sequence. The reaction can be separated into a quantitative PCR part and a slow continuous rise in temperature inducing melting of PCR products. The amount of double stranded DNA can be measured during this process. The typical temperature profile of the reaction is shown in Figure 2.1.

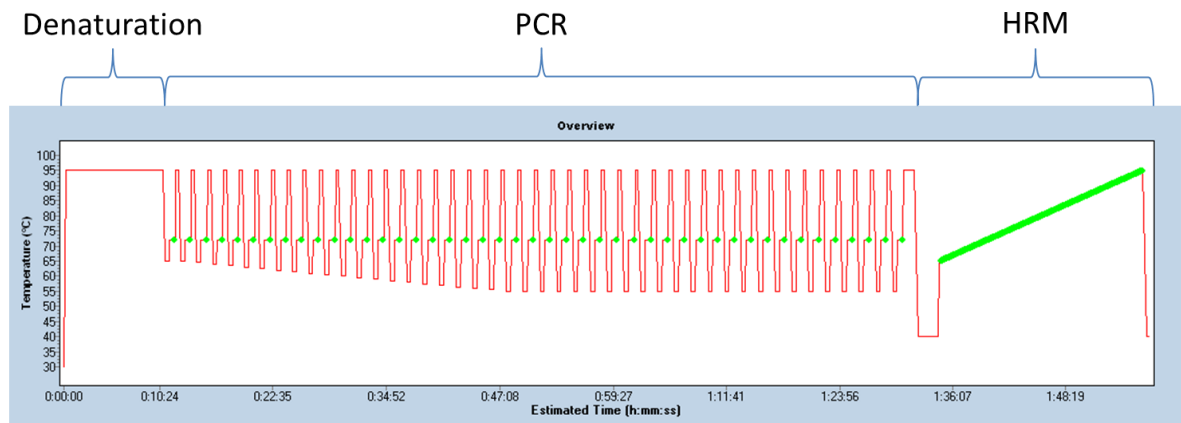


Figure 2.1: Temperature Profile HRM. This figure shows the temperature profile used in standard HRM experiments. The green dots represent the measuring points at which the fluorescence is measured (This figure is a screenshot from the LightCycler 480 Gene Scanning Software).

A fluorescent dye is used that intercalates with double stranded DNA and is incorporated during the PCR reaction. Fluorescence disappears upon denaturation of double stranded DNA. The fluorescence measurement points are shown in green in Figure 2.1. Point measurements in every PCR cycle are used to quantify the amplification. The melting curve is used to find the melting point and look at the melting behavior of the PCR products. All DNA strands are denatured slowly while the fluorescence is continuously measured. Before recording the melting curve the samples undergo a short denaturing step and are subsequently cooled down for 2 minutes to ensure that all strands are paired. In the wildtype sample the strands will always be matched with a perfect counterpart, forming homoduplexes. However if a variant is present on one allele and the wildtype on the other, it is possible that strands will pair up with one or more mismatches, forming heteroduplexes. These will show a different melting behavior compared to the homoduplexes in homozygous samples. This is shown in Figure 2.2. It implicates that HRM is more sensitive to detect heterozygous than homozygous sequence changes.

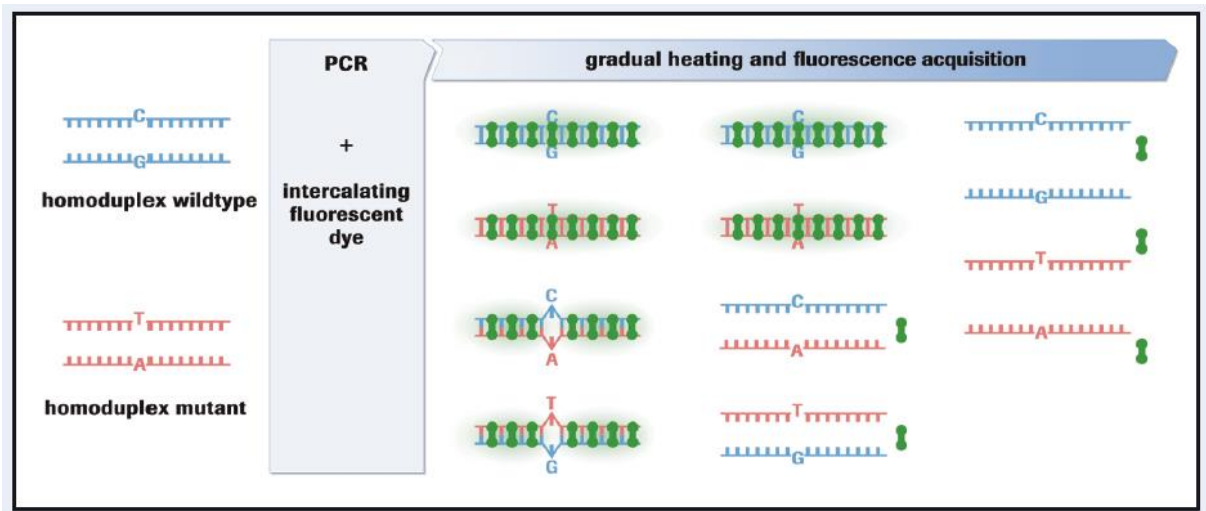


Figure 2.2: Technique of HRM analysis. This figure shows how sequence variants are made visible by fluorescence. Homoduplexes are matched perfectly whereas heteroduplexes include one or more mismatched basepairs. Sequences including one or more heteroduplexes show a different melting profile from sequences with only homoduplexes (Figure adopted from LightCycler 480 Technical Note, High Resolution Melting: Optimization Strategies, Roche, Mannheim, 2008).

2.1.5.1. Establishment of experimental method

The experimental process was established as part of this thesis. An original set of HRM primers had been designed by apl. Prof. Priv.-Doz. Dr. rer. nat. Wieland before the start of this thesis. During the establishment of this method, new primers were designed as needed for improvements and for new genes. For suitability for HRM the products are supposed to be no larger than 250 bp because changes in melting temperature are harder to detect in larger products. Primers also should be as close to the exon intron border as possible to ensure that as few SNPs as possible are in the product sequence. As a matter of principle the primer itself should not be designed to anneal to a sequence with a common SNP. Additionally HPLC (High Performance Liquid Chromatography) purification is recommended and was performed for all primers by the manufacturer. Otherwise the criteria for primers used in standard PCR reactions apply. A working dilution was made to 5 pmol/ μ l. For HRM forward and reverse primers were then mixed and stored at 4°C. A list of all primers used can be found in supplemental Table 6.5.

DNA was diluted 1/100 to a final concentration between 1 and 7 ng/ μ l. 5 μ l of that were used. The reagents were supplied in a LightCycler 480 High Resolution Melting Master Kit (Roche; Mannheim, Germany). Except for the DNA all reagents were mixed in a mastermix according to the recipe in Table 2.5.

Reagent	Amount
H ₂ O (provided in the Kit)	2 μ l
MgCl ₂ (25 mM, provided in Kit)	2 μ l
Primer Forward and Reverse (5 pmol/ μ l)	1 μ l
LightCycler® 480 High Resolution Melting Master	10 μ l
TOTAL	15 μ l

Table 2.5: Amount of the reagents used for a single HRM reaction during the establishment of the method.

Because of the fluorescent dye it was important that the prepared mix was not exposed to light for a long period of time. The DNA samples were pipetted into LightCycler 480 white 96 well plates (Roche; Mannheim, Germany) and the mastermix was added. Before loading the samples plates were briefly centrifuged and a LightCycler 480 Sealing Foil (Roche; Mannheim, Germany) was used to cover the plate. The samples were then loaded into a LightCycler 480 II (Roche; Mannheim, Germany) and the program shown in Table 2.6 was run.

2.1.5.2. Validation of the method

The primers were tested by standard PCR and gel electrophoresis. This was done according to the methods described in chapter 2.1.3 of this thesis. Here the correct product size was confirmed. The primers were also tested on the LightCycler 480 using control DNA, where they were evaluated using the T_m Calling Analysis Software (Roche; Mannheim, Germany). This program calculates the melting point of the sample and shows if one or multiple products with different melting temperatures are present in the sample. Ideally only one specific product is produced.

The method was also tested using DNA samples from 16 patients with known mutations. Here the Gene Scanning Software (Roche; Mannheim, Germany) was used as described below. It was established that the sequences with mutations were distinct from those without. Primers where either of the validation methods failed were redesigned and if no primer sequence worked that gene or exon was not analyzed using this method.

2.1.5.3. Analysis method

After the run the analysis program “Gene Scanning” supplied with the LightCycler 480 Software (Roche; Mannheim, Germany) was used. In the first step the amplification as well as the melting curves are evaluated (see Figure 2.3 panel A and B). If the amplification was too low, meaning clearly separate from the main group of samples, for one or more samples, these were excluded from the analysis. In the next step the normalization of the melting curves was

Program Name: Denaturation							
	Cycles: 1		Analysis Mode: None				
Target (°C)	Acquisition Mode	Hold (hh:mm:ss)	Ramp Rate (°C/s)	Acquisitions (per °C)	Sec Target (°C)	Step Size (°C)	Step Delay (cycles)
95	None	00:10:00	4.40				
Program Name: Amplification							
	Cycles: 45		Analysis Mode: Quantification				
Target (°C)	Acquisition Mode	Hold (hh:mm:ss)	Ramp Rate (°C/s)	Acquisitions (per °C)	Sec Target (°C)	Step Size (°C)	Step Delay (cycles)
95	None	00:00:10	4.40				
65	None	00:00:15	2.20		55	0.5	2
72	Single	00:00:25	4.40				
Program Name: High Resolution Melting							
	Cycles: 1		Analysis Mode: Melting Curves				
Target (°C)	Acquisition Mode	Hold (hh:mm:ss)	Ramp Rate (°C/s)	Acquisitions (per °C)	Sec Target (°C)	Step Size (°C)	Step Delay (cycles)
95	None	00:01:00	4.40				
40	None	00:02:00	2.20				
65	None	00:00:01	4.40				
95	Continuous		0.02	25			
Program Name: Cooling							
	Cycles: 1		Analysis Mode: None				
Target (°C)	Acquisition Mode	Hold (hh:mm:ss)	Ramp Rate (°C/s)	Acquisitions (per °C)	Sec Target (°C)	Step Size (°C)	Step Delay (cycles)
40	None	00:00:10	2.20				

Table 2.6: LightCycler Program for HRM. The standard program for the LightCycler is shown, including four main parts (denaturation, amplification, high resolution melting, and cooling). The first two steps are also part of a normal PCR reaction. The melting curve is specific for this reaction as was programmed as specified by the manufacturer. The cooling is done to cool down the plate before removal from the machine.

set manually. This step excludes the unimportant parts of the melting curve and focuses on the melting point. It also defines the maximum and minimum of the melting curve. By setting the pre- and post-curve sliding frames, depicted in green and blue, respectively (Figure 2.3 panel C), the initial and final fluorescence is defined. The sliders delimit the area, where all curves are set to 100% relative fluorescence pre-curve and 0% relative fluorescence post-curve. The standard analysis method was to put the pre-curve sliding frames (depicted in green, Figure 2.3 panel C) about 1°C apart from each other, 1-2°C from the start of the melt curve where all lines are still at maximum fluorescence. The post-curve melt sliders (depicted in blue, Figure 2.3 panel C) were put at the end of the melt curve, where all lines were at 0% fluorescence and about 1°C apart from each other. The normalized melt curves can be seen in Figure 2.3 panel D. In the next step “temperature shift” melting curves are automatically adjusted for artificial temperature differences. This setting was standardly at a threshold of 5%

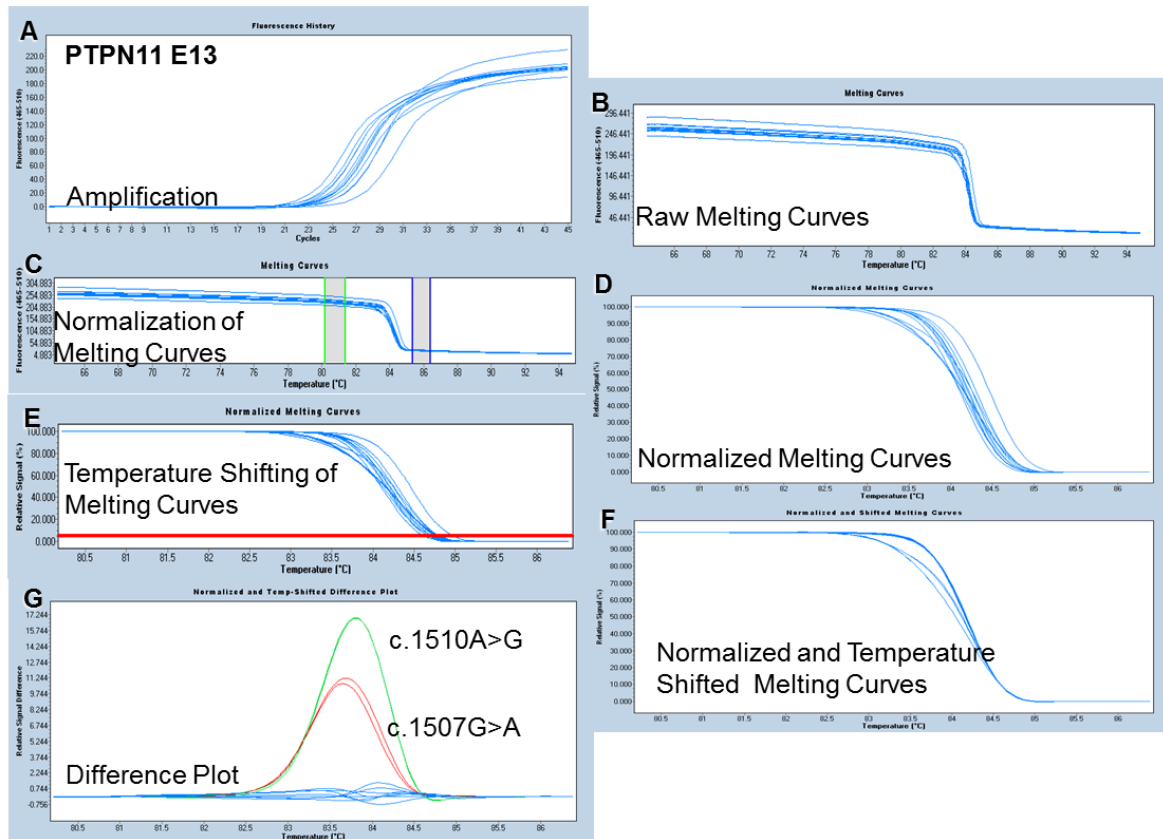


Figure 2.3: Example for a complete HRM Analysis of *PTPN11* Exon 13. A: Amplification curve of the samples confirming that in this experiment all samples showed efficient amplification. B: Raw melting curves as measured during the experiment. C: Normalization of melting curves: The sliding frames (green: pre-melt and blue: post-melt) define regions where fluorescence of all samples are set to maximum and minimum, respectively. D: Melting curves after normalization. E: Temperature shift allowing the normalization of the curves on the horizontal (temperature) axis. The red bar indicates the 5% mark on the relative signal axis, which is the standard temperature shift threshold. F: Final normalized and temperature shifted melting curves. These are then displayed in a difference plot in panel G. This plot is made by using one curve, always from the biggest group, as the baseline and displaying the other curves as differences from that (This figure was prepared with screenshots from the LightCycler 480 Gene Scanning Software).

(relative signal) as depicted in Figure 2.3 panel E (red bar). This adjustment allows for a correction due to the non-homogenic temperature on the reaction plate, by shifting the temperature axis to the point where the entire double-stranded DNA is denatured. The normalized and temperature shifted graph can be seen in Figure 2.3 panel F. On the basis of these adjusted melting curves the difference plot was calculated by the software, which takes one sample from the biggest group and calculates the difference from all other melting curves to that. This way curves deviating from the mean were easily visible as depicted in Figure 2.3 panel G. The pre- and post-curve melt sliders were then slightly changed in their position, to look at the samples again making sure that no deviation is missed. No reference sequences were used in this analysis and only patient samples compared with each other. In the case of

NS, only heterozygous changes are expected and not all patients have the exact same mutation, meaning the samples without a variant in a specific amplicon will act as referenes for those with variants.

After the analysis the samples from aberrant curves were sequenced using standard Sanger sequencing as previously described.

2.1.5.4. Standard protocol

The standard protocol that was established using the LightCycler 480 High Resolution Melting Master Kit (Roche; Mannheim, Germany) in the following set up:

Reagent	Amount
H ₂ O (provided in the Kit)	4 μ l
MgCl ₂ (25 mM, provided in Kit)	2 μ l
Primer Forward and Reverse (5 pmol/ μ l)	2 μ l
LightCycler® 480 High Resolution Melting Master	10 μ l
DNA (10 ng/ μ l)	2 μ l
TOTAL	20 μ l

Table 2.7: Amounts of reagents used in the standard HRM reaction

The composition described in Table 2.5 was used for HRM rounds 1-12 and the protocol in Table 2.7 was used for rounds 13-30. 12 patients were analyzed in each run and 32 amplicons were analyzed in each round divided up onto 4 plates as shown in Table 2.8.

Row \ Plate	1	2	3	4
A	<i>PTPN11</i> E02	<i>SOS1</i> E03	<i>SOS1</i> E10B	<i>KRAS</i> E02
B	<i>PTPN11</i> E03	<i>SOS1</i> E04	<i>SOS1</i> E10C	<i>KRAS</i> E03
C	<i>PTPN11</i> E07	<i>SOS1</i> E05	<i>SOS1</i> E10D	<i>KRAS</i> E05
D	<i>PTPN11</i> E08	<i>SOS1</i> E06	<i>SOS1</i> E11	<i>SHOC2</i> E02
E	<i>PTPN11</i> E11	<i>SOS1</i> E07	<i>SOS1</i> E13	<i>RAF</i> E07
F	<i>PTPN11</i> E12	<i>SOS1</i> E08	<i>SOS1</i> E14	<i>RAF</i> E12
G	<i>PTPN11</i> E13	<i>SOS1</i> E09	<i>SOS1</i> E16	<i>RAF</i> E14
H	<i>PTPN11</i> E14	<i>SOS1</i> E10A	<i>PTPN11</i> E04	<i>RAF</i> E17

Table 2.8: Standard plate set-up for HRM reactions. Four plates were used in each round of HRM analysis according to this diagram. The DNA was the same in all wells for each column and the primers were the same in all wells in each row.

After the plate was set up it was put into the LightCycler 480 II instrument (Roche; Mannheim, Germany) and program shown in Table 2.6 was run and the analysis was performed as described above.

2.1.6. Next Generation Sequencing

Next Generation Sequencing (NGS) or massive parallel sequencing is the umbrella term for several high-throughput sequencing techniques. Different technologies are available for the library preparation and sequencing. The technology used in the present work for the library preparation was the Nextera Rapid Capture Enrichment (Illumina, Inc.; San Diego, CA, USA). For the sequencing itself the method sequencing by synthesis (SBS) was used, which is the standard technique in sequencing instruments by Illumina, Inc. (San Diego, CA, USA).

A specific multigene panel enrichment was established, which includes all RASopathy genes that were known at the time of its design, genes for RASopathy-related differential diagnoses, including NF1 and LS, and candidate genes, which have not previously been described in RASopathies. These are functional candidates as well as candidates derived from exome sequencing studies performed in our European Consortium. A complete list of the genes can be found in Table 6.6 in the supplements. The results for the candidate genes will not be part of this thesis. The enrichment probes for this multigene panel were designed using the DesignStudio Sequencing Assay Designer (Illumina, Inc.; San Diego, CA, USA) by one of the scientists at our institute, Dr. rer. nat. Denny Schanze, with the support from the company. The experiments were performed in collaboration with the medical doctorate student, Julia Brinkmann. The experiments were run on an Illumina MiSeq System (Illumina, Inc.; San Diego, CA, USA).

2.1.6.1. Selection process

The DNA samples chosen for this analysis were from patients with a suspected RASopathy collected in the frame of our study (Molecular basis and genotype phenotype correlations of RASopathies) from international collaborators, as well as from our own genetic outpatient clinic, provided that patients or their legal guardians had given their consent for further analysis of their samples in a research context. 144 patients were chosen for this multigene panel, based on the confidence of the clinical diagnosis. This was established through a scoring system, where points are allocated for typical RASopathy symptoms (Pst, HCM, short stature, delayed development and others). Of the 144 patients, 15 had no previous genetic

testing, but the majority of patients had previously been analyzed by Sanger sequencing or HRM for a variable number of RASopathy genes.

2.1.6.2. Nextera rapid capture enrichment

The Nextera Rapid Capture Enrichment (Illumina, Inc.; San Diego, CA, USA) uses hybridization probes to enrich specific regions of the genome. After tagmentation, which fragments the genomic DNA and ligates universal adapters to these fragments, the DNA is amplified and indexes are added, which allow later identification of individual DNA samples after pooling of all samples. The DNA libraries from multiple patients are then combined into a single pool and biotinylated oligonucleotide probes are hybridized to the target regions. These target regions are captured by streptavidin coated magnetic beads, due to the binding affinity of biotin to the streptavidin, and amplified. After denaturation, the enriched library is loaded into the Illumina MiSeq System (Illumina, Inc.; San Diego, CA, USA).

2.1.6.3. Sequencing by synthesis

The flow cell, where the reaction takes place, is made up of lanes with a lawn of two different oligos. The enriched DNA libraries are bound to an oligo on the flow cell complementary to the library adapters. Through bridge amplification the strand is then replicated on the flow cell, generating a cluster of identical sequences. During the following sequencing procedure fluorescently labeled dNTPs are added to the reaction, similarly to Sanger sequencing. The difference is that the fluorescently labeled terminator does not stop the synthesis, but is reversible and another dNTP can be added in the next sequencing cycle. During each cycle all four dNTPs are available thus enabling a true base-by-base sequencing that has a low error rate. This way the sequences along with the indexes are read.

The individual reads are then aligned by the MiSeq Reporter software (Illumina, Inc.; San Diego, CA, USA) to the human reference genome (refGene) for each patient.

2.1.6.4. Sequence analysis

For sequence analysis the Variant studio by Illumina (San Diego, CA, USA) was used. Here all variants are shown with their quality score, cDNA and protein code, prediction results, and other external mutation databases like ClinVar or population frequency in ExAc. The program allows the application of filters. For this study a quality pass filter was chosen. This includes a coverage of >30 reads and reads of both forward and reverse sequence. Also the variant read

was set to >30%. Additionally a rare filter was applied, meaning that all variants identified with a global population frequency of more than 1 % were excluded.

2.1.6.5. Experimental procedure

Overall four runs were performed in this study. Runs 1 and 2 were performed with the standard enrichment protocol and for runs 3 and 4 a modified protocol was used. In the modified version 48 DNA samples were enriched instead of the 24 samples in the standard protocol, by using half of some reagents and adjusting the incubation times. The adjusted steps are marked in yellow in the experimental overview in Figure 2.4.

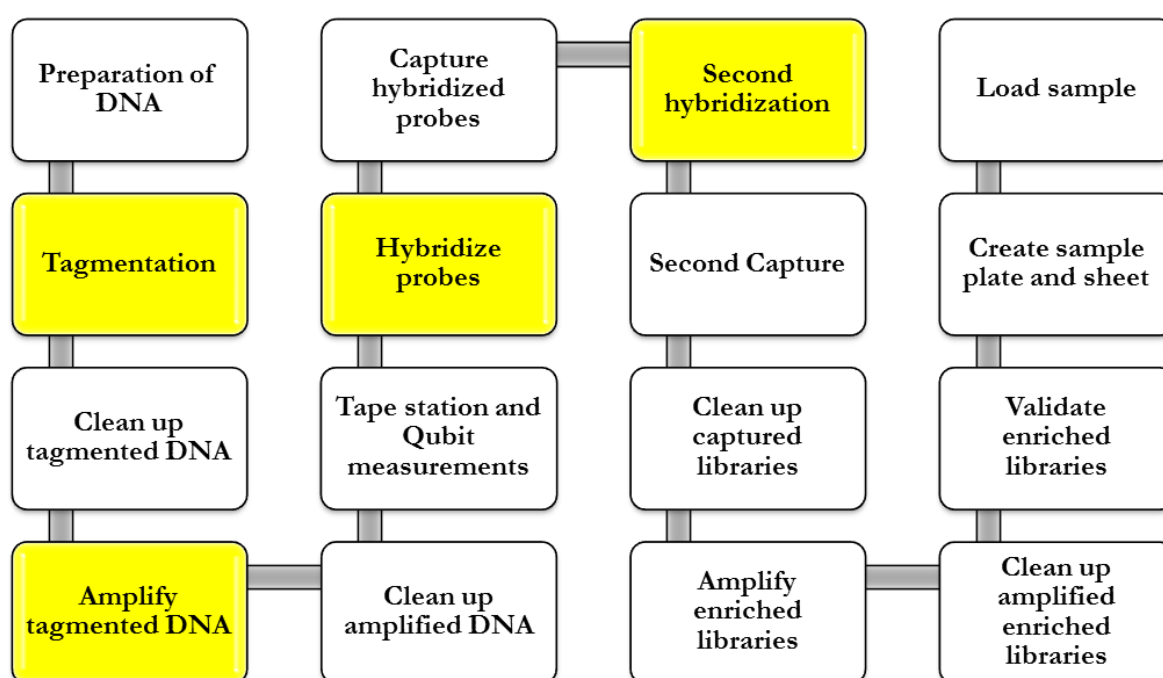


Figure 2.4: Sample preparation flow chart for NGS sequencing with Nextera Rapid Capture on a MiSeq system. Marked in yellow are the steps where adjustments were made in the modified protocol for runs 3 and 4. (This figure was prepared with information from the instruction manual supplied by Illumina, Inc. (San Diego, CA, USA)).

DNA quality was assessed using gel electrophoresis as described before. The DNA concentration was measured using the NanoDrop 2000/2000c UV-Vis spectrophotometer (Thermo Fisher Scientific Inc.; Waltham, MA, USA) as described before. According to these results the DNA solution was diluted to a concentration of 100 ng/ μ l using Tris HCl (Carl Roth GmbH + Co. KG; Karlsruhe, Germany) in a 10 μ l volume. The DNA concentration was then measured using the Qubit Fluorometric Quantitation System (Thermo Fisher

Scientific Inc.; Waltham, MA, USA) according to manufacturer's instructions. The Qubit only measures double stranded DNA, thus achieving a more accurate measurement of the amount of DNA present in the sample. The DNA was then further diluted to a concentration of 5 ng/ μ l in 10 μ l volume (5 ng/ μ l in 5 μ l for modified protocol) using Tris HCl. The complete solution was used in the further steps.

The manufacturer's instructions were followed in this study, except for the adjustments in the procedure made for the modified protocol. These are summarized in Table 2.9.

Step	Modified Protocol (48 samples)
Tagmentation	Half of the reagents
Clean Up tagmented DNA	No adjustments
Amplify tagmented DNA	Half of the reagents and 14 cycles in the PCR
Clean Up Amplified DNA	No adjustments
Tape Station and Qubit measurements	No adjustments
Hybridize probes	Longer incubation at 58°C (6 h)
Capture hybridized probes	No adjustments
Second hybridization	Incubation for at least 16 h
Second capture	No adjustments
Clean up captured libraries	No adjustments
Amplify enriched libraries	No adjustments
Clean up amplified enriched libraries	No adjustments
Validate enriched libraries	No adjustments
Create sample plate and sheet	No adjustments
Load sample	No adjustments

Table 2.9: Modifications of the protocol undertaken for runs 3 and 4 to double the sample number.

Before the libraries were loaded onto the MiSeq System (Illumina, Inc.; San Diego, CA, USA), they were quantified using the Qubit as previously described and the Agilent 4200 TapeStation System (Agilent Technologies; Santa Clara, CA, USA). The TapeStation was operated according to manufacturer's instructions. The quality is also assessed and was sufficient for all samples in this study. The results of the quantitation are used to calculate the concentration in nM according to the following formula.

$$\frac{\text{concentration in } \frac{ng}{\mu l}}{660 \frac{g}{mol} * \text{average library size}} * 10^6 = \text{concentration in nM}$$

For loading onto the MiSeq System (Illumina, Inc.; San Diego, CA, USA) final concentrations of 15 pM (runs 1, 2, and 4b) or 16 pM (runs 3a, 3b, and 4a) were used.

The system was started according to the general instructions.

2.1.6.6. Validation of variants

Confirmation of variants identified using NGS and exclusion of mix up of samples was done by Sanger sequencing according to the standard protocol described.

2.1.7. Classification of variants

All variants identified with HRM, Sanger sequencing, and NGS were searched against the NSEuroNet database since it includes all published mutations. When a previously unreported variant or one that was only published in a single publication was found, it was further classified. The database ClinVar (Landrum et al. 2014) was used, because it contains variants found by different laboratories with their classifications and reasoning behind the classification. Additionally prediction software was used. These programs analyze different aspects of the variant including conservations and the similarity between the exchanged amino acids. Here the programs MutationTaster (Schwarz et al. 2014), PolyPhen 2 (Adzhubei, Jordan and Sunyaev 2013, Adzhubei et al. 2010), MutPred (Li et al. 2009), and SIFT (Sim et al. 2012) were used. If possible, also the parental DNA was analyzed for segregation of the variant, since the a pathogenic variant is expected to be *de novo*, if the parents do not exhibit the phenotype and the variant is expected to segregate with the phenotype, if one of the parents has clinical signs for a RASopathy syndrome. The general criteria used at the beginning of this thesis are depicted in Figure 2.5.

More recently guidelines were published for the assessment of newly identified variants were published by the American College of Medical Genetics and Genomics (ACMG) (Richards et al. 2015). These include five categories for the classification of variants, namely pathogenic, likely pathogenic, uncertain significance, likely benign, and benign. Categorizing a variant is done by providing evidence that is rated from supporting to very strong. For example a moderate criterion would be a novel missense change at an amino acid where a different pathogenic change has been seen before. The only very strong criterion is the prediction of a null variant in a gene where loss of function is a known disease mechanism. They also distinguish between a *de novo* variant with unconfirmed maternity and paternity (moderate) and a *de novo* variant with confirmed maternity and paternity (strong). Combining the evidence criteria will then result in a category for the variant. For example 1 strong and 1-2 moderate criteria would result in a likely pathogenic variant, meaning a variant that is *de novo* with confirmed maternity and paternity, and at an amino acid where a pathogenic change has

already been seen would result in a likely pathogenic variant. These criteria include many of the aspects of our own validation process. All newly identified variants as well as variants only published once were reevaluated using the ACMG criteria.

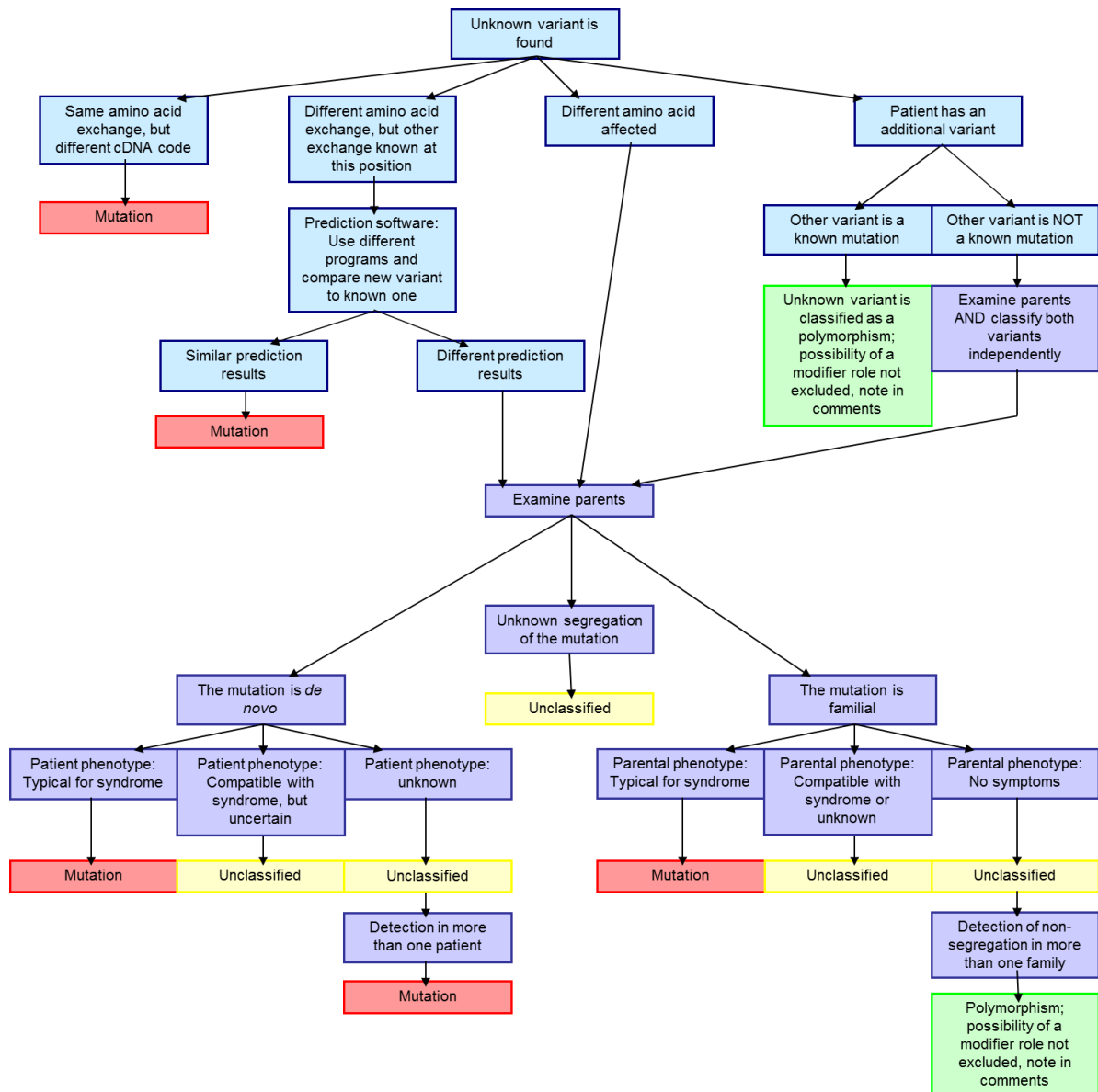


Figure 2.5: Flow chart for the evaluation of unknown variants. This flow chart depicts the evaluation of unpublished variants before classification guidelines were in place.

2.2. Database

As part of the NSEuroNet consortium a mutation database as well as a source for genotype-phenotype correlation with standardized phenotypic data was established. The process of

development is described in the following chapters focusing on the consensus-process, the structure of the database, ethical concerns, and the data input and analysis.

2.2.1. Consensus process

The first step to developing a new database was the design of a catalogue of questions. This questionnaire was of pivotal significance since the quality of the clinical information collected greatly depends on the quality of the questions. A list of the typical symptoms for patients with RASopathies is shown in Table 2.10.

Category	Symptom
Heart	Valvular pulmonary stenosis
	Hypertrophic Cardiomyopathy
	Atrial and Ventricular Septal Defect
	Rare other heart defect
Growth	Postnatal short stature
	Proportional short stature
	Relative macrocephaly
Craniofacial	Hypertelorism
	Downslanting palpebral fissures
	Ocular ptosis
	Broad forehead
	Low-set ears
	Short, broad neck / Pterygium colli
Skeletal system	Thorax anomalies: broad thorax, Pectus carinatum / excavatum
	Scoliosis
Skin and hair	Keratosis pilaris, Ichthyosis
	Ulerythema ophryogenes
	Pigmented skin lesions
	Curly hair
Development	Developmental delay of motor skills, speech, intelligence (variable)
Eyes	Refractive anomalies
	Strabism
	Nystagmus
Lymphatics	Fetal nuchal edema, pleural effusion, hydrops
	Neonatal or acquired lymphatic edema
Coagulation	Easy bruising
	Variable partial deficiencies of coagulation factors (Factor VIII, XI, XII, von Willebrand)
Urogenital	Cryptorchidism
	Unspecific renal anomalies
Neoplasms	Juvenile myelomonocytic leukemia
	Multiple granular cell tumors
	Leukemias, embryonal rhabdomyosarkomas, neuroblastomas, astrozytomas, and others

Table 2.10: Typical symptoms seen in patients with a RASopathy syndrome. (Adapted from (Zenker 2016))

According to the typical and rarer symptoms a questionnaire with appropriate answer choices was devised. This was then distributed to international partners of the NSEuroNet consortium as well as other international researchers with considerable experience in RASopathy research. Specifically the developmental section was prepared with the guidance and comment of the international consortium. This section includes questions about schooling, graduation and careers, which differs greatly from country to country and particularly in the special education field. The questions were adapted to reflect options presented internationally. With the feedback from the other researchers it was possible to modulate the questions and answer choices, resulting in a standardized questionnaire with international applicability.

The programming of the online questionnaire and the output of the database was done by an outside company (Dornheim Medical Images GmbH) with experience in databases. The website is on a server hosted by the Medizinisches Rechenzentrum of the University Hospital Magdeburg and open access as well as free of charge. The database is available online at www.nseuronet.com.

2.2.2. Structure

The NSEuroNet database has two main modules: the data submission and the data browser. The homepage with access to both modules is shown in Figure 2.6.

The screenshot shows the homepage of the NSEuroNet database. At the top left is the NSEuroNet logo, which includes a DNA double helix and the text 'NSEuroNet European Network on Noonan Syndrome and Related Disorders'. To the right of the logo are navigation links for 'Home' and 'Referencelist'. Below the header, the main content area is titled 'Welcome to the NSEuroNet database' and includes a link for 'About...'. The main content area is divided into two columns. The left column contains search options: 'Search by gene:' with a dropdown menu labeled 'please select...' and a 'Search' button, and 'Search by disease:' with a dropdown menu labeled 'please select...' and a 'Search' button. The right column contains a 'Submit data / Edit submissions' section with fields for 'username:' and 'password:', a 'Login' button, a link for 'forgot password?', and links for 'New Submitter?' and 'Register'. At the bottom of the page, there is a footer with links for 'Legal Information', 'Impressum', 'Disclaimer', and 'Haftungsausschluss'.

Figure 2.6: Homescreen of the NSEuroNet database. (Screenshot from www.nseuronet.com)

The data submission and editing module is password protected and contains the questionnaire developed in the consensus process. The data browser offers the option to show the available data by genes or diseases using a graphical and intuitive user interface.

2.2.2.1. Data submission

The consensus questionnaire was converted into a guided hierarchical online query module by Dornheim Medical Images GmbH. The queried items were divided into 15 categories, which can be seen in Figure 2.7.

Categories	
General Information	Renal and Urogenital
Clinical and Molecular	Ectodermal
Diagnosis	Skeletal
Perinatal	Hemato-oncology & Immunity
Feeding and Nutrition	Brain & Neurology
Heart	Ocular & Hearing
Lymphatics	Other Diseases
Growth	Overview
Development	

Figure 2.7: Categories. This figure depicts the categories featured in the database. (Figure prepared with screenshots from www.nseuronet.com)

The submitter is automatically guided through the menu, but can go back to each category throughout the data submission process. The answer options have four different layouts. The first is single choice answers, where only one of multiple answering options is applicable. The second layout is multiple choice answers, where more than one answering choice may be applicable to the patient. The third layout is drop-down menus, which are used because they are space-saving for short text answers and when only one option is applicable. The last layout is free text answers. These are used sparingly only for rare and uncommon symptoms because of difficulties with the standardization of entries.

The hierarchical structure of the online query module implies that sub-menus open up only if the “yes” button is marked in a superior hierarchical element. This process is displayed in Figure 2.8, showing the first page of the query module.

Additional to the hierarchical structure some items are hidden because of the age or gender of the patient. Certain aspects only apply to males, like cryptorchidism, whereas others only apply to females. The queries shown are only those relevant to the gender of the patient. Additionally certain items are only relevant to adult patients that cannot be answered for younger children. This is especially true in the developmental section where items like career or graduation are only shown for adults. The different sub-categories in the developmental section are shown in Figure 2.9.

Case 2604: General Information >

Age: 5 years 9 months

Age at data collection/last visit: 5 years 6 months

Gender: male female unknown

Ethnic background: german

Parental ages at birth: maternal 35 paternal 42

Patient has affected relatives: yes no unknown

Patient has affected relatives: yes no unknown

mother: unaffected father: unaffected

sibling(s): unaffected child/children: unaffected

Patient has died: yes no unknown

Patient has died: yes no unknown

cause of death: unknown

specify:

age at death:

Published case: yes no

Published case: yes no

Reference:

Bibliography: (will be entered by reviewer)

Figure 2.8: General Information. In this figure the first page of the database is shown. Highlighted by red boxes, the layout for the “yes” and “no” answer options with the sub-menus opened for the “yes” option are shown. (Figure prepared with screenshots from www.nseuronet.com)

5 years old	7 years old	20 years old
Development	Development	Development
Muscle Tone and Motor Milestones	Muscle Tone and Motor Milestones	Muscle Tone and Motor Milestones
Speech Development	Speech Development	Speech Development
Cognitive Development (Pre-school Age)	Cognitive Development (Primary School Age)	Cognitive Development (Secondary School Age)
	IQ measurement	Graduation Level
		Career
		IQ measurement

Figure 2.9: Developmental Categories. This figure shows the subcategories of the developmental section with the categories visible for 5, 7, and 20 year old patients. (Figure prepared with screenshots from www.nseuronet.com)

Once the data entry is finished, an overview of all entered data is displayed. After the submission process a reviewer validated all entries for consistency and plausibility, along with spelling and uniformity of free text entries. The reviewer also entered the growth percentile. If the patient had been published and a publication was noted in the online questionnaire, this was converted by the reviewer into the format recognized by the database. Reviewing submitted patient data was part of this thesis.

2.2.2.2. Data browser

The database can be browsed in two different ways: “search by gene” and “search by disease”. The search by gene opens a graphical user interface for the selected gene, which was created to resemble the design of the COSMIC database (Catalogue of somatic mutations in cancer) (Bamford et al. 2004). A graphical representation of the mutations found in the respective gene is displayed and additional information can be accessed in an intuitive and user friendly way. An overview of the browser is displayed in Figure 2.10.

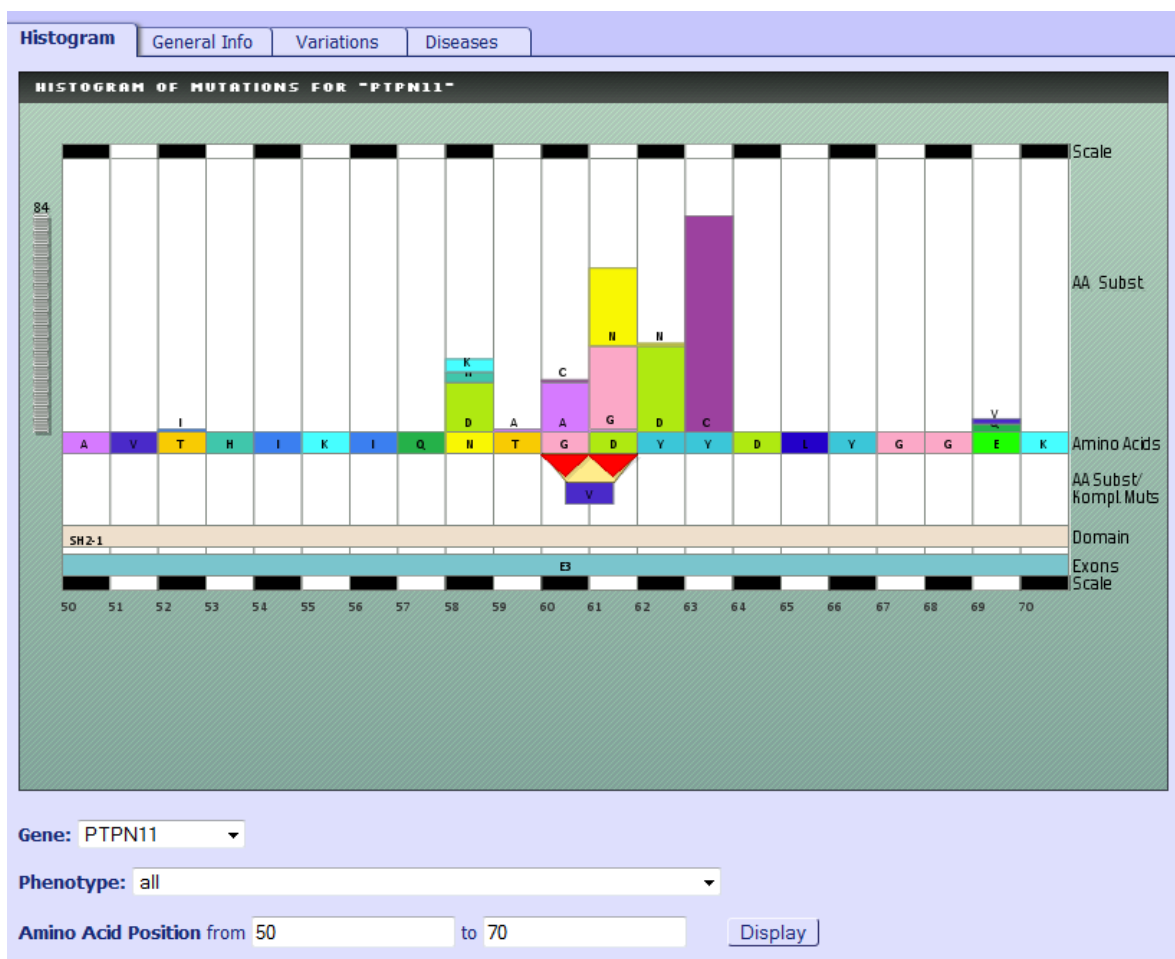


Figure 2.10: Overview output. This figure shows the graphical user interface in the data browser with the reference sequence shown in the “amino acids” line and the missense mutations displayed above and more complex mutations displayed below. (Screenshot from www.nseuronet.com)

Thereby the output webpage can be browsed for mutation data, links to publications, comments for specific mutations with certain risk factors or unknown consequences, and phenotypic data.

2.2.3. Ethical issues

In order to achieve a maximum protection of the privacy of patients whose genotype and phenotype data was included in the database no identifying information like names, addresses, abbreviation of names, or birth dates were used. Instead every dataset received a serial ID number. It is also not possible for the general public to access complete datasets of one single patient. In the data browser clinical information is shown in a summarized format without the ID numbers. Registered users, who are logged into the website, also called submitters, can only see individual datasets of their own patients, but not those from other submitters. According to guidelines published by Povey et al. consent for data entry was divided into four groups: published data, data existing as clinical reports, new diagnostic data, and research data (Povey et al. 2010). Published data was used with no restrictions, since publication had been consented to and the information was already available electronically. Although sharing of these data in a database, may not have been foreseen at the time of consent, only very limited information has been extracted from published records thus limiting the likelihood of reidentification. Diagnostic data, where consent was given for publication in a scientific journal and with the anonymity specifications in place, was used in this database. In the case of research data, informed consent was given by all study participants for publication of the data and thus it was entered into the database by the submitters. A number of study participants were recruited at the 2013 family meetings of the Noonan syndrome foundation, the CFC family group and the Costello network. These people had already been tested previously at different laboratories and a specific consent form for only the database was used, which was made according to the guidelines published by Povey and colleagues (Povey et al. 2010).

2.2.4. Data entry and analysis

Data entry was done for full clinical cases and literature cases. When the database was first programmed all patients published in the literature were entered and the data entry of published cases was regularly updated as part of this thesis work. To this end PubMed was utilized to identify all literature cases by searching for the gene names and syndrome names. It was determined that no detailed clinical information is entered from the literature cases, because of the strong heterogeneity in the presentation of clinical data in the literature, which

is not compatible with the standardization in this database. Instead the data entered from literature cases was restricted to genotype (as cDNA and protein code) and the published classification of the clinical syndrome (for example NS, CFCS, or CS). Additionally the publication reference as well as any oncologic manifestation, if present, was recorded. The rationale for including the information about oncologic manifestations but no other clinical data for literature cases was that we assumed that the presence of a cancer is likely to be mentioned even in very brief clinical reports.

Full clinical datasets from individual patients were entered for patients that were personally visited in our outpatient clinic or for patients seen by our collaborating clinicians. An example of the data entering process is illustrated below. The first page (Figure 2.8) queries general information including the age of the patient and ethnic background. The latter is important for the correct calculation of the growth percentile, since height varies in different ethnicities. On this page also the publication would be entered, if the patient had previously been published. This information allowed us to delete the respective literature case (with the same genotype) in order to avoid duplicates.

The second page (Figure 2.11) covers questions regarding the clinical and molecular diagnosis. The clinical diagnosis is queried and also a general classification of the craniofacial phenotype. In the latter the answer options are limited to “typical”, “suggestive”, and “atypical”.

Case 2604: Clinical and Molecular Diagnosis	
Most appropriate clinical category:	Noonan syndrome
Classify craniofacial phenotype:	typical
Genotype (Mutated gene):	PTPN11
Nucleotide code:	c.922A>G (example: c.922A>G)
Protein code:	p.N308D (example: p.N308D)
Other genetic variation apart from common SNPs:	<input type="radio"/> yes <input checked="" type="radio"/> no

Figure 2.11: Clinical and Molecular Diagnosis. This figure exemplary shows the entry of the mutation information as well as syndrome diagnosis and assessment of the facial phenotype. (Screenshot from www.nseuronet.com)

On this page any additional variants that were found in RASopathy genes in the same individual can also be entered (Figure 2.12). This information may be used to support the classification of rare variants, because any additional variant observed in an individual harboring a clearly disease-causing mutation that fully explains the phenotype, is likely to be a rare neutral polymorphism.

Other genetic variation apart from common SNPs: yes no

(Please use nomenclature on DNA level, e.g. c.322A>T)

Affected gene:

Nucleotide code:

Protein code:

Classification:

Comment:

Reference: (will be entered by reviewer)

Figure 2.12: Other variants. Depicted here is the form to enter other variants in RASopathy genes, mainly polymorphisms, or variants of unknown significance for an individual patient. (Screenshot from www.nseuronet.com)

The next page focuses on prenatal abnormalities, prenatal testing, gestational age at birth, and birth measurements (Figure 2.13).

Case 2604: Perinatal

Gestational age at birth: weeks

Birth weight: g

Birth length: cm

Head circumference: cm

Prenatal karyotyping done: yes no unknown

Result: normal abnormal

Antenatal ultrasound abnormalities: yes no unknown

fetal nuchal edema

polyhydramnios

fetal pleural effusion

fetal hydrops

fetal ascites

prenatally detected heart anomaly:

other:

(multiple selection possible)

Figure 2.13: Perinatal. This figure shows the entry form for all data related to pregnancy and birth. (Screenshot from www.nseuronet.com)

Page four of the questionnaire (Figure 2.14) then focuses on feeding difficulties. The questionnaire allows differentiation between reported poor feeding and the necessity (and duration) of gavage feeding. Additionally, failure to thrive (as defined by drop of BMI below the 3rd centile) and gastro-esophageal reflux are recorded, if present.

Figure 2.14: Feeding and Nutrition. This figure shows the part of the questionnaire for recording feeding issues. The top part of the figure shows the option “reported as poor feeder” and the bottom part shows the additional question that opens when the option “required gavage feeding” is chosen. (Figure prepared with screenshots from www.nseuronet.com)

The next page covers structural and functional cardiac anomalies (Figure 2.15). Here the therapeutic intervention, meaning surgery or medication, is also queried to determine if the defect was more severe or minor.

Figure 2.15: Heart Defects. This figure shows the page for recording heart issues the patient may have. The top question is regarding any structural anomalies and the bottom question regarding functional abnormalities has a similar menu available as the top question, when answered with “yes”. (Screenshot from www.nseuronet.com)

Page 6 is about the lymphatic anomalies that may arise in the newborn period or later in life (Figure 2.16).

Case 2604: Lymphatics

Lymphedema, chylothorax, or other lymphatic anomalies: yes no no data available

neonatal lymphedema

congenital chylothorax

pleural effusion/chylothorax (occurring after the newborn period)

lymphedema (occurring after the newborn period)

lymphangioma

other anomalies related to abnormal lymphatics:

(multiple selection possible)

Figure 2.16: Lymphatic anomalies. This figure shows the answer options if any lymphatic anomalies were noted in the patient history. (Screenshot from www.nseuronet.com)

Clinical data related to growth is recorded on page 7 of the questionnaire (Figure 2.17). The most recent measurements are entered and the age can be transferred from the first page. Parental height is needed to assess whether or not this patient's height is within their genetic range of target height. If additional growth data from previous measurements are available these can also be entered. Some patients with RASopathies receive growth hormone and thus the start age and pre-treatment height is entered additionally to the reason they receive the growth hormone treatment. The centile is entered by a reviewer and for the calculation the app Ped(z) was used (Gräfe 2016). For all patients with a German background the Kromeyer-Hauschild reference data were used and for all others the CDC/WHO data were used (Kromeyer-Hauschild et al. 2001, Kuczmarski et al. 2002).

The next big section of the questionnaire is regarding developmental issues (Figure 2.18). Here the age of the patient at acquisition of development data is entered or transferred from the first page. If this question is answered with no, the subsections will still open to give detailed answers for each of them, contrary to other "no" answers.

The first question in the developmental section is regarding muscle tone and motor development (Figure 2.19). Specific age ranges are given to assess the degree of delay. Also comments are possible, which is especially useful if the patient has not achieved a milestone yet, but may in the future and has not reached the maximum age (>18 months for sitting unaided, >36 months for walking unaided).

Case 2604: Growth	
Body height/length (last measurement):	<input type="text" value="102"/> cm
Weight:	<input type="text" value="15"/> kg
Occipito-frontal head circumference (OFC):	<input type="text" value="51"/> cm
Age at measurement:	<input type="text" value="5"/> years <input type="text" value="6"/> months use age entered on first page (age at last visit/data collection)
Parental height:	mother: <input type="text" value="164"/> cm father: <input type="text" value="175"/> cm
Previous measurements:	<input type="text" value="enter additional growth data"/>
Patient underwent growth hormone testing:	<input checked="" type="radio"/> yes <input type="radio"/> no <input type="radio"/> no data available
Result:	<input type="text" value="normal hormone levels"/>
Patient received growth hormone treatment:	<input type="radio"/> yes <input checked="" type="radio"/> no
Centile:	<input type="text" value="1"/> (will be entered by reviewer)

Figure 2.17: Growth data. This figure depicts the page for recording growth and growth hormone data. The current / most recent along with previous measurements can be entered additionally to information on growth hormone treatment and testing. (Screenshot from www.nseuronet.com)

Case 2604: Development	
Patient has/had any kind of developmental delay/deficits regarding motor, speech or cognitive development:	
<input checked="" type="radio"/> yes <input type="radio"/> no <input type="radio"/> no data available	
Age at acquisition of development data	
is:	<input type="text" value="5"/> years <input type="text" value="use age of data collection/last visit"/>

Figure 2.18: Developmental Section: Age. This figure shows the first page of the developmental section of the questionnaire where the age is entered. (Screenshot from www.nseuronet.com)

Case 2604: Muscle Tone and Motor Milestones	
Patient showed muscular hypotonia in infancy/childhood:	
<input checked="" type="radio"/> yes <input type="radio"/> no <input type="radio"/> no data available	
Patient showed delayed achievement of motor milestones (unsupported sitting later than 9 months; unsupported walking later than 18 months):	
<input checked="" type="radio"/> yes <input type="radio"/> no <input type="radio"/> no data available	
Achieved ability to sit without support:	<input checked="" type="radio"/> yes <input type="radio"/> no at age of: <input type="text" value="12-18 months"/>
Achieved ability to walk without support:	<input checked="" type="radio"/> yes <input type="radio"/> no at age of: <input type="text" value="24-36 months"/>
Additional comments:	<input type="text"/>
Received physical therapy:	<input checked="" type="radio"/> yes <input type="radio"/> no <input type="radio"/> no data available

Figure 2.19: Muscle Tone and Motor Milestones. This figure shows the questionnaire on hypotonia and the motor milestones. Also any additional comments can be entered. (Screenshot from www.nseuronet.com)

The second question in this subsection is about the speech development and current speech abilities (Figure 2.20). This question also has a comment option where the specific standing of a child can be documented if the child is still young and may achieve this milestone with a currently unknown delay.

Case 2604: Speech Development

Patient showed delayed speech development (simple two-word phrases later than 24 months; simple speech abilities for age):

yes no no data available

Is able to use simple two-word phrases: yes no

first simple two-word phrases at age: 36-48 months

Additional comments:

Current speech abilities: appropriate for age

Received speech therapy: yes no no data available

Figure 2.20: Speech Development. Depicted here is the entry form to register anomalies during speech development. (Screenshot from www.nseuronet.com)

The following cognitive development question is very specific to the age of the individual (Figure 2.21). For young children under 6 years of age (pre-school age) the degree of intellectual delay is only broadly categorized into mild, severe or not specified. For children aged between 6 and 10 years (primary school age) the assessment is a little more detailed. Here different options are given regarding the performance level in school and what kind of school the children go to (special education versus main stream schooling with additional help). The third schooling question will be open for everybody over the age of 10 and has more options than the primary school question.

For adults over the age of 18 the developmental questions continue (Figure 2.22). The graduation level and career questions assess the level of education achieved and to what degree independent living is possible for the individual.

If an IQ test has been performed the results are entered into the questionnaire on the same page as specific deficits in learning (Figure 2.23).

Case 2604: Cognitive Development (Pre-school Age)

Patient showed deficits in cognitive development during pre-school age:

yes no no data available

Intellectual delay:

Received occupational therapy or other supportive treatment: yes no no data available

Case 2604: Cognitive Development (Primary School Age)

Patient showed abnormalities in learning or intellectual capacities that required intervention (e.g repeating a grade, placement in special education, implementation of an individualized education plan):

yes no no data available

(tick most appropriate category)

attends/attended regular primary school, requires/required minor support

attends/attended regular primary school with major support or special primary school for children with learning disabilities (school aimed at the acquisition of reading, writing and math abilities)

attends/attended special school or institution aimed at acquisition of basic life skills

Case 2604: Cognitive Development (Secondary School Age)

Patient showed abnormalities in learning or intellectual capacities that led to school performance significantly below the level expected from family background and/or required intervention (e.g. repeating a grade, placement in special education, implementation of an individualized education plan):

yes no no data available

(tick most appropriate category)

attends/attended standard school with no or minor support, intellectual and school performance within the normal range but significantly lower than expected for family background

attends/attended standard school for many years with minor/major support or special school for children with learning disabilities

attends/attended standard school for a few years with major support or special school for children with learning disabilities; has simple reading, writing and math ability

special education; understands almost everything, makes use of small sentences and lots of signs

understands simple, daily sentences and single words; uses sentences of 2-3 words, and many signs

Understands a few words; usually walks, unsteadily, if supported; has no language or only a few words

Figure 2.21: Cognitive Development. This figure shows the different options available in the section on cognitive development, depending on the age of the proband. (Figure prepared with screenshots from www.nseuronet.com)

Case 2604: Graduation Level

Indicate school graduation level:

The patient has achieved or is aiming for:

(tick most appropriate category)

no regular school-leaving certificate qualifying for vocational training and is unable to live independently

lower level secondary general education certificate qualifying for vocational training and able to live independently with no or minor support

secondary general education certificate or regular high school diploma/certificate qualifying for apprenticeship in midlevel service vocations

university entrance diploma or regular high school diploma/certificate qualifying for university education (at least bachelors degree)

Case 2604: Career

Professional career:

(tick most appropriate category)

is under institutional care, unable to work, Day Habilitation Program

works in a sheltered workshop or receives extra assistance in a supported employment

works or has worked as an unskilled worker in gainful employment

has completed vocational training as a skilled worker or employee in a lower level service vocation

has completed vocational training as a skilled worker or employee in a midlevel service vocation or achieved an undergraduate profession (bachelor's degree)

has achieved a graduate profession (master's degree, postgraduate diploma, PhD, MD)

Figure 2.22: Graduation and Career. Depicted here are the answer options for the graduation level and professional career. (Figure prepared with screenshots from www.nseuronet.com)

Figure 2.23: IQ and specific Learning Disabilities. This figure shows the entry form for the IQ measurement and also specific deficits in learning, like legastheny or attention deficit. (Screenshot from www.nseuronet.com)

After the developmental section the questionnaire continues with the different organ systems that may be affected. First is the renal and urogenital system (Figure 2.24). The question about cryptorchidism is specific for male individuals. There are two questions here that are age specific. For individuals 15 and above a question about delayed puberty will appear and everyone over 18 will be asked about possible fertility issues.

Figure 2.24: Renal and Urogenital. Depicted here are the questions and answer options regarding renal anomalies, cryptorchidism (only shown for males), and fertility problems (only shown for adults). (Screenshot from www.nseuronet.com)

The next question is regarding skin and hair (Figure 2.25). In this section skin tumors are also entered and the type specified.

The next page is about the skeletal system (Figure 2.26) and following that is hemato-oncology and immunity (Figure 2.27). Here other neoplasms like leukemia or solid tumors are entered, if present, among other issues regarding bleeding disorders or the immune system.

Figure 2.25: Ectodermal. This figure shows the entry form for any anomalies regarding hair and skin. This section is divided into (from top to bottom) hair anomalies, hyperkeratotic skin lesions, pigmented skin lesions, hemangioma, and skin tumors. (Screenshot from www.nseuronet.com)

Figure 2.26: Skeletal. Depicted here are the answer options available for thorax anomalies, scoliosis and short or webbed neck. (Screenshot from www.nseuronet.com)

One of the last pages covers the brain and neurology (Figure 2.28). In the case of structural brain anomalies the “no data available” button was converted into a “no MRI/CT available”. This is to ensure that “no” is only answered in cases where the appropriate tests have been performed and were without pathological finding.

Case 2604: Hemato-oncology & Immunity

Patient has/had any of the following:

**Easy bruising reported/
coagulation disorder:** yes no no data available
 easy bruising reported, no further testing/specification
 confirmed coagulopathy

Hematologic disease/Leukemia: yes no no data available

**Solid tumors (benign, malignant,
tumor-like lesions):** yes no no data available

**Immunodeficiency/
frequent infections:** yes no no data available
 frequent infections in infancy/childhood reported by parents, no proven immunodeficiency
 frequent infections with proven immunologic defect such as antibody deficiency
specify defect:
 other:

Autoimmunity yes no no data available

Figure 2.27: Bruising, Oncology, and Immunity. This figure shows the entry form for anomalies regarding bruising, leukemia or hematologic diseases, solid tumors, and also immunity and autoimmunity. (Screenshot from www.nseuronet.com)

Case 2604: Brain & Neurology

Patient has/had any of the following:

Structural brain anomalies: yes no no MRI/CT available

Seizures: yes no no data available

Psychiatric disorder: yes no no data available

Other neurological diseases: yes no no data available

Figure 2.28: Brain and Neurology. Depicted here are the subsections in the brain and neurology category. (Screenshot from www.nseuronet.com)

The next section is regarding the eyes and ears (Figure 2.29). For the ocular ptosis and strabismus an individual drop-down menu opens giving answer options for the treatment, thus allowing a severity assessment. If the patient has permanent hearing deficits the subsection will open to ask if it is sensorineural or conductive hearing loss and if hearing aids are needed.

The next to last page is a free text field, where the submitter can enter anything else that the patient has, which was not previously covered (Figure 2.30).

Case 2604: Ocular & Hearing

Patient has/had any of the following:

Ocular ptosis: yes no no data available
 mild, no treatment

Refractive error/abnormal vision: yes no no data available
 (multiple selection possible) not specified myopia (mild or not specified)
 high myopia (-8 dpt or higher) hypermetropia
 astigmatism amblyopia

Strabismus: yes no no data available
 occlusion treatment

Nystagmus: yes no no data available

Permanent hearing deficits: yes no no data available

Figure 2.29: Ocular and Hearing. This figure shows the different anomalies queried regarding vision and hearing. (Screenshot from www.nseuronet.com)

Case 2604: Other Diseases

Other diseases or physical abnormalities not mentioned above, remarks:
 (please do not enter individual data)

talipes valgus, flat feet

Figure 2.30: Others. Depicted here is the entry field for all other extraordinary symptoms. (Screenshot from www.nseuronet.com)

The last page of the questionnaire is an overview which includes all data entered and the serial ID number (Figure 2.31). This was printed for all patients and is included in their file to ensure that reidentification is possible to make changes to the dataset in the future.

NSEuroNet
European Network on
Noonan Syndrome and
Related Disorders

Welcome, Christina Lissewski Home Referencelist Caselist Profile

Case 2604: Overview

General Information	
Age	5 years and 9 months
Age at data collection/last visit	5 years and 6 months
Gender	male
Ethnic background	german
Parental ages at birth	mother: 35; father: 42
Patient has affected relatives	no
Patient has died	no
Published case	no
Clinical and molecular diagnosis	
Most appropriate clinical category	Noonan syndrome
Craniofacial phenotype	typical
Genotype (Mutated gene)	PTPN11
Nucleotide code	c.922A>G
Protein code	p.N308D
Other genetic variation apart from common SNPs	undetermined; unclassified
Perinatal	
Birth measurements	age at birth: 39 weeks; birth weight: 3500 g; birth length: 52 cm; head circumference: 34 cm
Antenatal ultrasound abnormalities	fetal nuchal edema

Figure 2.31: Overview. This figure shows part of the overview, where all entries from the database are summarized. (Screenshot from www.nseuro.net)

2.3. Statistics

For comparison of phenotypic data the Fisher's exact test was used through the following website: <http://www.langsrud.com/stat/Fishertest.htm>. This test uses data from Agresti and colleagues (Agresti 1992).

Differences with a p-value of ≤ 0.05 (95% confidence interval) were deemed statistically significant.

3. RESULTS

3.1. Genotyping

Overall 606 patients were included in this study cohort during the time of this thesis. The DNA samples from these patients were analyzed by different methods. During the course of the project different methods became available and also new genes were identified, changing the analysis methods used. Additionally the analysis mode was dependent on the phenotypic features and syndrome classification. With the HRM method the hot spots in the genes *PTPN11*, *SOS1*, *RAF1*, *SHOC2*, and *KRAS* were analyzed, thus this method was only used for patients with a NS or NS-like diagnosis. Patients with a diagnosis of CFCS or CS were primarily analyzed using Sanger sequencing. The extent of genotyping by Sanger sequencing was dependent on the clinical data provided, the suggested diagnosis, and previous analyses. Some patients had previous testing done in external laboratories, which was not repeated in the primary analysis. After the conclusion of the HRM project and the establishment of the NGS panel all samples were analyzed using this newer method. The number of patients analyzed with each method and the outcome is shown in Figure 3.1.

Overall variants could be identified in 354 (58%) individuals. In 330 (54%) of them the variants were categorized as pathogenic or likely pathogenic.

3.1.1. HRM

3.1.1.1. Validation of the method

During the test runs of the HRM experiments 16 samples with known mutations were tested. In the first experiment four patients with mutations in *PTPN11* exon 3, *PTPN11* exon 8, *RAF1* exon 7, or *SOS1* exon 10A were tested. For each amplicon the mutation positive control, as well as two mutation negative samples, were amplified. The resulting difference plots can be seen in Figure 3.2.

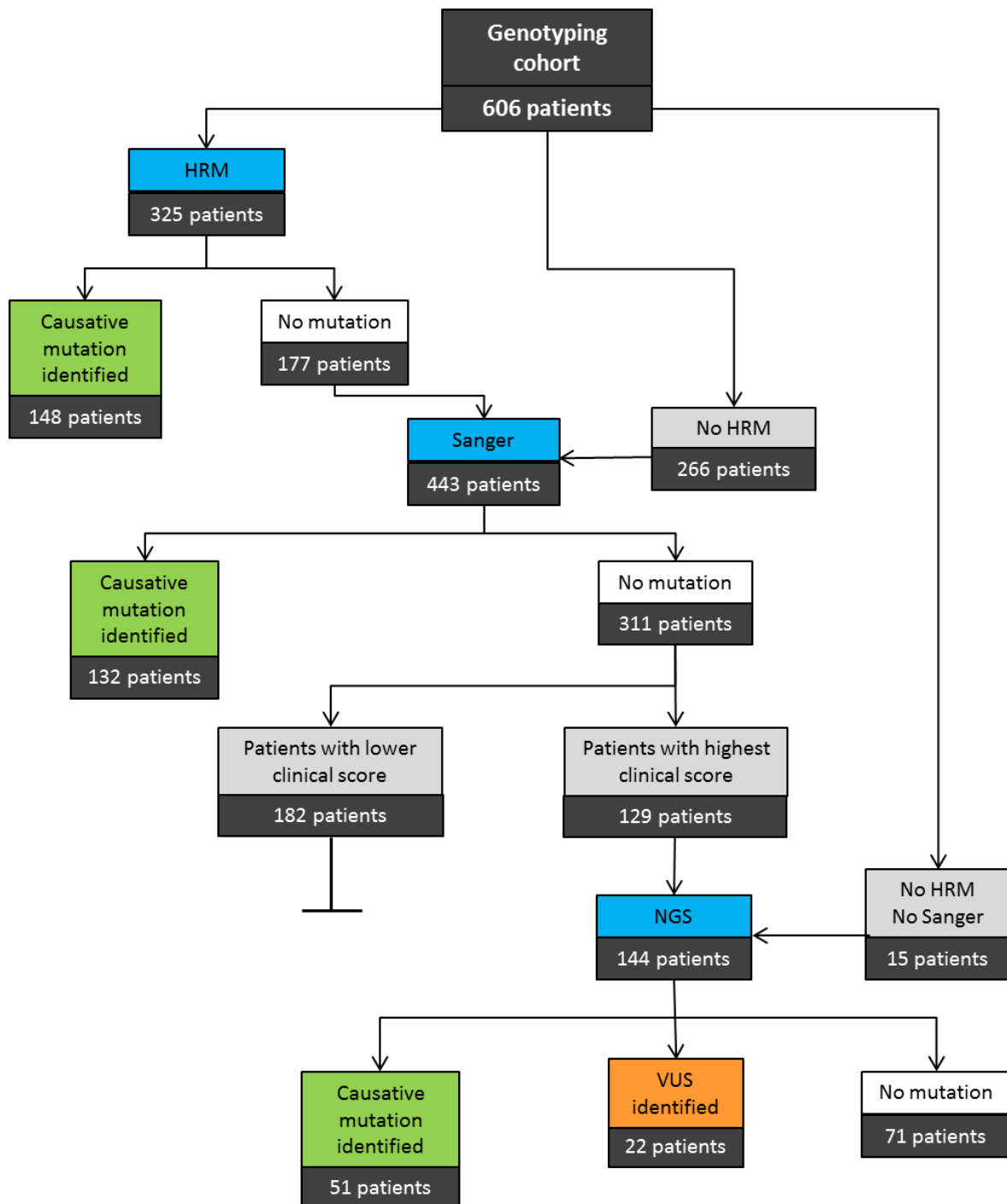


Figure 3.1: Genotyping flowchart. This figure is an overview of the genotyping cohort. It shows how many patients were analyzed with which method, for how many mutations or VUS were detected, and how many were analyzed with additional methods. The chosen method depended on the clinical diagnosis, possible previous analyses in external laboratories, and the time of inclusion into the study.

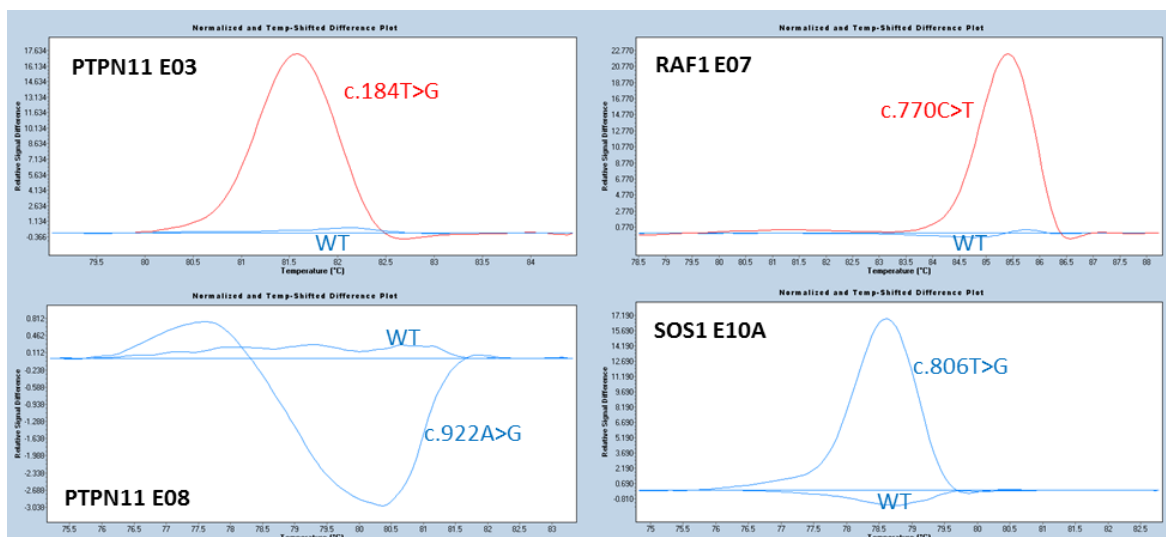


Figure 3.2: Test HRM analysis of samples with known mutations. This figure shows the difference plots for different amplicons, each containing one sample with a known mutation and several controls. *PTPN11* exon 03: The mutation positive sample is clearly visible in red with the mutation c.184T>G (p.Tyr62Asp). *RAF1* exon 07: Also here the mutation positive sample is clearly visible in red with the mutation c.770C>T (p.Ser257Leu). *PTPN11* exon 08: Here the aberrant curve does not have a different color and was thus not noticed as being different by the program, it is however visible as aberrant with the mutation c.922A>G (p.Asn308Asp). *SOS1* exon 10 amplicon A: Here the aberrant curve is also not differentiated by the software, but clearly visible with the mutation c.806T>G (p.Met269Arg). (This figure was prepared with screenshots from the LightCycler 480 Gene Scanning Software)

In the case of *PTPN11* exon 3 and *RAF1* exon 7 the aberrant curve resulting from the mutated samples is clearly recognized and color-coded by the program, whereas the program does not automatically recognize the aberrant curves in *PTPN11* exon 8 and *SOS1* exon 10A. Nevertheless in the latter case the aberrant curves are visible at manual inspection.

In the second and third experiments three samples were used for comparison of the comparability between duplicates and nine samples for comparison of different mutations in the same amplicon, respectively. Duplicates of a sample were chosen to evaluate the consistency of the aberrant curves. Samples with different mutations in the same amplicon were chosen to evaluate the specificity of the aberrant curves. In the latter experiment all samples were run in quintuplicate for better visibility. The results of these experiments can be seen in Figure 3.3.

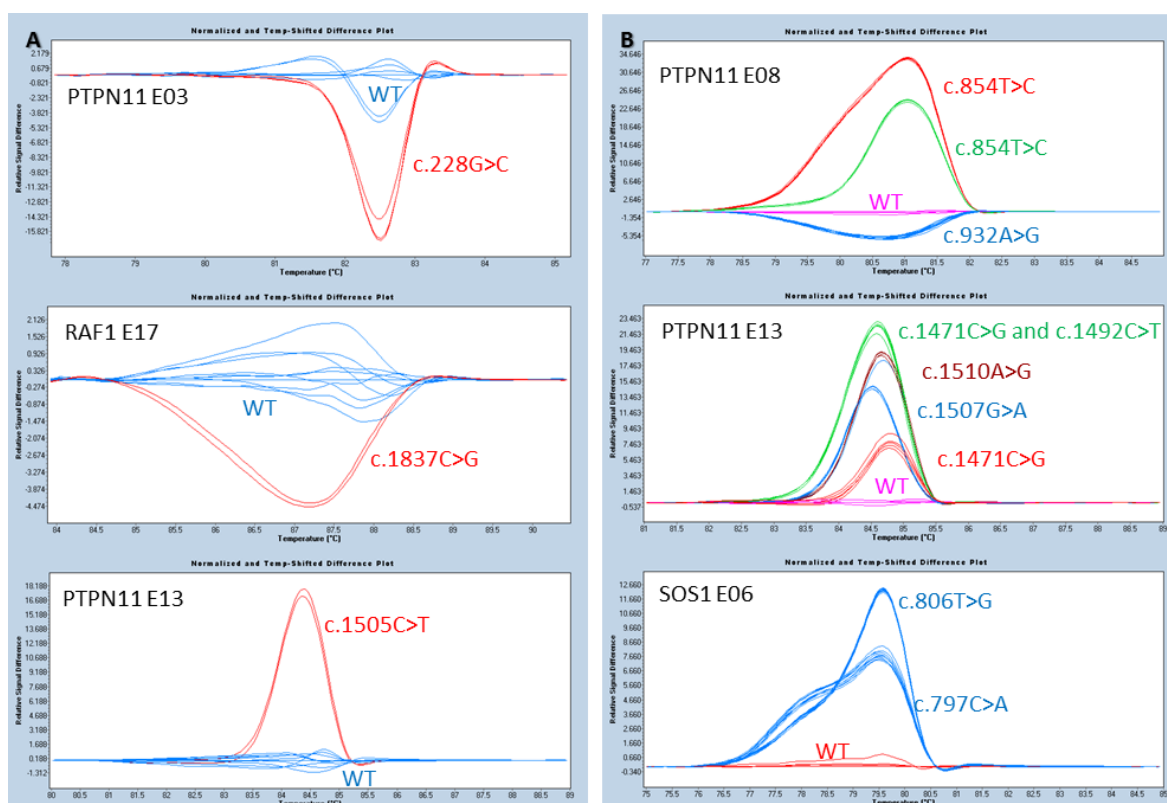


Figure 3.3: Test HRM Analysis with known mutations. Panel A: Difference plots from experiments with one sample with a known mutation run in duplicate and other mutation negative samples as controls in the same reaction. The aberrant curves are almost identical in the shown difference plots. Panel B: Difference plots from an experiment with multiple samples with different known mutations within the same amplicon and mutation negative controls. Here it is shown that the aberrant curves differ from WT as well as from each other depending on the precise nature of the mutation in the sample. (This figure was prepared with screenshots from the LightCycler 480 Gene Scanning Software).

In the second experiment the aberrant curves were always recognized by the program and the duplicates showed consistency in the difference plot. In the third experiment most aberrant curves are clearly distinguished depending on the mutation present in the DNA sample. For *PTPN11* exon 8 the pink lines represent the negative controls. The aberrant curves can clearly be identified and the different mutations are grouped separately by the program. For *PTPN11* exon 13 again the pink lines represent the mutation negative controls. Here the different mutations are clearly visible, but the difference between the c.1510A>G (p.Met504Val) and c.1507G>A (p.Gly503Arg), was not recognized by the program completely. For *SOS1* exon 6 the red lines are the mutation negative controls and again the program was not able to differentiate between the two mutation-positive groups, but this difference is clearly visible. Thus an aberrant melting curve was defined as one having a separate color from the main group and the term “borderline” was chosen for a curve that was visibly differing from the main group, but without recognition and color change otherwise made by the program.

3.1.1.2. HRM results and False-positives

DNA samples from 325 unrelated individuals were used for HRM analysis. Clinically these patients had a diagnosis of NS or other RASopathy, but not all patients fit strictly into the diagnostic criteria. For each of the patients 32 amplicons were analyzed as described in the methods section of this thesis, except for 7 patients, who were analyzed for everything but the *PTPN11* gene. Mutations in the *PTPN11* gene had been excluded by an external laboratory in these patients. Overall 542 out of 10337 amplicons (5%) had to be sequenced due to aberrant, meaning recognized by the program, or borderline melting profiles, meaning that they looked different from the other curves on inspection, but the program did not identify them as belonging to a different group. The results of the HRM runs are shown in Figure 3.4. 276 samples (51%) were confirmed to carry a variant in the respective amplicon, and 148 (54%) of these variants were pathogenic or likely pathogenic while 128 (46%) were benign or likely benign. This resulted in 148 patients with a confirmed diagnosis and 177 where no mutation could be identified.

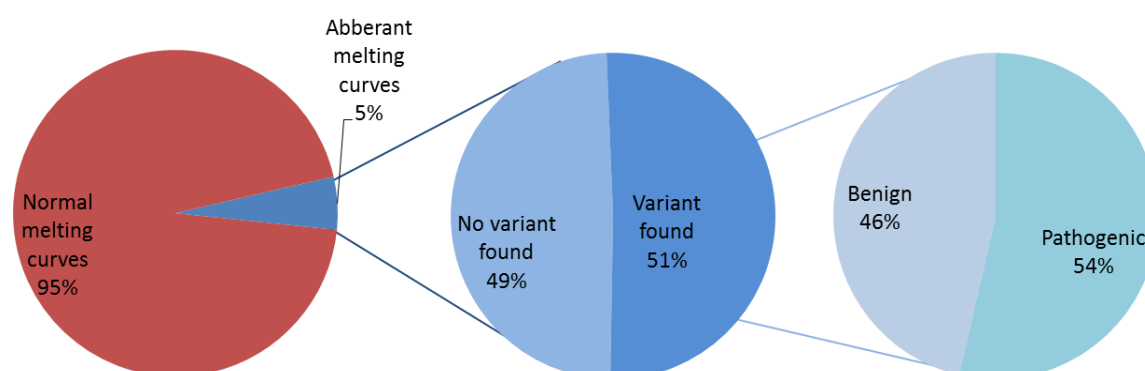


Figure 3.4: Overall results of all HRM runs. Normal melting curves were observed in 95% of cases. Of the 5% of aberrant curves variants were identified in 51% of cases and in 54% of this pathogenic variants could be found.

Of the 542 aberrant melting profiles 123 were only borderline aberrant. Variants were identified in 6 samples and the other 117 were artefacts without sequence variant. Of the 419 aberrant melting profiles, variants were identified in 270 of the samples, leaving 149 false-positive samples. The amplification and melting profiles for all false-positive samples, aberrant and borderline, were further analyzed. Examples are shown in Figure 3.5 and Figure 3.6 for the aberrant and borderline, respectively.

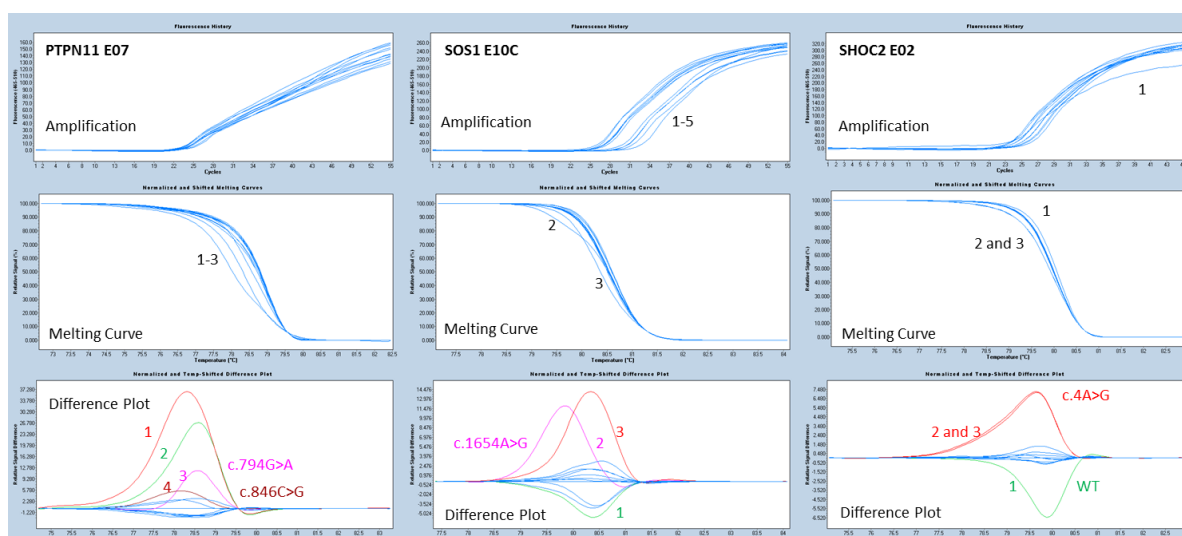


Figure 3.5: False-positives in aberrant melting profiles. *PTPN11* E07: In the amplification no samples deviated from the main group. In the melting curve three samples deviate and in the difference plot these curves and an additional one were sorted into a different group. Variants were present only in samples 3 and 4. *SOS1* E10C: In the amplification five samples deviate from the main group. In the melting curve two of those samples deviate and in the difference plot three samples were sorted into individual groups. Only sample 2 has a variant and the other two were wildtype sequences. *SHOC2* E02: In the amplification sample 1 deviates from the main group. This sample is also visible in the melting curve along with two other samples. The difference plot shows that samples 2 and 3 have the same variant and sample 1 is the wildtype sequence. (This figure was prepared with screenshots from the LightCycler 480 Gene Scanning Software).

The examples shown in Figure 3.5 highlight the importance of uniform amplification during the HRM analysis. In the first example (*PTPN11* E07) the overall amplification did not reach the plateau. In the difference plot four samples were sorted into individual groups, but only the two least apparent had a variant. This shows that aberrant amplification of all samples may obscure aberrant curves that would be more obvious if amplification had been optimal. In the next example (*SOS1* E10C) five samples show an amplification deviating from the main group. Two of those samples were also visible in the melting curve and three were sorted into different groups in the difference plot. However, only sample 2 had a variant. This shows that not all samples deviating from the main group in the amplification are aberrant in the difference plot and samples apparently aberrant due to an amplification problem may still have a variant. The last example (*SHOC2* E02) shows sample 1 differs from the main group and is also visible in the melting curve. Two additional samples are visible in the melting curve, are in the same group in the difference plot, and have the same variant. Sample 1 is in an individual group. This shows the expected outcome if the amplification is the reason for the aberrant curve, where no variant is present in the sample, but the sample is clearly sorted into a different group.

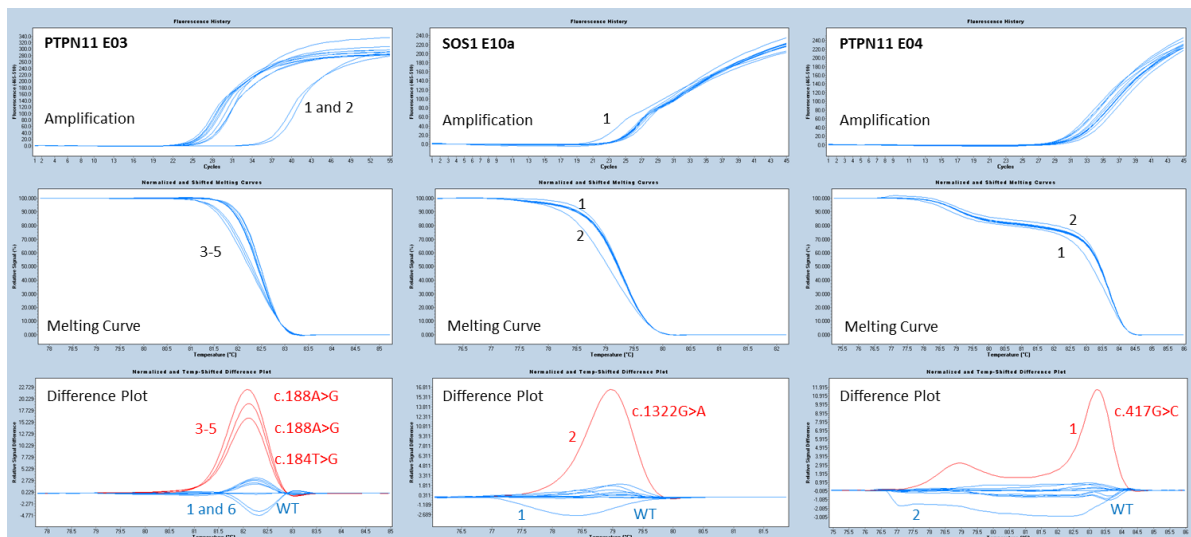


Figure 3.6: False-Positives in borderline melting profiles. *PTPN11* E03: In the amplification samples 1 and 2 deviate from the main group. In the melting curve three other samples deviate and in the difference plot these same samples can be seen in red. All three have a variant. One of the aberrant curves in the amplification also deviates from the main group in the difference plot, the other however, is in the main group. *SOS1* E10a: In the amplification sample 1 deviates from the main group. This sample is also visible in the melting curve along with sample 2. The difference plot shows that sample 2 is one with a variant and sample 1 is the wildtype sequence. *PTPN11* E04: In the amplification no sample deviates from the main group. In the melting curve samples 1 and 2 are visible. The difference plot shows that sample 1 has a variant and sample 2 is the wildtype sequence. (This figure was prepared with screenshots from the LightCycler 480 Gene Scanning Software).

The examples shown in Figure 3.6 show the borderline melting profiles. The first example (*PTPN11* E03) shows that differences in amplification may result in manually visible deviations in the difference plot (sample 1), but may also result in a curve not aberrant in the difference plot (sample 2). All three samples visually aberrant in the melting curve and distinguished in the difference plot were shown to carry a variant. In the second example (*SOS1* E10a) one of the samples (sample 1) shows aberrant amplification. This sample is also visible as different in the melting curve and difference plot showing that aberrant amplification may be the reason for an aberrant melting profile. The other sample (sample 2) is first manually visible in the melting curve and identified in the difference plot. This sample was shown to carry a variant. The last example (*PTPN11* E04) shows that aberrant amplification is not always the reason for an aberrant melting curve and difference plot. Here no sample is visible outside of the main group in amplification, but both samples are visible in the melting curve. Only one (sample 1) is identified in the difference plot, but sample 2 is also aberrant on manual inspection. However a variant is only present in sample 1. These examples in Figure 3.5 and Figure 3.6 show that not all melting curves and difference plot changes are explained by a differing amplification, but some are. However it cannot, in theory, be excluded that a sample with aberrant amplification and difference plot has no variant, thus all aberrant

and borderline melting profiles were sequenced. This results in a lower sensitivity of the method, but a better specificity, because the rate of false-negatives is presumably lower. Actual numbers of false-negatives are unknown, because no Sanger sequencing of amplicons already analyzed through HRM was performed. Some DNA samples were thoroughly analyzed using NGS and the results are shown in chapter 3.1.3 of this thesis.

3.1.1.3. Sequence-specificity of HRM

Several of the mutations have been identified multiple times. Since the analysis is based on the melting profile, which should be sequence-specific, similar aberrant curves, would be expected from samples with the same mutations. In the following example the difference plots of *PTPN11* Exon 8 from several runs (each containing 12 samples) are compared (Figure 3.7). In this exon a common polymorphism and the most common mutation are present in different combinations in multiple samples. The polymorphism rs41279090, *PTPN11* c.854-21C>T, has an allele frequency of 0.05919 according to ExAC. The mutations present in these samples are the most common *PTPN11* mutations c. 922A>G (p.Asn308Asp) or c. 923A>G (p.Asn308Ser).

In these difference plots the aberrant curves are visible, but not always recognized as such by the program (see R16, p.Asn308Asp). The polymorphism is always a peak above the baseline, whereas the mutation is under the baseline. The polymorphism seems to have a stronger impact on the melting curve, since the samples where both mutation and polymorphism are present, the curve looks more like the one with only the polymorphism.

As another example, results for *SOS1* exon 06 are shown, where two mutations were recurrently observed in this cohort, p.Met269Arg/Thr and p.Thr266Lys. (Figure 3.8).

The difference plots produced by DNA samples with these mutations are very similar in respect to the curve morphology. However an indication of mutation-specific differences, which are visible in Figure 3.8 (R6), is the absolute value of the y-axis “relative signal difference”. A comparison between these values is shown in Table 3.1.

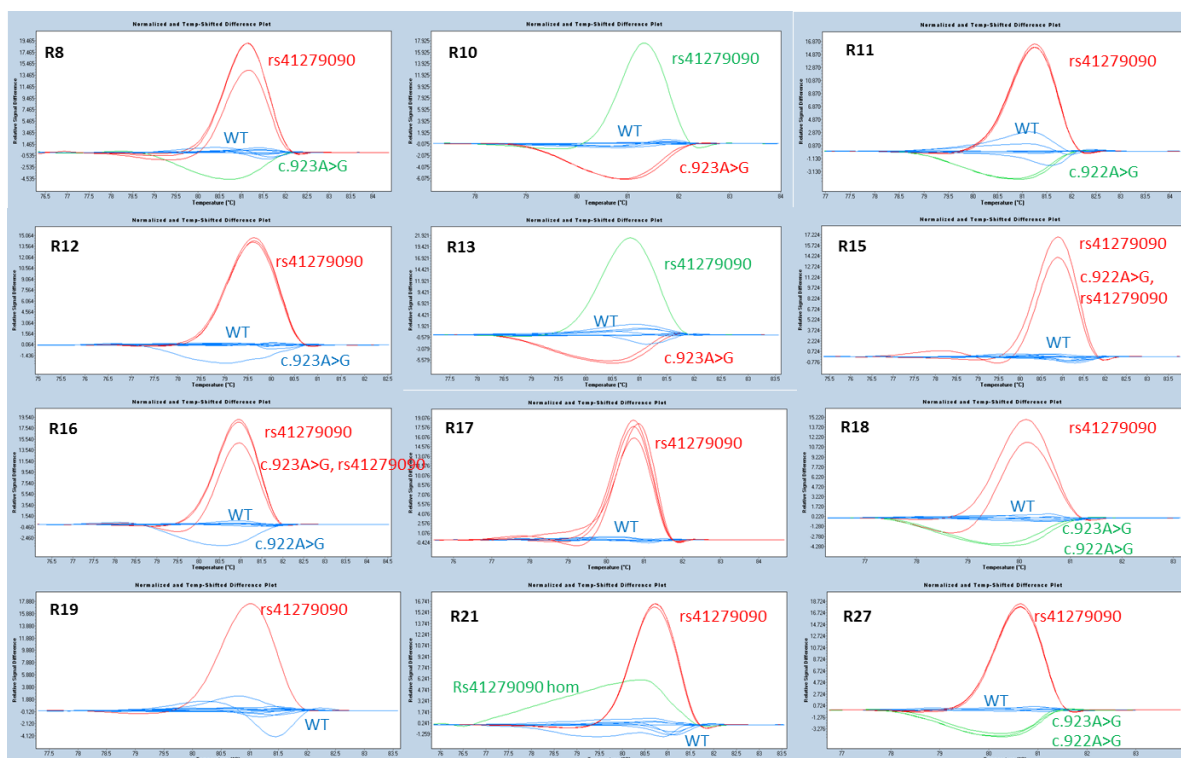


Figure 3.7: Difference Plots from *PTPN11* exon 08. This figure shows the results of different HRM runs for *PTPN11* exon 08. The annotated genotypes have been confirmed by Sanger sequencing. Notable is the comparison of the SNP (rs41279090) and the mutations c.922A>G, c.923A>G (p.Asn308Asp/Ser). In some difference plots both SNP and mutations are grouped in distinctive groups by the software (R8, R10, R11, R13, R18, R27), but in others the difference is visible, but not automatically detected by the software (R12, R16). Some samples had both variants and these curves are grouped with the SNP curves (R15, R16). In the picture from R17 only the SNP was present in any of the samples. In R19 one of the blue curves looks aberrant, but does not have a sequence variation. In R21 the SNP is not only present in the heterozygous state as in the other graphs, but also homozygous in one sample, which is shown in green and distinctive from the other curves. (This figure was prepared with screenshots from the LightCycler 480 Gene Scanning Software).

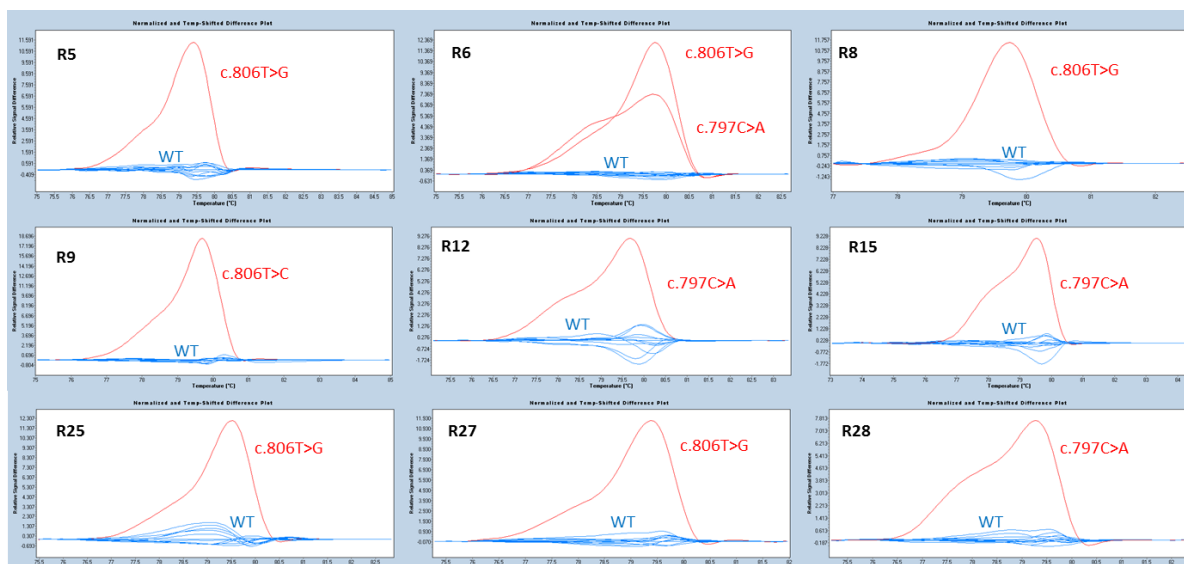


Figure 3.8: Difference Plots from *SOS1* exon 06. Depicted here are the results from the amplicon *SOS1* exon 06 where two different mutations have repeatedly been found in the samples. The p.Met269Arg/Thr mutation was identified in runs 5, 8, 9, 25, and 27 and the p.Thr266Lys in runs 12, 15, and 28. In run 6 both mutations were present in individual samples. The difference between the two curves is visible, but were not marked as different by the software. (This figure was prepared with screenshots from the LightCycler 480 Gene Scanning Software).

Round	Mutation	Maximum Peak
5	c.806T>G, p.Met269Arg	11.59
6	c.806T>G, p.Met269Arg	12.37
8	c.806T>G, p.Met269Arg	11.76
25	c.806T>G, p.Met269Arg	12.31
27	c.806T>G, p.Met269Arg	11.9
9	c.806T>C, p.Met269Thr	18.7
6	c.797C>A, p.Tyr266Lys	7.37
12	c.797C>A, p.Tyr266Lys	9.28
15	c.797C>A, p.Tyr266Lys	9.23
28	c.797C>A, p.Tyr266Lys	7.81

Table 3.1: Comparison of Relative Signal Differences. This table shows the value of the relative signal difference at the maximum peak of the difference plot shown in Figure 3.8.

The relative signal difference is comparable for the same variant in different experiments, but different for the individual variants.

3.1.1.4. Mutation Distribution

The distribution of the identified 148 pathogenic or likely pathogenic mutations among the different genes is shown in Figure 3.9. 68% (101 out of 148) of mutations were found in the *PTPN11* gene. The most common mutations in this gene are p.Asn308Ser (13 patients), p.Asn308Asp (10 patients), and p.Asp61Gly (9 patients). Overall mutations in the *SOS1* gene

were present in 20% (29 out of 148) of mutation positive individuals. Here the mutations p.Met269Arg (6 patients), p.Thr266Lys and p.Arg552Gly (4 patients each) were most common.

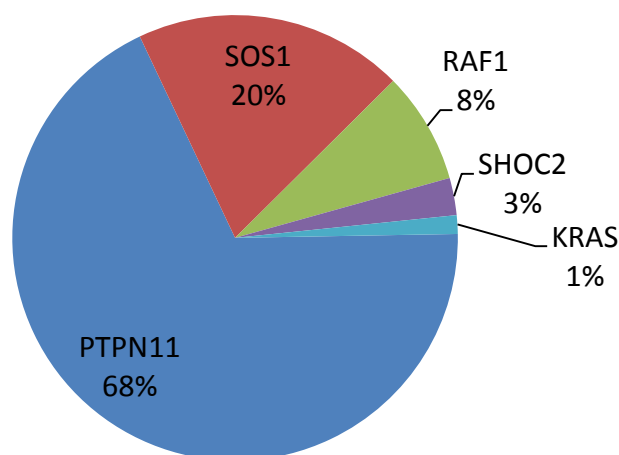


Figure 3.9: Distribution of mutations among genes. Depicted here are the percentages in which mutations in each of the genes were found.

Mutations in *RAF1*, *SHOC2*, and *KRAS* were identified in 8% (12 out of 148), 3% (4 out of 148), and 1% (2 out of 148) respectively. In this group the most common mutations were p.Ser257Leu in *RAF1* (6 patients) and p.Ser2Gly in *SHOC2* (4 patients).

3.1.2. Sanger sequencing

An overview of the patient flow is shown in the Figure 3.1 in the beginning of the results section. 266 patients of this study cohort underwent a primary mutation screening by Sanger sequencing only. The extent of the genetic analysis depended on the phenotype of the patient. Whereas patients with a CFCS diagnosis were analyzed for variants in *BRAF*, *MEK1*, *MEK2*, and *KRAS*, patients with a CS diagnosis were only analyzed for variants in *HRAS*. Where the phenotypes overlapped multiple genes were analyzed. 177 patients were analyzed with this method after no mutation could be found using HRM, but only for additional amplicons and not those that were analyzed using HRM. Overall 441 patient samples were sequenced. In 309 of these (70%) no mutation could be found. However not all patients were sequenced for the same genes and patients with very convincing phenotypes were analyzed for more genes than patients with an unclear diagnosis. One patient had a clinical diagnosis of NF1 and thus the *NF1* gene was sequenced directly. Mutations were found in 132 (30%) patients. Of these

mutations in the gene *PTPN11* were the most common with 29 patients (22%), followed by 22 (17%) patients with a mutation in *BRAF* (see Figure 3.10).

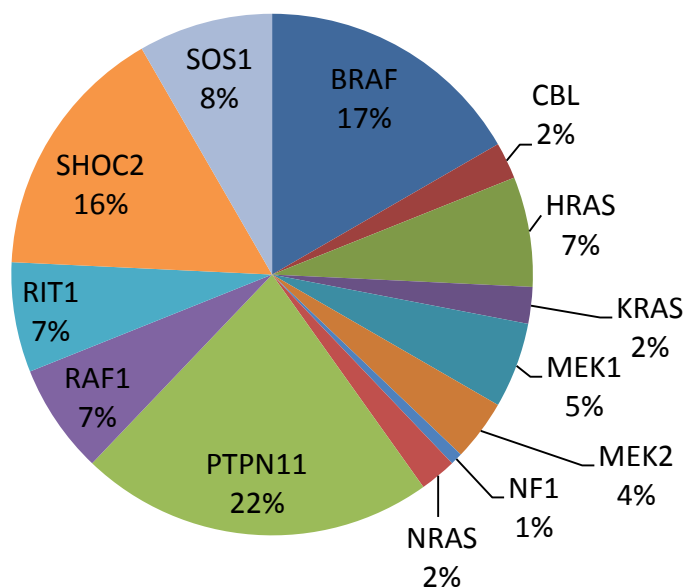


Figure 3.10: Distribution of genes in which mutations were found using Sanger sequencing. The figure shows the percentages in which mutations in specific genes have been found.

The most common mutation in the gene *PTPN11* was c.1403C>T; p.Thr468Met (6 patients) and in *BRAF* c.770A>G, p.Gln257Arg (5 patients). Also a large number of patients (21; 16%) were found to have a mutation in *SHOC2* (c.4A>G, p.Ser2Gly). Other genes represented here are *SOS1*, *RAF1*, *RIT1*, *NRAS*, *CBL*, *KRAS*, *MEK1*, *MEK2*, *HRAS*, and *NF1*. In *RAF1* the most common mutation was c.770C>T; p.Ser257Leu (5 patients). *HRAS* c.34G>A; p.Gly12Ser defining a diagnosis of CS was found in 4 patients.

Of the 160 patients who had previously been analyzed using HRM, 8 were found to have a mutation in one of the genes analyzed by Sanger sequencing. Two patients had a mutation in *BRAF*, two in *HRAS*, two in *MEK1* and one each in *MEK2* and *RIT1*.

3.1.3. Next Generation Sequencing

Overall 144 patients were analyzed using NGS. Of these, 46 had been previously analyzed using HRM and Sanger, 83 with Sanger sequencing only, and 15 had no previous testing performed in our laboratory. Variants or mutations were found in 73 individuals (51%) and for 71 (49%) no variant could be identified in any of the established genes. Differential diagnoses were established by molecular genetic testing for 6 patients, five of whom had

mutations in *NF1* and thus were diagnosed with NF1 or NF1-NS. One patient had a mutation in the *FGD1* gene and was diagnosed with Aarskog-Scott syndrome.

The distribution of the variants found among the genes can be seen in Figure 3.11.

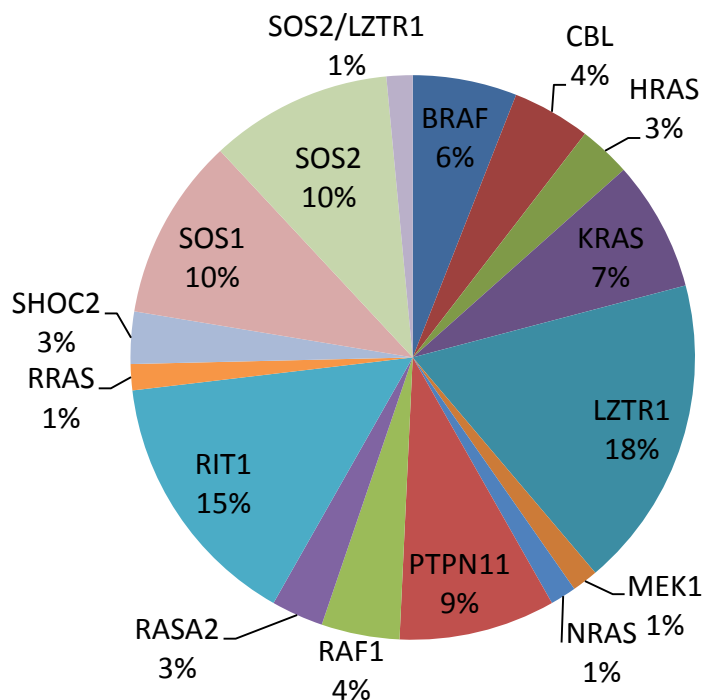


Figure 3.11: Variants found in patients using NGS sequencing. This figure shows the percentages of patients in whom variants were identified in the respective genes.

Most variants were found in the *LZTR1* gene (12 patients) followed by *RIT1* (10 patients), *SOS1*, and *SOS2* (7 patients each). Variants in *PTPN11* were identified in 6 patients. One patient was found to have a variant in *SOS2* and *LZTR1*. The novel or rarely described variants found here and through other methods will be described further in the following chapter. The known mutations found through NGS are shown in Table 3.2.

Gene	Mutation	Number of patients	Reference
<i>BRAF</i>	p.Gln257Arg	2	(Rodriguez-Viciano et al. 2006)
<i>BRAF</i>	p.Gln262Pro	1	(Ciara et al. 2015)
<i>CBL</i>	c.1096-1G>C	1	(Niemeyer et al. 2010)
<i>HRAS</i>	p.Gly12Ser	1	(Aoki et al. 2005)
<i>HRAS</i>	p.Thr58Ile	1	(Gripp et al. 2008)
<i>KRAS</i>	p.Asp153Val	1	(Nihori et al. 2006)
<i>KRAS</i>	p.Glu22Arg	1	(Zenker et al. 2007)
<i>KRAS</i>	p.Ile36Met	1	(Zenker et al. 2007)
<i>KRAS</i>	p.Phe156Leu	1	(Zenker et al. 2007)
<i>KRAS</i>	p.Thr58Ile	1	(Schubbert et al. 2006)
<i>LZTR1</i>	p.Arg284Cys	2	(Yamamoto et al. 2015)
<i>MEK1</i>	p.Asp67Asn	1	(Nava et al. 2007)
<i>NRAS</i>	p.Gly60Glu	1	(Cirstea et al. 2010)
<i>PTPN11</i>	p.Ala72Ser	1	(Tartaglia et al. 2001)
<i>PTPN11</i>	p.Asn308Asp	2	(Tartaglia et al. 2001)
<i>PTPN11</i>	p.Phe285Ser	1	(Tartaglia et al. 2002)
<i>PTPN11</i>	p.Thr2Ile	1	(Sarkozy et al. 2003)
<i>PTPN11</i>	p.Thr468Met	1	(Digilio et al. 2002)
<i>RAF1</i>	p.Ser257Leu	2	(Pandit et al. 2007)
<i>RIT1</i>	p.Ala57Gly	3	(Aoki et al. 2013)
<i>RIT1</i>	p.Ala77Ser	1	(Yoshida et al. 2004)
<i>RIT1</i>	p.Glu81Gly	1	(Aoki et al. 2013)
<i>RIT1</i>	p.Lys23Gln	1	(Nemcikova et al. 2016)
<i>RIT1</i>	p.Phe82Ile	1	(Karaer, Lissewski and Zenker 2015)
<i>RIT1</i>	p.Phe82Leu	1	(Aoki et al. 2013)
<i>RIT1</i>	p.Tyr89His	1	(Aoki et al. 2013)
<i>SHOC2</i>	p.Ser2Gly	2	(Cordeddu et al. 2009)
<i>SOS1</i>	p.Arg552Gly	1	(Roberts et al. 2007)
<i>SOS1</i>	p.Arg552Thr	1	(Beneteau et al. 2009)
<i>SOS1</i>	p.Glu846Lys	2	(Roberts et al. 2007)
<i>SOS1</i>	p.Trp432Arg	1	(Tartaglia et al. 2007)
<i>SOS2</i>	p.Met267Lys	1	(Yamamoto et al. 2015)
<i>SOS2</i>	p.Met267Lys/p.Glu266Asp	1	(Yamamoto et al. 2015) / unpublished
<i>SOS2</i>	p.Thr376Ser	1	(Yamamoto et al. 2015)

Table 3.2: Mutations found through NGS. This table shows the previously published mutations that were found using NGS technology.

The majority of mutations found were in genes not previously analyzed in the respective patient. In five cases the mutation was in a previously analyzed exon and in two the variant was in a previously analyzed gene, but that specific exon had not been sequenced, because only exons with known mutations had been sequenced. Previously unpublished variants are further classified in the following chapter. The five cases where a mutation had been

overlooked included one patient with the most common mutation in *PTPN11*: p.(Asn308Asp), one patient with the most common mutation in *SOS1*: p.(Arg552Gly), and one patient with the most common mutation in *HRAS*: p.(Gly12Ser). In all three cases the primary analysis had been done in an outside laboratory.

One patient was identified to carry the mutation c.468C>G, p.(Phe156Leu) in the *KRAS* gene (ENST00000311936). Sequencing of *KRAS* had previously been done in another diagnostic laboratory, but the sequence variant had been annotated as chr12:25362828G>C in the transcript isoform A (ENST00000256078) where it is located in the 3' untranslated region. Thus it was not further considered as a pathogenic change.

The last patient with a mutation that had remained undetected by the previous analysis was identified to carry a mutation in Exon 3 of *KRAS* (c.173C>T, p.(Thr58Ile)). The position had a read depth of 252 with an alternative read depth of 155 resulting in a 62.2% variant allele frequency, which is in the range for normal heterozygous variants. The patient had previously been analyzed with HRM showing abnormal results for *KRAS* exon 3 (Figure 3.12).

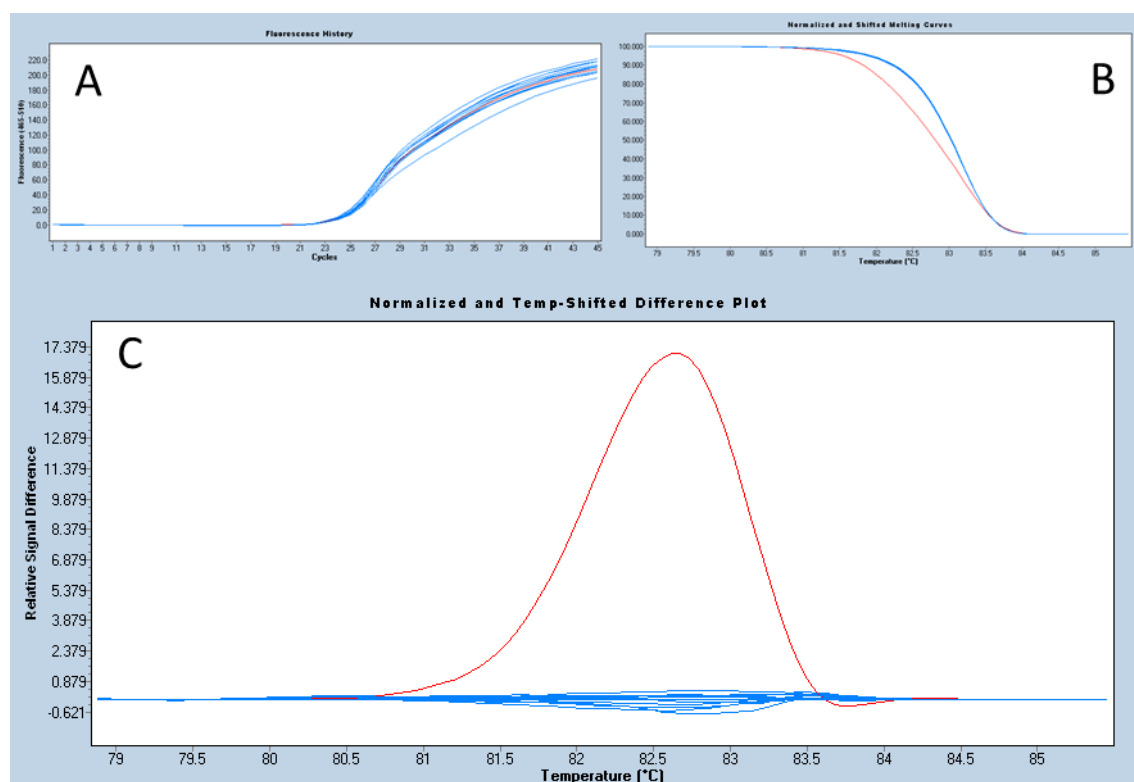


Figure 3.12: HRM Result *KRAS* exon 3. Here the amplification (panel A), melting curves (panel B), and difference plot (panel C) is shown. An aberrant curve is clearly visible in the melting profile and difference plot and was grouped separately by the software. (This figure was prepared with screenshots from the LightCycler 480 Gene Scanning Software).

This amplicon was then analyzed by Sanger sequencing, but no variant was over the detection threshold of the SeqPilot software. After obtaining the results of NGS sequencing the amplicon was reanalyzed by Sanger sequencing. The resulting electropherograms are shown in Figure 3.13. In order to circumvent the possibility of allele-specific PCR due to impaired binding of the primers to the mutated allele, sequencing was done with two different pairs of primers that have no overlap in their target sequence.

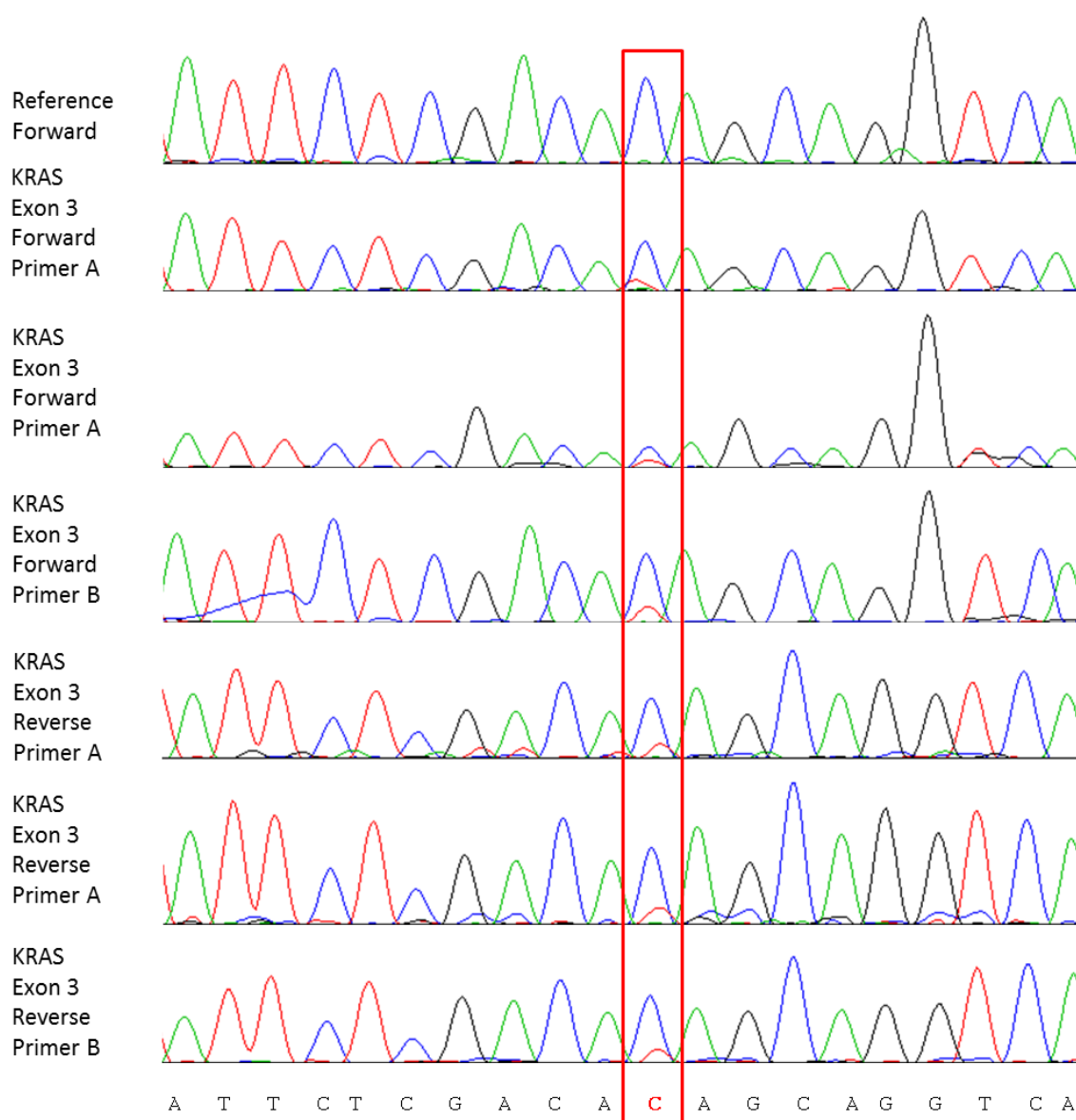


Figure 3.13: Electropherogram of the patient. Depicted here are the electropherograms obtained from Sanger sequencing of Exon 3 of the *KRAS* gene. The top sequence is a reference sequence with no variation at the position c.173 (red box). The remaining sequences are from the patient DNA, all of which show a low second peak, suggesting a mosaicism for this variant. (Primer A: amplicon size 280 bp; Primer B amplicon size: 293 bp, used for HRM). (This figure was prepared with screenshots from Chromas Lite (Technelysium Pty Ltd; South Brisbane, Australia))

Electropherograms obtained by bidirectional sequencing of amplicons of different size consistently showed a very small aberrant T peak at the site of the mutation detected by NGS. The cause of the failure to clearly detect the mutation by Sanger sequencing could not be resolved. The possibility of mosaicism is suggested by the Sanger sequencing results, but NGS of the same sample gave no hint at a possible mosaic.

3.1.4. Novel or rarely described variants

Overall 166 variants were identified in 354 individuals through any of the methods utilized in this study. Most of these variants found were known mutations that had been published multiple times and only 49 were unpublished variants or had been published just once. The latter group was classified into pathogenic, likely pathogenic or variant of unknown significance (VUS) according to the ACMG guidelines. Table 3.2 shows all variants that have been classified as pathogenic or likely pathogenic and Table 3.3 all VUS. Of these previously undescribed variant 21 were classified as pathogenic or likely pathogenic and 28 remained VUS.

Gene	cDNA	Protein	Count	Zygoty	Population database	Computational and predictive data	Functional data	<i>De novo</i> / Segregation data	Mutation database	Classification according to ACMG criteria
<i>NF1</i>	c.7549C>T	p.Arg2517*	1	heterozygous	absent	PVS1	PP2	unknown	pathogenic (LOVD)	pathogenic
<i>NF1</i>	c.5040delA	p.Gly1681Valfs*8	1	compound heterozygous	absent	PVS1	PM1	<i>De novo</i>	unknown	pathogenic
<i>RIT1</i>	c.229G>A	p.Ala77Thr	1	heterozygous	absent	PS1	PM1	unknown	pathogenic (ClinVar)	pathogenic
<i>BRAF</i>	c.1396_1397delinsTC	p.Gly466Ser	1	heterozygous	absent	PP3	PM1	<i>De novo</i>	unknown	likely pathogenic
<i>BRAF</i>	c.1798G>C	p.Val600Leu	1	heterozygous	absent	conflicting predictions	PS3	unknown	likely pathogenic (ClinVar)	likely pathogenic
<i>BRAF</i>	c.708C>G	p.Asn236Lys	1	heterozygous	absent	PP3	PP2	<i>De novo</i>	unknown	likely pathogenic
<i>BRAF</i>	c.1595_1605delinsACAGCTGG	p.Cys532_Ser535delinsTyrSerTrp	1	heterozygous	absent	PM5	PP2	<i>De novo</i>	unknown	likely pathogenic
<i>BRAF</i>	c.1395_1403del	p.Gly466_Phe468del	1	heterozygous	absent	PM5	PP2	<i>De novo</i>	unknown	likely pathogenic
<i>CBL</i>	c.1096-1G>T	-	1	heterozygous	absent	-	PM1	<i>De novo</i>	Pathogenic (ClinVar)	likely pathogenic
<i>CBL</i>	c.1096-4_1096-1delAAAG	-	1	heterozygous	absent	-	PM1	unknown	(likely) pathogenic (ClinVar)	likely pathogenic
<i>HRAS</i>	c.187_207dup	p.Glu63_Asp69dup	1	heterozygous	absent	-	PM1	<i>De novo</i> (confirmed parentage)	unknown	likely pathogenic
<i>LZTR1</i>	c.2062C>G	p.Arg688Gly	1	heterozygous	absent	PM5	PM1	unknown	unknown	likely pathogenic
<i>NF1</i>	c.4781A>G	p.Tyr1594Cys	1	heterozygous	absent	PP3	PM1	unknown	unknown	likely pathogenic
<i>PTPN11</i>	c.1471C>G	p.Pro491Ala	1	heterozygous	absent	conflicting predictions	PP2	<i>De novo</i>	likely pathogenic (ClinVar)	likely pathogenic
<i>PTPN11</i>	c.768_770dup	p.Gln257dup	1	heterozygous	absent	PM5	PP2	Inherited from affected parent	unknown	likely pathogenic
<i>PTPN11</i>	c.1282G>A	p.Val428Met	1	heterozygous	absent	PP3	PP2	Inherited from affected parent	likely pathogenic (ClinVar)	likely pathogenic
<i>RAF1</i>	c.1082G>C	p.Gly361Ala	1	heterozygous	absent	PP3	PP2	<i>De novo</i>	(likely) pathogenic (ClinVar)	likely pathogenic
<i>RRAS</i>	c.260A>T	p.Gln87Leu	1	heterozygous	absent	PP3	PP2	<i>De novo</i>	unknown	likely pathogenic
<i>SOS1</i>	c.571G>A	p.Glu191Lys	1	heterozygous	absent	PP3	PP2	Inherited from affected parent	VUS	likely pathogenic
<i>SOS1</i>	c.283G>A	p.Glu95Lys	1	heterozygous	absent	PP3	PP2	<i>De novo</i>	unknown	likely pathogenic
<i>SOS1</i>	c.512T>G	p.Val171Gly	1	heterozygous	absent	PP3	PP2	<i>De novo</i>	VUS	likely pathogenic

Table 3.3: Pathogenic or likely pathogenic variants. This table shows all previously unpublished pathogenic or likely pathogenic variants identified in this project and their classification criteria according to the ACMG guidelines (Richards et al. 2015). The same abbreviations were used as in the publication by Richards et al.: PM1: Mutational hot spot or well-studied functional domain without benign variant; PM5: Novel missense change at an amino acid residue where a different pathogenic missense change has been seen before; PP2: Missense in gene with low rate of benign missense variants and path. missenses common; PP3: Multiple lines of computational evidence support a deleterious effect on the gene/gene product; PS1: Same amino acid change as an established pathogenic variant; PS3: Well-established functional studies show deleterious effect; PVS1: Predicted null variant in a gene where loss-of-function is a known mechanism of disease.

Gene	cDNA	Protein	Count	Zygoty	Population database	Computational and predictive data	Functional data	<i>De novo</i> / Segregation data	Mutation database	Classification according to ACMG criteria
<i>CBL</i>	c.2513G>T	p.Gly838Val	1	heterozygous	absent	BP4	PP2	Nonsegregation with disease	unknown	VUS
<i>CBL</i>	c.2273C>T	p.Ala788Val	1	heterozygous	position is reported	conflicting predictions	PP2	unknown	unknown	VUS
<i>FGD1</i>	c.2002G>A	p.Glu668Lys	1	heterozygous	2.515e-05 (ExAC)	conflicting predictions	PP2	unknown	unknown	VUS
<i>LZTR1</i>	c.1856G>A	p.Arg619His	1	homozygous	absent	BP4	none	unknown	unknown	VUS
<i>SOS2</i>	c.2217G>T	p.Lys739Asn	1	heterozygous	2.471e-05 (ExAC)	BP4	PP2	Nonsegregation with disease	unknown	VUS
<i>LZTR1</i>	c.2090G>A	p.Arg697Glu	1	compound heterozygous	8.272e-06 (ExAC)	conflicting predictions	none	unknown	unknown	VUS
<i>LZTR1</i>	c.2407-2A>G	-	1	compound heterozygous	position is reported	-	none	unknown	unknown	VUS
<i>LZTR1</i>	c.361C>G	p.His121Asp	1	compound heterozygous	absent	PP3	none	Nonsegregation with disease	unknown	VUS
<i>LZTR1</i>	c.2264G>A	p.Arg755Gln	1	compound heterozygous	8.291e-06 (ExAC)	BP4	none	Nonsegregation with disease	unknown	VUS
<i>LZTR1</i>	c.2495A>G	p.Gln832Arg	1	heterozygous	absent	BP4	none	Nonsegregation with disease	unknown	VUS
<i>LZTR1</i>	c.271A>G	p.Met91Val	1	heterozygous	absent	conflicting predictions	none	unknown	unknown	VUS
<i>LZTR1</i>	c.614T>C	p.Ile205Thr	1	homozygous	absent	conflicting predictions	none	unknown	unknown	VUS
<i>LZTR1</i>	c.509G>A	p.Arg170Trp	1	homozygous	3.316e-05 (ExAC)	conflicting predictions	none	unknown	unknown	VUS
<i>LZTR1</i>	c.508C>T	p.Arg170Trp	1	heterozygous	1.658e-05 (ExAC)	conflicting predictions	none	unknown	unknown	VUS
<i>LZTR1</i>	c.509G>A	p.Arg170Gln	1	heterozygous	3.316e-05 (ExAC)	conflicting predictions	none	unknown	unknown	VUS
<i>LZTR1</i>	c.848G>A	p.Arg283Gln	2	heterozygous	absent	PP3	none	unknown	unknown	VUS
<i>MEK2</i>	c.376A>G	p.Asn126Asp	1	heterozygous	absent	conflicting predictions	PP2	unknown	unknown	VUS
<i>NF1</i>	c.4306G>A	p.Glu1415Lys	1	compound heterozygous	absent	conflicting predictions	PM1	Nonsegregation with disease	VUS (ClinVar)	VUS
<i>NF1</i>	c.5536C>T	p.Arg1846Trp	2	heterozygous	1.648e-05 (ExAC)	PP3	PM1	unknown	unknown	VUS
<i>NF1</i>	c.5669G>T	p.Gly1890Val	1	heterozygous	absent	PP3	PP2	unknown	unknown	VUS
<i>RASA2</i>	c.1532G>A	p.Arg511His	1	heterozygous	absent	PP3	PP2	inherited from father with unknown phenotype	unknown	VUS
<i>RASA2</i>	c.34T>A	p.Ser12Thr	1	heterozygous	position is reported	BP4	none	unknown	unknown	VUS
<i>SOS1</i>	c.3358G>A	p.Val1120Ile	1	heterozygous	absent	BP4	PP2	unknown	unknown	VUS
<i>SOS1</i>	c.375G>C	p.Gln125His	1	heterozygous	absent	conflicting predictions	PP2	strong benign	unknown	VUS
<i>SOS2</i>	c.1210C>A	p.Pro404Thr	1	heterozygous	position is reported	BP4	PP2	unknown	unknown	VUS
<i>SOS2</i>	c.3685A>T	p.Asn1229Tyr	1	heterozygous	absent	conflicting predictions	PP2	unknown	unknown	VUS
<i>SOS2</i>	c.3952C>T	p.Pro1318Ser	1	heterozygous	0.000602 (ExAC)	conflicting predictions	PP2	unknown	unknown	VUS
<i>SOS2</i>	c.929A>G	p.Asn310Ser	1	heterozygous	2.51e-05	BP4	PP2	unknown	unknown	VUS

Table 3.4: Variants of unknown Significance. This table shows all previously unpublished variants of unknown significance identified in this project and their classification criteria according to the ACMG guidelines (Richards et al. 2015). The same abbreviations were used as in the publication by Richards et al.: BP4: Multiple lines of computational evidence suggest no impact on gene/gene product; PM1: Mutational hot spot or well-studied functional domain without benign variant; PP2: Missense in gene with low rate of benign missense variants and path. missenses common ; PP3: Multiple lines of computational evidence support a deleterious effect on the gene/gene product.

3.2. Database

The NSEuroNet database was launched in 2011 and at first all literature cases with a confirmed mutation in one of the RASopathy genes were entered. This was regularly updated and thus resulted in the database being usable as a mutation database for published mutations. In addition, genotype and detailed phenotype data were entered from patients ascertained in our group. The database currently includes 2568 patients from the literature and 420 patients with full clinical information (see Table 3.5).

Gene	Literature patients	Patients with complete clinical information
<i>BRAF</i>	245	19
<i>CBL</i>	32	3
<i>HRAS</i>	583	6
<i>KRAS</i>	60	7
<i>LZTR1</i>	13	0
<i>MEK1</i>	48	7
<i>MEK2</i>	34	4
<i>NRAS</i>	12	17
<i>PTPN11</i>	1145	111
<i>RAF1</i>	87	40
<i>RIT1</i>	17	34
<i>RRAS</i>	2	2
<i>SHOC2</i>	46	107
<i>SOS1</i>	232	56
<i>SOS2</i>	12	7
TOTAL	2568	420

Table 3.5: NSEuroNet Literature Data. This figure shows the number of patients included in the NSEuroNet database sorted by genes.

The homepage of the database gives two different search options: search by gene and search by disease. The mutation spectrum for each gene is viewable through the “search by gene” function, and the genes found to be mutated in each syndrome is viewable through the “search by disease” option (Figure 3.14).

Welcome to the NSEuroNet database

Search by gene:
 please select...

Search by disease:
 please select...

Figure 3.14: Selection of search modus for the NSEuroNet database. This figure shows the homepage of the database where the data output is accessible either through searching for a specific gene or for a specific syndrome. (Screenshot from www.nseuro.net)

By choosing a gene and clicking “search” the mutation spectrum of the selected gene is visible as a histogram (see Figure 3.15).

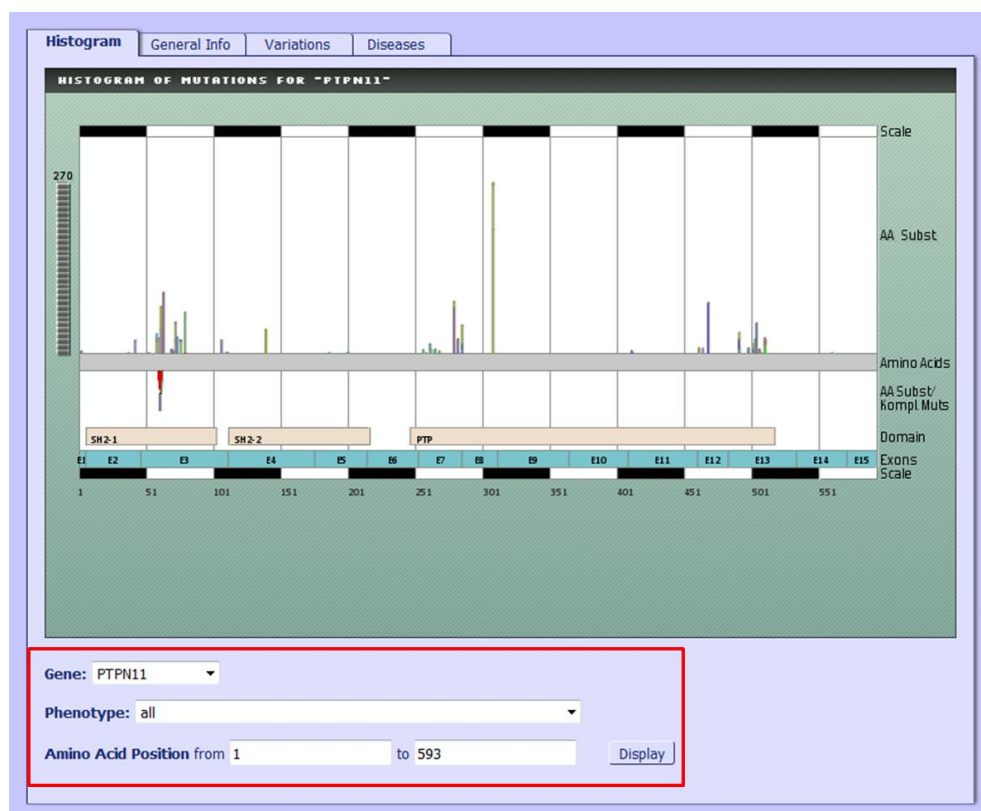


Figure 3.15: Mutation spectrum of *PTPN11*. This figure shows the overview for the *PTPN11* gene. The missense mutations are visible as bars above the grey line and deletions or complex mutations are visible below it. The black and white bar is the scale. The peach colored boxes show the domains and the turquoise colored boxes show the exons of the gene. In the red box the navigation for the page is visible. (Screenshot from www.nseuro.net)

Zooming into specific areas of the gene is possible by changing the amino acid range at the bottom of the screen (Figure 3.16).

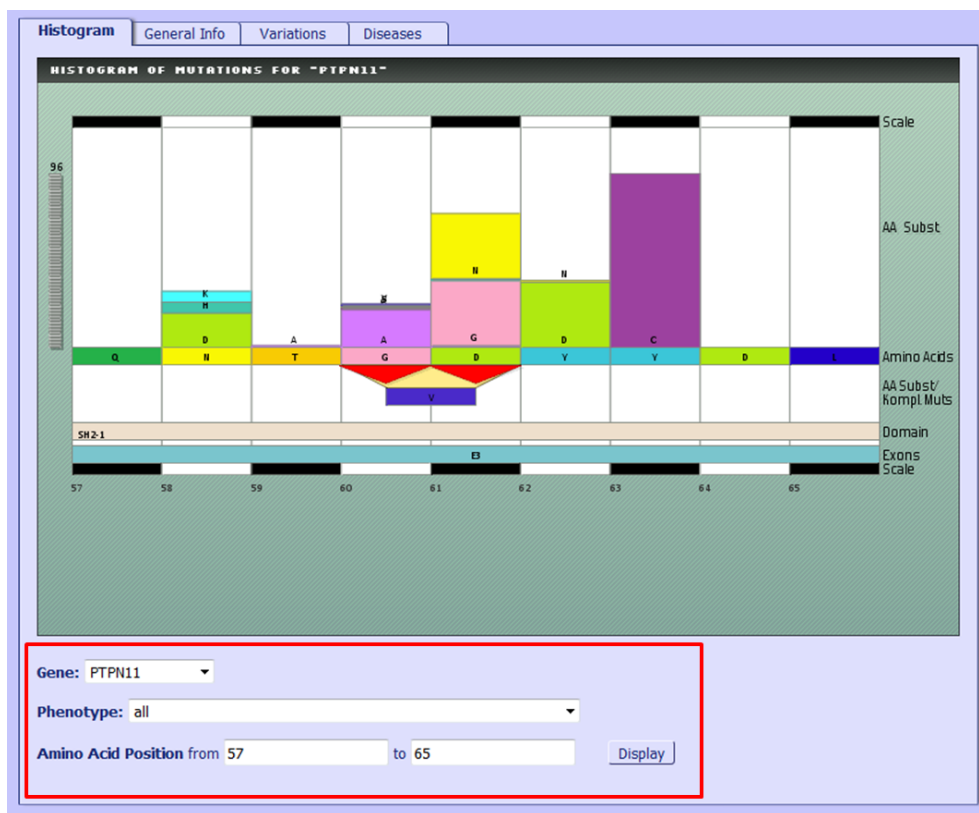


Figure 3.16: Mutation spectrum of *PTPN11* amino acid positions 57-65. This figure shows the amino acids 57-65 for the *PTPN11* gene. The missense mutations are visible as bars above the reference sequence and deletions or complex mutations are visible below it. The black and white bar is the scale. The peach colored boxes show the domains and the turquoise colored boxes the exons of the gene. In the red box the navigation for the page is visible. (Screenshot from www.nseuronet.com)

In the histogram a number of the items can be selected: the scale, the exon, the domain, the reference amino acid, and the mutation. By clicking on any of these items pop-up windows open with more detailed information about the mutations in the chosen range (Figure 3.17).

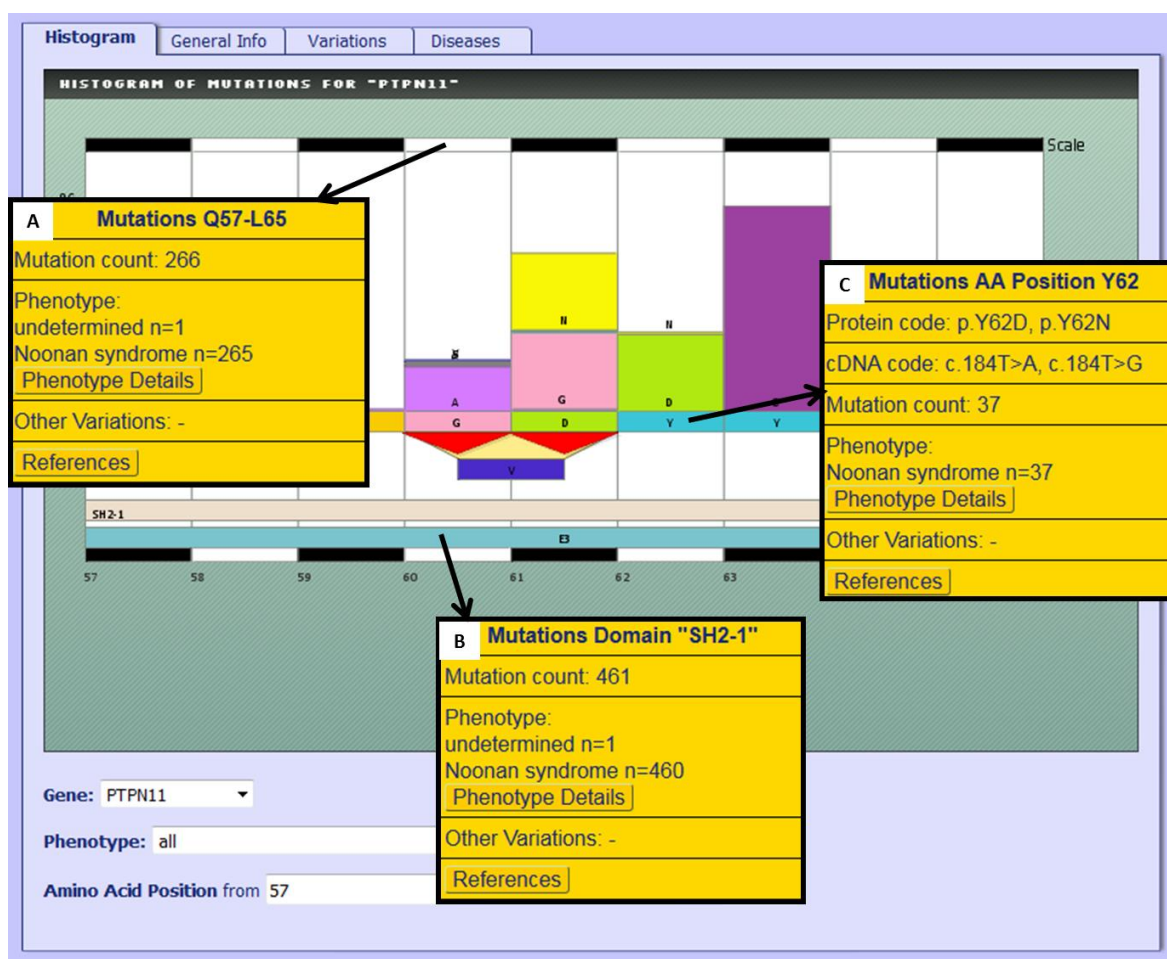


Figure 3.17: Pop-up windows. This figure shows three examples of possible pop-up windows available in the NSEuroNet database. Panel A: The details for the chosen region are shown including mutation count, phenotype, other variations and references. Panel B: The details for the SH2-1 domain are displayed and show the identical categories as in panel A. Panel C: The details for the amino acid position p.Y62 are shown. These include the categories previously described and also the protein codes of mutations at this position along with the entered cDNA codes. (Figure prepared with screenshots from www.nseuro.net.com)

In all pop up windows the number of cases entered (mutation count) is shown along with the phenotype makeup for that region. Literature cases were entered with the syndrome that they were published as having. A link to the references is also given. In the pop-up window for the reference amino acid or mutation the protein code and entered cDNA codes are also displayed. The button "phenotype details" opens a different pop up window displaying an overview of the clinical information entered from cases with full records (Figure 3.18).

Phenotype details for: Mutations from Position M1-R593			
		n	%
Population			
	total number of entries	1256	
	female/male	51:64	
	<4 / 4-18 / >18 years	26:59:10	
	sporadic/familial	67:41	
	died from complications of underlying disease	3/99	3.03%
Clinical diagnosis			
	Noonan syndrome	1060/1256	84.39%

Figure 3.18: Phenotype details for patients with a mutation in *PTPN11*. This figure shows the summary of the phenotypic information entered for all patients with mutations in the given range. (Screenshot from www.nseuronet.com)

Not all variants found were classified as pathogenic or likely pathogenic. All variants that do not fit into these categories are viewable under the “other variations” button (see Figure 3.19). The references for all entries in the specified area can be viewed by clicking on “references”.

Other Variations					
cDNA	Protein	Classification	Count	Reference	Comment
c.781C>T	p.L261F	unclassified	1	Pannone	on same allele as p.R265Q
-	p.I309V	polymorphism	1	-	-
c.925A>G	p.I309V	unclassified	1	Jongmans, 2011	originally published by Tartaglia, 2002 as mutation, but due to new evidence more likely polymorphism
c.925A>G	p.I309V	unclassified	1	Pergament, 2011	-
c.925A>G	p.I309V	unclassified	1	Tartaglia, 2002	-
c.925A>G	p.I309V	unclassified	1	Tartaglia, 2006	-
c.925A>G	p.I309V	unclassified	1	Wang, 2013	-

Figure 3.19: Other variations for *PTPN11*. This figure shows the other variations that have been entered for the *PTPN11* gene with their frequency and reference as well as a comment that has been entered by a reviewer. (Screenshot from www.nseuronet.com)

Comments are entered by the reviewers if additional information for this mutation would be beneficial for the user. Comments include information on associations with JMML or MPDs, if lethality has been observed frequently, and pathogenicity.

On the page that is reached by a “search by gene” there are 3 additional tabs that can be selected besides the histogram which is the first page displayed in this search option and has been described in the paragraph above. The “general Info” tab (Figure 3.20) contains information on the gene and respective protein.

GENERAL INFO ABOUT "PTPN11"

Gene Symbol (HGNC Symbol): PTPN11
 Gene Name: protein tyrosine phosphatase, non-receptor type 11
 Synonyms: BPTP3, PTP2C, SH-PTP2, SHP-2, SHP2
 Chromosomal Location: 12q24.1
 Protein Name: Tyrosine-protein phosphatase non-receptor type 11
 Alternative Name: Protein-tyrosine phosphatase 1D, Protein-tyrosine phosphatase 2C, SH-PTP2, SH-PTP3
 FASTA Sequences: cDNA: [NM_002834.3](#) protein: [NP_002825.3](#)
 Isoforms: none

External databases:

- OMIM: [176876](#)
- Ensembl:
 - Gene: [ENSG00000179295](#)
 - Transcript: [ENST00000351677](#)
- NCBI Entrez Gene: [5781](#)
- HGNC:
- COSMIC: [PTPN11](#)
- CCDS: [9163.1](#)
- Uniprot: [Q06124](#)

Statistic:

- Total number of disease-causing mutations for this gene: 96
- Total number of entries in database: 1257

Figure 3.20: General information about *PTPN11*. Depicted here is the page displayed under the “General Info” tab for the *PTPN11* gene. The sources of sequence, domain, and exon information are shown along with other external databases. (Screenshot from www.nseurionet.com)

The official gene name, protein name, synonyms as well as chromosomal position are shown. This page also provides the information which reference sequence was used for annotation, and the user can easily be directed to NCBI Gene to view FASTA sequences. Additionally the page contains other links to outside sources for further information including OMIM, NCBI, COSMIC and Uniprot. At the bottom of the page the statistics are given about how many entries are in the database for this gene and how many distinct mutations have been entered for this protein.

The “Variations” tab leads the user to a list of all variations contained in this database for the respective gene (Figure 3.21).

cDNA	Protein	Classification	Count	Phenotype	Reference	Comment
c.218C>T	p.T37I	mutation	1	Show	Show	Show
c.124A>G	p.T42A	mutation	21	Show	Show	Show
c.155C>T	p.T52I	mutation	1	Show	Show	Show
c.172A>G	p.N58D	mutation	19	Show	Show	Show
c.174C>G	p.N58K	mutation	5	Show	Show	Show
c.172A>C	p.N58H	mutation	6	Show	Show	Show
c.174C>A	p.N58K	mutation	1	Show	Show	Show
c.175A>G	p.T59A	mutation	1	Show	Show	Show
c.179G>C	p.G60A	mutation	21	Show	Show	Show
c.178G>T	p.G60C	mutation	1	Show	Show	Show
c.179_181del	p.G60del	mutation	1	Show	Show	Show
c.178G>A	p.G60S	mutation	1	Show	Show	Show
c.179C>T	p.G60V	mutation	1	Show	Show	Show
c.179_182delinsT	p.G60_D61delinsV	mutation	1	Show	Show	Show
c.182A>G	p.D61G	mutation	36	Show	Show	Show
c.182A>C	p.D61A	mutation	1	Show	Show	Show
c.181G>A	p.D61N	mutation	36	Show	Show	Show
c.181_183del	p.D61del	mutation	1	Show	Show	Show
c.181G>C	p.D61H	mutation	1	Show	Show	Show
c.184T>G	p.Y62D	mutation	36	Show	Show	Show
c.184T>A	p.Y62N	mutation	1	Show	Show	Show
c.188A>G	p.Y63C	mutation	96	Show	Show	Show
c.206A>T	p.E69V	mutation	2	Show	Show	Show
c.205G>C	p.E69Q	mutation	5	Show	Show	Show

Figure 3.21: Variations Tab. This figure shows the page displayed under the variations tab for *PTPN11*. All variants in this gene that have been entered into the database are shown with their classification, phenotype and references, if available. The red boxes highlight that this list is referring to the cDNA code, thus the same mutation on the protein level may have more than one entry. (Screenshot from www.nseuronet.com)

Under this tab all variations, including mutations, polymorphisms and variants of unknown significance are linked with their specific references, phenotype, and possible comment. Additionally the number of cases in the database with the specific variation is displayed. In this list all information is referring to the cDNA code and not to the amino acid position. This means that the same mutation on the protein level may have more than one line in this list (red boxes in Figure 3.21).

The “Diseases” tab leads to a pie chart of all syndromes associated with mutations in the selected gene (Figure 3.22).

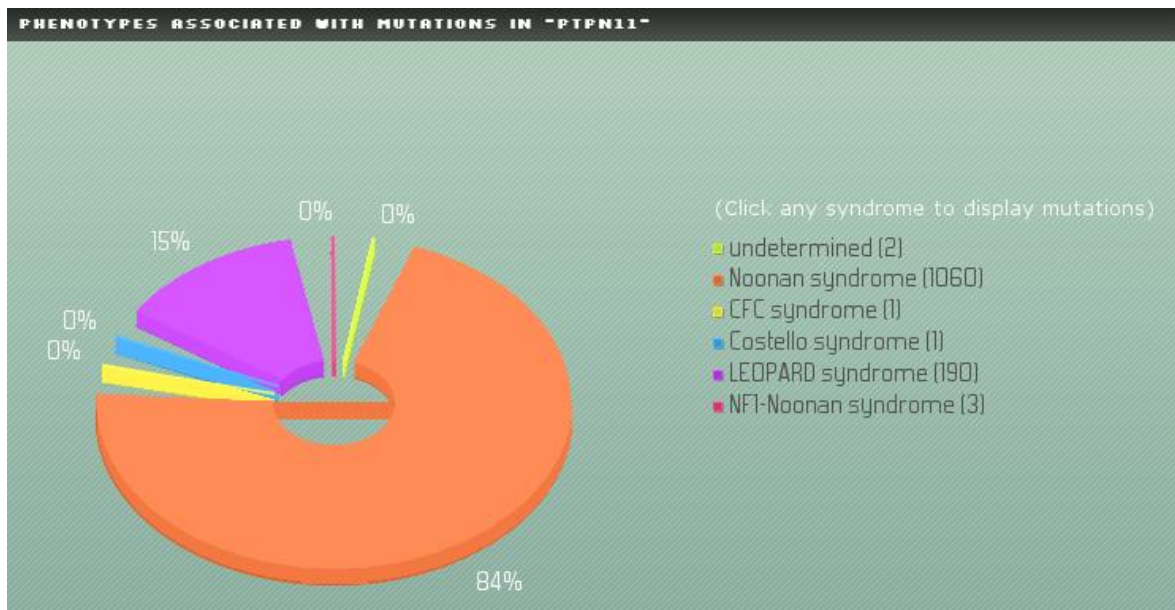


Figure 3.22: Phenotypes associated with mutations in *PTPN11*. This figure shows the page displayed under the “Diseases” tab. Here the syndromes associated with mutations in *PTPN11* are shown and their percentages. (Screenshot from www.nseuronet.com)

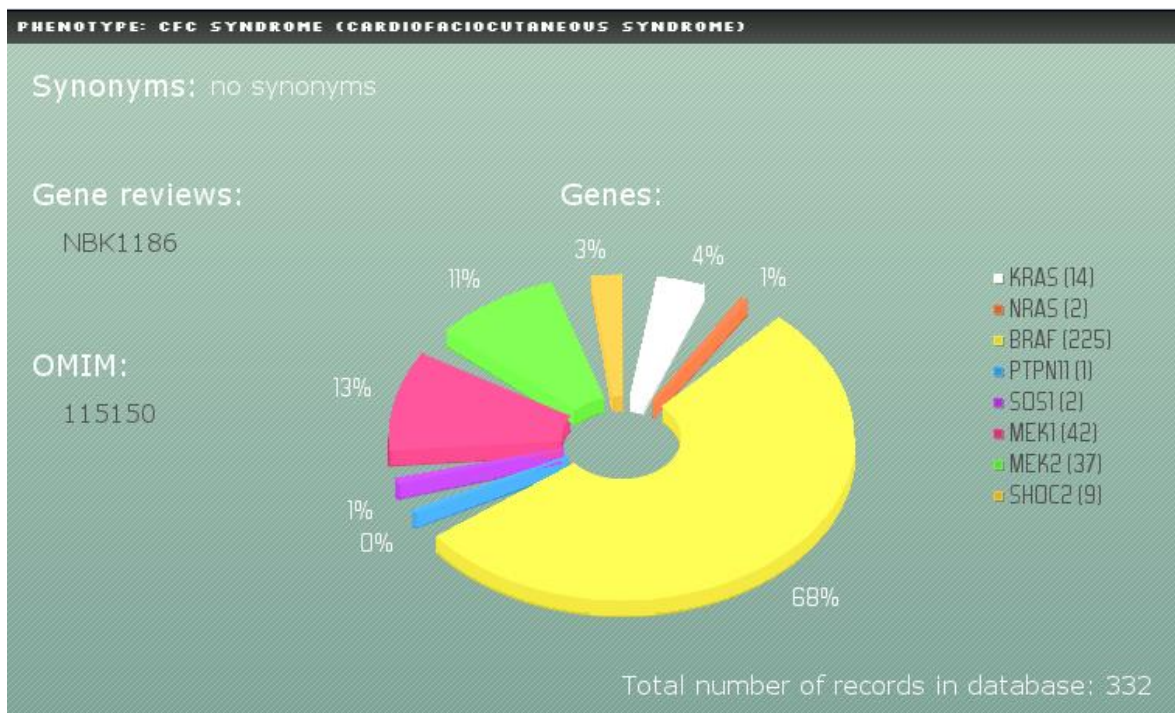


Figure 3.23: Search by disease for CFCS. In this figure the distribution of mutations in different genes is shown for patients diagnosed clinically as having CFCS. (Screenshot from www.nseuronet.com)

The pie chart in Figure 3.22 shows the number and percentage of patients with mutations in the chosen gene, here *PTPN11*, for each clinically diagnosed syndrome. Thereby the most

common syndrome associated with mutations in the respective gene can easily be identified. It is possible to click on the syndrome names. This will result in a popup window showing the mutation spectrum that is filtered for the protein and syndrome.

The “search by disease” option gives an overview of the genes most affected in patients with a certain syndrome (see Figure 3.23). This page also has links to Gene reviews and OMIM for more information on the syndromes. It also shows the total number of records with the specific syndrome in the database including published and unpublished cases. By clicking on a gene the “Histogram” page described above (Figure 3.15) opens, but with the mutations filtered for the specific syndrome, thus showing a syndrome-specific mutation pattern of the respective gene.

In order to use the database as a mutation database, the search for a mutation of interest can easily be done through the “search by gene” option. After choosing the appropriate gene the displayed range can be narrowed to get a higher resolution of the histogram (see Figure 3.15: red box). A range of 10-20 amino acids around the position of interest is most suitable. In this view (example shown in Figure 3.16) the mutation is visible if it has been entered and classified as a pathogenic variant. By clicking on the mutation, further information is available in the pop up window (example shown in Figure 3.17 Panel C). If the variant is not displayed, clicking on the reference amino acid will produce a pop up window that may show other variations annotated in the database (see Figure 3.24).

Mutations AA Position I309	Other Variations					
	cDNA	Protein	Classification	Count	Reference	Comment
Protein code: no data	-	p.I309V	polymorphism	1	-	-
cDNA code: no data	-	p.I309V	polymorphism	1	-	-
Mutation count: 0	c.925A>G	p.I309V	unclassified	1	Jongmans, 2011	originally published by Tartaglia, 2002 as mutation, but due to new evidence more likely polymorphism
Phenotype: -	c.925A>G	p.I309V	unclassified	1	Pergament, 2011	-
Other Variations	c.925A>G	p.I309V	unclassified	1	Tartaglia, 2002	-
References	c.925A>G	p.I309V	unclassified	1	Tartaglia, 2006	-
	c.925A>G	p.I309V	unclassified	1	Wang, 2013	-

Figure 3.24: Other variations. Depicted here is the detailed view for a specific amino acid position on the left side with other variations annotated in the database for this position. The right side of the figure (red box) shows the list of other variations that have been entered for this amino acid together with their reference and comments. (Screenshot from www.nseuronet.com)

Variations listed under “Other Variations” are classified as either polymorphism or unclassified, a reference is given and a comment for the evidence of classification.

In the following chapters specific statistical analyses facilitated by the NSEuroNet database are presented.

3.2.1. SHOC2

Specific efforts were made to collect full genotype phenotype datasets from patients with mutations in the *SHOC2* gene, because this was one of the genes newly published as a RASopathy gene during the time of this thesis and quite little was known about this subtype of NS called NSLAH or Mazzanti syndrome. Clinical findings in 72 previously unpublished individuals with the p.Ser2Gly mutation in *SHOC2* (34 females, 36 males, and 2 with unknown sex) are summarized in Table 6.1 in the supplements. Of those 23 are from our genotyping study. The median age in the cohort was 7.4 years. Other patient datasets were collected from multiple collaborators. Overall, the clinical phenotype is characteristic of NS. In all subjects, the craniofacial phenotype was evaluated by experienced RASopathy specialists (members of the NSEuroNet consortium) on the basis of personal examination or photographs. In all of the patients variable combinations of craniofacial dysmorphisms characteristic of NS were recognized, such as broad forehead, hypertelorism, downslanting palpebral fissures, ptosis, broad nasal bridge, low set ears and short neck; all faces were classified as typical or suggestive of NS (Figure 3.25 and data not shown).

Prenatal abnormalities were recorded in 20 out of 31 (65%) patients. The most common findings were polyhydramnios (n=10) and fetal nuchal edema (n=10). Five affected fetuses had either isolated pleural effusions or hydrops fetalis. A fetal heart defect/anomaly was suspected in only one case. In 61 of 64 individuals (95%) feeding difficulties in infancy were reported, and 25 patients required gavage feeding, seven of them for more than 12 months. The majority of patients had a congenital heart defect (55/67; 82%) with pulmonary valve stenosis (Pst, 22/67; 33%), hypertrophic cardiomyopathy (HCM, 20/67; 30%), and septal defects (16/67; 24%) occurring with almost similar frequencies in this cohort. One of the patients with HCM died in childhood due to cardiac problems. Short stature (height SD below -2.00; 3rd centile) was found in 42/52 individuals (81%), and another five patients had a height below -1.25 SD (10th centile). The average SD for height was -2.48 in this cohort. Fifteen patients had received growth hormone treatment. Eleven out of 15 (73%) had a proven GH deficiency or neurosecretory dysfunction. Motor developmental delay was observed in 30/34 subjects (88%) and was frequently associated with muscular hypotonia. In 17 of them, delay in the achievement of motor milestones was mild (unaided walking between 18 and 24 months) or not specified. Seven individuals showed moderate delay in motor

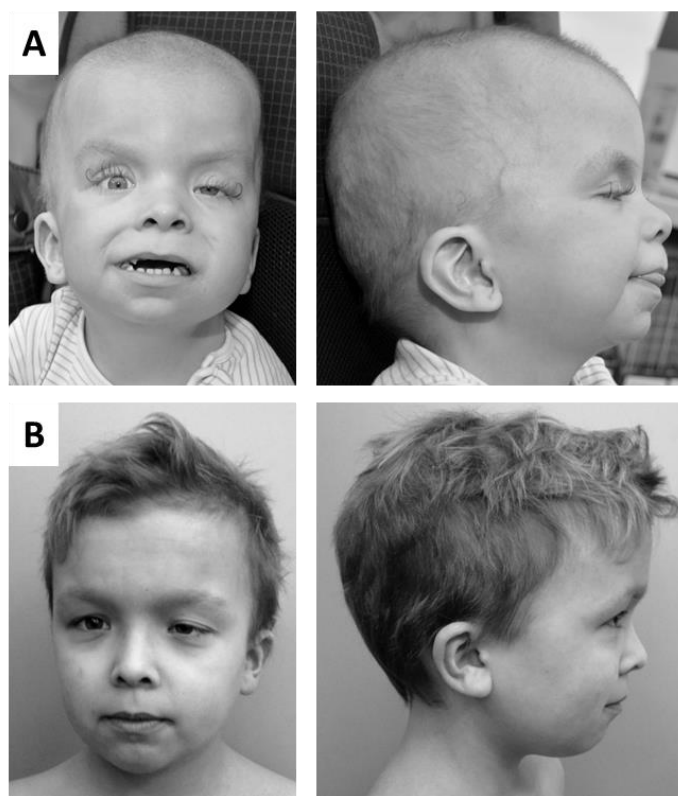


Figure 3.25: Facial features of two *SHOC2* mutation-positive patients. The photographs are shown exemplary for patients with *SHOC2* mutations. Photographs are not part of the database. Both patients have suggestive facial features for NS. Panel A: 2-year old boy with sparse hair, pronounced trichomegaly, left-sided ptosis, and low-set ears. Panel B: 13.5-year old boy with sparse hair, slight hypertelorism, slight left-sided ptosis, and low-set ears.

milestones (unaided walking between 24 and 36 months) and six a severe delay (unaided walking later than 36 months). Learning or intellectual disabilities were reported in 14/19 (74%) of our *SHOC2* mutation-positive subjects aged 5 years or older. 17/37 male patients (46%) had cryptorchidism. Loose anagen hair or easily pluckable hair was described in 35 out of 64 (55%) individuals. Keratosis pilaris was found in 12 out of 64 (19%) subjects. A short, broad and/or webbed neck was present in 55/63 (87%) individuals and pectus deformities in 17/63 (27%). In 18 out of 34 individuals (53%) bleeding diathesis were reported, but abnormal coagulation tests were recorded in only three, including one patient with von Willebrand, one with a platelet dysfunction, and one with a factor VIII deficiency. Ocular ptosis was present in 21 out of 47 individuals (45%) and refractive errors in 19 out of 45 (42%). Four patients had other eye abnormalities ranging from pale optic nerves with abnormal retinal function to exophthalmos, bilateral optic disc coloboma, and one patient was registered as being partially sighted. Four patients had hydrocephalus, one of them was additionally diagnosed with saggital suture synostosis. Hearing was abnormal in five patients. Of these, 3 had hearing deficits and 2 hyperacusis. Three patients each had hepato- or

hepatosplenomegaly. Three patients had hydronephrosis but no other renal anomalies were reported. Two individuals had documented systemic lupus erythematosus. Two patients had brain anomalies including ventricular dilatation and hypoplasia of the corpus callosum. One patient had hemangiomas and another had Kasabach-Merritt syndrome as well as a vascular tumor type hemangioendothelioma kaposiform of the spleen.

3.2.2. RIT1

RIT1-mutations were detected in 20 individuals in our genotyping cohort. Nineteen of these have been published along with 18 further individuals identified by our close collaborators in Hamburg (Kouz et al. 2016). One new patient has been identified after publication.

We identified eleven different *RIT1* missense mutations in a total of 43 patients from 38 unrelated families. In the complete cohort five of the missense changes have not been described previously: c.91G>C (p.(Gly31Arg)), c.229G>A (p.(Ala77Thr)), c.229G>T (p.(Ala77Ser)), c.245T>C (p.(Phe82Ser)), and c. 244T>A (p.(Phe82Ile)) however, a different *RIT1* mutation affecting codon 77 (c.229G>C, p.(Ala77Pro)) and two others changing codon 82 (c.244T>G, p.(Phe82Val) and c.246T>G, p.(Phe82Leu)) have already been reported (Aoki et al. 2013, Chen et al. 2014b). The p.(Gly31Arg) variant is absent from the databases dbSNP, 1,000 genomes and ExAC Browser and predicted to be damaging by the Mutation Taster, and others.

For seven mutations *de novo* occurrence was demonstrated by parental testing. Four mutations were familial, with five additional affected family members being confirmed carriers of the respective mutation (patients R1-2, R4-2, R4-3, R7-2, and R26-2), including a mother and her daughter carrying the novel mutation p.(Gly31Arg). These familial cases expand the number of *RIT1* mutation-positive individuals to 43. Segregation of the *RIT1* mutation could not be investigated in 32 individuals as DNA samples of one or both parents were not available.

Clinical findings in 43 individuals with a *RIT1* mutation (27 females and 16 males) are summarized in Table 6.2 in the supplements. Overall, the clinical phenotype is characteristic of NS. In all subjects, the craniofacial phenotype was evaluated by experienced RASopathy specialists on the basis of personal examination or photographs. In all of the patients we found variable combinations of craniofacial dysmorphisms characteristic of NS, such as broad forehead, hypertelorism, downslanting palpebral fissures, ptosis, broad nasal bridge, low set ears and short neck; all faces were classified as typical or suggestive of NS (Figure 3.26 and data not shown).

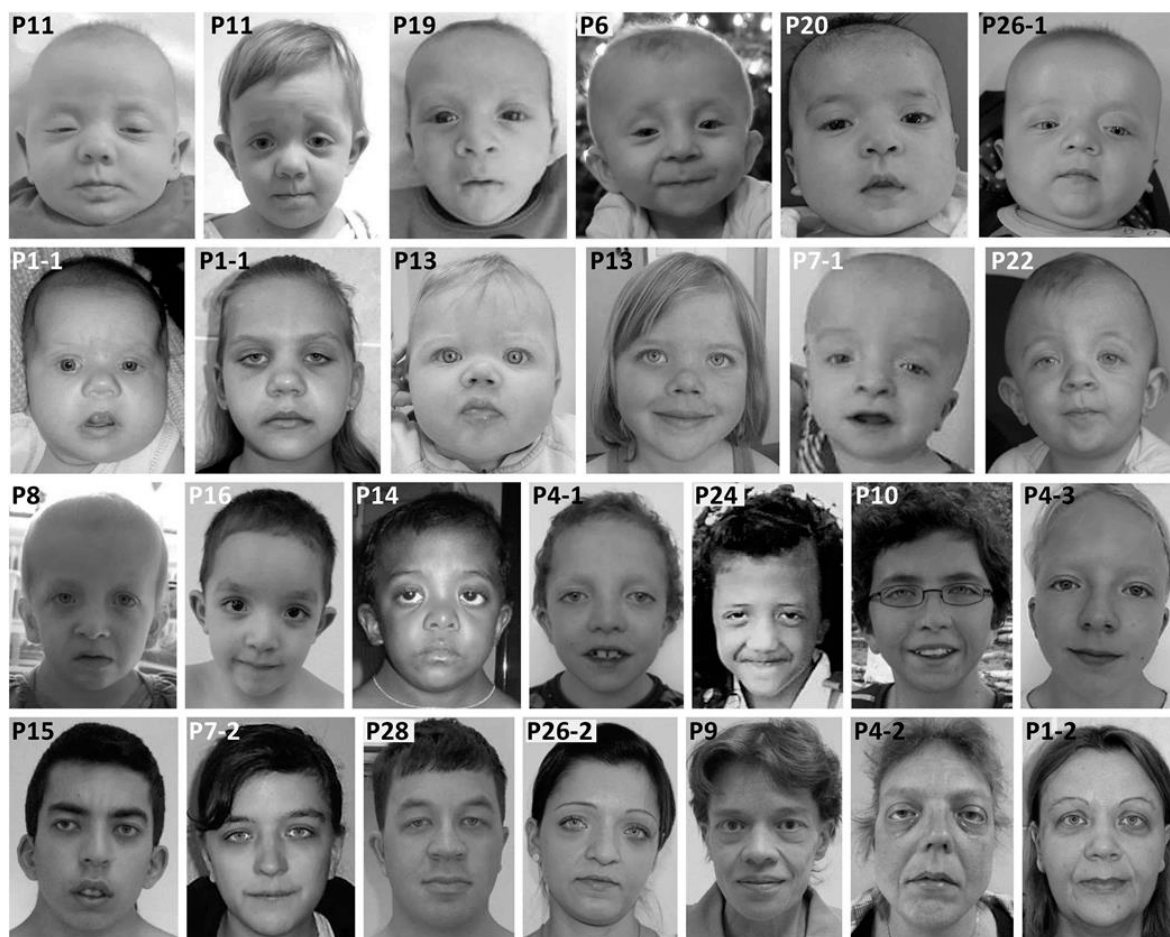


Figure 3.26: Craniofacial phenotype in patients with *RIT1* mutation. Facial photographs of 23 individuals from our cohort displaying the spectrum of *RIT1* mutation–associated facial dysmorphism from infancy to adulthood. Patients R11, R1-1, and R13 are shown at different ages (infancy vs. 2.6, 8.5, and 4.7 years, respectively) to document evolution of the craniofacial phenotype. All affected individuals exhibit recognizable dysmorphic features of NS, although the expression is quite variable. Previously published in (Kouz et al. 2016)

Prenatal abnormalities were recorded in 19/33 (58%) patients. The most common findings were fetal nuchal edema (n=11) and polyhydramnios (n=10). Nine affected fetuses had either isolated pleural effusions or hydrops fetalis. A fetal heart defect/anomaly was suspected in only five cases. Premature birth was quite common: 16/32 (50%) were born before the 37th week of gestation and six of them before the 34th week of gestation. In 15 of 30 individuals (50%) feeding difficulties in infancy were reported, and six patients required gavage feeding for several weeks. In the latter case, infants were born prematurely with one exception. Two children had gastro-esophageal reflux. Almost all patients had congenital heart defect (42/43; 98%), with Pst being the most common anomaly (34/43; 79%), but also a high rate of HCM was observed (21/43; 49%). 14/43 (33%) had septal defects, mainly atrial septum defect. Postnatal lymphatic anomalies were noted in 22/43 (51%). Notably, acquired lymphedema (occurring after the newborn period), such as lymphedema of lower limbs and genitalia,

acquired chylothorax, or a combination of both was found in 8 out of 39 individuals, and another one (patient R24) had intestinal lymphangiectasis with protein-losing enteropathy, resulting in a percentage of 23% for late-onset lymphatic complications which leads to significant morbidity. Short stature (height SD below -2.00; 3rd centile) was found only in 14/39 individuals (36%). Two patients had received growth hormone treatment. Motor developmental delay was observed in 11/32 subjects (34%) and was frequently associated with muscular hypotonia. Learning or intellectual disabilities were reported in 6/24 (25%) of our *RIT1* mutation-positive subjects aged 5 years or older. In four of six individuals mental disabilities were mild. Learning difficulties were associated with attention deficit disorder in three individuals. Seven out of twelve male patients (58%) had cryptorchidism. Skin and hair abnormalities were found in 13/33 individuals (39%), with curly hair and cutaneous hemangioma as the most common findings in five individuals each. Keratosis pilaris was found in only two patients. A short, broad and/or webbed neck was present in 18/39 (46%) individuals and pectus deformities in 20/39 (51%). In six out of 32 individuals (19%) easy bruising was reported, but abnormal coagulation tests were recorded in none. Ocular ptosis was observed in 25 out of 39 subjects (64%). Ocular ptosis was significant in three individuals where surgical correction was either planned or performed. Refractive errors were present in 13/33 (39%). Three individuals had cataracts. Four patients developed benign or malignant neoplasias including multiple giant cell tumors of the jaws in patient R2, B-cell acute lymphoblastic leukemia in patient R14, two independent tumors of the stomach (a gastrointestinal stromal tumor and a neuroendocrine tumor) in patient R9, and a lipoma in patient R28. Three patients had hydronephrosis requiring surgery and four other showed minor renal anomalies. Three individuals had documented hypothyroidism or autoimmune thyroiditis. Three subjects had deafness requiring hearing aids, but in one of them (patient R4-3) this is possibly a genetic trait segregating independently in the family.

3.2.3. NRAS

NRAS-mutations were detected in four individuals in our genotyping cohort. All of these have been published along with 7 further families and a total of 19 individuals identified by our international collaborators (Altmüller et al. 2017). One additional patient has been identified by another collaborator after publication.

We identified 20 affected individuals from twelve unrelated families with mutations in *NRAS*. In sporadic cases, *de novo* occurrence of the mutation was proven by testing of parental DNA, if available. In four instances of familial NS, the respective *NRAS* mutation was demonstrated

to co-segregate with the phenotype. In total nine different heterozygous *NR4S* mutations were identified. All changes affected highly conserved residues. Of note, the mutations segregating in the four families, c.71T>A (p.(Ile24Asn)), c.149C>T (p.(Thr50Ile)) and c.179G>A (p.(Gly60Glu)), had previously been documented in NS (Cirstea et al. 2010, Denayer et al. 2012, Runtuwene et al. 2011). Five changes, c.34G>C (p.(Gly12Arg)), c.35G>A (p.(Gly12Asp)), c.34G>A (p.(Gly12Ser)), c.35G>T (p.(Gly12Val)), c.112-1_113dupGGA (p.(Glu37dup)) and c.173C>T (p.(Thr58Ile)), had not been described as germline mutations in NS, and occurred in sporadic cases. *De novo* occurrence was demonstrated for the missense changes c.34G>C (p.(Gly12Arg)), c.35G>A (p.(Gly12Asp)), c.34G>A (p.(Gly12Ser)) and c.35G>T (p.(Gly12Val)). The germline nature of the variants c.34G>C (p.(Gly12Arg)), c.35G>A (p.(Gly12Ser)), c.34G>A (p.(Gly12Asp)), and c.173C>T (p.(Thr58Ile)) was further supported by their occurrence in a heterozygous pattern in non-hematopoietic tissues. Regarding the c.112-1_113dupGGA (p.(Glu37dup)) variant, the father was unavailable for testing, and in the case of c.173C>T (p.(Thr58Ile)) the father was found to have a mosaicism for the mutation in his peripheral blood leukocytes.

Our cohort of individuals with heterozygous *NR4S* mutations consisted of ten males and ten females with a median age of 7 years (range: 3 months - 50 years). The majority (17 patients) had a clinical diagnosis of NS. However, in two patients the proposed diagnosis based on clinical assessment was CFCS, and in one patient aged one-year CS was initially suspected. One case was a prenatal diagnosis where genetic testing for a RASopathy was performed because of a large hygroma colli. The clinical data are summarized in Table 6.3 in the supplements.

All assessed subjects had craniofacial features that were classified as typical or suggestive for a RASopathy (Figure 3.27 and data not shown).



Figure 3.27: Clinical photographs documenting the craniofacial phenotype of patients with heterozygous NRAS variants. N1: p.(Gly12Ser), 4 years old; N3-1, N3-2, N3-3: p.(Ile24Asn), familial observation with affected family members shown at age 10, 13, and 36 years, respectively; N5-1: p.(Gly60Glu), 17 years old; N7: p.(Glu37dup), 6 month old; N10-1: p.(Gly60Glu), 18 years old; N11: p.(Thr50Ile), 11 years old; N13: p.(Gly12Asp), 1 year old. Previously published in (Altmuller et al. 2017)

Short and broad or webbed neck was found in 94% (17 out of 18 patients), and ocular ptosis in 83% (15/18) of the cases. Twelve out of 19 patients (63%) had cardiac anomalies with hypertrophic cardiomyopathy (HCM) being present in 32% of the cases. Of note, septal defects and Pst were reported only in a minority of our cohort (16% and 11%, respectively). Similarly, short stature was present in only five out of 17 cases (29%). Motor delay and intellectual or learning disabilities were recorded in 40% (6/15) and 43% (6/14) of patients, respectively. Learning disabilities, if present, were of mild degree except for patient 7 who had severe global developmental delay (discussed below). In addition, the majority of patients had prenatal abnormalities (71%, 10/14) with polyhydramnios being reported in 50% of the cases. Nuchal edema and fetal chylothorax/hydrops as prenatal abnormalities were seen in 21%. Cryptorchidism occurred in 56% (5/9) of males. Bleeding diathesis was reported in 3 out of

17 individuals (18%), but only one patient had a confirmed coagulopathy (von Willebrand disease, patient N8). Neoplasias were observed in two individuals: one patient had a JMML-like myeloproliferative disorder (patient 13) and another patient had a brain tumor of unclear aetiology (patient N12). Selected patients are presented in more detail in the following.

Patient N1 (c.34G>A, p.(Gly12Ser)) presented with typical physical signs of NS: facial anomalies (Figure 3.27), left ventricular hypertrophy, atrial and ventricular septal defects (corrected by surgery), a persistent ductus arteriosus, and short stature. She exhibited marked muscular hypotonia in infancy. Her development was mildly delayed; she was able to walk freely with 2.3 years and spoke 2-3 word sentences at the age of 2.5 years. Her language skills at last evaluation at the age of 5.5 years were classified as normal for age. Intellectual development was also tested normal for age, but deficits were noted in spatial performance and attention. She had regular follow-up in the paediatric hemato-oncology during infancy, and had no signs of myeloproliferative disorder. The heterozygous *NRAS* mutation was found in leukocyte DNA, confirmed in DNA from buccal mucosal epithelial cells and finger nail keratinocytes, and was absent in the parents.

Patient N2 (c.35G>T, p.(Gly12Val)) was a fetus with a suspected RASopathy based on the finding of a very large cystic nuchal hygroma (14.3 mm) at twelve weeks of gestation. Progressive hydrops fetalis developed, eventually leading to intrauterine death at 22 weeks of gestation. No autopsy data were available but hydropic appearance of the fetus was reported. No heart defect could be detected. Fetal karyotyping was performed on a chorionic villus sample and resulted in a normal male karyotype. The heterozygous *NRAS* mutation was demonstrated in DNA from cultured chorionic villus fibroblasts. Parents were negative for the mutation.

Patient N5-2 (c.179G>A, p.(Gly60Glu)) is an affected child of a three generation family with obvious features of NS in her father and grandfather. She died on the first day of life from severe hydrops. Post-mortem MRI revealed bilateral pleural effusions, a small pericardial effusion and left ventricular hypertrophy.

Patient N7 (c.112-1_113dupGGA, p.(Glu37dup)) came to medical attention because of developmental issues and an atrial septal defect. She had a prenatal history of fetal nuchal edema, polyhydramnios, an intracerebral arachnoid cyst, and bilateral hydronephrosis detected by antenatal ultrasound. Subcutaneous edema was noted at birth. She required gavage feeding due to severe failure to thrive. In addition, she developed epilepsy and a sleep disorder. She had duplex collecting system and recurrent urinary tract infections due to ureteroceles

requiring surgical treatment. An MRI in the newborn period revealed thinning of the cortex with white matter changes, consistent with hypoxic ischemic encephalopathy. At the age of 2 years and 5 months her stature was below third centile (-2.69 SD) and she had a short webbed neck, shield chest, wide-spaced nipples, while facial anomalies were less typical (Figure 3.27). She was suspected to have CFCS because of her severe developmental delay, hypotonia and ectodermal abnormalities. She continued to demonstrate head lag at age 4 years old and unsupported sitting was not possible. Other features included microcephaly (43 cm at 2y5m (-3.27 SD)), ocular abnormalities including nystagmus and strabismus, hearing deficits and hemangioma. The *NR4S* mutation was detected in leukocyte DNA. Additionally, she was identified to harbor a 1.24 Mb gain from chromosome 22q11.23 detected by array CGH analysis (arr[GRCh38] 22q11.23(23408742_24595702)x3). This duplication was considered to have an impact on phenotypic complexity and modification of the RASopathy phenotype, specifically the severity of neurodevelopmental issues. Neither genetic abnormality was detected in the mother, but the father was unavailable for testing.

Patient N8 (c.173C>T, p.(Thr58Ile)) presented with suggestive facial features of NS, ocular ptosis, strabismus, and pectus excavatum, but without cardiac anomalies and short stature. She displayed muscular hypotonia and mild motor delay. The germline origin of the mutation was supported by its identification in DNA from urine, saliva, and peripheral blood. The patient's father was found to have a mosaicism for the mutation in his peripheral blood.

Patient N11 (c.149C>T, p.(Thr50Ile)) presented with typical facial features of a RASopathy, and mitral valve prolapse. At age 11, her height was in the low normal range (-1.47 SD). The suspected clinical diagnosis was CFCS because of typical facial features with substantial supraorbital hypoplasia and prominent ectodermal findings (curly hair, sparse eyebrows, keratosis pilaris, facial keratosis and multiple nevi), while her motor and intellectual development was only mildly delayed (IQ 65). Her perinatal history was characterized by multiple complications that may have contributed to her developmental problems. She had perinatal asphyxia (Apgar scores 2/5/7) and required mechanical ventilation for 17 days. Also she developed sepsis and portal vein thrombosis after umbilical vein catheter. She was discharged from the hospital at 45 days of life. Brain MRI at 4 months of age revealed non-obstructive hydrocephalus requiring ventriculoperitoneal shunting at 6 months. The *NR4S* mutation was demonstrated in leukocyte DNA.

Patient N12 (c.34G>C, p.(Gly12Arg)) had a RASopathy-typical facial phenotype, short webbed neck, macrocephaly and HCM. She was born at 36 weeks of gestation after a

pregnancy complicated by polyhydramnios. Birth weight was increased at 4,145 g. The postnatal period was complicated by prolonged hyperinsulinemic hypoglycemia, severe feeding difficulties including oral aversion and respiratory difficulties due to upper airway collapse. She was treated with a percutaneous gastrostomy and a tracheostomy with continuous positive airway pressure ventilation. The tracheostomy has been removed at 1 year and 8 months. A brain MRI at 8 months of age revealed an expansive lesion of 0.8x0.7x0.6 cm in the hypothalamus proposed to represent a hamartoma or lipoma, but neither surgery nor biopsy have been performed, so far, because of the absence of any endocrinological or specific neurological deficits attributable to this lesion.. Her EEG was normal, and she has been followed by a clinical neurologist. Her early motor development was delayed (unsupported sitting at age 10 months), but she started walking age appropriately at 1 year and 5 months. She had sparse, thin hair, full lips, deep palmar and plantar creases, several small nevi and one café-au-lait spot. Based on the clinical findings, CS was suggested, but no *HRAS* mutation was found. The heterozygous *NRAS* mutation was detected by WES. It was confirmed in DNA obtained from fingernail keratinocytes by Sanger sequencing, and was not found in DNA samples from both parents.

Patient N13 (c.35G>A, p.(Gly12Asp)) is a male born after an uneventful pregnancy except for mild fetal pyelocalyceal dilatation (7 mm) of the left kidney detected on ultrasound scans. Birth weight at term was 4,060 g, body length 51 cm, and head circumference 37.5 cm. He had no feeding problems and no lymphatic anomalies. A few café-au-lait spots were noted on neonatal examination, and he was therefore followed up because of a suspected diagnosis of NF1. At the age of three months, a blood cell count showed leucocytosis with 3% blast cells on a peripheral blood smear, mild anaemia and thrombocytopenia. On examination, he showed four café-au-lait spots over 0.5 cm diameter and three melanocytic nevi on lower limbs and buttocks, macrocephaly with suggestive facial features of NS (Figure 3.27), short neck but no thorax deformities, hepatosplenomegaly (4 and 3 cm, respectively), normal male genitalia with descended testes, and normal hands and feet. Bone marrow biopsy showed findings consistent with a myeloproliferative disorder. A brain MRI showed subdural fluid accumulations but no brain structural anomalies. Cardiological examination and echocardiography were normal. The heterozygous *NRAS* mutation was identified in leukocyte DNA and later confirmed in DNA extracted from skin fibroblasts, but was absent in both parents. Although he met clinical and analytical/cytological criteria for the diagnosis of JMML, in view of the stability of the blood cell counts and absence of complications it was decided not to start treatment and follow him up closely. Until the age of 11 months, this child has

remained stable hematologically, without proliferative phenomena or infectious complications. He was not short in stature, and his motor development was still within the normal range. A detailed developmental assessment was not possible yet due to his young age.

3.3. CBL

Variants in the CBL gene were detected in eight individuals in our genotyping cohort. Four patients of our genotyping cohort and one additional patient identified through our diagnostic department have been published as presented in Table 3.6 (Bulow et al. 2015, Martinelli et al. 2015). Five additional patients have been identified after publication.

Overall in our cohort we were able to identify seven individuals with variants in the *CBL* gene (see Table 3.6).

Patient	cDNA	Protein	Classification	Publication
C1	c.1100A>C	p.(Gln367Pro)	Pathogenic	(Bulow et al. 2015)
C2	c.1096-1G>T		Pathogenic	(Bulow et al. 2015, Martinelli et al. 2015)
C3	c.1100A>C	p.(Gln367Pro)	Pathogenic	(Bulow et al. 2015)
C4	c.1104_1112del	p.(Glu369_Tyr371del)	Pathogenic	(Martinelli et al. 2015)
C5	c.1096-4_1096-1delAAAAG		Pathogenic	
C6	c.1096-1G>C		Pathogenic	
C7	c.2513G>T	p.(Gly838Val)	Inherited by healthy father, VUS	
C8	c.2273C>T	p.(Ala788Val)	VUS	
C9	c.1423G>A	p.(Gly475Ser)	Likely benign, patient has a known <i>PTPN11</i> mutation (p.Glu139Asp)	

Table 3.6: CBL variants. This table shows *CBL* variants identified in our genotyping cohort and the two patients identified by the diagnostic department (C4 and C5).

Patients C7-9 have been excluded of further analysis because the *CBL* variant may not be responsible for the phenotype.

The clinical presentation in individuals with disease-causing CBL mutations was quite variable. Patient C1 was noted to have pleural effusions at 21 weeks of gestation, which did not improve and bilateral thoracocentesis was performed at 27 weeks. Delivery at 31+1 weeks was necessitated by placental insufficiency. Birth measurements were in the normal range. A respiratory distress syndrome, intraventricular hemorrhage, supraventricular pulmonary stenosis and chylothorax were diagnosed shortly after birth. Chylothorax resolved at 9 months of age. Her development was delayed with independent walking at 35 months and usage of three-

word sentences at 5 3/12 years old. Her facial appearance and symptoms were suggestive of a RASopathy (see Figure 3.28 panel A).



Figure 3.28: Clinical photographs. The pictures of patient C1 are shown in panel A. The wide set eyes, low nasal bridge, low set ears can be noted. Panel B shows the pictures of patient C3. The wide set eyes can be noted in the left photograph, the low set ears in the middle and the prominent belly in the right photograph. Previously published in (Bulow et al. 2015)

Patient C2 was noted to have a left-sided hydrothorax, mild skin edema, and ascites (hydrops fetalis) as well as hepatosplenomegaly and polyhydramnios. He was born at 36 weeks gestation and intubated soon after due to cyanosis. The hydrothorax was drained and did not recur. The patient was diagnosed with a mild valvular pulmonary stenosis. His development was delayed with walking at 3 years and usage of single words at 2 years of age. His facial appearance and symptoms were suggestive of a RASopathy.

Patient C3 was noted to have polyhydramnios, fetal hydrops and bilateral pleural effusions at 31 weeks of gestation necessitating premature delivery. Normal birth parameters were noted. The patient was then diagnosed to have an atrial septal defect, right inguinal hernia, bilateral undescended testes, and hepatosplenomegaly. JMML was diagnosed at 3 weeks of age. He was developmentally delayed. His facial appearance and symptoms were suggestive of a RASopathy (see Figure 3.28 panel B).

Patients C4 was a 3.4 year old boy with a significant developmental delay and facial features suggestive of NS. He had normal growth parameters and no malignancy was reported. He had a mild Pst and a congenital cataract in the left eye. No information was available from the prenatal period.

Patient C5 was a 1 month old boy with VSD, undescended testis, feeding difficulties, and an increased white blood count. His facial features were suggestive of NS, but he had strong temporal constrictions of unknown origin. No information was available for the prenatal period.

Patient C6 was a 3 year old boy with a Pst and VSD. He also had undescended testis and a severe developmental delay. His facial features were suggestive of NS and he had sparse hair. No information was available about the prenatal period.

3.4. HRAS

HRAS-mutations were identified in twelve individuals in this study. Five of these had the most common mutation p.Gly12Ser. Other previously described mutations (p.Gly12Ala, p.Gly13Cys, p.Lys117Arg, and p.Thr58Ile) were found in all but one patient, who is subsequently described in more detail.

The 18 year old patient from turkey was female and clinical examination revealed short stature, coarse facial features with ptosis and hypertelorism, HCM, mild feeding problems, and mild intellectual disability. She also had hyperkeratotic skin lesions on the ankles and multiple lentiginos on the face. No oncogenic manifestations were noted. These symptoms were evaluated to be a mild form of CS. Sanger sequencing of *HRAS* revealed a 21 bp duplication in exon 3 (c.187_207dup) predicting a 7 amino acids duplication p.(Glu63_Asp69dup) (see Figure 3.29). This duplication was not found in either of the parents. Clinical photographs and the electropherogram are shown in Figure 3.29.

Similar to NS, the by far most common mutation type in CS is missense. A few small deletions or duplications of one amino acid have also been reported, but a duplication of this size has never been described. The duplication found in this patient (p.(Glu63_Asp69dup) is partially including the HRAS switch II domain, which mediates binding of HRAS with various regulator and effector proteins (Boriack-Sjodin et al. 1998, Polakis and McCormick 1993, Scheffzek et al. 1997, Stieglitz et al. 2008, Vetter and Wittinghofer 2001). This domain is also known as a hotspot for gain-of-function mutations. Functionally, this variant has been analyzed by our collaborators in Hamburg showing that it induces hyperactivation of the RAF/MAPK, but not the PI3K-Akt signaling cascade. It has however also been shown to affect both pathways in respect to hyporeagibility. These results have been published by Lorenz et al. (Lorenz et al. 2013).

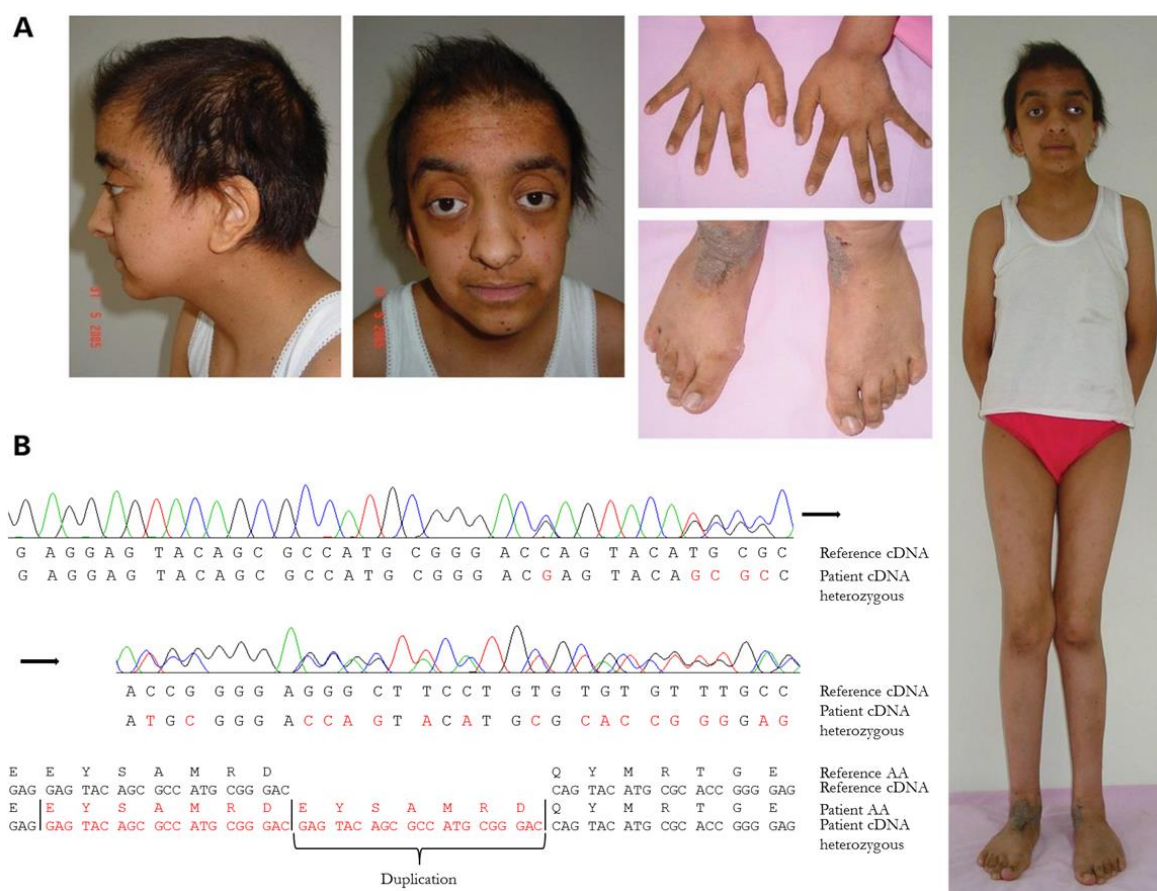


Figure 3.29: Photographs and electropherogram of patient with *HRAS* duplication. Panel A shows the facial features, hand, feet and whole body picture of the proband. These were previously published in (Lorenz et al. 2013). Panel B shows the electropherogram of the sequence detected in the patient sample. Under the sequence the reference cDNA sequence and the aberrant sequence identified in the patient is shown with the aberrant nucleotides highlighted in red. At the bottom is the sequence shown in a codon format with the corresponding amino acids. The duplicated region is shown in red.

3.5. Copy number changes containing RAS-MAPK genes

In an international collaboration we have collected two cases with CNVs containing known RAS-MAPK pathway genes. The clinical description of these cases and the critical discussion of the role of RAS-MAPK pathway genes in those CNVs was published by Lissewski, et al. (Lissewski et al. 2015).

Two patients with duplications including RAS pathway genes were identified through array CGH in the labs of collaborating partners. Patient X1 was 15 years old with height and weight under the 3rd centile. His OFC was on the 25th centile. He had a learning disability and was also diagnosed with ADHD. His mother and maternal grandmother also had mild learning difficulties. His mother's height was normal (10-25th centile) and his grandmothers height was

under the 3rd centile. Both had a normal OFC (50th centile). None of them had cardiac anomalies or other congenital malformations. Using a CytoScan HD Array a 1.2 Mb duplication at chromosome 19p13.3 (chr19:3947246-5098336, hg 19) was found in all three family members. This duplication includes the gene *MEK2* and others (see Figure 3.30).



Figure 3.30: Facial photographs of patients and schematic presentation of duplications. Panel a and b show facial photographs of patient X1 with a broad nasal bridge, “interrupted” eyebrows and otherwise normal hair and no other anomalies. Panel c shows the mother of patient X1 displaying no obvious craniofacial dysmorphism. Panel d shows the facial aspect of the index patient’s maternal grandmother with a broad nasal bridge and no other anomalies. Panel e is a schematic presentation of the 1.2 Mb duplication on chromosome 19 that was found in all three family members. The duplication includes *MAP2K2* (*MEK2*; grey shadow) as well as multiple other genes. Panel f and g show the facial photographs of patient X2 with mild dysmorphism including a long philtrum, slightly down-slanting palpebral fissures and fleshy, slightly low-set ears. Panel h is a schematic presentation of the 0.16 Mb duplication on chromosome 3 identified in patient X2, which includes *RAF1* (grey shadow) and a few other genes. It is slightly smaller than the one described by Luo et al. (Luo, Yang et al. 2012) (both schematic presentations were generated with the help of the UCSC Genome Browser at <http://genome.ucsc.edu>) (previously published in (Lissewski et al. 2015))

Patient X2 was born at 37 weeks of gestation with a birth weight of 3300 g (75th centile). He had no congenital anomalies, but his expressive language development was delayed. His height and weight at 3.5 years is on the 75th centile with a normal OFC (25-50th centile). The father of the patient had a normal intellect, normal height and no dysmorphic features. An Illumina

HumanCytoSNP-12 v2.1 Array identified a 0.16 Mb duplication on 3p25.2 (chr3:12558126-12778794, hg19) present in the patient and his father.

3.6. Novel genes for RASopathies

During the preparation of this thesis several new genes were discovered to be causative for RASopathies. The genes are *LZTR1*, *RASA2*, *RRAS*, and *SOS2*. The patients in this study cohort identified with variants in these genes are presented in Table 3.7.

ID	Gen(e)	Variant(s)	Inheritance	Methods			Classification
G01	<i>LZTR1</i>	p.Arg284Cys	unknown		Sanger	NGS	Pathogenic
G02	<i>LZTR1</i>	p.Arg688Gly	unknown		Sanger	NGS	Likely pathogenic
G03	<i>LZTR1</i>	p.Arg283Gln	unknown		Sanger	NGS	VUS
G04	<i>LZTR1</i>	p.Arg170Gln	unknown	HRM	Sanger	NGS	VUS
G05	<i>LZTR1</i>	p.His121Asp/ p.Arg755Gln	Paternal / Maternal		Sanger	NGS	VUS/VUS
G06	<i>LZTR1</i>	p.Arg170Trp	unknown		Sanger	NGS	VUS
G07	<i>LZTR1</i>	p.Ile205Thr(hom)/ p.Arg170Trp(hom)	Mother and father heterozygous for both		Sanger	NGS	VUS/VUS
G08	<i>LZTR1</i>	p.Arg284Cys	unknown		Sanger	NGS	Pathogenic
G09	<i>LZTR1</i>	p.Met91Val	unknown			NGS	VUS
G10	<i>LZTR1</i>	p.Arg697Glu/ c.2407-2A>G	Paternal / Maternal		Sanger	NGS	VUS/VUS
G11	<i>LZTR1</i>	p.Gln832Arg	Maternal		Sanger	NGS	VUS
G12	<i>LZTR1</i>	p.Arg283Gln	unknown		Sanger	NGS	VUS
G13	<i>RASA2</i>	p.Ser12Thr	unknown	HRM	Sanger	NGS	VUS
G14	<i>RASA2</i>	p.Arg511His	Paternal (healthy father)		Sanger	NGS	VUS
G15	<i>RRAS</i>	p.Gln87Leu	<i>De novo</i>		Sanger	NGS	Likely pathogenic
G16	<i>SOS2</i>	p.Asn310Ser	unknown	HRM	Sanger	NGS	VUS
G17	<i>SOS2</i>	p.Asn1229Tyr	unknown	HRM	Sanger	NGS	VUS
G18	<i>SOS2</i>	p.Pro1318Ser	unknown		Sanger	NGS	VUS
G19	<i>SOS2</i>	p.Thr376Ser	Segregation with disease	HRM	Sanger	NGS	Pathogenic
G20	<i>SOS2</i>	p.Pro404Thr	unknown		Sanger	NGS	VUS
G21	<i>SOS2</i>	p.Glu266Asp / p.Met267Lys (in trans)	unknown		Sanger	NGS	Pathogenic
G22	<i>SOS2</i>	p.Met267Lys	unknown		Sanger	NGS	Pathogenic
G23	<i>SOS2</i> / <i>LZTR1</i>	p.Lys739Asn/ p.Arg619His(hom)	unknown		Sanger	NGS	VUS/VUS

Table 3.7. Variants in novel genes. This table shows the variants found through NGS in the novel genes that may be associated with RASopathies. The inheritance of the variant is shown where known. The methods column shows which methods the patients DNA have been analyzed with. The classification for the variant is also shown.

All of the variants shown in Table 3.8 were identified through our NGS multigene panel and confirmed by Sanger sequencing. Variants in *LZTR1* were identified in 13 individuals. In three cases the variants were classified as pathogenic. Of the other 10 individuals, two had had two different variants (G05 and G10), one had a homozygous variant (G23) additional to a variant in *SOS2*, and one even had two homozygous variants (G07). The p.(Arg170Trp) variant, homozygous in patient G07, was heterozygous in patient G06. The variants p.(Arg283Gly) and p.(Arg284Cys) were both found in two unrelated individuals each. None of these patients, except for G2, had a pathogenic variant or VUS in any other of the genes included in this NGS multigene panel. The clinical data available from these patients is shown in Table 3.8.

Patient ID	Amino acid substitution	Prenatal findings	Heart defects/anomalies	Short stature	Developmental delay
G01	p.Arg284Cys	PH	ASD, VSD, aortic coarctation	ND	ND
G02	p.Arg688Gly	PH, NE	HCM	yes	yes
G03	p.Arg283Gln	NE	PDA	yes	yes
G04	p.Arg170Gln	ND	Pst, HCM, mitral regurgitation	yes	yes
G05	p.His121Asp/ p.Arg755Gln	NE	septum hypertrophy, VSD, ASD	ND	ND
G06	p.Arg170Trp	ND	no	yes	yes
G07	p.Ile205Thr(hom)/ p.Arg170Trp(hom)	ND	ASD, Pst, HCM	yes	yes
G08	p.Arg284Cys	ND	ND	ND	ND
G09	p.Met91Val	NE	Pst	no	no
G10	p.Arg697Gln/ c.2407- 2A>G	NE, HF	VSD, Pst, ASD, HCM	yes	yes
G11	p.Gln832Arg	ND	VSD	yes	yes
G12	p.Arg283Gln	PH	Pst, HCM	no	yes
G23	p.Lys739Asn (<i>SOS2</i>)/ p.Arg619His(hom)	NE, PH	Pst, HCM	no	yes

Table 3.8: Phenotypic features of the patients with *LZTR1* variants. Abbreviations: ASD: atrial septal defect; HCM: hypertrophic cardiomyopathy; HF: hydrops fetalis; ND: no data; NE: fetal nuchal edema; PH: polyhydramnios; PDA: Patent ductus arteriosus; Pst: pulmonary valve stenosis; VSD: ventricular septal defect.

Two variants were found in *RASA2* in one individual each. Patient G13 had the variant c.34T>A, p.(Ser12Thr) and the patient G14 c.1532G>A, p.(Arg511His) both in a heterozygous state. The variant in patient G14 was inherited by an apparently healthy father and no parental DNA was available for patient G13. Patient G13 was a 9-year-old male born to Turkish parents. His facial features were suggestive for a RASopathy. He had feeding difficulties in the neonatal period. He was short in stature (<3rd percentile) and he had a VSD that required surgical intervention. Walking was delayed (>24 months) and he had a mild

speech delay. He had an IQ between 70 and 79. No clinical information was available from patient G14.

The *RRAS* variant (c.260A>T, p.(Gln87Leu)) was identified in a 4.7-year-old girl of Malaysian Chinese descent who passed away due to RSV pneumonia while waiting for a heart transplant due to severe HCM. She also had a Pst and arrhythmia. She was born at 35 weeks gestation with a birth weight of 3620 g, length of 48 cm, and head circumference of 35 cm. During pregnancy polyhydramnios were reported. She had feeding difficulties and failure to thrive along with short stature (-5.40 SD, WHO growth charts), but no testing for GH deficiency was performed. Her motor development was slightly delayed with unsupported walking achieved between 18 and 24 months. She had renal impairment possibly due to cardiac failure and hepatosplenomegaly. Photographs of this patient are shown in Figure 3.31. The *RRAS* variant was proven to be *de novo*, but no additional material to prove the germline status of the mutation was available.



Figure 3.31: Photographs of patient G15 with a likely pathogenic variant in *RRAS* (c.260A>T, p.(Gln87Leu)). Panel A and B: Facial photos of 4.7 year-old-patient with a high forehead, hypertelorism, flat nasal bridge, and low-set ears. Panel C: Full-body photo showing dystrophic appearance.

Variants in *SOS2* were identified in eight individuals from our study cohort, one of whom was published along with six other individuals from five families by an international collaborative group (Cordeddu, et al. 2015). The variants, including the one previously mentioned in patient G23 with *LZTR1* and *SOS2*, found in three additional patients were classified as VUS as shown in Table 3.4. The other variants were classified as pathogenic and these patients are described in more detail in the following. One variant (p.(Met267Lys)) was found in two unrelated individuals. At the same codon two additional unrelated individuals were identified

with the variant c.800T>G (p.(Met267Arg)). One patient had the c.791C>A (p.(Thr264Lys)) variant, which was proven to be *de novo* with confirmed paternity. The variant c.1127C>G (p.(Thr376Ser)) was detected in two familial cases. All codons identified here with pathogenic variants are known mutational hotspots in the homologous SOS1 gene. The position p.Thr264 in SOS2 corresponds to the codon p.Thr266 in SOS1, the position p.Met267 to p.Met269, and p.Thr376 to p.Thr378.

The clinical information of all patients with pathogenic variants in *SOS2* is shown in Table 6.4 in the supplements. The *SOS2* mutation-positive cohort consisted of four males and five females with a median age of 13 (range 2 months – 42 years). Of the nine individuals four were familial cases from two families and the remaining five were sporadic cases. All assessed individuals had craniofacial features that were classified as typical or suggestive for a RASopathy. Short and broad or webbed neck was found in 71% (5 out of 7 patients), and ocular ptosis in 75% (6/8) of the cases. Five out of eight patients (63%) had cardiac anomalies with septal defects being present in 50% of the cases. Of note, HCM and Pst were reported in only 13% and 25%, respectively. Short stature was present in two out of eight cases (25%). Motor delay was noted in only one individual and intellectual or learning disabilities were recorded 2 out of 8 patients. One patient showed easy bruising, but no patient had a confirmed coagulopathy. One patient had a rhabdomyoma of the right ventricle, which spontaneously resolved.

4. DISCUSSION

4.1. Detection and prevalence of mutations

Overall 606 patients were in this cohort and disease-causing variants were identified in 330 of them (54%). In clinically well characterized, not previously analyzed cohorts with NS the detection rate for mutations in *PTPN11*, *SOS1*, *KRAS*, *NRAS*, *RAF1*, *BRAF*, and *MEK1* was reported to be approximately 70% (Tartaglia, Zampino and Gelb 2010). With the identification of new genes since this publication, the detection rate can be assumed to be even higher now, but this rate is strongly dependent on the clinical inclusion criteria and previous genetic testing before inclusion in the study. In the clinically heterogeneous cohort here, a lower mutation detection rate is not expected. One possible explanation is, that some of the patients had been tested negative for mutations in the more commonly mutated genes (*PTPN11*, and others) prior to inclusion in our study cohort, and thus the cohort is depleted from cases with detectable mutations in those genes. This explanation corresponds with a relatively low rate of *PTPN11* mutation positive individuals in our cohort (41% of all mutation-positive cases; Figure 4.1). Another reason is the strong clinical heterogeneity of our cohort where some patients had a clinical diagnosis of NS, CFCS, CS, or NF1-NS, and in some the phenotype remained undetermined between these entities or did only partially match with any RASopathy. The HRM cohort consisted of 325 individuals and for 148 (46%) of them a disease-causing variant was found. The cohort for Sanger sequencing consisted of 441 individuals of whom a disease-causing variant was found in 132 (30%). The NGS cohort consisted of 144 individuals and for 51 (35%) of them a disease-causing variant was found. These differences in the mutation detection rates likely reflect pre-selection and pre-testing status in the respective fractions of patients, and not the sensitivity of the methods. Of the overall 330 mutation-positive patients the mutations were most commonly found in the genes *PTPN11* (136/330; 41%), *SOS1* (45/330; 14%), *SHOC2* (27/330; 8%), *BRAF* (26/330; 8%) and *RAF1* (24/330; 7%) (Figure 4.1).

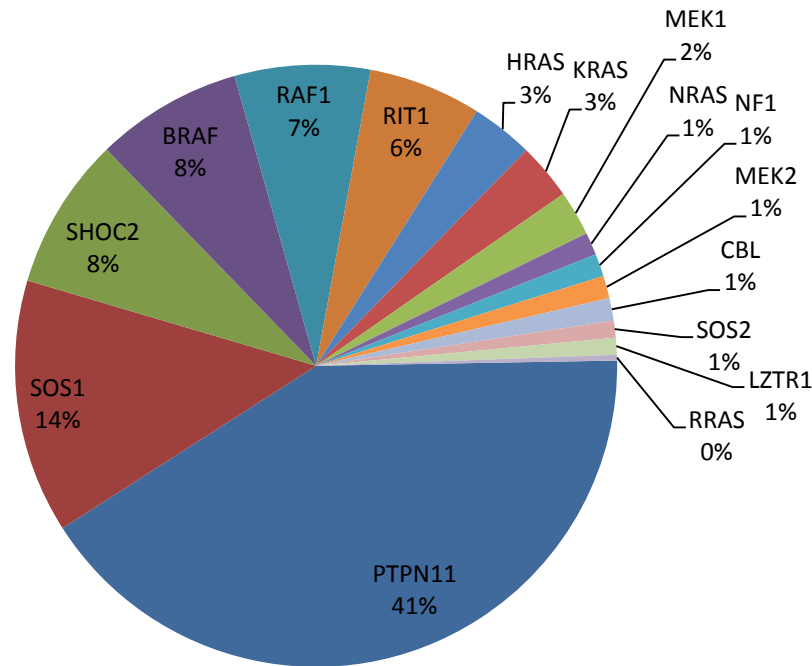


Figure 4.1: Overall distribution of gene mutations found using all three methods. This figure shows the percentages in which mutations in each of the genes have been found.

In the literature *PTPN11* mutations are reported to account for about half of the cases with NS, which is more than what we have found (41%) (Roberts et al. 2013). Mutations in *SOS1* have been described in 10% of individuals, which is slightly higher in our cohort (14%). In both cases the difference may be explained because our cohort included some patients who had previously been tested for *PTPN11*, but none of the other genes, thus resulting in less *PTPN11* positive results and more *SOS1* positive results, since this is the second most commonly mutated gene in NS. In our cohort we found *RAF1* mutations in 7%, which is in line with the literature (5-15%) (Roberts et al. 2013). *BRAF* mutations are mainly described in CFCS (75%) and also in a minority of NS patients (Rauen 2013, Roberts et al. 2013), but no exact numbers are known of the incidence in an overall RASopathy cohort. Mutations in *SHOC2* and *RIT1* were also relatively common in our cohort and present in 8% and 6%, respectively. The *SHOC2* mutation is specific for NSLAH, but no incidence has been reported. Mutations in *RIT1* have been found in about 5% - 10% of individuals with NS (Zenker 2016). This is in line with what we have found in this research cohort (6%). Disease-causing mutations in the other genes were less frequently identified in this cohort, but this was to be expected. *HRAS*, *KRAS*, and *NRAS* are only responsible for a small number of cases with RASopathies (Rauen 2013). In essence, although the mutation distribution found in this

study is roughly in line with previously published figures, it has to be pointed out that it does not reflect the precise distribution in the population, because the cohort was underlying several modes of recruitment bias as outlined above. The relatively low rate of mutation-positive individuals (54%) reflects the fact that we deliberately chose less stringent clinical criteria for inclusion in order to have the chance to detect mutations also in less typical phenotypes.

During the evolution of this project, different methods of mutation screening were applied. Screening with NGS multigene panels covering the entire coding sequence of all known RASopathy genes is the most comprehensive method and has meanwhile become standard in diagnostics.

In the fraction of patients studied by such an NGS multigene panel mutations were identified in seven patients in genes that had previously been analyzed. In two cases the mutation was found in a gene that had been analyzed, but the specific exon had not, because no mutations were previously found in these exons. Since the clustered gain-of-function mutations found in RASopathies are recurring, this procedure has been useful to limit costs with covering what is known, but it entails the risk that rare mutations in other exons of this gene are overlooked. Since the advent of NGS technology variants in previously unstudied exons are appearing not only in RASopathies and thus including all coding exons in the analysis is becoming increasingly important. HRM allows a rapid pre-screening of sequences, but is also limited in the number of amplicons that can be tested in one run (Lo et al. 2009).

In five cases the mutation identified was in a previously analyzed exon and thus overlooked by the method or analysis. Three of these are cases where the initial analysis had been done in a different laboratory, so no details on method or analysis program are known and thus the cause of failure to detect these mutations could not be elucidated. In one case the oversight to identify the mutation was shown to be an annotation problem, where the wrong isoform was chosen in the original analysis. This shows the crucial importance that the correct reference sequence is used in the analysis. In the last case an abnormality was detected using HRM analysis, but the following Sanger validation was false-negative for what the cause could not be determined.

Thus, in our hands, all three methods employed had a very high sensitivity for detecting mutations in the parts of the genes covered by the respective analysis. Only the last case was really confirmed as false-negative by Sanger sequencing, while HRM screening was positive. Mutation screening by HRM was established and evaluated in the first part of this study. It proved to be useful for a screening for mutations in RASopathy genes. The fact that mutations leading to RASopathies are always heterozygous, restricted to the coding sequence of genes, and that these genes are relatively poor in polymorphisms in their coding sequences, makes these genes good candidates for a highly sensitive screening by HRM, in principle. However, the increasing number of known RASopathy genes and thereby increased size of coding sequence to be analyzed strongly limits the usefulness of HRM for this purpose. On the other hand, the availability of NGS-based sequencing in the routine in research and diagnostics has made HRM disappear from the scientific literature as well as in genetic laboratories, as it is the case in our laboratory. Although it is still true that RASopathy-associated mutations show strong clustering to certain regions in the respective genes, a targeted sequencing of mutation hotspots only seems to be no longer state of the art.

This evolution of methods and the resultant broadening of molecular analyses made it necessary to develop stringent and standardized classification criteria for previously undescribed variants. In 2015, Richards and colleagues (Richards et al. 2015) published classification criteria that have been accepted widely and are now used standardly. These guidelines were also employed in this study.

4.2. The NSEuroNet database and its uses

Different mutation databases including the RASopathy genes currently exist. There are databases collecting mutations or variants, somatic mutations, limited phenotype information, and published mutations. The Leiden Open Variation Database (LOVD), the Catalogue of Somatic Mutations in Cancer (COSMIC), the Human Gene Mutation Database (HGMD), and the Clinical Variation database (ClinVar) are established resources including data on mutations and variations in RASopathy genes and others. However, the actual content, information about related phenotypes, and/or curation status varies strongly. LOVD collects DNA variations and is sorted by genes (Fokkema et al. 2011). Some submitters provide additional information like references, method of detection, and consequences for splice variants if known. It is free to use and no registration is needed. The database is gene specific and curated, but the currentness of data, completeness and quality of curation is depending on the activity of voluntary submitters and curators, which is very variable. Phenotype information is

scarce. COSMIC is a database for somatic variations in cancer (Bamford, Dawson et al. 2004). Two main types of data exist in this database: Curated data from publications and variants from genome wide screens. All variants are shown in a graphic overview and details are available, e.g. what tissue the variant was found in. HGMD (public version) is also a locus specific mutation database and includes published mutations (Bamford et al. 2004). Access to the database is only possible through registration and additional information is only available to professional account holders or subscribers. More recently ClinVar was established (Landrum et al. 2014). In this database all variants found through exome/genome sequencing or targeted sequencing are entered and classified by the submitter. In most cases the reasons for the classification is given and can thus be recapitulated. No detailed phenotypic data are available from the patients, but the clinical diagnosis is given. While all these databases include valuable information, none of them combine the detailed and standardized phenotypic information with a mutation database. This is what the NSEuroNet database was set out to achieve in order to allow more detailed genotype-phenotype comparisons. This database is a joint project of the NSEuroNet consortium and was developed in Magdeburg as one major part of this thesis.

Since its launch in 2011, the NSEuroNet database has continuously been fed with published mutations. This made the database immediately available as a curated mutation database. The graphical user interface is similar to that of COSMIC and the mutation spectrum is visible for each gene. Also references are readily available for each known mutation. In addition to the literature cases with limited clinical information, full records with a large set of standardized clinical data, and the related genotype can be entered. Currently the database still mainly holds published data, but the number of datasets with complete clinical information is continuously rising. Full clinical records of patients are available, but not in large numbers yet for all genes. The database currently comprises 2568 literature cases and 420 entries with complete clinical information. The phenotype information that is collected through the standardized online questionnaire is unique to any of the other databases relevant for RASopathies. The more clinical data becomes available, the more precise genotype-phenotype correlations can be established, which increases the understanding of clinical variability among RASopathies and may also help families with newly diagnosed children and in other clinical and genetic counseling decisions.

In the future the NSEuroNet database will have a new analysis tool for clinical data so that the clinical information available in the database can be analyzed more detailed by every user. It is

also planned that a data exchange will take place between ClinVar and the NSEuroNet database so both databases can benefit.

The NSEuroNet database has already proven useful in several large cohort genotype-phenotype studies, which were performed for *RIT1*, *SHOC2*, and *NRAS* mutation positive patients. The details of these studies will be discussed further in the following chapters. Clinical data from these cohorts was compared to clinical data from the *PTPN11*, *SOS1*, and *RAF1* cohorts that have also been entered into the NSEuroNet database.

4.2.1. SHOC2 mutations and Mazzanti syndrome

Our database comprises the largest collection of clinical data of patients with NS caused by a *SHOC2* mutation. Data are available from 72 unrelated and previously unpublished *SHOC2* mutation-positive patients from our cohort and collaborators. All of these patients had the same c.4A>G (p.(Ser2Gly)) variant. To better define the phenotype associated with a *SHOC2* mutation, we summarized the clinical features observed in our 72 patients and compared the frequency of clinical features with those in a total 79 individuals described as case reports and small series in the literature (Table 4.1) (Bader-Meunier et al. 2013, Baldassarre et al. 2014, Capalbo et al. 2012, Choi et al. 2015, Cizmarova et al. 2016, Cordeddu et al. 2009, Croonen et al. 2013, da Silva et al. 2016, Digilio et al. 2011, Ekvall et al. 2011, Ferrero et al. 2012, Garavelli et al. 2015, Gargano et al. 2014, Gripp et al. 2013, Hoban et al. 2012, Justino et al. 2015, Komatsuzaki et al. 2010, Lee et al. 2011, Lo et al. 2015, Mazzanti et al. 2013, Quaiò et al. 2013, Simsek-Kiper et al. 2013, Takasawa et al. 2015, Takenouchi et al. 2014, Timeus et al. 2013, Zmolikova et al. 2014).

We also compared the frequency of phenotypic features in our *SHOC2* mutation-positive cohort with patients harboring a *PTPN11*, *SOS1* or *RAF1* mutation, whose phenotype data had been collected using the same standardized form of the NSEuroNet database (Table 4.2).

	Total Publications	This study	Total	Total %
n	79	72		
Males/Females	48/29	37/34	85/63	
Median age (in years)	9	7.4	7.8	
Prenatal abnormalities	12/23	20/31	32/54	59%
Polyhydramnios	9/35	10/31	19/66	29%
Nuchal edema	4/16	10/31	14/47	30%
Fetal chylothorax/hydrops	2/13	3/31	5/44	11%
Feeding difficulties	26/34	61/64	87/98	89%
Cardiac anomaly	59/71	55/67	114/138	83%
Pst	20/71	22/67	42/138	30%
ASD/VSD	26/68	16/67	42/135	31%
HCM	19/70	20/67	39/137	28%
Short stature	64/68	42/52	106/120	88%
GH deficiency or neurosecretary dysfunction	29/38	11/15	40/53	75%
Motor delay	25/30	30/34	55/64	86%
Intellectual/learning disabilities	44/55	14/19	58/74	78%
Cryptorchidism in males	15/35	8/28	23/63	37%
Loose anagen or easily pluckable hair	17/17	35/64	53/81	65%
Keratosis pilaris	15/43	12/64	27/107	25%
Scoliosis	2/6	6/63	8/69	12%
Pectus deformity	36/58	17/63	53/121	44%
Short/broad/webbed neck	45/60	55/63	100/123	81%
Ocular ptosis	16/29	21/47	37/76	49%
Bleeding diathesis	14/40	18/34	32/74	43%
Neoplasia (benign and malignant)	3/19	1/72	4/91	4%

Table 4.1: Combined data from *SHOC2* publications. This table shows the combined data from all *SHOC2* publications and the data compiled in this study.

The essential findings in the analysis of the *SHOC2* mutation-positive patients were the high incidence of prenatal abnormalities, feeding difficulties in the neonatal period, short stature with GH deficiency, and intellectual deficits. These findings are confirmed in the total of all previously published patients (Table 4.1). Compared to *PTPN11* a significantly higher frequency of prenatal abnormalities was observed in the *SHOC2* cohort (28% vs 65%). Overall feeding issues appeared to occur more frequently in individuals with a *SHOC2* mutation compared with NS-affected individuals linked to other genes, however, this difference did not reach statistical significance in our dataset. Pulmonary stenosis was significantly less common compared to 79% in patients with a *SOS1* mutation and also observed less frequently than in patients with *PTPN11* mutation (56%) without reaching statistical significance. Compared to individuals with a *RAF1* mutation (15%) this was more common in the *SHOC2* cohort. HCM was present in about a third of our cohort and compared to *PTPN11* (12%) and *SOS1* (12%) more frequent, but only statistically significant in comparison with the *PTPN11* cohort. HCM in the *SHOC2* mutation-positive cohort was statistically less frequent in comparison with the *RAF1* cohort (83%). The frequency is increased compared to the genes *PTPN11* (74%), *SOS1* (59%) and *RAF1* (60%), but not

	<i>SHOC2</i>	<i>PTPN11</i>	p-value	<i>SHOC2</i>	<i>SOS1</i>	p-value	<i>SHOC2</i>	<i>RAF1</i>	p-value
Males/Females	37/34	51/43		37/34	27/27		37/34	22/19	
Median age (in years)	7.4	7.1		7.4	7.7		7.4	5.1	
Prenatal abnormalities	20/31	24/86	0.02*	20/31	23/36	1	20/31	23/32	0.84
Polyhydramnios	10/31	15/86	0.22	10/31	15/36	0.64	10/31	14/32	0.63
Nuchal edema	10/31	12/86	0.08	10/31	3/36	0.07	10/31	14/32	0.63
Fetal chylothorax/hydrops	3/31	5/86	0.68	3/31	2/36	0.66	3/31	2/32	1
Feeding difficulties	61/64	52/86	0.08	61/64	20/34	0.19	61/64	22/32	0.33
Cardiac anomaly	55/67	70/89	0.90	55/67	45/52	0.89	55/67	38/40	0.66
Pst	22/67	50/89	0.08	22/67	41/52	0.008*	22/67	6/40	0.12
ASD/VSD	16/67	31/89	0.31	16/67	14/52	0.84	16/67	14/40	0.40
HCM	20/67	11/89	0.03*	20/67	6/52	0.08	20/67	33/40	0.004*
Short stature	42/52	64/87	0.79	42/52	27/46	0.34	42/52	18/30	0.47
Motor delay	30/34	35/75	0.05*	30/34	14/33	0.08	30/34	12/26	0.15
Intellectual/learning disabilities	14/19	18/45	0.18	14/19	8/38	0.02*	14/19	9/21	0.43
Cryptorchidism in males	8/28	36/47	0.04*	8/28	16/24	0.14	8/28	13/17	0.11
Keratosis pilaris	12/64	2/88	0.001*	12/64	19/47	0.07	12/64	3/29	0.55
Scoliosis	6/63	7/88	0.78	6/63	6/48	0.76	6/63	2/31	1
Pectus deformity	17/63	50/91	0.03*	17/63	39/47	0.001*	17/63	26/37	0.01*
Short/broad/webbed neck	55/63	52/91	0.10	55/63	38/51	0.67	55/63	26/37	0.53
Ocular ptosis	21/47	52/86	0.36	21/47	38/49	0.13	21/47	23/36	0.36
Bleeding diathesis	18/34	26/78	0.26	18/34	10/47	0.05*	18/34	4/24	0.07
Neoplasia (benign and malignant)	1/72	11/88	0.01*	1/72	7/49	0.02*	1/72	0/29	1

Table 4.2: Frequency of phenotypic features in the *SHOC2* cohort compared to the *PTPN11*, *SOS1*, and *RAF1* cohorts. This table shows the frequency of specific phenotypic features and the p-values obtained by Fisher's exact test. *statistical significance ($p \leq 0.05$)

statistically significant. Growth hormone deficiency has been reported in *SHOC2* mutation positive cohorts and was found in 40 out of 53 individuals (75%). This number also includes patients with neurosecretory dysfunction. However this was not tested in all individuals and thus a real frequency is unknown. Learning difficulties and intellectual disability were less frequent in the *PTPN11* (40%), *RAF1* (43%), and *SOS1* mutation-positive cohorts (31%), reaching statistical significance in the latter. Keratosis pilaris was significantly more common in the *SHOC2* mutation-positive cohort compared to the *PTPN11* cohort (2%), and lower compared to the *SOS1* cohort (40%, no significance). Loose anagen or easily pluckable hair was present in more than half of the individuals with *SHOC2* mutations (53/81; 65%). This is a unique feature of patients with *SHOC2* mutations and has been described well in the literature (Cordeddu et al. 2009, Mazzanti et al. 2003). A neoplasia has only been reported in one of our patients (1/72; 1%), which makes the incidence significantly lower when compared to the *PTPN11* (11/88; 13%) and *SOS1* (7/49; 14%) cohorts.

NSLAH was thought to be genetically homogenous with only one mutation (c.4A>G; p.(Ser2Gly)) present in all affected individuals, but in 2014 a patient and her father with a different variant (c.519G>A; p.(Met173Ile)) were identified (Hannig et al. 2014). However, these patients do not exhibit classic symptoms of NS, NSLAH or CFC. They are of normal height, have no heart defects and the daughter had no delay in development. The father had an intellectual disability. Both had sparse hair (Hannig et al. 2014). Since the symptoms do not qualify for a clinical diagnosis of a RASopathy it is unlikely that the variant found causes a RASopathy.

Overall the clinical data obtained from the previous literature is generally in line with our findings. The specific *SHOC2* phenotype is marked by loose anagen or easily pluckable hair, thus called NSLAH. Short stature with GH deficiency is also a common feature in these patients (Tartaglia and Gelb 2010, Zenker 2011). Ectodermal anomalies are also commonly associated, especially darkly pigmented skin and keratosis pilaris (Tartaglia and Gelb 2010). Heart anomalies are present in the majority of individuals with *SHOC2* mutation, but the spectrum is different from patients with mutations in the other NS genes (Zenker 2011). Also NSLAH may not have the previously thought homogeneity, since another variant was identified (Hannig et al. 2014). However further studies are necessary to determine if the patients with other variants than the typical p.Ser2Gly alteration in *SHOC2* also have NSLAH.

4.2.2. Genotype phenotype correlations with germline *RIT1* mutations

RIT1-mutations were detected in 20 individuals in our genotyping cohort. Nineteen of these have been published along with 18 further individuals identified by our close collaborators in Hamburg (Kouz et al. 2016). One new patient has been identified after publication. Overall we identified *RIT1* mutations in 38 unrelated individuals with a clinical diagnosis of NS; none of them had been suspected to have CFCS or CS. Two previous studies by Aoki et al. (2013) and Bertola et al. (2014) reported a *RIT1* mutation detection rate of approximately 9% in cohorts of patients that had been tested negative for mutations in the previously known genes (Aoki et al. 2013, Bertola et al. 2014). In contrast, Gos et al. (2014) found only 3.8% of their mutation-negative cases with NS to carry a heterozygous *RIT1* mutation (Gos et al. 2014). The differences in the detection rates, however, are likely to be explained by more or less strict clinical inclusion criteria, and these figures do not reflect the prevalence of *RIT1* alterations in an unselected cohort of NS-affected subjects. To provide a better estimate of the contribution of *RIT1* mutations to NS, we calculated the relative frequency of mutations in the NS-linked genes among 507 individuals tested positive for NS at the University of Magdeburg since

2009: *PTPN11*: 54%; *SOS1*: 18%; *RAF1*: 11%, *RIT1*: 5%; *KRAS*: 3%; *CBL*: 2%; *NRAS*: 1%. This cohort is not free from any bias, and compared to an unselected patient population these figures may be an overestimation for mutations in *SOS1* and *RAF1*, but an underestimation for *RIT1* alterations. Nevertheless, these numbers indicate that *RIT1* mutations are quite common, and *RIT1* is among the four major genes for NS accounting for at least 5% of molecularly confirmed NS-affected cases. In the 38 *RIT1* mutation-positive index patients reported here, the majority of mutations was found to affect codon 82 (n=10), giving rise to amino acid substitution of phenylalanine to valine, leucine, isoleucine or serine. The two other most common *RIT1* codons mutated in NS-affected individuals are 57 (n=9) and 95 (n=4). Clustering of disease-causative variants at codons 57, 82 and 95 has already been observed (Aoki et al. 2013, Gos et al. 2014). The *RIT1* mutation p.(Gly31Arg) identified in this study is novel and alters a functionally relevant amino acid residue. Glycine 31 in *RIT1*, located in the G1 motif, corresponds to glycine 13 in the RAS GTPases. Glycine 13 of *HRAS* is mutated in individuals with CS (p.(Gly13Cys)) (Gripp et al. 2011). These findings together with pathogenicity prediction and segregation of the variant with disease provide strong evidence for causality of the *RIT1* amino acid substitution p.(Gly31Arg).

To better define the phenotype associated with a *RIT1* mutation, we summarized the clinical features observed in our 43 patients and reviewed those in 90 individuals described in the literature (Table 4.3) (Aoki et al. 2013, Bertola et al. 2014, Calcagni et al. 2016, Cave et al. 2016, Chen et al. 2014b, Gos et al. 2014, Justino et al. 2015, Koenighofer et al. 2016, Milosavljevic et al. 2016, Nemcikova et al. 2016, Yaoita et al. 2016).

We also compared the frequency of phenotypic features in our *RIT1* mutation-positive cohort with patients harboring a *PTPN11*, *SOS1* or *RAF1* mutation, whose phenotype data had been collected using the same standardized form (NSEuroNet database; Table 4.4).

	All publications	This study	Total	%
n	90	43	133	
Males/Females	35/46	16/27	51/73	
Median age (in years)	8.5	6.5	7.5	
Prenatal abnormalities	18/27	19/33	37/60	62%
Polyhydramnios	18/61	10/33	28/94	30%
Nuchal edema	18/47	11/33	29/80	36%
Fetal chylothorax/hydrops	12/53	9/33	21/86	24%
Feeding difficulties	30/49	15/30	45/79	57%
Cardiac anomaly	85/89	42/43	127/132	96%
Pulmonary/pulmonary valve stenosis	61/84	34/43	95/127	75%
ASD/VSD	36/77	14/43	50/120	42%
HCM	40/81	21/43	61/124	49%
Acquired lymphatic disorder	4/20	8/39	12/59	20%
Short stature	23/67	14/39	37/106	35%
Motor delay	11/43	11/32	22/75	29%
Intellectual/learning disabilities	11/52	6/24	17/76	22%
Cryptorchidism in males	19/29	7/12	26/41	63%
Curly hair	25/63	5/39	30/102	29%
Keratosis pilaris	10/42	2/39	12/81	15%
Scoliosis	4/24	2/39	6/63	10%
Pectus deformity	27/64	20/39	47/103	46%
Short/broad/webbed neck	52/69	18/39	70/108	65%
Ocular ptosis	29/60	25/39	54/99	55%
Bleeding diathesis	9/62	6/32	15/94	16%
Neoplasia (benign and malignant)	4/80	4/43	8/123	7%

Table 4.3: Combined data from RIT1 publications. This table shows the combined data from all RIT1 publications and the data compiled in this study.

In more than half of the *RIT1* mutation-positive cases, prenatal abnormalities were observed including nuchal edema as the most common finding but also polyhydramnios, fetal pleural effusions, and hydrops fetalis. The frequency of prenatal abnormalities was comparable between our cohort and previously published cases with *RIT1* mutation. Compared to *PTPN11* and *SOS1* a higher frequency of fetal nuchal edema (33%), fetal chylothorax and/or fetal hydrops (27%) was observed, reaching statistical significance for both in *SOS1* and for the latter in *PTPN11*. Notably, *RIT1* mutation-positive individuals from our cohort also had a higher incidence (21%) of lymphatic disorders occurring later in life, which was significant in comparison to patients with *PTPN11* and *RAF1* mutations. Four cases with *RIT1* mutation and acquired lymphatic disorders were also reported in the literature (Table 4.3). A significant proportion of all patients with a *RIT1* germline mutation in our cohort (50%) and previously reported cases (57%) had feeding difficulties, however, in our cohort we could relate the more severe feeding difficulties to premature birth (data not shown). Overall feeding issues appear to occur less frequently in individuals with a *RIT1* mutation compared with NS-affected individuals linked to other genes (Kobayashi et al. 2010), however, this difference does not reach statistical significance in our dataset. Cardiovascular abnormalities were seen in

n	<i>RIT1</i>	<i>PTPN11</i>	p-value	<i>RIT1</i>	<i>SOS1</i>	p-value	<i>RIT1</i>	<i>RAF1</i>	p-value
Males/Females		51/43			27/27			22/19	
Median age (in years)	6.5	7.1		6.5	7.7		6.5	5.1	
Prenatal abnormalities	19/33	24/86	0.06	19/33	23/36	0.8	19/33	23/32	0.7
Polyhydramnios	10/33	15/86	0.24	10/33	15/36	0.6	10/33	14/32	0.5
Nuchal edema	11/33	12/86	0.08	11/33	3/36	0.04*	11/33	14/32	0.6
Fetal chylothorax/ hydrops	9/33	5/86	0.01	9/33	2/36	0.05*	9/33	2/32	0.1
Feeding difficulties	15/30	52/86	0.7	15/30	20/34	0.8	15/30	22/32	0.5
Cardiac anomaly	42/43	70/89	0.5	42/43	45/52	0.8	42/43	38/40	1
Pulmonary/pulmonary valve stenosis	34/43	50/89	0.2	34/43	41/52	1	34/43	6/40	0.0003*
ASD/VSD	14/43	31/89	1	14/43	14/52	0.7	14/43	14/40	0.1
HCM	21/43	11/89	0.001*	21/43	6/52	0.004*	21/43	33/40	0.2
Acquired lymphatic disorder	8/39	3/92	0.006*	8/39	4/49	0.2	8/39	0/34	0.02*
Short stature	14/39	64/87	0.05*	14/39	27/46	0.3	14/39	18/30	0.29
Motor delay	11/32	35/75	0.6	11/32	14/33	0.8	11/32	12/26	0.6
Intellectual/ learning disabilities	6/24	18/45	0.5	6/24	8/38	0.8	6/24	9/21	0.6
Cryptorchidism in males	7/12	36/47	0.8	7/12	16/24	1	7/12	13/17	0.8
Keratosi pilaris	2/39	2/88	0.6	2/39	19/47	0.002*	2/39	3/29	0.6
Scoliosis	2/39	7/88	0.7	2/39	6/48	0.5	2/39	2/31	1
Pectus deformity	20/39	50/91	0.9	20/39	39/47	0.2	20/39	26/37	0.5
Short/broad/ webbed neck	18/39	52/91	0.6	18/39	38/51	0.2	18/39	26/37	0.3
Ocular ptosis	25/39	52/86	0.9	25/39	38/49	0.6	25/39	23/36	1
Bleeding diathesis	6/32	26/78	0.4	6/32	10/47	1	6/32	4/24	1
Neoplasia (benign and malignant)	4/43	11/88	0.8	4/43	7/49	0.8	4/43	0/29	0.3

Table 4.4: Frequency of phenotypic features in the *RIT1* cohort compared to the *PTPN11*, *SOS1*, and *RAF1* cohorts. This table shows the frequency of specific phenotypic features and the p-values obtained by Fisher's exact test. *statistical significance ($p \leq 0.05$)

almost all individuals with a *RIT1* alteration (combined frequency 127/132; 96%). This is higher than in patients with *PTPN11* mutation (78%) and also higher than the frequency reported for NS overall (81%; no patients with *RIT1* mutation included) (Prendiville et al. 2014). The most prevalent heart defect was pulmonary or pulmonary valve stenosis found in a total of 95 out of 127 *RIT1* mutation-positive individuals (75%) compared to 56% in patients with *PTPN11* mutation, 15% in those with *RAF1* mutation, reaching statistical significance, and 57% reported in molecularly confirmed patients with NS overall (Prendiville et al. 2014). A high incidence of HCM in NS-affected subjects with *RIT1* mutation has already been noticed by Aoki et al. (2013) (Aoki et al. 2013). There is a total prevalence of HCM of 49% (61/124) in individuals with a *RIT1* mutation compared to 16% in reported individuals with a molecularly confirmed diagnosis of NS in general (without *RIT1*) (Aoki et al. 2013). We found significant differences compared to individuals with *PTPN11* or *SOS1* mutation (12% each) in our dataset that is consistent with published data (Kobayashi et al. 2010). These findings corroborate that *RIT1* is the second most important NS gene associated with HCM; only

RAF1 germline mutations show a higher association with HCM (about 80%) (Kobayashi et al. 2010). NS-affected individuals with HCM show a significant early mortality (22% by the age of one year) (Wilkinson et al. 2012). However, there was no instance of cardiac death related to HCM in our cohort of *RIT1* mutation-positive patients as well as in other reported patients (Aoki et al. 2013, Bertola et al. 2014, Chen et al. 2014b, Gos et al. 2014, Justino et al. 2015, Koenighofer et al. 2016, Nemcikova et al. 2016) suggesting that HCM associated with *RIT1* mutations has a more benign course. Atrial or ventricular septal defects were found in a proportion of subjects with *RIT1* mutation that is comparable to individuals with mutations in other genes (Table 4.4) (Kobayashi et al. 2010). Short stature, which is a common feature in NS (van der Burgt et al. 2007), was consistently found at a relatively low frequency, affecting in total only 37 of 106 individuals with *RIT1* alteration (35%). The frequency of short stature in *RIT1* mutation-positive individuals is lower than in patients with alteration in *PTPN11*, *SOS1* and *RAF1*, reaching statistical significance in *PTPN11* in our dataset. Accordingly, Kobayashi et al. (2010) recorded a higher incidence of short stature, particularly in patients with a *RAF1* (82%) or *PTPN11* (56%) mutation (Kobayashi et al. 2010). Consistent with our data, a relatively low percentage of subjects with a *RIT1* mutation were recorded to have intellectual/learning disabilities (17/76; 22% in total) that corresponds well to 21% of individuals with *SOS1* mutation in our cohort and 18% reported in the literature (Kobayashi et al. 2010). Conversely, in patients with *RAF1* and *PTPN11* mutation a frequency of 43% and 40%, respectively, was recorded for intellectual/learning disabilities in our data that is consistent with published data (Kobayashi et al. 2010). However, differences in the overall prevalence of intellectual/learning disabilities between patients with *RIT1*, *PTPN11*, *SOS1*, and *RAF1* mutation in our cohort did not reach statistical significance, probably because of a limited sample size. A more detailed analysis of the degree of intellectual impairment showed that the recorded deficits were usually mild in the *RIT1* mutation-positive patients described here. Specific learning disabilities were uncommon, but again numbers were too small to achieve statistically significant differences. Ectodermal abnormalities such as curly hair and hyperkeratosis are relatively uncommon in *RIT1* mutation-positive subjects from our cohort as well as in previously published cases. Significantly higher frequencies of ectodermal abnormalities were recorded in individuals with *SOS1* mutation in our dataset, which fits well with data from the literature (Kobayashi et al. 2010). Pectus deformities and a short, broad or webbed neck are consistently observed in NS-affected individuals with mutations in different genes (Kobayashi et al. 2010, Koenighofer et al. 2016). We observed lower frequencies for these anomalies in patients with a *RIT1* mutation compared to *SOS1* and *RAF1*, without reaching statistical significance in this dataset. Bleeding diathesis was rarely observed in

patients with *RIT1* mutation (19%) from our cohort, but is not significantly different from the rate in patients carrying mutations in *PTPN11*, *SOS1*, and *RAF1* (33%, 21% and 17%, respectively). In our cohort, bleeding problems were rather mild and without any severe complications (data not shown). Ocular ptosis was seen quite often in our *RIT1* mutation-positive cohort (64%) as well as in a total of 54 out of 99 (55%) individuals with *RIT1* alteration. This association is quite similar in all other patient groups with molecularly confirmed NS (60-78% in our cohort and 62-79% reported in (Kobayashi et al. 2010)). However, severe ptosis requiring surgical interventions appears to be rare in *RIT1*-mutated patients (three individuals in our cohort and no documentation in previous studies).

Somatic mutations in *RIT1* have recently been identified in myeloid malignancies and lung adenocarcinomas (2014, Berger et al. 2014, Gomez-Segui et al. 2013). The *RIT1* mutational spectrum found in human cancers significantly overlaps with *RIT1* germline alleles: all oncogenic mutations clustered around glutamine 79 in the switch II region (p.(Ala77Pro), p.(Glu81Gly), p.(Phe82Leu/Val) and p.(Met90Ile)) and induced cellular transformation (2014, Berger et al. 2014, Gomez-Segui et al. 2013). A recent study on cancer spectrum and frequency in patients with RASopathies demonstrated an 8.1-fold increased risk of all childhood tumors in NS-affected children (Kratz et al. 2015), but as this study included only patients with a molecularly confirmed diagnosis of a RASopathy before 2013, no cases with a *RIT1* mutation were included. We identified the second cases of *RIT1* mutation-associated NS with acute lymphoblastic leukemia and multiple giant cell lesions of the jaws (Table 6.2 in the supplements and (Aoki et al. 2013, Bertola et al. 2014)), suggesting that individuals carrying a *RIT1* germline mutation might be at increased risk for developing these types of neoplasia. Two other patients of our cohort developed malignant or benign tumors (a gastrointestinal stromal and a neuroendocrine tumor in the same individual, and a lipoma in another patient), thus bringing the total number of *RIT1* mutation-positive individuals with any type of neoplasia to eight out of 123 (7%) including three cases of malignancy. The three subjects with a malignant tumor had alterations affecting codons 81 and 82 that are common sites of somatic *RIT1* mutations in cancer (2014, Berger et al. 2014, Gomez-Segui et al. 2013). The two patients reported with giant cell tumors of the jaws (our cohort and (Bertola et al. 2014)) shared the *RIT1* mutation p.(Ala57Gly). In summary, these findings indicate that NS-associated *RIT1* germline mutations do confer susceptibility to neoplasia; however, further studies are needed to determine the risk for malignancies in this particular NS patient group.

We conclude that *RIT1* is one of the four most frequently mutated genes in patients with a clinical phenotype of NS. By careful clinical evaluation of our patient cohort and review of

previously reported cases, we delineated in more detail the clinical characteristics of *RIT1*-associated NS: we found a high frequency of cardiovascular abnormalities with particular risk of HCM and a predisposition to lymphatic problems, while short stature, developmental delay, bleeding diathesis, and ectodermal abnormalities occurred at lower frequencies compared to NS in general. We add the three novel amino acid substitutions p.(Gly31Arg), p.(Ala77Thr) and p.(Phe82Ser) to eleven already reported NS-associated *RIT1* alterations. The majority of *RIT1* germline mutations cluster at codons 57, 82 and 95, and the mutation spectrum in NS-affected individuals significantly overlaps with that of somatic mutations in tumors. We found a possible hint at increased risk of neoplasia in subjects with *RIT1* mutation-associated NS.

4.2.3. Genotype phenotype correlations with germline *NRAS* mutations

NRAS mutations were detected in four individuals in our genotyping cohort. All of these have been published along with 7 further families identified by our international collaborators in a total of 19 individuals (Altmuller et al. 2017). One additional patient has been identified by another collaborator after publication. Overall we describe 20 new patients with a RASopathy due to germline *NRAS* mutations. The size of this cohort exceeds the total number of previously reported patients harboring germline mutations in *NRAS* (Cirstea et al. 2010, Denayer et al. 2012, Digilio et al. 2011, Ekvall et al. 2015, Kraoua et al. 2012, Runtuwene et al. 2011). We report *de novo* as well as familial occurrence of the already known changes c.71T>A (p.(Ile24Asn)), c.149C>T (p.(Thr50Ile)), and c.179G>A (p.(Gly60Glu)), confirming these codons to be hotspots for RASopathy-associated germline mutations in *NRAS*. In addition, we identified six novel mutations affecting residues Gly12, Glu37, and Thr58 to cause a RASopathy phenotype.

The assumption that the novel sequence variants, c.34G>C, 35G>A, 34G>A, c.35G>T (p.(Gly12Arg/Asp/Ser/Val) respectively), c.112-1_113dupGGA (p.(Glu37dup)), and c.173C>T (p.(Thr58Ile)), indeed represent pathogenic mutations is supported by several lines of evidence: All amino acid substitutions affect highly conserved residues of *NRAS*, and they are located at or near known hotspots for somatic or germline *NRAS* mutations. Additionally all novel *NRAS* mutations described here have previously been reported as pathogenic mutations in the other RAS genes *KRAS* and/or *HRAS*, and the activating effects have been shown in functional studies (Ahmadian et al. 1999, Aoki et al. 2005, Cirstea et al. 2010, Fasano et al. 1984, Gremer et al. 2010, Gremer et al. 2011, Schubbert et al. 2006, Wey et al. 2013).

Missense changes affecting p.Gly12 in *NRAS* or other RAS proteins are among the most common somatic changes in cancer, and result in impaired GTPase activity and GAP

resistance, leading to constitutive activation (Ahmadian et al. 1999, Gremer et al. 2011, Schubbert et al. 2006, Wey et al. 2013). While for position p.Glu37 in NRAS neither somatic nor germline mutations had previously been described, the same duplication p.(Glu37dup) in HRAS has been reported in a case of CS (Gremer et al. 2010). Mutant HRAS^{E37dup} was shown to predominate in the active GTP-bound state due to lower intrinsic GTPase activity and complete resistance to GAP, but its impact on signal flux through the MAPK and PI3K-AKT cascades was found to be milder compared to HRAS^{G12V}, because of reduced binding affinities for effector proteins (Gremer et al. 2010). The missense mutations resulting in p.(Thr58Ile) have been described eight times in HRAS as a cause of CS and six times in *KRAS* mainly associated with NS (www.nseuronet.com). Additionally, this mutation has occasionally been observed in RAS isoforms as a somatic mutation in various types of malignancy (COSMIC) (Forbes et al. 2015). Previous functional characterization of the KRAS^{Thr58Ile} mutant provided evidence for a mild over-activated behaviour of the GTPase and enhanced activation of downstream effectors (Gremer et al. 2011, Schubbert et al. 2006). The four novel RASopathy-associated NRAS variants affecting p.Gly12 represent well-known oncogenic mutations that occur with decreasing prevalence (p.Gly12Asp > p.Gly12Ser > p.Gly12Val > p.Gly12Arg) as somatic changes in various tumors, particularly in hematopoietic and lymphoid malignancies (COSMIC database) (Forbes et al. 2015). The previously reported spectrum of NRAS germline mutations appeared to spare the classical oncogenic hotspots p.Gly12, p.Gly13, and p.Gln61, suggesting that the occurrence of oncogenic NRAS alterations in the germline might lead to embryonic lethality (Cirstea et al. 2010). This is therefore the first report to show that apparent non-mosaic germline changes in NRAS affecting one of these hotspots for oncogenic mutations may be compatible with life and lead to a clearly recognizable RASopathy phenotype. An overlap of the germline mutation spectrum with oncogenic mutation hotspots has very rarely been observed for germline *KRAS* mutations in CFCS (Nava et al. 2007), while it is regularly observed for germline *HRAS* mutations leading to CS. This has been correlated with the significantly increased tumor risk in this particular type of RASopathy. Consistently, one of the present subjects carrying a missense change at codon 12 of NRAS had a tumor-like lesion in the hypothalamus the precise nature of which was not delineated by the time of this report, and another one had a JMML-like myeloproliferative disorder. Of note, JMML and JMML-like myeloproliferative disorders (MPDs) are particularly related to NS and to somatic mutations in RASopathy genes, including *NRAS* (Caye et al. 2015, Kratz et al. 2005, Niemeyer 2014, Stieglitz et al. 2015, Strullu et al. 2014). Also, for the stillbirth with the mutation p.(Gly12Val, patient N2) we do not have sufficient data to exclude a myeloproliferative disease or other kind of neoplasia.

There is one previously published case report of suggestive germline status for the NRAS mutation p.(Gly13Asp) in a patient with JMML (De Filippi et al. 2009). The infant who was affected by JMML was reported to have short stature and dysmorphic features reminiscent of NS. In this case the mutation was not only in buccal cells and hair bulbs, but also in fibroblasts, suggesting that the mutation was indeed not restricted to hematopoietic tissue. Nevertheless, a mosaic status for the mutation cannot be excluded, in principle. Notably, another patient affected by ALPS and no clinical signs of NS was erroneously reported to have a germline event solely based on the demonstration of this change in DNA from a buccal swab (Oliveira et al. 2007). During follow-up the mutation was not retrieved in DNA samples from hair bulbs and a repeat buccal swab, thus disproving the germline status (personal communication J. B. Oliveira, February 2010). This is pointing to the difficulties in assessing the germline status of a mutation, which is also a possible limitation in the data presented here. It is known that hematopoietic cells may migrate and reside in non-hematopoietic tissues including buccal mucosa and fingernails (Hiramoto et al. 2015, Imanishi et al. 2007). However, cultured fibroblasts that could be tested in some of the patients are devoid of contamination with hematopoietic cells (Caye et al. 2015, Kraoua et al. 2012, Stieglitz et al. 2015). Together with the systemic clinical features observed in all our patients it is likely that NRAS changes affecting Gly12 were indeed of germline origin.

Our findings suggest that clinically obvious RASopathy features constitute the major phenotype caused by activating *NRAS* mutations occurring in the germline, whereas hematological abnormalities do not invariably emerge even in the presence of mutations at oncogenic hotspots. Comparing the clinical symptoms recorded in our patients to previously reported cases with germline *NRAS* mutations we generally found high congruency regarding the frequency of clinical findings in various organ systems. Taking together the clinical data from a total of 38 affected individuals allows us to further delineate the RASopathy phenotype associated *NRAS* mutations (Table 4.5).

	Cristea, 2010	Runtuwene, 2011	Digilio, 2011	Denayer, 2012	Kraoua, 2012	Ekvall, 2015	Present Study	Total	%
Males/Females	3/2	1/0	0/1	4/3	1/1	1/1	10/10	20/18	
Median age (in years)	14	30	2	20	10,5	45	7	14	
Prenatal abnormalities	3/5	ND	0/1	ND	2/2	0/2	10/14	15/24	63
Polyhydramnios	2/5	ND	0/1	ND	1/2	0/2	7/14	10/24	42
Nuchal edema	1/5	ND	0/1	ND	0/2	0/2	3/14	4/24	17
Fetal chylothorax/hydrops	0/5	ND	0/1	ND	0/2	0/2	3/14	3/24	13
Feeding difficulties	ND	ND	0/1	1/7	2/2	ND	5/15	8/25	32
Cardiac anomaly	3/5	0/1	1/1	1/7	1/2	2/2	12/19	20/37	54
Pst	2/5	0/1	1/1	0/7	1/2	0/2	2/19	6/37	16
ASD/VSD	0/5	0/1	0/1	0/7	0/2	1/2	3/19	4/37	11
HCM	2/5	0/1	1/1	0/7	0/2	1/2	6/19	10/37	27
Acquired lymphatic disorder	0/5	ND	ND	ND	ND	ND	0/19	0/24	0
Short stature	3/5	1/1	1/1	4/7	1/2	0/2	5/17	15/35	43
Motor delay	5/5	ND	1/1	1/2	1/2	ND	6/15	14/25	56
Intellectual/learning disabilities	2/5	1/1	0/1	0/7	0/2	0/2	6/14	9/32	28
Cryptorchidism in males	2/3	1/1	NA	2/2	0/1	0/1	5/9	10/17	59
Curly Hair	3/5	ND	0/1	ND	1/2	1/2	3/17	8/27	30
Keratosis pilaris	4/5	ND	0/1	ND	1/2	0/2	4/17	9/27	33
Scoliosis	1/5	ND	ND	ND	1/2	ND	0/18	2/25	8
Pectus deformity	4/5	1/1	1/1	2/7	2/2	0/2	6/18	16/36	44
Short/broad/webbed neck	4/5	1/1	1/1	2/2	2/2	2/2	17/18	29/31	84
Ocular ptosis	1/5	ND	0/1	ND	2/2	0/2	15/18	18/28	64
Bleeding diathesis	0/5	ND	ND	2/7	1/2	1/2	3/17	7/33	21
Neoplasia (benign and malignant)	0/5	0/1	0/1	0/7	0/2	0/2	3/18	3/36	8

Table 4.5: Clinical data from *NRAS* publications. This table shows the clinical data from all *NRAS* publications and the data compiled in this study.

Cardiac anomalies are present in approximately half of cases, but contrasting to what is generally observed in NS, Pst is significantly less common (16%), while HCM is the most prevalent cardiac finding (27%), with a slightly higher prevalence compared to the general NS population (Roberts et al. 2013). Septal defects also represent a relatively common cardiac feature, occurring in 11% of cases (Marino et al. 1999). The typical craniofacial appearance is commonly seen and indistinguishable from NS of other etiologies. Short or webbed neck and ocular ptosis were highly prevalent among patients with *NRAS* mutations (84% and 64%, respectively). Notably, short stature was only present in 43% of patients, which is less prevalent than in NS in general. Motor delay is quite frequent (56%), while learning disabilities are observed in a similar frequency as in NS of other genetic aetiologies (28%).

Cryptorchidism in males (59%) and the occurrence of prenatal abnormalities are also quite frequent (63%) and comparable to their general frequency in NS (Roberts, Allanson et al. 2013).

While all previously reported patients had a clinical diagnosis of NS, three patients in this cohort were diagnosed as having CFCS or CS based on their clinical features. For patient N7 a working diagnosis of CFCS was initially made primarily based on her striking craniofacial features, profound hypotonia, significant developmental delay, and feeding issues. In addition to the *NR4S* mutation she was found to have a 1.24 Mb duplication on chromosome 22q11.23, corresponding to the region between LCR-F and LCR-H, whose *de novo* occurrence could not be confirmed. Similar 22q11.23 duplications have been found in individuals with variable clinical features, including muscular hypotonia, developmental delay, and seizures, with *de novo* occurrence but also inherited from apparently healthy parents (Chang et al. 2015, Coppinger et al. 2009). It is therefore possible that this copy number change might contribute to the severity of the developmental phenotype and some atypical features described in this patient. Similarly, patient N11, who carried the c.149C>T (p.(Thr50Ile)) variant, was clinically classified as having CFCS because of significantly delayed motor development, mild intellectual disability (IQ of 65), and prominent ectodermal abnormalities (keratosis pilaris, multiple nevi, sparse eyebrows and curly, sparse hair). Of note, the same mutation had previously been reported in patients with a NS phenotype and no or only mild developmental problems (Cirstea et al. 2010, Denayer et al. 2012). Patient N12 (p.(Gly12Arg)) showed severe perinatal complications typically seen in newborns with CS, including polyhydramnios, neonatal hyperinsulinemic hypoglycemia, severe feeding difficulties and respiratory problems. Furthermore, she had deep palmar and plantar creases and a tumor-like lesion of unknown etiology in the hypothalamus. Her motor development was delayed. This constellation prompted the diagnosis of CS, but the patient was very young at last follow-up and the phenotype may still change with age.

Considering the relatively severe expression of NS in patient N1 (p.(Gly12Ser)) and patient N13 (p.(Gly12Asp)), the CS-like neonatal presentation in patient N12 (p.(Gly12Arg)), and intrauterine death of patient N2 (p.(Gly12Val)), it is tentative to speculate that this may be related to the more severe functional impact of these mutations at Gly12. Among these, the p.(Gly12Val) change that was associated with intrauterine death is the most common oncogenic mutation at codon 12 in *NRAS* and demonstrated to represent the strongest effect on downstream signaling, while the others have somewhat weaker activating potential (Ahmadian et al. 1999, Fasano et al. 1984). Similarly, gradual differences in the phenotypic

severity have also been proposed for different *HRAS* p.Gly12 mutations in CS (Lorenz et al. 2012). Regarding clinical management it has to be considered that *NRAS* mutations corresponding with CS-associated *HRAS* changes may also share a similar risk of malignancy as seen in CS. However, the number of patients is still limited and the observation period for the patients reported here was too short to draw definite conclusions about possible genotype-phenotype correlations.

In summary, we have presented the largest cohort to date of patients with germline *NRAS* mutations and their association with the typical clinical phenotype of RASopathies. We showed that mutations affecting Gly12 might be compatible with life when occurring in the germline. This is comparable to the germline mutation spectrum previously documented in *HRAS* (Aoki et al. 2005), but different to the one in *KRAS* where RASopathy-associated germline mutations and somatic changes occurring in cancer hardly overlap (Zenker et al. 2007). Our findings emphasize the obvious RASopathy phenotype associated with activating germline *NRAS* mutations, thus challenging the germline status of oncogenic *NRAS* mutations in previous reports with hematological phenotypes. More data is required to ascertain the risk of malignancy in patients with oncogenic *NRAS* mutations in the germline.

4.3. Prenatal symptoms in CBL syndrome

Variants in the *CBL* gene were detected in eight individuals in our genotyping cohort. Four patients of our genotyping cohort and one additional patient identified through our diagnostic department have been published as presented in Table 3.6 (Bulow et al. 2015, Martinelli et al. 2015). Five additional patients have been identified after publication. Pathogenic variants were identified in six patients.

In the six patient cohort with mutations in the *CBL* gene, we identified patients C1 and C3 with the same missense mutation that has already been described in the literature (Martinelli et al. 2010). Patient C2, C4, C5, and C6 had splice mutations c.1096-1G>T, c.1104_1112del, c.1096-4_1096-1del, and c.1096-1G>C respectively. Two of these have not been published, but at position c.1096-1 a G>C exchange has been reported (Niemeyer et al. 2010). Both variants have been found in other patients with a RASopathy according to the ClinVar database.

CBL mutations have been described as somatic mutations in various leukemias (Loh et al. 2009, Schnittger et al. 2012) and as germline mutations in patients showing variable developmental abnormalities with or without JMML. Most of the *CBL* mutations found as

germline and somatic events are located in the linker and ring finger domain (RF) encoded by exons 7–9 (Schnittger et al. 2012). Patients C1 and C3 had an identical mutation in exon 8, c.1100A>C (p.Gln367Pro), which had been previously identified in a patient with developmental delay, cafe-au-lait macules, enlarged left atrium, and transient chaotic ventricular dysrhythmias (Martinelli et al. 2010) and in a patient with primary lymphedema and teratoma (Hanson et al. 2014). The mutation detected in Patient C2 (c.1096–1G>T) and C6 (c.1096–1G>C) has only been published in the latter form in a patient with developmental delay, cryptorchidism, juvenile xanthogranuloma (JXG), and JMML (Niemeyer et al. 2010). The present patients all had craniofacial features compatible with a Noonan-like syndrome, including congenital heart defects typical of RASopathies, short stature, and/or delayed development. We assume that perinatal complications and/or JMML may have contributed to their developmental delay. Only 14 (56%) of the 25 previously reported NSLL patients were diagnosed with developmental delay (Table 4.6); 11 patients showed normal development and in one girl with developmental delay in childhood had caught up at age 15 years (Martinelli et al. 2010).

	Martinelli, 2010	Perez, 2010	Niemeyer, 2010	Hanson, 2014	Hyakuna, 2015	This study	Total	%
Short stature, postnatal onset	1/4	3/3	4/17	0/1	1/1	2/4	11/30	37%
Microcephaly	0/4	2/3	ND	0/1	ND	0/3	2/11	18%
Dysmorphic features	4/4	3/3	ND	1/1	1/1	6/6	15/15	100%
Thorax abnormality	3/4	1/3	ND	1/1	1/1	2/3	8/12	67%
Cafe-au-lait spots	2/4	2/3	4/17	0/1	ND	0/3	8/28	29%
Cardiac malformations	3/4	0/3	ND	1/1	0/1	6/6	10/15	67%
Cardiomyopathy	0/4	0/3	2/17	0/1	0/1	0/5	2/31	6%
Hypertension	0/4	0/3	4/17	0/1	ND	0/5	4/30	13%
Developmental delay	3/4	1/3	9/17	1/1	1/1	5/5	20/31	65%
Pleural effusion	0/4	0/3	ND	0/1	ND	3/3	3/11	27%
JMML	0/4	3/3	17/17	0/1	1/1	1/3	22/29	76%
Lymphedema	ND	ND	ND	1/1	ND	1/3	2/4	50%
Teratoma	0/4	0/3	1/17	1/1	0/1	0/4	2/30	7%
Cryptorchidism (males)	0/1	0/0	3/9	0/0	NA	3/4	6/14	43%

Table 4.6: Clinical data from *CBL* publications. This table shows the clinical data from all *CBL* publications and the data compiled in this study.

It has been increasingly recognized that the RAS-MAPK pathway plays a major role in the signaling of lymphangiogenesis (Coso, Bovay and Petrova 2014). Remarkably, some of our patients had a history of prenatal pleural effusions, congenital hydro-/chylothorax, and/or hydrops fetalis. While such complications have not previously been described in individuals

with *CBL* germline mutations, they belong to a spectrum of prenatal abnormalities that are typically associated with the RASopathies. The most frequent prenatal findings in NS and related disorders include increased nuchal translucency and cystic hygroma, but pleural effusions, hydrops, and lymphedema have also been reported (Baldassarre et al. 2011, Witt et al. 1987, Witters et al. 2002, Yoshida et al. 2004). These abnormalities may be regarded as a continuous spectrum caused by impaired fetal lymphatic drainage probably related to lymphatic dysplasia or delayed maturation of lymphatic vessels. The lymphedema of the feet and legs in Patient C1 and in another patient with the same c.1100A>C mutation (Hanson et al. 2014) points to an underlying abnormality of the lymphatic system (Roberts et al. 2013, Witt et al. 1987) and further documents the pathophysiological relationship of the *CBL* syndrome with the RASopathies. Spontaneous resolution is common, but in some cases lymphedema and lymphatic/chylous effusions may persist until and beyond birth. As the outcome of fetal hydrops is generally poor, Witters et al. (2002) found it noteworthy that in a patient with NS, hydrops resolved spontaneously. However, the outcome of NS-related hydrops is not always favorable and lethality of NS-associated hydrops, particularly intrauterine lethality, may be largely underestimated (Lee et al. 2009, Yoshida et al. 2004). More recently, a patient with hydrops fetalis, severe ascites, pleural effusion, and the p.Ser2Gly SHOC2 mutation was described (Gargano et al. 2014). He died two days after he was born at 30 5/7 weeks gestation due to the severity of his symptoms. Previously described patients with a *CBL* germline mutation were selected either through their Noonan-like features or through being affected by JMML. Taking these cohorts together, it can be concluded that the clinical phenotype associated with *CBL* mutations generally includes developmental and physical abnormalities that overlap with NS or the RASopathy pattern of anomalies (Digilio et al. 2011, Martinelli et al. 2010, Niemeyer et al. 2010, Perez et al. 2010). This is in line with the experimental findings showing that the mutated protein has a similar effect on the RAS/MAPK pathway as NS-associated mutations. However, it is likewise apparent that the Noonan-like features are more variable, and not all patients would be classified as having NS on a clinical basis alone. Therefore, it was debated whether this syndrome should be classified as Noonan-like or rather as a distinct “*CBL* syndrome”. The clinical observations presented here further support the similarities between the *CBL* mutation-associated syndrome and NS, as we can document that these conditions also share a typical (albeit not specific) pattern of prenatal abnormalities. It is obvious that at least part of the typical craniofacial phenotype of NS (e.g., pterygium colli, low posterior hairline, and low-set ears) is the consequence of a fetal nuchal edema. Last not least, the presented cases underline that *CBL* mutations have to be

included in the differential diagnosis of fetal pleural effusions, hydrops fetalis, and probably also fetal nuchal edema.

4.4. Copy number changes containing RAS-MAPK genes

There are a small number of case reports associating larger genomic duplications encompassing RASopathy genes with NS or NS-like phenotypes. These reports have raised the hypothesis that increased protein expression of one of these signaling molecules could be an alternative pathomechanism for RASopathies. In an international collaboration we have collected two cases with CNVs containing known RAS-MAPK pathway genes. The clinical description of these cases and the critical discussion of the role of RAS-MAPK pathway genes in those CNVs was published by Lissewski, et al. (Lissewski et al. 2015).

Shchelochkov et al. described a patient born with aortic coarctation, ASD and VSD (Shchelochkov et al. 2008). The patient also exhibited muscular hypotonia, delayed development, failure to thrive, hip dysplasia, velopharyngeal incompetence, microcephaly (OFC: -4.5SD), and had low normal body height (10th centile) at 3 years and 8 months. Her facial anomalies were considered to be consistent with NS. By array-CGH, a 10 Mb duplication of chromosome 12q24 was found, including *PTPN11* and several other genes.

A slightly smaller duplication of 12q24 (8.98 Mb in size) including the *PTPN11* gene was identified in a patient presenting with short stature (just below 3rd centile), mild mitral valve regurgitation, muscular hypotonia, developmental delays, feeding difficulties, and pyloric stenosis (Graham et al. 2009). He also had some minor craniofacial features that are common in RASopathies.

More recently, Chen et al. reported a 14 year-old girl with a 24 Mb duplication including the *PTPN11* gene (Chen et al. 2014a). The patient had severe intellectual disability, ventricular septal defect, pectus excavatum, and a body height on the 3rd centile. The authors argued that most features were compatible with a RASopathy.

Luo et al. described a male patient with tetralogy of Fallot, atrial septal defect and a persistent left superior vena cava. He also had a right upper limb anomaly with radial aplasia and 2-5 syndactyly, some lentiginos, as well as a malformed left ear with sensorineural hearing loss (Luo et al. 2012). He had no delays in his psychomotor development, and his height was on the 3rd percentile. The patient was originally diagnosed as having Holt-Oram syndrome, but following the detection of a 0.25 Mb duplication of 3p25.2 including the *RAF1* gene by SNP

array the diagnosis was changed to NS / NSML. The authors proposed that CNVs might be a rare cause for syndromic CHD resembling NS.

These patients as well as the ones described here share some clinical features that are frequent in RASopathies but also in many other genetic syndromes, such as delays of growth and development. Although some of them had congenital heart defects, they are not the typical ones associated with RASopathies (pulmonary stenosis or hypertrophic cardiomyopathy). Some of the other reported anomalies, such as microcephaly, radial aplasia, ear malformation, and severe intellectual disability, would be considered unusual for NS. The recognition of the craniofacial characteristics of NS is critical for the clinical diagnosis (van der Burgt 2007). After careful review of all published photographs, however, we came to the conclusion that none of these cases have a facial gestalt that is really typical of a RASopathy, and in some of them hardly any NS-like features are present. Likewise, the clinical diagnosis of a RASopathy appears not to have been considered prior to molecular karyotyping in any of the patients except for the case reported by Graham et al. (Graham et al. 2009). In all others, NS instead seems to be a post hoc diagnosis, where the finding that a RASopathy gene was located in the duplicated region may have caused a significant bias. Clinical findings in five individuals affected by duplications containing *RAF1* and *MEK2*, respectively, as presented here further support the notion that phenotypes associated with these duplications are rather non-specific and have no obvious resemblance to NS. This is in line with the fact that the two published studies using a systematic screening for copy number variations in patients with the clinical diagnosis of a RASopathy failed to detect any anomalies: Graham et al. were unable to detect *PTPN11* deletions or duplications by quantitative PCR in over 250 mutation-negative NS patients (Graham et al. 2009) and another study using MLPA analysis of the genes *PTPN11*, *SOS1*, *RAF1*, *KRAS*, *BRAF*, *MEK1*, and *MEK2* was negative in 44 individuals with a clinical diagnosis of NS (Nystrom et al. 2010). Although the number of patients enrolled in these studies was limited, it still holds true that copy number changes affecting RASopathy genes have never been found in patients with a primary and clinically convincing diagnosis of NS or a related disorder.

The fact that RAS pathway genes are located in the respective duplicated regions is of course not sufficient to conclude they are responsible for the duplication-associated phenotype. All of these duplications include one or more other genes and some of them could reasonably contribute to the phenotype, such as *TBX3* and *TBX5* in the duplications of 12q24 (Graham et al. 2009, Shchelochkov et al. 2008). Notably, the smallest duplications containing RASopathy genes, as documented in family 2 reported here, are also associated with the

mildest and least NS-specific phenotypes. The *RAF1* duplication in this family was observed also in the completely normal father, thus questioning the contribution of this CNV to the phenotype in the index patient.

Although it seems to be a reasonable hypothesis that whole gene duplications may lead to increased protein expression and that this, in the case of a signaling molecule, may in turn lead to increased signaling, such speculations have significant shortcomings and lack experimental evidence, so far. First, it cannot be taken for granted that expression of all proteins encoded by genes contained in a genomic duplication is actually above normal level. No experimental confirmation for increased expression levels of the respective gene products has been provided in the reported cases of genomic duplications containing RAS pathway genes. Unfortunately, no adequate material was available to us to perform appropriate expression studies in our patients. Second, even if expression was abnormal, reasonable doubt would remain regarding the potential of quite modest changes in expression levels (+50%) to alter signaling in a similar way as known disease-associated mutations in these genes do. In fact, the activation mechanisms of mutant proteins in the RAS-MAPK pathway is very specific, e.g. by change in conformation or phosphorylation, and this is unlikely to be influenced by the level of expression. There is so far no robust experimental proof for gene dosage effects of RAS pathway components on signaling activity. Accordingly, to our knowledge, no whole RAS pathway gene duplications have been observed as oncogenic events in tumors. In fact, duplications of RAF genes (*BRAF*, *RAF1*) that have been reported in astrocytomas actually lead to fusion genes of KIAA1549:BRAF, FAM131B:BRAF, or SRGAP3:RAF1 acting through abnormal activation of the gene product and not through a dosage effect (Cin et al. 2011, Jones et al. 2008).

To further question the hypothesis that RAS-MAPK pathway genes are dosage-sensitive, we also reviewed recent publications claiming haploinsufficiency of genes encoding RAS pathway components. Nowaczyk et al. described seven patients with a relatively distinct phenotype who had 19p13.3 deletions of varying size and a minimal region of overlap encompassing the *MEK2* locus, including a single case whose deletion apparently contained only the *MEK2* gene (Nowaczyk et al. 2013). In epidermal growth factor-stimulated fibroblasts from one patient with a 1.6 Mb deletion, they found that the amount of total MEK2 and phosphorylated MEK1/2 was significantly decreased whereas the amount of phosphorylated ERK remained unchanged. The authors postulated that haploinsufficiency of MEK2 was a new model of a RASopathy, where a deletion of one of the components of the pathway resulted in what they considered to be a “RASopathy-like phenotype”. Recently, Chen et al. reported a 183 kb *de*

novi deletion including *SHOC2* and at least one other gene (*BBIP1*) in a patient with a complex heart defect, preaxial polydactyly of the right hand, facial dysmorphism, and microcephaly, and normal height and intellectual function. The authors suggested that haploinsufficiency of *SHOC2* can result in a “RASopathy-like phenotype” (Chen et al. 2014a). In both studies, however, the evidence that the deletion of *MEK2* and *SHOC2*, respectively, is indeed the critical mechanism for the phenotype remains rudimentary. Loss-of-function point mutations of *MEK2* and *SHOC2*, respectively that would support this hypothesis have not been reported so far. Regarding *PTPN11*, heterozygous loss-of-function mutations have no developmental phenotype when occurring in the germline, but they give rise to metachondromatosis on the basis of somatic second hits (Bowen et al. 2011). A single frameshift mutation of the *SOS1* gene, c.3248dup; p.(Arg1084Lysfs*23) (published as c.3248_3249insC), has been reported in a family with hereditary gingival fibromatosis (Hart et al. 2002), but this association has never been replicated in a second family.

We conclude that phenotypes observed in patients with CNVs including RASopathy genes lack specificity for a RASopathy, and accordingly, most of the reported patients did not have a pre-test clinical suspicion of a RASopathy disorder. The phenotypes associated with such genomic aberrations have to be regarded as contiguous gene syndromes for which the contribution by these genes is still unclear and may rather be of minor or even no significance. There is currently insufficient evidence for altered dosage of RAS pathway genes to be the critical mechanism for the phenotype associated with CNVs including RASopathy loci. The speculations raised on the basis of a small number of case reports rather document that the interpretation of causal relationships as well as of phenotypic similarities is extremely prone to bias, if the gene for a known developmental disorder is contained in a CNV found in a patient with a non-specific phenotype. These cases highlight that the role of single genes in contiguous gene deletions / duplications should be evaluated with caution.

4.5. Novel RASopathy genes

With the advent of NGS, specifically exome sequencing, and its increasing usage in medical genetic research, new possibly causative genes for RASopathies have been identified. Chen et al. (Chen et al. 2014b) completed exome sequencing in a cohort of 27 patients with a clinical diagnosis of NS and found variants in previously described genes and also in *RASA2*, *SPRY1*, and *MAP3K8*. In the case of *RASA2* three individuals with different missense variants were identified including one patient who also had a known pathogenic *RIT1* mutation. One patient harboring the mutation p.(Arg511Cys) was found to have Pst, an ASD and short

stature. She was two years old and had no developmental delay. Another patient (mutation p.(Tyr326Asn)) was an 11-year-old male with short stature, no heart defect, but a developmental delay of unspecified severity. The third patient had a variant in *RASA2* (p.(Tyr326Cys)) and the known *RIT1* mutation p.(Phe82Val). She was 10 years old and had short stature. She had multiple cardiac anomalies including Pst, ASD, branch pulmonary artery stenosis, PDA, and a dilated main pulmonary artery. She also had an unspecified developmental delay. In this case, however, it remains uncertain whether the *RASA2* variant had a modifying role of the clinical phenotype or whether the *RIT1* mutation fully explains this phenotype. In our cohort we also identified two individuals with variants in this gene. One patient had a variant inherited from the father with no obvious Noonan phenotype (p.(Arg511His)), and for the variant identified in the other patient (p.(Ser12Thr)) segregation could not be analyzed. The former variant affects exactly the same codon that has been described with a variant in one NS patient by Chen and colleagues in one of their patients (p.(Arg511Cys)) with unknown inheritance (Chen et al. 2014b). Our patient's phenotype included short stature and developmental delay, which fits with the patients described previously. However the number of patients with *RASA2* variants is too small to draw genotype-phenotype conclusions. Chen et al. also analyzed the p.(Arg511Cys) variant functionally and showed that a reduction of *RASA2* levels in HEK293 cells increases phosphorylated ERK levels in EGF-stimulated cells. They postulated that this variant has a dominant-negative effect. Both variants found here have been classified as VUS. Missense mutations in *RASA2* have also been described in various cancers (Chen et al. 2014b). Since this initial publication no further patients with possible mutations in *RASA2* have been published. Functional evidence exists, but for the published variant the inheritance is unknown and in our case the mutation was inherited from the father with an unspecified phenotype. It remains questionable if *RASA2* is indeed a new RASopathy gene. The pathogenic significance of the variants in *SPRY1* and *MAP3K8* also remained uncertain and further functional studies were considered necessary to determine the pathogenicity (Chen et al. 2014b).

Likewise through exome sequencing a variant in the *RRAS* gene (c.163G>A (p.(Val55Met))) was identified by Flex and colleagues (Flex et al. 2014). Through targeted sequencing they identified another patient with the variant c.116_118dup (p.(Gly39dup)). By analyzing bone marrow aspirates or circulating leukocytes from non-syndromic patients with JMML they also identified the c.260A>T (p.Gln87Leu) variant as a somatic event. They showed that the p.(Gly39dup) variant leads to decreased intrinsic GTPase activity and that an overexpression of mutant proteins leads to increased RAS/MAPK signaling (Flex et al. 2014). In our cohort

we identified another patient (G15) with a *de novo* *RRAS* alteration (c.260A>T (p.(Gln87Leu)). The position p.Gln87 in *RRAS* aligns with p.Gln61 in *HRAS*, *KRAS* and *NRAS*, which is a known hotspot for oncogenic mutations (Simanshu et al. 2017). The phenotypic features of patient G15 as described in chapter 3.6 of this thesis fulfil the clinical criteria for a diagnosis of NS. Even though *RRAS* is not directly involved in the RAS/MAPK pathway its dysregulated function was shown to perturb signal flow through the cascade, thus supporting *RRAS* mutations as a rare cause for a RASopathy phenotype (Flex et al. 2014). Our patient with a *de novo* mutation at a critical position of the protein further supports this assumption. Notably, the mutation found in our patient has previously been described only as somatic mutation in leukemia. Carrying such an oncogenic mutation in the germline could be an explanation for the severe expression of the phenotype in this child. However, we could not definitely exclude the possibility that the mutation was a clonal event restricted to hemoatopoetic tissue.

Another one of the novel genes identified through exome sequencing is *A2ML1* (Vissers et al. 2015). It was described in one case as a *de novo* event and two cases of familial NS. The phenotype was variable and while some individuals have a phenotype somewhat resembling NS, other mutation carriers in the familial cases showed no obvious symptoms of a RASopathy. Two different variants were identified and both were functionally characterized using a zebrafish model, which showed developmental defects resembling the effects of other RASopathy mutations in this model system, including facial features and heart defects, but none of them showed increased levels of phosphorylated ERK, which is considered as a surrogate marker for RAS-MAPK pathway activation and a common finding in functional experiments on mutations in previously identified genes. We have screened 144 patients for mutations in *A2ML1* (the gene was included in our NGS panel). The variant p.(Arg802His) that was published by Vissers et al. as a disease-causing mutation was also found in one of the patients in our study cohort, but this patient also had the known *RAF1* mutation p.(Ser257Leu) that fully explained the patient's phenotype (Vissers et al. 2015). This observation challenges the pathogenic significance of this *A2ML1* variant for a Noonan syndrome phenotype. Together with the absence of other *A2ML1* mutations in our cohort and the fact that no other cases have been published since 2015, it has to be concluded that the role of *A2ML1* as a gene for Noonan syndrome remains uncertain and it is unlikely that *A2ML1* mutations really cause a typical RASopathy.

Also in 2015 Yamamoto and colleagues identified variants in *SOS2* and *LZTR1* to be associated with NS (Yamamoto et al. 2015). The disease-associated variants identified in *SOS2* were p.(Met267Lys) and p.(Thr376Ser). *SOS2* was confirmed in the same year as a novel gene

for Noonan syndrome by Cordeddu and colleagues (Cordeddu et al. 2015) who described mutations at the same position and at a neighbouring codon (mutation p.(Thr264Lys)). This publication included also one of the patients from this cohort (G19). Functional studies revealed higher levels of GTP-bound Ras and increased RAS/MAPK signaling in all three variants identified in the latter study. The same functional consequences had also been described in *SOS1* mutations (Tartaglia et al. 2007). The positions affected by these activating mutations in *SOS2* correspond to established mutation hotspots in *SOS1*. In our cohort a total of eight individuals were identified with variants in *SOS2* (see Table 3.7) including the published patient, but only three of those variants could be classified as pathogenic. Two patients had the p.(Met267Lys) variant and one the p.(Thr376Ser) variant, both of which have previously been described (Cordeddu et al. 2015, Yamamoto et al. 2015). The other variants had not been described before. In an alignment with the *SOS1* sequence no published *SOS1* mutations were found at exactly the corresponding positions, but for two variants *SOS1* mutations close to the corresponding positions were found (Table 4.7).

Patient	SOS2	SOS1	Published SOS1 mutations	Classification
G16	p.Asn310Ser	p.Leu312	p.Asp309Tyr (Roberts et al. 2007)	VUS
G17	p.Asn1229Tyr	p.Ser1227	None	VUS
G18	p.Pro1318Ser	p.Pro1318	p.His1320Arg (Tartaglia et al. 2007)	VUS
G19	p.Thr376Ser	p.Thr378	p.Thr378Ser (Yamamoto et al. 2015)	pathogenic
G20	p.Pro404Thr	p.Arg406	None	VUS
G21	p.Glu266Asp / p.Met267Lys (in trans)	p.Glu 268 / p.Met269	None / p.Met269Lys (Roberts et al. 2007)	pathogenic
G22	p.Met267Lys	p.Met269	p.Met269Lys (Roberts et al. 2007)	pathogenic
G23	p.Lys739Asn (LZTR1 p.Arg619His(hom))	p.Lys741	None	VUS

Table 4.7: *SOS2* variants and their corresponding positions and known mutations in *SOS1*

The aligned positions in Table 4.7 also show if the regular amino acids at the corresponding positions are identical in the two SOS isoforms. This is only the case for the variants found in patients G18 and G23. For the RAS isoforms it has been shown repeatedly that mutations at corresponding positions have similar functional impact on the protein (Ahmadian et al. 1999, Aoki et al. 2005, Cirstea et al. 2010, Fasano et al. 1984, Gremer et al. 2010, Gremer et al. 2011, Schubert et al. 2006). The same may be true for *SOS1* and *SOS2*, but corresponding mutations have not been described for all variants found in this study.

The clinical data of the patients from this study with likely pathogenic or pathogenic variants and our international collaboration published in Cordeddu et al. are shown in comparison to the clinical data from Yamamoto et al. in Table 4.8 (Cordeddu et al. 2015, Yamamoto et al. 2015).

	Yamamoto, 2015	This study	Total	Percent
n	5	9	14	
Males/Females	1/4	4/5	5/9	
Median age (in years)	13	13	13	
Prenatal abnormalities	ND	4/4	4/4	100%
Polyhydramnios	ND	3/4	3/4	75%
Nuchal edema	ND	2/4	2/4	50%
Fetal chylothorax/hydrops	ND	1/4	1/4	25%
Feeding difficulties	ND	3/5	3/5	60%
Cardiac anomaly	3/5	5/8	8/13	62%
Pst	1/5	2/8	3/13	23%
ASD/VSD	1/5	4/8	5/13	38%
HCM	0/5	1/8	1/13	8%
Acquired lymphatic disorder	ND	4/8	4/8	50%
Short stature	1/4	2/8	3/12	25%
Motor delay	2/5	1/8	3/13	23%
Intellectual/learning disabilities	2/5	2/8	4/13	31%
Cryptorchidism in males	1/1	3/3	4/4	100%
Keratosis pilaris	3/5	4/8	7/13	54%
Pectus deformity	0/5	6/8	6/13	46%
Short/broad/webbed neck	5/5	5/7	10/12	83%
Ocular ptosis	ND	6/8	6/8	75%
Bleeding diathesis	2/2	1/7	3/9	33%
Neoplasia (benign and malignant)	0/5	1/9	1/14	7%

Table 4.8: Clinical Data of patients with *SOS2* mutations. This table shows the clinical data from all *SOS2* publications and the data compiled in this study.

The clinical data is comparable from the two cohorts in respect to cardiac anomalies, short stature, and developmental delay. Clinically the patients have been described with typical NS had many similarities to what is specifically known for patients with *SOS1* mutations, but mutations in *SOS2* are much rarer (Cordeddu et al. 2015). Thus the size of the cohort is currently too small to draw conclusions about genotype-phenotype correlations. The role of mutations in *SOS2* as a rare cause for RASopathies has been confirmed also in our cohort. The characterization of the new variants found here has been shown in chapter 3.1.4 and for the variants identified as VUS further evidence and functional studies are necessary to characterize these variants fully.

Yamamoto and colleagues also identified variants in *LZTR1* in patients with an NS phenotype (Yamamoto et al. 2015). Somatic mutations of this gene had previously been described in patients with glioblastoma, and germline mutations in patients with schwannomatosis (Piotrowski et al. 2014). Functionally the effect of NS-associated variants on the RAS/MAPK

pathway has not been analyzed. Thus it is unknown if they increase RAS/MAPK signaling, which would be expected for a RASopathy (Tidyman and Rauen 2016). In our cohort we identified 13 patients with variants in this gene (see Table 4.9).

ID	Variant(s)	Segregation	Publication	Classification
G01	p.Arg284Cys	unknown	NS (Yamamoto et al. 2015)	Pathogenic
G02	p.Arg688Gly	unknown	Schwannomatosis (p.Arg688Cys, (Piotrowski et al. 2014))	Likely pathogenic
G03	p.Arg283Gln	unknown	None	VUS
G04	p.Arg170Gln	unknown	None	VUS
G05	p.His121Asp/ p.Arg755Gln	Paternal / Maternal	None	VUS/VUS
G06	p.Arg170Trp		None	VUS
G07	p.Ile205Thr(hom)/ p.Arg170Trp(hom)	Mother and father heterozygous for both	None	VUS/VUS
G08	p.Arg284Cys	unknown	NS (Yamamoto et al. 2015)	Pathogenic
G09	p.Met91Val	unknown	None	VUS
G10	p.Arg697Glu/ c.2407-2A>G	Paternal / Maternal	None	VUS/VUS
G11	p.Gln832Arg	Maternal	None	VUS
G12	p.Arg283Gln	unknown	None	VUS
G23	p.Arg619His(hom)	unknown	None	VUS

Table 4.9: LZTR1 variants. This table shows the LZTR1 variants found in this study with the segregation in the specific case, the publication in either patients with NS or schwannomatosis, and the classification according to ACMG criteria.

In the cohort published by Yamamoto and colleagues heart defects were identified in 8 out of 12 (67%) of individuals, which is less frequent compared to our cohort with *LZTR1* variants (11 out of 12 (92%)). Short stature was found in only 4 out of 13 (31%) individuals by Yamamoto and colleagues, but in 7 out of 10 (70%) individuals in our cohort and developmental delay was reported in our cohort in 9 out of 10 (90%) compared to 2 out of 13 (15%) in the published cohort (Yamamoto et al. 2015). These discrepancies may be due to the small sample size or because not all of the patients in our cohort have disease-causing variants in *LZTR1*.

For most patients only one variant was found, but in four of them biallelic (compound heterozygous or homozygous) variants were identified. In patient G05 and G10 two variants were identified and each inherited from a parent, meaning that the variants are in a compound heterozygous state. A homozygous variant was found in a patient G23, who also has an unknown *SOS2* variant. Two homozygous variants were identified in patient G07. One of

these variants was also found in another patient in a heterozygous state. These observations would be compatible with recessive inheritance in some instances of *LZTR1*-associated NS. Homozygous or compound heterozygous mutations in other RASopathy genes are generally not seen in patients with NS and related conditions. One case has been published with an early fetal death and a compound heterozygous state of *PTPN11* mutations (Becker et al. 2007). Thus it is assumed that biallelic mutations of one of the established RASopathy genes are probably not compatible with life. However, the existence of a subtype of NS with autosomal recessive inheritance had already been proposed before the first gene for NS was published (van Der Burgt and Brunner 2000). It has not been confirmed until now. In the majority of our patients with *LZTR1* variants these were only on one allele, thus suggesting autosomal dominant inheritance as initially published for *LZTR1*-related NS. Some of the variants identified have been described previously either with NS or with schwannomatosis. While our results strongly support *LZTR1* being a novel gene for NS, the genetic and molecular basis of dominant and recessive mutations as well as the relation with schwannomatosis is incompletely understood. Also the precise pathogenic mechanisms for *LZTR1* mutations have remained unclear and further studies will be necessary for elucidation of these open questions.

The gene *PPP1CB* has also been identified through exome sequencing being associated with a Noonan-like disorder (Gripp et al. 2016). Gripp et al identified two variants in four unrelated patients. The patients were found to share similarities with the phenotype of *SHOC2* patients. Three of the individuals had slow growing hair, but even though three patients had short stature, a GH deficiency has not been reported. They also did not show generalized hyperpigmentation or hyperkeratosis often seen in patients with a *SHOC2* mutation (Gripp et al. 2016). They did however have ocular anomalies and macrocephaly with enlarged ventricles and arachnoid spaces as seen in patients with *SHOC2* mutations (Baldassarre et al. 2014, Gripp et al. 2013). Since the initial publication further patients have been identified to carry a mutation in *PPP1CB* which enhances the evidence that this is really a new RASopathy gene (Bertola et al. 2017, Zambrano et al. 2017). *PPP1CB* was not included in the NGS panel used in the study presented here, because it was not known as a RASopathy gene at the time of the design of the enrichment kit. Therefore, our cohort has not yet been screened for mutations in this gene.

More recently a mutation in the gene *MRAS* was identified through exome sequencing of a patient and her parents (Higgins et al. 2017). The variant c.68G>T (p.(Gly23Val)) was identified in the patient and absent on both parents. Higgins et al. also analyzed the *MRAS*

gene by targeted sequencing in a cohort of 109 additional patients and found a second patient with an *MRAS* variant (c.203C>T (p.(Thr68Ile)) (Higgins et al. 2017). Interestingly both patients had HCM. The positions affected by NS-associated mutations in *MRAS*, p.Gly23 and p.Thr68, correspond to the known mutation hotspots p.Gly13 and p.Thr58, respectively, in *HRAS*, *KRAS* and *NRAS* isoforms ((Gripp et al. 2010); this study). *MRAS* was included as an obvious candidate gene in our NGS panel. The analysis of this gene in 144 patients did not detect either of the published mutations, nor other variants affecting positions that are known mutational hotspots in other *RAS* isoforms. One patient was found to have a c.16G>A (p.(Val6Ile)) variant. This variant is not present in the ClinVar database and was found on one allele out of 120912 in ExAc. Valine at position 6 of *MRAS* has no corresponding amino acid in *HRAS*, *KRAS* or *NRAS* (Higgins et al. 2017). This variant would thus be classified as a variant of unknown significance. Testing of parental DNAs is pending, and if the variant can be proven to be *de novo*, functional studies will be helpful to determine its validity.

The *RAS*/MAPK pathway and its relation to *RAS*opathies as shown in the beginning of this dissertation (Figure 1.1) has experienced substantial further evolution during the time of this thesis and the work presented here has made significant contributions to this evolution. Figure 4.2 shows the pathway and associated phenotypes in a revised version including the more recently established genes.

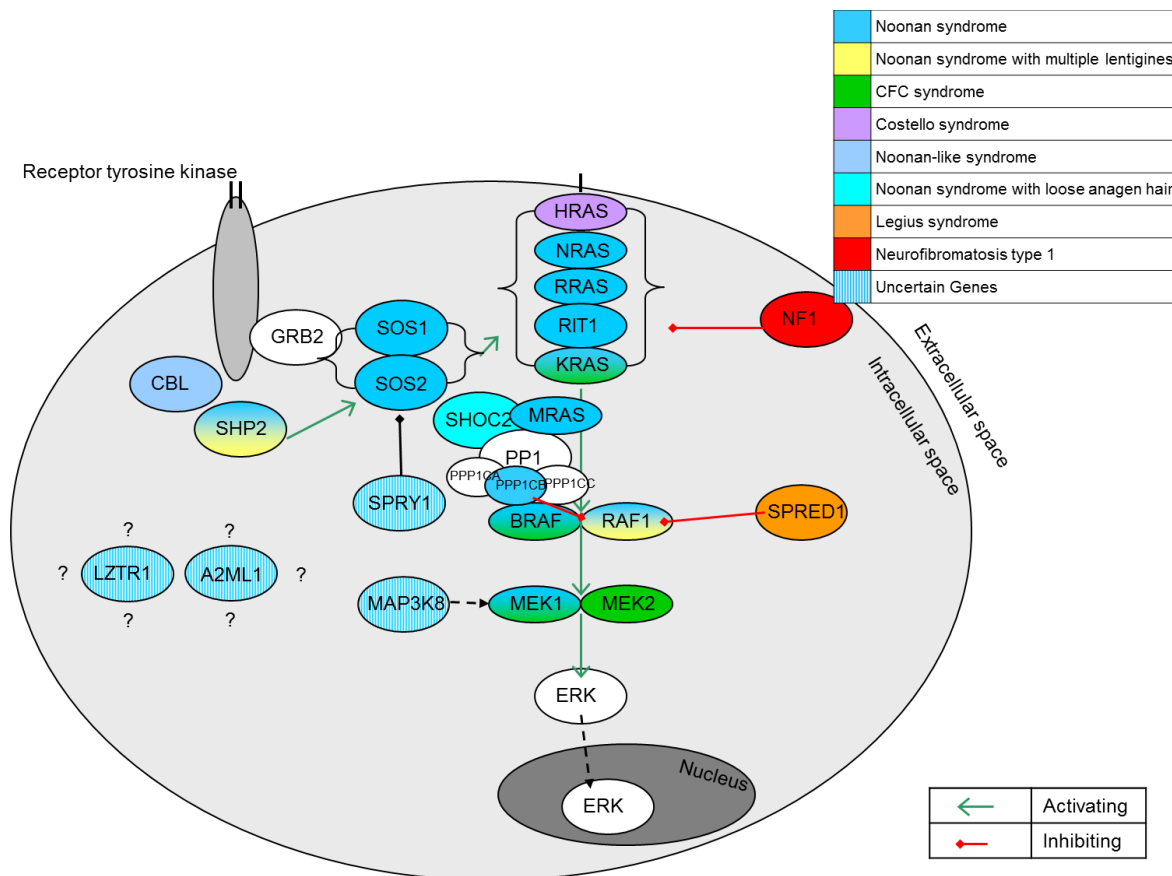


Figure 4.2: The new RAS/MAPK pathway. Shown here is the RAS/MAPK pathway including all genes in which mutations have been associated with RASopathies. The exact function and localization of LZTR1 and A2ML1 in this pathway are unknown.

In conclusion, the experience made during this study underscore the importance of a careful analysis of all variants, including also a critical reappraisal of variants previously published as disease-causing mutations in order to prevent false diagnoses and premature conclusions. Novel findings may challenge the pathogenicity of a variant, the proposed mode of inheritance (as suggested for *LZTR1*), and even the causality of a gene (as suggested for *A2ML1*). The ACMG criteria provide rules for classification of the pathogenicity of novel variants, which are rather conservative. They may underestimate pathogenicity of variants in genes where no previous mutations are known, but they prevent premature classification as disease-causing mutations. This is reflected by a relatively high number of variants in novel genes identified through this study, which just receive a classification as VUS. The quality of clinical phenotyping of the patients is also vital. The identification of new candidate mutations in individuals whose phenotype is not specific for a RASopathy is insufficient for establishing a new RASopathy gene. The existence of a functional link to the RAS/MAPK pathway is the hallmark for genes causing RASopathies. Thus for new genes it is important to assess their

functional impact on this pathway. This is not understood sufficiently for genes like *LZTR1* and particularly *A2ML1*.

4.6. Conclusion and outlook

The work of this PhD thesis has significantly contributed to the delineation of phenotypes and molecular understanding of RASopathies. The NSEuroNet database established in the frame of this thesis has proven to be a great asset in determining genotype-phenotype correlations in RASopathies. Standardized data collection has been used for the cohorts with *SHOC2*, *RIT1* and *NRAS* mutations and for each of these a more specific phenotype could be determined. The same is to be done for other genes and may be interesting for the newer genes as patient numbers increase. This kind of analysis overcomes the strong limitations of metaanalyses of published phenotype data, which are caused by lack of standardization.

The cohort of patients with *SHOC2* mutations is a genetically homogenous cohort with the prominent features of LAH, short stature often with GH deficiency, and ectodermal anomalies. The cohort of patients with *RIT1* mutations is noticeable by the high prevalence of HCM, lymphatic anomalies, and possible increased risk of cancer. Affected individuals less frequently have short stature. The spectrum of *RIT1* mutations was expanded as a result of this thesis. The cohort of patients with *NRAS* mutations mainly resembles the average NS cohort. Specific genotype-phenotype correlations have not emerged, yet, but this could also be due to a still quite low number of patients. It was shown that mutations at G12 are compatible with life, although the phenotype may be more severe for these patients. Patients with *CBL* mutations were found to have prenatal symptoms that are part of the RASopathy phenotype, which enhances the evidence that *CBL* really is a RASopathy gene.

The NSEuroNet database will be further updated with published mutations to preserve this function. Moreover new functions will be added to the database to allow individual submitters to analyze their data in more detail and a link to the ClinVar database will be added to make this data readily available for users.

It was shown in this study cohort that, while most mutations are found in the known hot spot regions of the genes, some may also be in parts of genes that might not have been considered when mutation screening by Sanger sequencing was used. Thus complete analysis of all exons in a gene is preferable, which can be easily achieved today by using the NGS technology. We have also seen in this cohort, that a mutation may be missed in Sanger sequencing due to currently unknown reasons. The most comprehensive analysis for patients with a RASopathy

phenotype is NGS panels. The classification of new variants is extremely important and appropriate guidelines are in place. More new variants will be identified in the future. The possible identification and suitable classification of these variants will help in diagnosis and patient counseling.

The critical review of newly identified genes also remains important. Through exome sequencing possible new genes are identified, but the connection to RASopathies is not always clear. The clinical phenotype of the patients needs to be convincing and the mutation should have a functional impact on the RAS/MAPK pathway as minimum requirements to be considered as causative for a RASopathy. The same is true for contiguous gene deletions or duplications, which have been shown to be too unspecific for a RASopathy diagnosis.

5. REFERENCES

- (1988) National Institutes of Health Consensus Development Conference Statement: neurofibromatosis. Bethesda, Md., USA, July 13-15, 1987. *Neurofibromatosis*, 1, 172-8.
- (2014) Comprehensive molecular profiling of lung adenocarcinoma. *Nature*, 511, 543-50.
- Adzhubei, I., D. M. Jordan & S. R. Sunyaev (2013) Predicting functional effect of human missense mutations using PolyPhen-2. *Current protocols in human genetics / editorial board, Jonathan L. Haines ... [et al.]*, Chapter 7, Unit 7 20.
- Adzhubei, I. A., S. Schmidt, L. Peshkin, V. E. Ramensky, A. Gerasimova, P. Bork, . . . S. R. Sunyaev (2010) A method and server for predicting damaging missense mutations. *Nature methods*, 7, 248-9.
- Agresti, A. (1992) A Survey of Exact Inference for Contingency Tables. 131-153.
- Ahmadian, M. R., T. Zor, D. Vogt, W. Kabsch, Z. Selinger, A. Wittinghofer & K. Scheffzek (1999) Guanosine triphosphatase stimulation of oncogenic Ras mutants. *Proceedings of the National Academy of Sciences of the United States of America*, 96, 7065-70.
- Allanson, J. E., J. G. Hall & M. I. Van Allen (1985) Noonan phenotype associated with neurofibromatosis. *American journal of medical genetics*, 21, 457-62.
- Altmuller, F., C. Lissewski, D. Bertola, E. Flex, Z. Stark, S. Spranger, . . . M. Zenker (2017) Genotype and phenotype spectrum of NRAS germline variants. *European journal of human genetics : EJHG*.
- Aoki, Y., T. Niihori, T. Banjo, N. Okamoto, S. Mizuno, K. Kurosawa, . . . Y. Matsubara (2013) Gain-of-function mutations in RIT1 cause Noonan syndrome, a RAS/MAPK pathway syndrome. *American journal of human genetics*, 93, 173-80.
- Aoki, Y., T. Niihori, H. Kawame, K. Kurosawa, H. Ohashi, Y. Tanaka, . . . Y. Matsubara (2005) Germline mutations in HRAS proto-oncogene cause Costello syndrome. *Nature genetics*, 37, 1038-40.
- Bader-Meunier, B., H. Cave, N. Jeremiah, A. Magerus, N. Lanzarotti, F. Rieux-Laucat & V. Cormier-Daire (2013) Are RASopathies new monogenic predisposing conditions to the development of systemic lupus erythematosus? Case report and systematic review of the literature. *Seminars in arthritis and rheumatism*, 43, 217-9.
- Baldassarre, G., A. Mussa, E. Banaudi, C. Rossi, M. Tartaglia, M. Silengo & G. B. Ferrero (2014) Phenotypic variability associated with the invariant SHOC2 c.4A>G (p.Ser2Gly) missense mutation. *American journal of medical genetics. Part A*, 164A, 3120-5.
- Baldassarre, G., A. Mussa, A. Dotta, E. Banaudi, S. Forzano, A. Marinosci, . . . G. B. Ferrero (2011) Prenatal features of Noonan syndrome: prevalence and prognostic value. *Prenatal diagnosis*, 31, 949-54.
- Bamford, S., E. Dawson, S. Forbes, J. Clements, R. Pettett, A. Dogan, . . . R. Wooster (2004) The COSMIC (Catalogue of Somatic Mutations in Cancer) database and website. *British journal of cancer*, 91, 355-8.
- Becker, K., H. Hughes, K. Howard, M. Armstrong, D. Roberts, E. J. Lazda, . . . M. Tartaglia (2007) Early fetal death associated with compound heterozygosity for Noonan syndrome-causative PTPN11 mutations. *American journal of medical genetics. Part A*, 143A, 1249-52.
- Beke, A., J. G. Joo, A. Csaba, L. Lazar, Z. Ban, C. Papp, . . . Z. Papp (2009) Incidence of chromosomal abnormalities in the presence of fetal subcutaneous oedema, such as nuchal oedema, cystic hygroma and non-immune hydrops. *Fetal diagnosis and therapy*, 25, 83-92.
- Beneteau, C., H. Cave, A. Moncla, N. Dorison, A. Munnich, A. Verloes & B. Leheup (2009) SOS1 and PTPN11 mutations in five cases of Noonan syndrome with multiple giant cell lesions. *European journal of human genetics : EJHG*, 17, 1216-21.
- Bentires-Alj, M., M. I. Kontaridis & B. G. Neel (2006) Stops along the RAS pathway in human genetic disease. *Nature medicine*, 12, 283-5.
- Berger, A. H., M. Imielinski, F. Duke, J. Wala, N. Kaplan, G. X. Shi, . . . M. Meyerson (2014) Oncogenic RIT1 mutations in lung adenocarcinoma. *Oncogene*, 33, 4418-23.
- Bertola, D., G. Yamamoto, M. Buscarilli, A. Jorge, M. R. Passos-Bueno & C. Kim (2017) The recurrent PPP1CB mutation p.Pro49Arg in an additional Noonan-like syndrome individual: Broadening the clinical phenotype. *American journal of medical genetics. Part A*, 173, 824-828.

- Bertola, D. R., G. L. Yamamoto, T. F. Almeida, M. Buscarilli, A. A. Jorge, A. C. Malaquias, . . . A. C. Pereira (2014) Further evidence of the importance of RIT1 in Noonan syndrome. *American journal of medical genetics. Part A*, 164A, 2952-7.
- Bianchessi, D., S. Morosini, V. Saletti, M. C. Ibba, F. Natacci, S. Esposito, . . . M. Eoli (2015) 126 novel mutations in Italian patients with neurofibromatosis type 1. *Molecular genetics & genomic medicine*, 3, 513-25.
- Boriack-Sjodin, P. A., S. M. Margarit, D. Bar-Sagi & J. Kuriyan (1998) The structural basis of the activation of Ras by Sos. *Nature*, 394, 337-43.
- Bowen, M. E., E. D. Boyden, I. A. Holm, B. Campos-Xavier, L. Bonafe, A. Superti-Furga, . . . M. L. Warman (2011) Loss-of-function mutations in PTPN11 cause metachondromatosis, but not Ollier disease or Maffucci syndrome. *PLoS genetics*, 7, e1002050.
- Brady, A. F., C. R. Jamieson, I. van der Burgt, A. Crosby, M. van Reen, H. Kremer, . . . S. Jeffery (1997) Further delineation of the critical region for noonan syndrome on the long arm of chromosome 12. *European journal of human genetics : EJHG*, 5, 336-7.
- Brems, H., M. Chmara, M. Sahbatou, E. Denayer, K. Taniguchi, R. Kato, . . . E. Legius (2007) Germline loss-of-function mutations in SPRED1 cause a neurofibromatosis 1-like phenotype. *Nature genetics*, 39, 1120-6.
- Brems, H. & E. Legius (2013) Legius syndrome, an Update. Molecular pathology of mutations in SPRED1. *The Keio journal of medicine*, 62, 107-12.
- Brosius, S. (2010) A history of von Recklinghausen's NF1. *Journal of the history of the neurosciences*, 19, 333-48.
- Bulow, L., C. Lissewski, R. Bressel, A. Rauch, Z. Stark, M. Zenker & O. Bartsch (2015) Hydrops, fetal pleural effusions and chylothorax in three patients with CBL mutations. *American journal of medical genetics. Part A*, 167A, 394-9.
- Calcagni, G., A. Baban, F. R. Lepri, B. Marino, M. Tartaglia & M. C. Digilio (2016) Congenital heart defects in Noonan syndrome and RIT1 mutation. *Genetics in medicine : official journal of the American College of Medical Genetics*, 18, 1320.
- Capalbo, D., D. Melis, L. De Martino, L. Palamaro, S. Riccomagno, G. Bona, . . . M. Salerno (2012) Noonan-like syndrome with loose anagen hair associated with growth hormone insensitivity and atypical neurological manifestations. *American journal of medical genetics. Part A*, 158A, 856-60.
- Cave, H., A. Caye, N. Ghedira, Y. Capri, N. Pouvreau, N. Fillot, . . . A. Verloes (2016) Mutations in RIT1 cause Noonan syndrome with possible juvenile myelomonocytic leukemia but are not involved in acute lymphoblastic leukemia. *European journal of human genetics : EJHG*, 24, 1124-31.
- Cawthon, R. M., R. Weiss, G. F. Xu, D. Viskochil, M. Culver, J. Stevens, . . . et al. (1990) A major segment of the neurofibromatosis type 1 gene: cDNA sequence, genomic structure, and point mutations. *Cell*, 62, 193-201.
- Caye, A., M. Strullu, F. Guidez, B. Cassinat, S. Gazal, O. Fenneteau, . . . H. Cave (2015) Juvenile myelomonocytic leukemia displays mutations in components of the RAS pathway and the PRC2 network. *Nature genetics*, 47, 1334-40.
- Chang, J., L. Zhao, C. Chen, Y. Peng, Y. Xia, G. Tang, . . . L. Wu (2015) Pachygyria, seizures, hypotonia, and growth retardation in a patient with an atypical 1.33Mb inherited microduplication at 22q11.23. *Gene*, 569, 46-50.
- Chen, C. H., T. H. Chen, S. J. Kuo, C. P. Chen, D. J. Lee, Y. Y. Ke, . . . M. Chen (2009) Genetic evaluation and management of fetal chylothorax: review and insights from a case of Noonan syndrome. *Lymphology*, 42, 134-8.
- Chen, J. L., X. Zhu, T. L. Zhao, J. Wang, Y. F. Yang & Z. P. Tan (2014a) Rare copy number variations containing genes involved in RASopathies: deletion of SHOC2 and duplication of PTPN11. *Molecular cytogenetics*, 7, 28.
- Chen, P. C., J. Yin, H. W. Yu, T. Yuan, M. Fernandez, C. K. Yung, . . . R. Kucherlapati (2014b) Next-generation sequencing identifies rare variants associated with Noonan syndrome. *Proceedings of the National Academy of Sciences of the United States of America*, 111, 11473-8.
- Choi, J. H., M. Y. Oh, M. S. Yum, B. H. Lee, G. H. Kim & H. W. Yoo (2015) Moyamoya syndrome in a patient with Noonan-like syndrome with loose anagen hair. *Pediatric neurology*, 52, 352-5.
- Ciara, E., M. Pelc, D. Jurkiewicz, M. Kugaudo, D. Gieruszczak-Bialek, A. Skorka, . . . M. Krajewska-Walasek (2015) Is diagnosing cardio-facio-cutaneous (CFC) syndrome still a challenge?

- Delineation of the phenotype in 15 Polish patients with proven mutations, including novel mutations in the BRAF1 gene. *European journal of medical genetics*, 58, 14-20.
- Cin, H., C. Meyer, R. Herr, W. G. Janzarik, S. Lambert, D. T. Jones, . . . S. M. Pfister (2011) Oncogenic FAM131B-BRAF fusion resulting from 7q34 deletion comprises an alternative mechanism of MAPK pathway activation in pilocytic astrocytoma. *Acta neuropathologica*, 121, 763-74.
- Cirstea, I. C., K. Kutsche, R. Dvorsky, L. Gremer, C. Carta, D. Horn, . . . M. Zenker (2010) A restricted spectrum of NRAS mutations causes Noonan syndrome. *Nature genetics*, 42, 27-9.
- Cizmarova, M., K. Hlinkova, S. Bertok, P. Kotnik, H. C. Duba, R. Bertalan, . . . D. Ilencikova (2016) New Mutations Associated with Rasopathies in a Central European Population and Genotype-Phenotype Correlations. *Annals of human genetics*, 80, 50-62.
- Coppinger, J., D. McDonald-McGinn, E. Zackai, K. Shane, J. F. Atkin, A. Asamoah, . . . L. G. Shaffer (2009) Identification of familial and de novo microduplications of 22q11.21-q11.23 distal to the 22q11.21 microdeletion syndrome region. *Human molecular genetics*, 18, 1377-83.
- Cordeddu, V., E. Di Schiavi, L. A. Pennacchio, A. Ma'ayan, A. Sarkozy, V. Fodale, . . . M. Tartaglia (2009) Mutation of SHOC2 promotes aberrant protein N-myristoylation and causes Noonan-like syndrome with loose anagen hair. *Nature genetics*, 41, 1022-6.
- Cordeddu, V., J. C. Yin, C. Gunnarsson, C. Virtanen, S. Drunat, F. Lepri, . . . M. Tartaglia (2015) Activating Mutations Affecting the Dbl Homology Domain of SOS2 Cause Noonan Syndrome. *Human mutation*.
- Coso, S., E. Bovay & T. V. Petrova (2014) Pressing the right buttons: signaling in lymphangiogenesis. *Blood*, 123, 2614-24.
- Costello, J. M. (1977) A new syndrome: mental subnormality and nasal papillomata. *Australian paediatric journal*, 13, 114-8.
- Croonen, E. A., W. Nillesen, C. Schrandt, M. Jongmans, H. Scheffer, C. Noordam, . . . H. G. Yntema (2013) Noonan syndrome: comparing mutation-positive with mutation-negative dutch patients. *Molecular syndromology*, 4, 227-34.
- da Silva, F. M., A. A. Jorge, A. Malaquias, A. da Costa Pereira, G. L. Yamamoto, C. A. Kim & D. Bertola (2016) Nutritional aspects of Noonan syndrome and Noonan-related disorders. *American journal of medical genetics. Part A*, 170, 1525-31.
- De Filippi, P., M. Zecca, D. Lisini, V. Rosti, C. Cagioni, C. Carlo-Stella, . . . C. Danesino (2009) Germ-line mutation of the NRAS gene may be responsible for the development of juvenile myelomonocytic leukaemia. *British journal of haematology*, 147, 706-9.
- Denayer, E., H. Peeters, L. Sevenants, M. Derbent, J. P. Fryns & E. Legius (2012) NRAS Mutations in Noonan Syndrome. *Molecular syndromology*, 3, 34-38.
- Digilio, M. C., E. Conti, A. Sarkozy, R. Mingarelli, T. Dottorini, B. Marino, . . . B. Dallapiccola (2002) Grouping of multiple-lentigines/LEOPARD and Noonan syndromes on the PTPN11 gene. *American journal of human genetics*, 71, 389-94.
- Digilio, M. C., F. Lepri, A. Baban, M. L. Dentici, P. Versacci, R. Capolino, . . . B. Dallapiccola (2011) RASopathies: Clinical Diagnosis in the First Year of Life. *Molecular syndromology*, 1, 282-289.
- Ekvall, S., L. Hagenas, J. Allanson, G. Anneren & M. L. Bondeson (2011) Co-occurring SHOC2 and PTPN11 mutations in a patient with severe/complex Noonan syndrome-like phenotype. *American journal of medical genetics. Part A*, 155A, 1217-24.
- Ekvall, S., M. Wilbe, J. Dahlgren, E. Legius, A. van Haeringen, O. Westphal, . . . M. L. Bondeson (2015) Mutation in NRAS in familial Noonan syndrome--case report and review of the literature. *BMC medical genetics*, 16, 95.
- Estep, A. L., W. E. Tidyman, M. A. Teitell, P. D. Cotter & K. A. Rauen (2006) HRAS mutations in Costello syndrome: detection of constitutional activating mutations in codon 12 and 13 and loss of wild-type allele in malignancy. *American journal of medical genetics. Part A*, 140, 8-16.
- Farrell, S. A., L. J. Warda, P. LaFlair & W. Szymonowicz (1993) Adams-Oliver syndrome: a case with juvenile chronic myelogenous leukemia and chylothorax. *American journal of medical genetics*, 47, 1175-9.
- Fasano, O., T. Aldrich, F. Tamanoi, E. Taparowsky, M. Furth & M. Wigler (1984) Analysis of the transforming potential of the human H-ras gene by random mutagenesis. *Proceedings of the National Academy of Sciences of the United States of America*, 81, 4008-12.
- Fernandez Alvarez, J. R., K. D. Kalache & E. L. Grauel (1999) Management of spontaneous congenital chylothorax: oral medium-chain triglycerides versus total parenteral nutrition. *American journal of perinatology*, 16, 415-20.

- Ferrero, G. B., G. Picco, G. Baldassarre, E. Flex, C. Isella, D. Cantarella, . . . E. Medico (2012) Transcriptional hallmarks of Noonan syndrome and Noonan-like syndrome with loose anagen hair. *Human mutation*, 33, 703-9.
- Flex, E., M. Jaiswal, F. Pantaleoni, S. Martinelli, M. Strullu, E. K. Fansa, . . . M. Tartaglia (2014) Activating mutations in RRAS underlie a phenotype within the RASopathy spectrum and contribute to leukaemogenesis. *Human molecular genetics*, 23, 4315-27.
- Fokkema, I. F., P. E. Taschner, G. C. Schaafsma, J. Celli, J. F. Laros & J. T. den Dunnen (2011) LOVD v.2.0: the next generation in gene variant databases. *Human mutation*, 32, 557-63.
- Forbes, S. A., D. Beare, P. Gunasekaran, K. Leung, N. Bindal, H. Boutselakis, . . . P. J. Campbell (2015) COSMIC: exploring the world's knowledge of somatic mutations in human cancer. *Nucleic acids research*, 43, D805-11.
- Garavelli, L., V. Cordeddu, S. Errico, P. Bertolini, M. E. Street, S. Rosato, . . . M. Tartaglia (2015) Noonan syndrome-like disorder with loose anagen hair: a second case with neuroblastoma. *American journal of medical genetics. Part A*, 167A, 1902-7.
- Gargano, G., I. Guidotti, E. Balestri, F. Vagnarelli, S. Rosato, G. Comitini, . . . L. Garavelli (2014) Hydrops fetalis in a preterm newborn heterozygous for the c.4A>G SHOC2 mutation. *American journal of medical genetics. Part A*, 164A, 1015-20.
- Gelb, B. D., A. E. Roberts & M. Tartaglia (2015) Cardiomyopathies in Noonan syndrome and the other RASopathies. *Progress in pediatric cardiology*, 39, 13-19.
- Gomez-Segui, I., H. Makishima, A. Jerez, K. Yoshida, B. Przychodzen, S. Miyano, . . . J. P. Maciejewski (2013) Novel recurrent mutations in the RAS-like GTP-binding gene RIT1 in myeloid malignancies. *Leukemia : official journal of the Leukemia Society of America, Leukemia Research Fund, U.K.*, 27, 1943-6.
- Gorlin, R. J., R. C. Anderson & M. Blaw (1969) Multiple lentigenes syndrome. *American journal of diseases of children*, 117, 652-62.
- Gos, M., S. Fahiminiya, J. Poznanski, J. Klapecki, E. Obersztyn, M. Piotrowicz, . . . J. Majewski (2014) Contribution of RIT1 mutations to the pathogenesis of Noonan syndrome: four new cases and further evidence of heterogeneity. *American journal of medical genetics. Part A*, 164A, 2310-6.
- Gräfe, D. 2016. Ped(z).
- Graham, J. M., Jr., N. Kramer, B. A. Bejjani, C. T. Thiel, C. Carta, G. Neri, . . . M. Zenker (2009) Genomic duplication of PTPN11 is an uncommon cause of Noonan syndrome. *American journal of medical genetics. Part A*, 149A, 2122-8.
- Gremer, L., A. De Luca, T. Merbitz-Zahradnik, B. Dallapiccola, S. Morlot, M. Tartaglia, . . . G. Rosenberger (2010) Duplication of Glu37 in the switch I region of HRAS impairs effector/GAP binding and underlies Costello syndrome by promoting enhanced growth factor-dependent MAPK and AKT activation. *Human molecular genetics*, 19, 790-802.
- Gremer, L., T. Merbitz-Zahradnik, R. Dvorsky, I. C. Cirstea, C. P. Kratz, M. Zenker, . . . M. R. Ahmadian (2011) Germline KRAS mutations cause aberrant biochemical and physical properties leading to developmental disorders. *Human mutation*, 32, 33-43.
- Gripp, K. W., K. A. Aldinger, J. T. Bennett, L. Baker, J. Tusi, N. Powell-Hamilton, . . . W. B. Dobyns (2016) A novel rasopathy caused by recurrent de novo missense mutations in PPP1CB closely resembles Noonan syndrome with loose anagen hair. *American journal of medical genetics. Part A*, 170, 2237-47.
- Gripp, K. W., E. Hopkins, D. Doyle & W. B. Dobyns (2010) High incidence of progressive postnatal cerebellar enlargement in Costello syndrome: brain overgrowth associated with HRAS mutations as the likely cause of structural brain and spinal cord abnormalities. *American journal of medical genetics. Part A*, 152A, 1161-8.
- Gripp, K. W., E. Hopkins, K. Sol-Church, D. L. Stabley, M. E. Axelrad, D. Doyle, . . . A. E. Lin (2011) Phenotypic analysis of individuals with Costello syndrome due to HRAS p.G13C. *American journal of medical genetics. Part A*, 155A, 706-16.
- Gripp, K. W., A. M. Innes, M. E. Axelrad, T. L. Gillan, J. S. Parboosingh, C. Davies, . . . K. Sol-Church (2008) Costello syndrome associated with novel germline HRAS mutations: an attenuated phenotype? *American journal of medical genetics. Part A*, 146A, 683-90.
- Gripp, K. W., D. J. Zand, L. Demmer, C. E. Anderson, W. B. Dobyns, E. H. Zackai, . . . K. Sol-Church (2013) Expanding the SHOC2 mutation associated phenotype of Noonan syndrome with loose anagen hair: structural brain anomalies and myelofibrosis. *American journal of medical genetics. Part A*, 161A, 2420-30.

- Gutmann, D. H., R. E. Ferner, R. H. Listernick, B. R. Korf, P. L. Wolters & K. J. Johnson (2017) Neurofibromatosis type 1. *Nature reviews. Disease primers*, 3, 17004.
- Gutmann, D. H., D. L. Wood & F. S. Collins (1991) Identification of the neurofibromatosis type 1 gene product. *Proceedings of the National Academy of Sciences of the United States of America*, 88, 9658-62.
- Hannig, V., M. Jeoung, E. R. Jang, J. A. Phillips, 3rd & E. Galperin (2014) A Novel SHOC2 Variant in Rasopathy. *Human mutation*, 35, 1290-4.
- Hanson, H. L., M. J. Wilson, J. P. Short, B. A. Chioza, A. H. Crosby, R. M. Nash, . . . S. Mansour (2014) Germline CBL mutation associated with a noonan-like syndrome with primary lymphedema and teratoma associated with acquired uniparental isodisomy of chromosome 11q23. *American journal of medical genetics. Part A*, 164A, 1003-9.
- Hart, T. C., Y. Zhang, M. C. Gorry, P. S. Hart, M. Cooper, M. L. Marazita, . . . D. Pallos (2002) A mutation in the SOS1 gene causes hereditary gingival fibromatosis type 1. *American journal of human genetics*, 70, 943-54.
- Higgins, E. M., J. M. Bos, H. Mason-Suares, D. J. Tester, J. P. Ackerman, C. A. MacRae, . . . M. J. Ackerman (2017) Elucidation of MRAS-mediated Noonan syndrome with cardiac hypertrophy. *JCI insight*, 2, e91225.
- Hiramoto, R., T. Imamura, H. Muramatsu, X. Wang, T. Kanayama, M. Zuiki, . . . H. Hosoi (2015) Serial investigation of PTPN11 mutation in nonhematopoietic tissues in a patient with juvenile myelomonocytic leukemia who was treated with unrelated cord blood transplantation. *International journal of hematology*, 102, 719-22.
- Hoban, R., A. E. Roberts, L. Demmer, R. Jethva & B. Shephard (2012) Noonan syndrome due to a SHOC2 mutation presenting with fetal distress and fatal hypertrophic cardiomyopathy in a premature infant. *American journal of medical genetics. Part A*, 158A, 1411-3.
- Imanishi, D., Y. Miyazaki, R. Yamasaki, Y. Sawayama, J. Taguchi, H. Tsushima, . . . M. Tomonaga (2007) Donor-derived DNA in fingernails among recipients of allogeneic hematopoietic stem-cell transplants. *Blood*, 110, 2231-4.
- Jamieson, C. R., I. van der Burgt, A. F. Brady, M. van Reen, M. M. Elswawi, F. Hol, . . . E. Mariman (1994) Mapping a gene for Noonan syndrome to the long arm of chromosome 12. *Nature genetics*, 8, 357-60.
- Jones, D. T., S. Kocialkowski, L. Liu, D. M. Pearson, L. M. Backlund, K. Ichimura & V. P. Collins (2008) Tandem duplication producing a novel oncogenic BRAF fusion gene defines the majority of pilocytic astrocytomas. *Cancer research*, 68, 8673-7.
- Justino, A., P. Dias, M. Joao Pina, S. Sousa, L. Cirnes, A. Berta Sousa, . . . J. L. Costa (2015) Comprehensive massive parallel DNA sequencing strategy for the genetic diagnosis of the neuro-cardio-facio-cutaneous syndromes. *European journal of human genetics : EJHG*, 23, 347-53.
- Kabbani, M. S., S. Giridhar, M. Elbarbary, M. A. Elgamal, H. Najm & M. Godman (2005) Postoperative cardiac intensive care outcome for Down syndrome children. *Saudi medical journal*, 26, 943-6.
- Karaer, K., C. Lissewski & M. Zenker (2015) Familial cardiofaciocutaneous syndrome in a father and a son with a novel MEK2 mutation. *American journal of medical genetics. Part A*, 167A, 385-8.
- Keilhack, H., F. S. David, M. McGregor, L. C. Cantley & B. G. Neel (2005) Diverse biochemical properties of Shp2 mutants. Implications for disease phenotypes. *The Journal of biological chemistry*, 280, 30984-93.
- Kobayashi, T., Y. Aoki, T. Niihori, H. Cave, A. Verloes, N. Okamoto, . . . Y. Matsubara (2010) Molecular and clinical analysis of RAF1 in Noonan syndrome and related disorders: dephosphorylation of serine 259 as the essential mechanism for mutant activation. *Human mutation*, 31, 284-94.
- Koenighofer, M., C. Y. Hung, J. L. McCauley, J. Dallman, E. J. Back, I. Mihalek, . . . O. A. Bodamer (2016) Mutations in RIT1 cause Noonan syndrome - additional functional evidence and expanding the clinical phenotype. *Clinical genetics*, 89, 359-66.
- Komatsuzaki, S., Y. Aoki, T. Niihori, N. Okamoto, R. C. Hennekam, S. Hopman, . . . Y. Matsubara (2010) Mutation analysis of the SHOC2 gene in Noonan-like syndrome and in hematologic malignancies. *Journal of human genetics*, 55, 801-9.
- Kouz, K., C. Lissewski, S. Spranger, D. Mitter, A. Riess, V. Lopez-Gonzalez, . . . M. Zenker (2016) Genotype and phenotype in patients with Noonan syndrome and a RIT1 mutation. *Genetics in medicine : official journal of the American College of Medical Genetics*, 18, 1226-1234.

- Kraoua, L., H. Journal, P. Bonnet, J. Amiel, N. Pouvreau, C. Baumann, . . . H. Cave (2012) Constitutional NRAS mutations are rare among patients with Noonan syndrome or juvenile myelomonocytic leukemia. *American journal of medical genetics. Part A*, 158A, 2407-11.
- Kratz, C. P., L. Franke, H. Peters, N. Kohlschmidt, B. Kazmierczak, U. Finckh, . . . M. Zenker (2015) Cancer spectrum and frequency among children with Noonan, Costello, and cardio-facio-cutaneous syndromes. *British journal of cancer*, 112, 1392-7.
- Kratz, C. P., C. M. Niemeyer, R. P. Castleberry, M. Cetin, E. Bergstrasser, P. D. Emanuel, . . . M. L. Loh (2005) The mutational spectrum of PTPN11 in juvenile myelomonocytic leukemia and Noonan syndrome/myeloproliferative disease. *Blood*, 106, 2183-5.
- Kromeyer-Hauschild, K., M. Wabitsch, D. Kunze, F. Geller, H. C. Geiß, V. Hesse, . . . J. Hebebrand (2001) Perzentile für den Body-mass-Index für das Kindes- und Jugendalter unter Heranziehung verschiedener deutscher Stichproben. *Monatsschrift Kinderheilkunde*, 149, 807-818.
- Kuczmariski, R. J., C. L. Ogden, S. S. Guo, L. M. Grummer-Strawn, K. M. Flegal, Z. Mei, . . . C. L. Johnson (2002) 2000 CDC Growth Charts for the United States: methods and development. *Vital and health statistics. Series 11, Data from the national health survey*, 1-190.
- Landrum, M. J., J. M. Lee, G. R. Riley, W. Jang, W. S. Rubinstein, D. M. Church & D. R. Maglott (2014) ClinVar: public archive of relationships among sequence variation and human phenotype. *Nucleic acids research*, 42, D980-5.
- Lee, B. H., J. M. Kim, H. Y. Jin, G. H. Kim, J. H. Choi & H. W. Yoo (2011) Spectrum of mutations in Noonan syndrome and their correlation with phenotypes. *The Journal of pediatrics*, 159, 1029-35.
- Lee, K. A., B. Williams, K. Roza, H. Ferguson, K. David, K. Eddleman, . . . R. Kornreich (2009) PTPN11 analysis for the prenatal diagnosis of Noonan syndrome in fetuses with abnormal ultrasound findings. *Clinical genetics*, 75, 190-4.
- Legius, E., E. Schollen, G. Matthijs & J. P. Fryns (1998) Fine mapping of Noonan/cardio-facio cutaneous syndrome in a large family. *European journal of human genetics : EJHG*, 6, 32-7.
- Lepri, F. R., R. Scavelli, M. C. Digilio, M. Gnazzo, S. Grotta, M. L. Dentici, . . . B. Dallapiccola (2014) Diagnosis of Noonan syndrome and related disorders using target next generation sequencing. *BMC medical genetics*, 15, 14.
- Li, B., V. G. Krishnan, M. E. Mort, F. Xin, K. K. Kamati, D. N. Cooper, . . . P. Radivojac (2009) Automated inference of molecular mechanisms of disease from amino acid substitutions. *Bioinformatics*, 25, 2744-50.
- Lisewski, C., S. G. Kant, Z. Stark, I. Schanze & M. Zenker (2015) Copy number variants including RAS pathway genes-How much RASopathy is in the phenotype? *American journal of medical genetics. Part A*.
- Lo, F. S., J. D. Luo, Y. J. Lee, S. G. Shu, M. T. Kuo & C. C. Chiou (2009) High resolution melting analysis for mutation detection for PTPN11 gene: applications of this method for diagnosis of Noonan syndrome. *Clinica chimica acta; international journal of clinical chemistry*, 409, 75-7.
- Lo, F. S., C. J. Wang, M. C. Wong & N. C. Lee (2015) Moyamoya disease in two patients with Noonan-like syndrome with loose anagen hair. *American journal of medical genetics. Part A*, 167, 1285-8.
- Loh, M. L., D. S. Sakai, C. Flotho, M. Kang, M. Fliegau, S. Archambeault, . . . C. M. Niemeyer (2009) Mutations in CBL occur frequently in juvenile myelomonocytic leukemia. *Blood*, 114, 1859-63.
- Lorenz, S., C. Lisewski, P. O. Simsek-Kiper, Y. Alanay, K. Boduroglu, M. Zenker & G. Rosenberger (2013) Functional analysis of a duplication (p.E63_D69dup) in the switch II region of HRAS: new aspects of the molecular pathogenesis underlying Costello syndrome. *Human molecular genetics*, 22, 1643-53.
- Lorenz, S., C. Petersen, U. Kordass, H. Seidel, M. Zenker & K. Kutsche (2012) Two cases with severe lethal course of Costello syndrome associated with HRAS p.G12C and p.G12D. *European journal of medical genetics*, 55, 615-9.
- Luo, C., Y. F. Yang, B. L. Yin, J. L. Chen, C. Huang, W. Z. Zhang, . . . Z. P. Tan (2012) Microduplication of 3p25.2 encompassing RAF1 associated with congenital heart disease suggestive of Noonan syndrome. *American journal of medical genetics. Part A*, 158A, 1918-23.
- Marchuk, D. A., A. M. Saulino, R. Tavakkol, M. Swaroop, M. R. Wallace, L. B. Andersen, . . . F. S. Collins (1991) cDNA cloning of the type 1 neurofibromatosis gene: complete sequence of the NF1 gene product. *Genomics*, 11, 931-40.

- Marino, B., M. C. Digilio, A. Toscano, A. Giannotti & B. Dallapiccola (1999) Congenital heart diseases in children with Noonan syndrome: An expanded cardiac spectrum with high prevalence of atrioventricular canal. *The Journal of pediatrics*, 135, 703-6.
- Martinelli, S., A. De Luca, E. Stellacci, C. Rossi, S. Checquolo, F. Lepri, . . . M. Tartaglia (2010) Heterozygous germline mutations in the CBL tumor-suppressor gene cause a Noonan syndrome-like phenotype. *American journal of human genetics*, 87, 250-7.
- Martinelli, S., E. Stellacci, L. Pannone, D. D'Agostino, F. Consoli, C. Lisewski, . . . M. Tartaglia (2015) Molecular Diversity and Associated Phenotypic Spectrum of Germline CBL Mutations. *Human mutation*, 36, 787-96.
- MayoClinic. 2016. Pulmonary Valve Stenosis.
- MayoClinic. 2017. Hypertrophic Cardiomyopathy.
- Mazzanti, L., E. Cacciari, A. Cicognani, R. Bergamaschi, E. Scarano & A. Forabosco (2003) Noonan-like syndrome with loose anagen hair: a new syndrome? *American journal of medical genetics. Part A*, 118A, 279-86.
- Mazzanti, L., F. Tamburrino, E. Scarano, A. Perri, B. Vestrucci, M. Guidetti, . . . M. Tartaglia (2013) GH Therapy and first final height data in Noonan-like syndrome with loose anagen hair (Mazzanti syndrome). *American journal of medical genetics. Part A*, 161A, 2756-61.
- Mensink, K. A., R. P. Ketterling, H. C. Flynn, R. A. Knudson, N. M. Lindor, B. A. Heese, . . . D. Babovic-Vuksanovic (2006) Connective tissue dysplasia in five new patients with NF1 microdeletions: further expansion of phenotype and review of the literature. *Journal of medical genetics*, 43, e8.
- Messiaen, L. M., T. Callens, G. Mortier, D. Beysen, I. Vandenbroucke, N. Van Roy, . . . A. D. Paeppe (2000) Exhaustive mutation analysis of the NF1 gene allows identification of 95% of mutations and reveals a high frequency of unusual splicing defects. *Human mutation*, 15, 541-55.
- Milosavljevic, D., E. Overwater, S. Tamminga, K. de Boer, M. W. Elting, M. E. van Hoorn, . . . A. C. Houweling (2016) Two cases of RIT1 associated Noonan syndrome: Further delineation of the clinical phenotype and review of the literature. *American journal of medical genetics. Part A*, 170, 1874-80.
- Moerman, P., K. Vandenberghe, H. Devlieger, C. Van Hole, J. P. Fryns & J. M. Lauweryns (1993) Congenital pulmonary lymphangiectasis with chylothorax: a heterogeneous lymphatic vessel abnormality. *American journal of medical genetics*, 47, 54-8.
- Nava, C., N. Hanna, C. Michot, S. Pereira, N. Pouvreau, T. Niihori, . . . H. Cave (2007) Cardio-facio-cutaneous and Noonan syndromes due to mutations in the RAS/MAPK signalling pathway: genotype-phenotype relationships and overlap with Costello syndrome. *Journal of medical genetics*, 44, 763-71.
- Nemcikova, M., S. Vejvalkova, F. Fencel, M. Sukova & A. Krepelova (2016) A novel heterozygous RIT1 mutation in a patient with Noonan syndrome, leukopenia, and transient myeloproliferation-a review of the literature. *European journal of pediatrics*, 175, 587-92.
- Niemeyer, C. M. (2014) RAS diseases in children. *Haematologica*, 99, 1653-62.
- Niemeyer, C. M., M. W. Kang, D. H. Shin, I. Furlan, M. Erlacher, N. J. Bunin, . . . M. L. Loh (2010) Germline CBL mutations cause developmental abnormalities and predispose to juvenile myelomonocytic leukemia. *Nature genetics*, 42, 794-800.
- Niihori, T., Y. Aoki, Y. Narumi, G. Neri, H. Cave, A. Verloes, . . . Y. Matsubara (2006) Germline KRAS and BRAF mutations in cardio-facio-cutaneous syndrome. *Nature genetics*, 38, 294-6.
- Noonan, J. A. (1968) Hypertelorism with Turner phenotype. A new syndrome with associated congenital heart disease. *American journal of diseases of children*, 116, 373-80.
- Noonan, J. A. E., D. A. (1963) Associated noncardiac malformations in children with congenital heart disease. *Journal of Pediatrics*, 63, 468-470.
- Nowaczyk, M. J., B. A. Thompson, S. Zeesman, U. Moog, P. A. Sanchez-Lara, P. L. Magoulas, . . . K. A. Rauen (2013) Deletion of MAP2K2/MEK2: a novel mechanism for a RASopathy? *Clinical genetics*.
- Nystrom, A. M., S. Ekvall, A. C. Thuresson, E. Denayer, E. Legius, M. Kamali-Moghaddam, . . . M. L. Bondeson (2010) Investigation of gene dosage imbalances in patients with Noonan syndrome using multiplex ligation-dependent probe amplification analysis. *European journal of medical genetics*, 53, 117-21.

- Oliveira, J. B., N. Bidere, J. E. Niemela, L. Zheng, K. Sakai, C. P. Nix, . . . M. J. Lenardo (2007) NRAS mutation causes a human autoimmune lymphoproliferative syndrome. *Proceedings of the National Academy of Sciences of the United States of America*, 104, 8953-8.
- Pandit, B., A. Sarkozy, L. A. Pennacchio, C. Carta, K. Oishi, S. Martinelli, . . . B. D. Gelb (2007) Gain-of-function RAF1 mutations cause Noonan and LEOPARD syndromes with hypertrophic cardiomyopathy. *Nature genetics*, 39, 1007-12.
- Perez, B., F. Mechinaud, C. Galambrun, N. Ben Romdhane, B. Isidor, N. Philip, . . . H. Cave (2010) Germline mutations of the CBL gene define a new genetic syndrome with predisposition to juvenile myelomonocytic leukaemia. *Journal of medical genetics*, 47, 686-91.
- Pierpont, E. I., M. E. Pierpont, N. J. Mendelsohn, A. E. Roberts, E. Tworog-Dube & M. S. Seidenberg (2009) Genotype differences in cognitive functioning in Noonan syndrome. *Genes, brain, and behavior*, 8, 275-82.
- Piotrowski, A., J. Xie, Y. F. Liu, A. B. Poplawski, A. R. Gomes, P. Madanecki, . . . L. M. Messiaen (2014) Germline loss-of-function mutations in LZTR1 predispose to an inherited disorder of multiple schwannomas. *Nature genetics*, 46, 182-7.
- Polakis, P. & F. McCormick (1993) Structural requirements for the interaction of p21ras with GAP, exchange factors, and its biological effector target. *The Journal of biological chemistry*, 268, 9157-60.
- Povey, S., A. I. Al Aqeel, A. Cambon-Thomsen, R. Dagleish, J. T. den Dunnen, H. V. Firth, . . . R. G. Cotton (2010) Practical guidelines addressing ethical issues pertaining to the curation of human locus-specific variation databases (LSDBs). *Human mutation*, 31, 1179-84.
- Prasad, R., K. Singh & R. Singh (2002) Bilateral congenital chylothorax with Noonan syndrome. *Indian pediatrics*, 39, 975-6.
- Prendiville, T. W., K. Gauvreau, E. Tworog-Dube, L. Patkin, R. S. Kucherlapati, A. E. Roberts & R. V. Lacro (2014) Cardiovascular disease in Noonan syndrome. *Archives of disease in childhood*, 99, 629-34.
- Quaio, C. R., T. F. de Almeida, A. S. Brasil, A. C. Pereira, A. A. Jorge, A. C. Malaquias, . . . D. R. Bertola (2013) Tegumentary manifestations of Noonan and Noonan-related syndromes. *Clinics*, 68, 1079-83.
- Rauen, K. A. (2013) The RASopathies. *Annual review of genomics and human genetics*, 14, 355-69.
- Razzaque, M. A., T. Nishizawa, Y. Komoike, H. Yagi, M. Furutani, R. Amo, . . . R. Matsuoka (2007) Germline gain-of-function mutations in RAF1 cause Noonan syndrome. *Nature genetics*, 39, 1013-7.
- Reynolds, J. F., G. Neri, J. P. Herrmann, B. Blumberg, J. G. Coldwell, P. V. Miles & J. M. Opitz (1986) New multiple congenital anomalies/mental retardation syndrome with cardio-facio-cutaneous involvement--the CFC syndrome. *American journal of medical genetics*, 25, 413-27.
- Richards, S., N. Aziz, S. Bale, D. Bick, S. Das, J. Gastier-Foster, . . . H. L. Rehm (2015) Standards and guidelines for the interpretation of sequence variants: a joint consensus recommendation of the American College of Medical Genetics and Genomics and the Association for Molecular Pathology. *Genetics in medicine : official journal of the American College of Medical Genetics*, 17, 405-24.
- Roberts, A. E., J. E. Allanson, M. Tartaglia & B. D. Gelb (2013) Noonan syndrome. *Lancet*, 381, 333-42.
- Roberts, A. E., T. Araki, K. D. Swanson, K. T. Montgomery, T. A. Schiripo, V. A. Joshi, . . . R. S. Kucherlapati (2007) Germline gain-of-function mutations in SOS1 cause Noonan syndrome. *Nature genetics*, 39, 70-4.
- Rodriguez-Viciano, P., O. Tetsu, W. E. Tidyman, A. L. Estep, B. A. Conger, M. S. Cruz, . . . K. A. Rauen (2006) Germline mutations in genes within the MAPK pathway cause cardio-facio-cutaneous syndrome. *Science*, 311, 1287-90.
- Runtuwene, V., M. van Eekelen, J. Overvoorde, H. Rehmann, H. G. Yntema, W. M. Nillesen, . . . J. den Hertog (2011) Noonan syndrome gain-of-function mutations in NRAS cause zebrafish gastrulation defects. *Disease models & mechanisms*, 4, 393-9.
- Sarkozy, A., E. Conti, D. Seripa, M. C. Digilio, N. Grifone, C. Tandoi, . . . B. Dallapiccola (2003) Correlation between PTPN11 gene mutations and congenital heart defects in Noonan and LEOPARD syndromes. *Journal of medical genetics*, 40, 704-8.
- Scheffzek, K., M. R. Ahmadian, W. Kabsch, L. Wiesmuller, A. Lautwein, F. Schmitz & A. Wittinghofer (1997) The Ras-RasGAP complex: structural basis for GTPase activation and its loss in oncogenic Ras mutants. *Science*, 277, 333-8.

- Schnittger, S., U. Bacher, T. Alpermann, A. Reiter, M. Ulke, F. Dicker, . . . T. Haferlach (2012) Use of CBL exon 8 and 9 mutations in diagnosis of myeloproliferative neoplasms and myelodysplastic/myeloproliferative disorders: an analysis of 636 cases. *Haematologica*, 97, 1890-4.
- Schubbert, S., M. Zenker, S. L. Rowe, S. Boll, C. Klein, G. Bollag, . . . C. P. Kratz (2006) Germline KRAS mutations cause Noonan syndrome. *Nature genetics*, 38, 331-6.
- Schwarz, J. M., D. N. Cooper, M. Schuelke & D. Seelow (2014) MutationTaster2: mutation prediction for the deep-sequencing age. *Nature methods*, 11, 361-2.
- Shchelochkov, O. A., A. Patel, G. M. Weissenberger, A. C. Chinault, J. Wiszniewska, P. H. Fernandes, . . . V. R. Sutton (2008) Duplication of chromosome band 12q24.11q24.23 results in apparent Noonan syndrome. *American journal of medical genetics. Part A*, 146A, 1042-8.
- Sim, N. L., P. Kumar, J. Hu, S. Henikoff, G. Schneider & P. C. Ng (2012) SIFT web server: predicting effects of amino acid substitutions on proteins. *Nucleic acids research*, 40, W452-7.
- Simanshu, D. K., D. V. Nissley & F. McCormick (2017) RAS Proteins and Their Regulators in Human Disease. *Cell*, 170, 17-33.
- Simsek-Kiper, P. O., Y. Alanay, B. Gulhan, C. Lisewski, D. Turkyilmaz, D. Alehan, . . . K. Boduroglu (2013) Clinical and molecular analysis of RASopathies in a group of Turkish patients. *Clinical genetics*, 83, 181-6.
- Stieglitz, B., C. Bee, D. Schwarz, O. Yildiz, A. Moshnikova, A. Khokhlatchev & C. Herrmann (2008) Novel type of Ras effector interaction established between tumour suppressor NORE1A and Ras switch II. *The EMBO journal*, 27, 1995-2005.
- Stieglitz, E., A. N. Taylor-Weiner, T. Y. Chang, L. C. Gelston, Y. D. Wang, T. Mazor, . . . M. L. Loh (2015) The genomic landscape of juvenile myelomonocytic leukemia. *Nature genetics*, 47, 1326-33.
- Strullu, M., A. Caye, J. Lachenaud, B. Cassinat, S. Gazal, O. Fenneteau, . . . H. Cave (2014) Juvenile myelomonocytic leukaemia and Noonan syndrome. *Journal of medical genetics*, 51, 689-97.
- Takasawa, K., S. Takishima, C. Morioka, M. Nishioka, H. Ohashi, Y. Aoki, . . . T. Morio (2015) Improved growth velocity of a patient with Noonan-like syndrome with loose anagen hair (NS/LAH) without growth hormone deficiency by low-dose growth hormone therapy. *American journal of medical genetics. Part A*, 167A, 2425-9.
- Takenouchi, T., Y. Sakamoto, T. Miwa, C. Torii, R. Kosaki, K. Kishi, . . . K. Kosaki (2014) Severe craniosynostosis with Noonan syndrome phenotype associated with SHOC2 mutation: clinical evidence of crosslink between FGFR and RAS signaling pathways. *American journal of medical genetics. Part A*, 164A, 2869-72.
- Tartaglia, M. & B. D. Gelb (2005) Noonan syndrome and related disorders: genetics and pathogenesis. *Annual review of genomics and human genetics*, 6, 45-68.
- Tartaglia, M. & B. D. Gelb (2010) Disorders of dysregulated signal traffic through the RAS-MAPK pathway: phenotypic spectrum and molecular mechanisms. *Annals of the New York Academy of Sciences*, 1214, 99-121.
- Tartaglia, M., K. Kalidas, A. Shaw, X. Song, D. L. Musat, I. van der Burgt, . . . B. D. Gelb (2002) PTPN11 mutations in Noonan syndrome: molecular spectrum, genotype-phenotype correlation, and phenotypic heterogeneity. *American journal of human genetics*, 70, 1555-63.
- Tartaglia, M., S. Martinelli, L. Stella, G. Bocchinfuso, E. Flex, V. Cordeddu, . . . B. D. Gelb (2006) Diversity and functional consequences of germline and somatic PTPN11 mutations in human disease. *American journal of human genetics*, 78, 279-90.
- Tartaglia, M., E. L. Mehler, R. Goldberg, G. Zampino, H. G. Brunner, H. Kremer, . . . B. D. Gelb (2001) Mutations in PTPN11, encoding the protein tyrosine phosphatase SHP-2, cause Noonan syndrome. *Nature genetics*, 29, 465-8.
- Tartaglia, M., L. A. Pennacchio, C. Zhao, K. K. Yadav, V. Fodale, A. Sarkozy, . . . B. D. Gelb (2007) Gain-of-function SOS1 mutations cause a distinctive form of Noonan syndrome. *Nature genetics*, 39, 75-9.
- Tartaglia, M., G. Zampino & B. D. Gelb (2010) Noonan syndrome: clinical aspects and molecular pathogenesis. *Molecular syndromology*, 1, 2-26.
- Tidyman, W. E. & K. A. Rauen (2009) The RASopathies: developmental syndromes of Ras/MAPK pathway dysregulation. *Current opinion in genetics & development*, 19, 230-6.
- Tidyman, W. E. & K. A. Rauen (2016) Expansion of the RASopathies. *Current genetic medicine reports*, 4, 57-64.

- Timeus, F., N. Crescenzo, G. Baldassarre, A. Doria, S. Vallero, L. Foglia, . . . G. B. Ferrero (2013) Functional evaluation of circulating hematopoietic progenitors in Noonan syndrome. *Oncology reports*, 30, 553-9.
- Uusitalo, E., J. Leppavirta, A. Koffert, S. Suominen, J. Vahtera, T. Vahlberg, . . . S. Peltonen (2015) Incidence and mortality of neurofibromatosis: a total population study in Finland. *The Journal of investigative dermatology*, 135, 904-906.
- van der Burgt, I. (2007) Noonan syndrome. *Orphanet journal of rare diseases*, 2, 4.
- van der Burgt, I., E. Berends, E. Lommen, S. van Beersum, B. Hamel & E. Mariman (1994) Clinical and molecular studies in a large Dutch family with Noonan syndrome. *American journal of medical genetics*, 53, 187-91.
- van Der Burgt, I. & H. Brunner (2000) Genetic heterogeneity in Noonan syndrome: evidence for an autosomal recessive form. *American journal of medical genetics*, 94, 46-51.
- van der Burgt, I., W. Kupsky, S. Stassou, A. Nadroo, C. Barroso, A. Diem, . . . M. Zenker (2007) Myopathy caused by HRAS germline mutations: implications for disturbed myogenic differentiation in the presence of constitutive HRas activation. *Journal of medical genetics*, 44, 459-62.
- Vetter, I. R. & A. Wittinghofer (2001) The guanine nucleotide-binding switch in three dimensions. *Science*, 294, 1299-304.
- Viskochil, D., A. M. Buchberg, G. Xu, R. M. Cawthon, J. Stevens, R. K. Wolff, . . . et al. (1990) Deletions and a translocation interrupt a cloned gene at the neurofibromatosis type 1 locus. *Cell*, 62, 187-92.
- Visser, L. E., M. Bonetti, J. Paardekooper Overman, W. M. Nillesen, S. G. Frints, J. de Ligt, . . . J. den Hertog (2015) Heterozygous germline mutations in A2ML1 are associated with a disorder clinically related to Noonan syndrome. *European journal of human genetics : EJHG*, 23, 317-24.
- Wallace, M. R., D. A. Marchuk, L. B. Andersen, R. Letcher, H. M. Odeh, A. M. Saulino, . . . et al. (1990) Type 1 neurofibromatosis gene: identification of a large transcript disrupted in three NF1 patients. *Science*, 249, 181-6.
- Wey, M., J. Lee, S. S. Jeong, J. Kim & J. Heo (2013) Kinetic mechanisms of mutation-dependent harvey ras activation and their relevance for the development of costello syndrome. *Biochemistry*, 52, 8465-79.
- Wilkinson, J. D., A. M. Lowe, B. A. Salbert, L. A. Sleeper, S. D. Colan, G. F. Cox, . . . S. E. Lipshultz (2012) Outcomes in children with Noonan syndrome and hypertrophic cardiomyopathy: a study from the Pediatric Cardiomyopathy Registry. *American heart journal*, 164, 442-8.
- Williams, V. C., J. Lucas, M. A. Babcock, D. H. Gutmann, B. Korf & B. L. Maria (2009) Neurofibromatosis type 1 revisited. *Pediatrics*, 123, 124-33.
- Witt, D. R., H. E. Hoyme, J. Zonana, D. K. Manchester, J. P. Fryns, J. G. Stevenson, . . . J. G. Hall (1987) Lymphedema in Noonan syndrome: clues to pathogenesis and prenatal diagnosis and review of the literature. *American journal of medical genetics*, 27, 841-56.
- Witters, I., B. Spitz, C. Van Hole, K. Devriendt, J. P. Fryns & K. Verbek (2002) Resolution of non-immune hydrops in Noonan syndrome with favorable outcome. *American journal of medical genetics*, 110, 408-9.
- Yamamoto, G. L., M. Agüena, M. Gos, C. Hung, J. Pilch, S. Fahiminiya, . . . D. R. Bertola (2015) Rare variants in SOS2 and LZTR1 are associated with Noonan syndrome. *Journal of medical genetics*, 52, 413-21.
- Yaoita, M., T. Niihori, S. Mizuno, N. Okamoto, S. Hayashi, A. Watanabe, . . . Y. Aoki (2016) Spectrum of mutations and genotype-phenotype analysis in Noonan syndrome patients with RIT1 mutations. *Human genetics*, 135, 209-22.
- Yoshida, R., M. Miyata, T. Nagai, T. Yamazaki & T. Ogata (2004) A 3-bp deletion mutation of PTPN11 in an infant with severe Noonan syndrome including hydrops fetalis and juvenile myelomonocytic leukemia. *American journal of medical genetics. Part A*, 128A, 63-6.
- Zambrano, R. M., M. Marble, S. A. Chalew, C. Lilje, A. Vargas & Y. Lacassie (2017) Further evidence that variants in PPP1CB cause a rasopathy similar to Noonan syndrome with loose anagen hair. *American journal of medical genetics. Part A*, 173, 565-567.
- Zenker, M. (2009) Genetic and pathogenetic aspects of Noonan syndrome and related disorders. *Hormone research*, 72 Suppl 2, 57-63.
- Zenker (2011) Clinical manifestations of mutations in RAS and related intracellular signal transduction factors. *Current opinion in pediatrics*, 23, 443-51.

- Zenker, M., K. Lehmann, A. L. Schulz, H. Barth, D. Hansmann, R. Koenig, . . . K. Kutsche (2007) Expansion of the genotypic and phenotypic spectrum in patients with KRAS germline mutations. *Journal of medical genetics*, 44, 131-5.
- Zenker, M. K., K. (2016) RASopathien. *Medizinische Genetik*, 28, 15-38.
- Zmolikova, M., A. Puchmajerova, P. Hecht, J. Lebl, M. Trkova & A. Krepelova (2014) Coarctation of the aorta in Noonan-like syndrome with loose anagen hair. *American journal of medical genetics. Part A*, 164A, 1218-21.

5.1. Online Resources

All online resources were last accessed on 17.10.2017.

CCDS (<https://www.ncbi.nlm.nih.gov/projects/CCDS/CcdfsBrowse.cgi>)

ClinVar (<https://www.ncbi.nlm.nih.gov/clinvar/>)

COSMIC (<http://cancer.sanger.ac.uk/cosmic>)

Ensembl (<http://www.ensembl.org/index.html>)

Fisher's exact test (<http://www.langsrud.com/stat/Fishertest.htm>)

HGNC (<https://www.genenames.org/>)

Mutation Taster (<http://www.mutationtaster.org/>)

MutPred (<http://mutpred.mutdb.org/>)

NCBI Gene (<https://www.ncbi.nlm.nih.gov/gene>)

NSEuroNet (<https://nseuronet.com/php/>)

OMIM (<https://www.omim.org/>)

PolyPhen2 (<http://genetics.bwh.harvard.edu/pph2/>)

Primer3 (<http://primer3.ut.ee/>)

PubMed (<https://www.ncbi.nlm.nih.gov/pubmed/>)

SIFT (<http://sift.jcvi.org/>)

UniProt (<http://www.uniprot.org/>)

6. SUPPLEMENTS

6.1. Clinical tables

6.1.1. SHOC2

ID	S01	S02	S03	S04	S05	S06	S07	S08	S09	S10
Age	22,0	7,0	15,2	35,0	7,9	5,4	16,0	6,0	8,8	25,0
Gender	f	m	m	f	m	m	f	f	f	f
Affected relatives	-	-	-	-	-	-	-	-	-	-
Prenatal findings	NE, HF	-	-	-	-	-	-	PE, HD	-	ND
Feeding problems	+	+	+	+	+	+	+	+	+	+
Heart defects	Pst	Pst, ASD	pericardial effusion at age 14	-	-	HCM	Pst	supravalvular aortic stenosis, coarctation	-	MVA
Lymphatic abnormalities	ND	ND	-	-	-	-	-	-	-	-
SDS	-0,95	1,75	-3,43	-2,18	-4,55	-2,95	-2,57	-2,04	-1,88	ND
Short Stature	+	-	+	+	+	+	+	+	-	ND
GH deficiency	ND	ND	-	confirmed GH deficiency	neurosecretor y dysfunction	confirmed GH deficiency	neurosecretory dysfunction	ND	ND	ND
Motor Delay	+	+	+	+	-	+	+	+	+	+
Intellectual/learning disabilities	+	ND	+	+	+	ND	+	-	+	+
Cryptorchidism	ND	-	-	ND	-	+	ND	ND	ND	ND
Skin and Hair	SH	SH, LAH, KP, EC, Atopic Dermatitis	SH, EPH, SGH, KP, EC	SH, EPH, LAH	SH, EPH, LAH, IC, EC	SH, EPH, LAH, KP, EC	SH, EPH, LAH	SH, EPH, LAH, EC, HA	SH, EPH, LAH, EC	IC, EC
Skeletal	SN	SN	SN	SN	SN	TH, SN	TH, SN	-	-	-
Bleeding diathesis	-	-	-	-	-	-	van Willebrand	-	-	-
Seizures	-	-	-	-	-	epilepsy, resolved after transient treatment	-	-	-	ND
Ocular	-	PT, RE, ST	PT, ST	RE	-	PT, RE, ST, NY	PT, RE	PT, ST	PT, RE, ST, NY	-
Other diseases	-	-	head tilt	Deterioration in mobility with hyperreflexia and unsteady gait at age 35	Enamel dysplasia	Hyperacusis, Registered partially sighted, Severe allergies	juvenile idiopathic arthritis	-	Bilateral optic disc colobomata	Malrotation requiring surgery, depression

continued on next page

ID	S11	S12	S13	S14	S15	S16	S17	S18	S19	S20
Age	11,0	7,8	11,4	1,5	11,0	20,0	13,0	14,5	6,8	18,5
Gender	f	m	f	m	m	m	m	m	f	f
Affected relatives	-	Sibling	-	-	-	-	unknown	unknown	unknown	unknown
Prenatal findings	-	ND	NE, HF, PH	NE	-	HF	ND	ND	PH	ND
Feeding problems	+	+	+	+	+	+	ND	+	+	+
Heart defects	MVA, myxomatous mitral and tricupsid valves with trivial incompetence	Supravalvular PVS	Pst, HCM, ASD	Pst	-	Pst	Pst, HCM	ASD	atrial septum aneurysm, portal vein stenosis	aortic coarctation, Arrhythmia
Lymphatic abnormalities	-	ND	-	-	-	-	ND	ND	ND	ND
SDS	ND	-3,27	-2,86	-4,93	-2,89	-2,06	-3,92	-3,04	-2,02	-0,17
Short Stature	ND	+	+	+	+	+	+	+	+	+
GH deficiency	-	ND	neurosecretory dysfunction	normal hormone levels	ND	ND	ND	ND	ND	confirmed GH deficiency
Motor Delay	+	ND	+	+	+	+	-	ND	ND	ND
Intellectual/learning disabilities	+	ND	+	ND	+	+	-	ND	ND	ND
Cryptorchidism	ND	-	ND	-	+	ND	-	ND	ND	ND
Skin and Hair	SH, KP, HA	CH, SH, SGH	SH, EPH, SGH, KP, EC, CAS	SH, EPH, SGH, EC	CH, SH	ND	SH, EPH, KP, EC	SH, EC, MN	CH, SH, KP, EC, MN, HA	FH
Skeletal	SN	SC, SN	SN	SN	SN	ND	TH, SN	SC, SN	TH, SN	ND
Bleeding diathesis	easy bruising	ND	easy bruising	-	-	platelet dysfunction	-	ND	ND	easy bruising
Seizures	-	ND	-	-	-	epilepsy, ongoing treatment	-	ND	ND	ND
Ocular	RE	RE	PT, ST	PT	PT	PT, RE, NY	ND	RE	ND	PT, RE, ST
Other diseases	Hyperacusis, Hypopigmented skin lesion, Enamel dysplasia primary dentition	-	Hepatomegaly	Presented with fractured femur and T12 and L1 fractures at age 15 months. Found to have generalised osteopaenia with normal Vitamin D status. Treated with Pamidronate.	-	Idiopathic thrombocytopenic purpura	-	-	-	-

continued on next page

ID	S21	S22	S23	S24	S25	S26	S27	S28	S29	S30
Age	0,5	2,3	14,5	2,3	4,3	3,2	1,3	0,7	7,8	11,0
Gender	m	m	f	m	m	f	f	f	m	f
Affected relatives	unknown	unknown	unknown	unknown	unknown	unknown	unknown	unknown	Sibling	unknown
Prenatal findings	ND	NE	NE	PH	ND	ND	NE	ND	ND	ND
Feeding problems	+	+	+	+	+	+	+	+	+	-
Heart defects	HCM	HCM	Pst, ASD	HCM	ND	-	HCM, VSD	HCM, ASD	VSD, Supravalvular PVS	HCM, MVA
Lymphatic abnormalities	ND	ND	ND	ND	ND	ND	ND	ND	ND	-
SDS	-1,96	-2,24	-2,36	-3,56	-5,08	-2,33	ND	ND	-3,27	-2,58
Short Stature	-	+	+	+	+	+	+	+	+	+
GH deficiency	ND	ND	confirmed GH deficiency	ND	ND	ND	ND	ND	ND	normal hormone levels
Motor Delay	ND	ND	ND	ND	ND	ND	ND	ND	ND	+
Intellectual/learning disabilities	ND	ND	ND	ND	ND	ND	ND	ND	ND	ND
Cryptorchidism	+	-	ND	-	-	ND	ND	ND	-	ND
Skin and Hair	FH	SH, SGH, EC	SH, LAH, KP	SH, LAH	SH	SH	SH, LAH, EC	SH, HA	CH, SH, SGH	LAH, CAS, HA
Skeletal	TH	SN	SN	SN	SN	-	SN	SN	SC, SN	SN
Bleeding diathesis	ND	ND	easy bruising	easy bruising	ND	ND	ND	ND	ND	ND
Seizures	ND	ND	ND	ND	ND	ND	ND	ND	ND	-
Ocular	RE	ND	ND	PT, ST	ND	ND	ND	ND	RE	-
Other diseases	-	-	-	-	-	-	-	patient has died due to unknown causes, Hepatomegaly	-	-

continued on next page

ID	S31	S32	S33	S34	S35	S36	S37	S38	S39	S40
Age	4,5	12,0	7,8	13,0	17,1	6,5	5,0	1,8	30,0	13,8
Gender	m	m	f	m	f	m	f	f	m	f
Affected relatives	unknown	unknown	unknown	unknown	unknown	unknown	unknown	unknown	unknown	unknown
Prenatal findings	ND	ND	ND	ND	ND	ND	PH	ND	ND	ND
Feeding problems	-	+	+	+	+	+	+	+	+	+
Heart defects	Pst, ASD	HCM	partial atrioventricular canal	Pst, MVA	MVA	HCM	HCM	Pst, ASD	ASD	Pst, VSD
Lymphatic abnormalities	ND	ND	ND	ND	ND	ND	ND	ND	ND	ND
SDS	-0,26	-2,24	-3,61	-3,36	-2,31	-2,63	-2,33	-4,48	-3,54	-3,93
Short Stature	-	+	+	+	+	+	+	+	+	+
GH deficiency	ND	ND	ND	confirmed GH deficiency	confirmed GH deficiency	ND	ND	ND	ND	ND
Motor Delay	ND	ND	ND	ND	+	ND	ND	ND	ND	ND
Intellectual/learning disabilities	ND	ND	ND	ND	ND	ND	ND	ND	ND	ND
Cryptorchidism	-	ND	ND	+	ND	+	ND	ND	-	ND
Skin and Hair	SH, SGH, EC	SH, LAH, HA	SH, LAH	SH, LAH, KP, EC	SH, LAH	SH, LAH, KP, HA	SH, CAS	SH, CAS	SH	SH, LAH
Skeletal	SN	SN	SC, SN	SN	SC, SN	SN	SN	SN	SN	TH
Bleeding diathesis	ND	ND	ND	ND	ND	ND	ND	ND	ND	ND
Seizures	ND	ND	ND	ND	ND	ND	ND	ND	ND	ND
Ocular	ND	RE, ST	ND	ND	ST	RE, ST	RE, ST	ND	ST	ST
Other diseases	Hepatospl enomegaly	-	-	Hydrocephalus, colpocephaly	Hydrocephalus	-	Hepatomegaly	-	-	-

continued on next page

ID	S41	S42	S43	S44	S45	S46	S47	S48	S49	S50
Age	6,5	2,0	34,0	9,5	14,0	1,5	0,5	0,3	8,7	38,0
Gender	f	f	m	f	m	f	m	f	m	m
Affected relatives	unknown	unknown	unknown	unknown	unknown	unknown	unknown	unknown	-	-
Prenatal findings	ND	ND	ND	NE, PH	PH	PH	ND	NE	bilateral renal pelvis dilatation	-
Feeding problems	+	+	+	+	+	+	ND	+	+	+
Heart defects	Pst, HCM, ASD	HCM	Pst	-	Pst, ASD	Pst, ASD	Pst, aortic valve stenosis, PFO	HCM, aortic coarctation	Pst	MVA
Lymphatic abnormalities	ND	ND	ND	ND	ND	ND	ND	ND	-	-
SDS	ND	ND	ND	ND	ND	ND	ND	ND	-3,18	-2,21
Short Stature	ND	ND	ND	ND	ND	ND	ND	ND	+	+
GH deficiency	ND	ND	ND	ND	ND	ND	ND	ND	ND	confirmed GH deficiency
Motor Delay	ND	ND	ND	ND	ND	ND	ND	ND	+	+
Intellectual/learning disabilities	ND	ND	ND	ND	ND	ND	ND	ND	+	-
Cryptorchidism	ND	ND	-	ND	ND	ND	ND	ND	-	+
Skin and Hair	SH, LAH, HA	SGH, EC	SGH, EC	LAH, HA	SGH, CAS	SGH, EC	ND	ND	FH, SH, EPH	SH, ML
Skeletal	TH, SN	SN	TH, SN	TH, SN	TH, SN	SN	ND	ND	TH, SN	TH, SN
Bleeding diathesis	easy bruising	ND	easy bruising	easy bruising	easy bruising	easy bruising	ND	ND	easy bruising	easy bruising
Seizures	ND	ND	ND	ND	ND	ND	ND	ND	benign seizures (e.g. febrile or transient) required - treatment	-
Ocular	ST	ND	ST	RE, ST	ND	ND	ND	ND	PT, RE	PT, RE, ST
Other diseases	-	-	-	hearing deficit	hearing deficit	-	-	-	pale optic nerves, poor VEPs, abnormal retinal function, recurrent otitis media (tubes)	multiple surgeries on legs, Hydrocephalus

continued on next page

ID	S51	S52	S53	S54	S55	S56	S57	S58	S59	S60
Age	1,8	3,0	3,0	3,5	3,8	16,8	15,2	18,0	0,0	4,3
Gender	m	m	m	f	m	f	m	f	unknown	f
Affected relatives	-	unknown	unknown	unknown	unknown	unknown	-	-	unknown	-
Prenatal findings	-	ND	ND	ND	ND	ND	ND	ND	ND	ND
Feeding problems	+	+	+	+	+	+	ND	+	+	ND
Heart defects	Pst, HCM	-	ND	ND	HCM, MVA	Pst	ND	ASD	-	MVA, aneurysm of spetum
Lymphatic abnormalities	-	ND	ND	ND	ND	ND	lymphadenopathy	ND	-	ND
SDS	-1,39	ND	-4,46	ND	-1,6	ND	-3,47	-2,33	-1,49	-2,22
Short Stature	-	ND	+	ND	-	ND	+	+	-	+
GH deficiency	ND	ND	ND	ND	ND	ND	ND	ND	ND	ND
Motor Delay	+	ND	+	ND	+	+	ND	-	ND	+
Intellectual/learning disabilities	ND	ND	ND	ND	ND	+	ND	-	ND	ND
Cryptorchidism	-	+	-	ND	-	ND	ND	ND	-	ND
Skin and Hair	FH, SH, EC	SH, EPH	SH, EPH	CH	SH, EPH, HA	FH, KP	ND	SH, EPH	SH, EPH, HA	SH, EPH, HA
Skeletal	SN	-	TH, SN	ND	SN	TH, SC, SN	ND	TH, SN	SN	-
Bleeding diathesis	-	-	ND	ND	-	-	ND	-	ND	ND
Seizures	-	-	ND	ND	-	-	ND	-	ND	-
Ocular	ST	ND	ND	ND	ND	ST	ND	RE	PT	ST
Other diseases	congenital CMV infection, thrompocytopenia 5G/l, atopic eczema, cow's milk and egg allergy, G6PD deficiency	-	-	-	ventricular dilatation and hypoplasia of the corpus callosum	-	hepatospleno megaly	hearing deficit	lateral ventricle dilatation	-

continued on next page

ID	S61	S62	S63	S64	S65	S66	S67	S68	S69	S70	S71	S72
Age	2,8	1,4	5,5	14,0	1,3	19,6	1,7	4,0	3,1	13,5		
Gender	f	f	m	f	f	m	m	m	f	m	ND	m
Affected relatives	-	-	-	-	-	-	-	-	-	-	ND	-
Prenatal findings	ND	ND	ND	ND	ND	ND	PH	NE	NE, PE, PH	PH, macrocephaly, suspected skeletal dysplasia	ND	ND
Feeding problems	+	ND	-	+	+	+	ND	+	+	+	ND	ND
Heart defects	-	Pst	-	-	-	Pst, VSD	HCM	aortic isthmus stenosis	persistent foramen ovale	HCM, MVA, atrial septal aneurysm	ND	HCM
Lymphatic abnormalities	-	ND	-	-	-	ND	ND	-	-	-	ND	ND
SDS	0,05	ND	-3,09	-2,27	ND	-3,15	ND	-3,06	-3,26	-2,97	ND	ND
Short Stature	-	ND	+	+	ND	+	ND	+	+	+	ND	ND
GH deficiency	ND	ND	ND	ND	ND	ND	ND	ND	confirmed GH deficiency	unknown	ND	ND
Motor Delay	+	ND	+	-	ND	+	ND	+	+	+	ND	+
Intellectual/learning disabilities	ND	ND	ND	-	ND	ND	ND	ND	ND	+	ND	ND
Cryptorchidism	ND	ND	-	ND	ND	ND	ND	+	ND	-	ND	ND
Skin and Hair	ND	CH	SH, EPH, HA	SH, EPH, HA	SH, EPH, HA	EPH	ND	CH, FH, SH	FH, SH, KP, EC, HP	FH, SH, EPH, IC, HP	ND	HA, SH, CAL
Skeletal	SN	SN	SN	TH, SN	SN	TH, SN	SN	SN	TH, SN	ND	ND	ND
Bleeding diathesis	ND	ND	ND	ND	ND	ND	ND	factor VIII deficiency	-	easy bruising	ND	ND
Seizures	-	ND	-	-	-	-	ND	benign seizures	-	-	ND	ND
Ocular	-	-	ST	PT	PT	PT	ND	PT, ST	PT, ST	PT	ND	ND
Other diseases	-	-	exophthalmos	-	-	rhabdomyolysis	vascular tumor type hemangioendothelioma kaposiform of the spleen and a Kasabach Meritt syndrome	prenatal sagittal suture synostosis (operated at age of 1 year), Hydrocephalus	-	hepatosplenomegaly, hypermobility	-	passed away due to cardiac problems

Table 6.1: Clinical Data of the *SHOC2* cohort. All patients shown here have the mutation c.4A>G; p.(S2G). Abbreviations: -: absent; +: present; ASD: atrial septal defect; CAS: Café-au-lait spots; CH: curly hair; EC: eczema; EPH: easily pluckable hair; f: female; FH: fine hair; HA: hemangioma; HCM: hypertrophic cardiomyopathy; HD: prenatal heart defect; HF: hydrops fetalis; HP: hyperpigmentation; IC: ichthyosis; KP: keratosis pilaris; LAH: loose anagen hair; m: male; ML: multiple lentiginos; MN: multiple naevi; MVA: mitral valve anomaly; NA: not applicable; ND: no data; NE: nuchal edema; NY: nystagmus; PE: pleural effusion; PFO: persistent foramen ovale; PH: polyhydramnios; Pst: pulmonary stenosis; PT: ptosis; PVS: pulmonary valve stenosis; RE: refractive error; SC: scoliosis; SGH: slow growing hair; SH: sparse hair; SN: short neck / webbed neck; ST: strabismus; TH: thorax anomaly; VSD: ventricular septal defect; y: year(s).

6.1.2. RIT1

Patient ID	R1-1	R1-2	R2	R3	R4-1	R4-2	R4-3	R5	R6	R7-1
Age	8 y	47 y	11 y	13 y	8 y	42 y	14 y	4 y	1 y	6 y
Gender	f	f	f	f	m	f	m	f	f	m
RIT1 amino acid substitution	p.Gly31 Arg	p.Gly31 Arg	p.Ala57Gly	p.Phe82 Val	p.Gly95Ala	p.Gly95 Ala	p.Gly95Ala	p.Lys23Asn	p.Ala57Gly	p.Ala57Gly
Inheritance	inherited	not known	not known	<i>de novo</i>	inherited	not known	inherited	<i>de novo</i>	<i>de novo</i>	inherited
Prenatal findings	–	ND	–	NE, PE, HF	–	–	–	NE	NE, PE, PH	PH, HD
Premature birth (< 37 weeks GA)	ND	–	–	+	–	+	–	–	+	+
Feeding difficulties	–	–	ND	–	+	–	–	+	+	+
Heart defects/anomalies	PST	PST	PST, HCM	PST, HCM	PST	ASD, VSD	PST	PST, ASD	PST, HCM	PST, ASD, VSD
Lymphatic anomalies	–	–	aLE	nLE, nCT	–	–	–	–	cCT, nAS	–
SDS	0.07	-0.33	-3.42	-1.18	-1.52	0.61	-0.90	-0.27	-3.15	-1.37
Short stature	–	–	+	–	–	–	–	–	+	–
Motor developmental delay	–	–	–	–	+	–	–	+	+	+
Intellectual/learning disabilities	–	–	–	–	ND	–	–	ND	ND	+
Cryptorchidism	NA	NA	NA	NA	–	NA	NA	NA	NA	+
Skin and hair abnormalities	–	–	–	–	CH	CH	CH	–	–	–
Skeletal anomalies	TH, SN	–	TH, SN	SN	TH	SC	–	–	TH, SN	TH
Easy bruising	–	–	–	–	–	–	–	–	–	–
Ocular abnormalities	PT	PT	PT	PT	PT, RE	PT, RE	PT, RE	–	PT	PT
Other anomalies	–	–	giant cell tumor of jaws	–	–	depression	sensorineural hearing deficit	minor renal anomalies	–	hydrocephalus

continued on next page

Patient ID	R7-2	R8	R9	R10	R11	R12	R13	R14	R15	R16
Age	29 y	5 y	38 y	16 y	3 y	1 y	5 y	5 y	24 y	11 y
Gender	f	f	f	f	f	f	f	f	m	m
RIT1 amino acid substitution	p.Ala57Gly	p.Phe82Leu	p.Phe82Leu	p.Thr83Pro	p.Met90Ile	p.Ser35Thr	p.Ser35Thr	p.Phe82Leu	p.Gly95Ala	p.Ser35Thr
Inheritance	not known	<i>de novo</i>	not known	not known	not known	<i>de novo</i>	<i>de novo</i>	not known	not known	not known
Prenatal findings	ND	NE, HF, RA	ND	-	-	-	PH	PH	-	-
Premature birth (< 37 weeks GA)	ND	-	-	+	+	+	-	-	-	+
Feeding difficulties	ND	+	-	+	-	+	-	ND	-	+
Heart defects/anomalies	PST	HCM, ASD, MVA	PST, MVA	HCM	PST, ASD, MVA	PST	PST, HCM	PST, HCM	MVA	PST, HCM
Lymphatic anomalies	-	nLE, aLE	aLE, aCT	-	nCT	-	-	-	aLE	-
SDS	-0.80	-2.52	-1.11	-0.37	-1.97	ND	-1.99	-2.96	0.54	-0.19
Short stature	-	+	-	-	-	ND	-	+	-	-
Motor developmental delay	ND	+	-	-	+	ND	-	-	-	-
Intellectual/learning disabilities	ND	-	-	-	ND	ND	-	-	+	+
Cryptorchidism	NA	NA	NA	NA	NA	NA	NA	NA	+	-
Skin and hair abnormalities	-	-	-	KP, HA	HA	-	HA	CH	HA	-
Skeletal anomalies	-	TH, SN	-	-	-	SN	SN	TH, SN	TH, SC, SN	TH, SN
Easy bruising	+	-	-	+	-	ND	ND	-	+	+
Ocular abnormalities	-	PT, RE	glaucoma	RE, ST	RE, CT	PT	-	PT, RE	PT, RE, ST	PT, RE
Other anomalies	hypothyroidism	benign seizures, minor renal anomalies	autoimmune thyroiditis, NET and GIST of the stomach	HN	hernia umbilicalis	-	-	B-ALL	-	-

continued on next page

Patient ID	R17	R18	R19	R20	R21	R22	R23	R24	R25	R26-1	R26-2	R27
Age	11 y	13 y	2 m	6 m	3 y	7 y	1 y	15 y	11 y	5 m	32 y	21 y
Gender	m	f	m	f	f	m	f	f	m	m	f	m
amino acid substitution	p.Phe82Leu	p.Phe82Leu	p.Ala57Gly	p.Ala57Gly	p.Ala77Thr	p.Ala57Gly	p.Phe82Leu	p.Gly95Ala	p.Gly95Ala	p.Ala57Gly	p.Ala57Gly	p.Ala77Thr
Inheritance	not known	not known	not known	not known	not known	<i>de novo</i>	not known	not known	not known	inherited	not known	not known
Prenatal findings	PH	–	NE, HF, PH, HD	–	PH	NE, PE, PH, HD	NE, PE, HF	NE, PH	NE, RA	PH	ND	ND
Premature birth (< 37 weeks GA)	+	–	+	–	–	+	+	+	+	–	ND	ND
Feeding difficulties	ND	–	–	+	–	+	+	+	–	–	ND	ND
Heart defects/anomalies	PST, HCM, ASD	PST	PST, HCM, VSD	PST, HCM, ASD, VSD	PST, ASD	HCM, MVA	PST, HCM, ASD	ASD	PST, ASD	PST, HCM	PST	PST, MVA
Lymphatic anomalies	aLE, aCT	–	nLE	nLE	ND	nLE, nCT	aCT	IL	–	–	–	–
Short stature (SD)	(-1.91)	+ ^a	(-2.10)	(-2.31)	(-2.21)	(-0.03)	(-1.21)	(-2.11)	(-1.16)	(0.38)	(-0.80)	(1.07)
Motor developmental delay	+	–	ND	ND	+	+	ND	+	–	ND	–	–
Intellectual/learning disabilities	+	–	ND	ND	ND	–	ND	+	+	ND	–	–
Cryptorchidism	+	NA	–	NA	NA	+	NA	NA	+	+	NA	–
Skin and hair abnormalities	–	–	CH	–	–	MN	–	HA	KP, MN	–	–	MN
Skeletal anomalies	TH	–	SN	SN	TH	TH	TH, SN	SN	SN	–	–	TH
Easy bruising	–	+	–	–	ND	+	–	–	–	–	–	ND
Ocular abnormalities	PT, RE, ST	PT	PT	PT	–	PT, ST	–	RE	PT, RE, CT	–	–	PT, RE, ST
Other anomalies	benign seizures, HN	–	–	–	–	HN	nephrocalcinosis	submucosal cleft palate	minor renal anomalies, deafness, hypothyroidism	–	–	minor renal anomalies

continued on next page

Patient ID	R28	R29	R30	R31	R32	R33	R34	R35	R36	R37	R38
Age	29 y	4 y	2 y	4	1	0,1	33	6	18	3	3
Gender	m	f	m	m	m	f	m	m	f	f	f
amino acid substitution	p.Phe82Ser	p.Phe82Ile	p.Ala77Thr	p.Ala57Gly	p.Tyr89His	p.Ala57Gly	p.Ala77Ser	p.Phe82Leu	p.Lys23Gln	p.Glu81Gly	p.Ala57Gly
Inheritance	not known	not known	not known	not known	not known	not known	not known	not known	not known	not known	not known
Prenatal findings	-	HD	ND	ND	ND	HF	ND	HF, NE	ND	-	NE, HD, hypoxia
Premature birth (< 37 weeks GA)	+	-	ND	ND	ND	ND	ND	ND	ND	-	+
Feeding difficulties	+	-	ND	ND	+	ND	ND	ND	ND	+	ND
Heart defects/anomalies	-	PST, HCM, MVA, PFO	PST, HCM, VSD	PST, HCM, VSD, PFO	PST, HCM	HCM	slight thickening of multiple valves	PST, HCM, aortic-isthmus stenosis	PST	PST, oHCM, heart insufficiency	PST, MVA, HCM, subaortic stenosis
Lymphatic anomalies	-	-	-	-	ND	hydrops	aLE	ND	ND	Chylothorax	nLE
Short stature (SD)	+ ^a	(-0.76)	+	ND	ND	ND	+	-	+	- (-0,14)	+
Motor developmental delay	-	-	+	-	ND	ND	ND	ND	-	-	ND
Intellectual/learning disabilities	-	ND	ND	-	ND	ND	ND	ND	-	ND	ND
Cryptorchidism	-	NA	ND	+	ND	NA	ND	ND	NA	NA	NA
Skin and hair abnormalities	-	-	-	ND	CAL	ND	ML, CAL	ND	ND	-	-
Skeletal anomalies	SN	TH	TH	TH, SN	ND	ND	TH	ND	ND	TH	TH, SN
Easy bruising	-	-	ND	-	ND	ND	ND	ND	ND	-	ND
Ocular abnormalities	PT, ST	-	PT	ND	ND	ND	PT	PT	ND	-	-
Other anomalies	lipoma	-	-	-	ND	died at a young age	bilateral hearing loss	hemangioma	Moyamoya	-	-

Table 6.2: Clinical data of the *RIT1* cohort. *RIT1* mutations are described in the three-letter code according to the short isoform NP_008843.1. Abbreviations: -: absent; +: present; aCT: acquired chylothorax; aLE: acquired lymphedema (after newborn period); ASD: atrial septal defect; B-ALL: B-cell acute lymphoblastic leukemia; CH: curly hair; CT: cataract; F: female; GIST: gastrointestinal stromal tumor; HA: hemangioma; HCM: hypertrophic cardiomyopathy; HD: suspected fetal heart defect/anomaly; HF: hydrops fetalis; HN: hydronephrosis; IL: intestinal lymphangiectasis; KP: keratosis pilaris; m: month(s); M: male; MN: multiple nevi; MVA: mitral valve anomalies; NA: not applicable; nAS: neonatal ascites; nCT: neonatal/congenital chylothorax; ND: no data; NE: fetal nuchal edema; NET: neuroendocrine tumor; nLE: neonatal lymphedema; PE: fetal pleural effusions; PH: polyhydramnios; PST: pulmonary valve stenosis; PT: ocular ptosis; RA: fetal renal anomaly; RE: refractive error; SC: scoliosis; SN: short, broad, or webbed neck; ST: strabismus; TH: thorax deformity; VSD: ventricular septal defect; y: year(s).

6.1.3. NRAS

Patient ID	N1	N2	N3-1	N3-2	N3-3	N4-1	N4-2	N5-1	N5-2	N5-3
Age at last follow-up	5y	IUFD at 22+3 weeks	13y8m	10y3m	36y	6y8m	42y	21y	1 day	50
Gender	f	m	m	m	f	f	f	m	f	m
Genotype	p.Gly12Ser	p.Gly12Val	p.Ile24Asn	p.Ile24Asn	p.Ile24Asn	p.Thr50Ile	p.Thr50Ile	p.Gly60Glu	p.Gly60Glu	untested
Segregation	<i>de novo</i>	<i>de novo</i>	maternally inherited	maternally inherited	?	maternally inherited	likely <i>de novo</i>	likely paternally inherited	likely paternally inherited	possibly maternally inherited
Mutation confirmed in non-hematopoietic tissue	finger nails, buccal cells									
Phenotype	NS	ND	NS	NS	NS	NS	NS	NS	NS	NS
Prenatal findings	-	NE, HF	PH	-	ND	PH, HD	ND	PH, PST	PE, FA	ND
Feeding difficulties	+	ND	-	-	ND	-	ND	ND	-	ND
Heart defects/anomalies	VSD, ASD, HCM, PDA	ND	HCM	HCM	HCM	HCM	-	PST, VSD	HCM	-
Lymphedema	-	ND	-	-	-	-	-	-	nLE	-
Height SDS	-2.91	ND	-2.60	-1.91	-1.41	0.13	ND	0.32 (at 12y)	ND	-1.81
Developmental delay	MD	ND	ID(m)	MD, ID(m)	ID(m)	-	-	ID(m)	ND	-
Cryptorchidism	NA	ND	+	+	NA	NA	NA	+	NA	+
Hair and skin	CH	ND	WH, MN	WH	CH, MN, HA	SH, CH, SE, KP	-	ML	ND	ML
Skeletal	SN	ND	SN	SN	SN	TH, SN	SN	TH, SN	ND	TH, SN
Bleeding diathesis	-	ND	+	+	-	-	-	-	ND	-
Ocular abnormalities	PT	ND	PT	PT, RE	PT	PT	PT	PT	ND	PT
Additional									died on 1st day of life from severe hydrops; post mortem MRI: left ventricular hypertrophy	

continued on next page

Patient ID	N6	N7	N8	N9	N10-1	N10-2	N11	N12	N13	N14
Age at last follow-up	2y5m	2y5m	7y1m	2y1m	18y4m	8y11m	11y3m	1y0m	1y0m	4y8m
Gender	f	f	f	m	m	m	f	f	m	m
Genotype	p.Gly60Glu	p.Glu37dup	p.Thr58Ile	p.Thr50Ile	p.Gly60Glu	p.Gly60Glu	p.Thr50Ile	p.Gly12Arg	p.Gly12Asp	p.Gly60Glu
Segregation	<i>de novo</i>	father untested, mother no mutation	mosaicism in father	parents untested	?	paternally inherited	?	<i>de novo</i>	<i>de novo</i>	parents untested
Mutation confirmed in non-hematopoietic tissue			saliva, urine					finger nails	skin fibroblasts	
Phenotype	NS	CFCS	NS	NS	NS	NS	CFCS	CS	NS	NS
Prenatal findings	NE, PE, mild VM, congenital chylothorax	NE, PH, intracerebral arachnoid cyst, bilateral hydro-nephrosis	ND	ND	-	PH	-	PH	PH, mild pyelocalyceal dilatation left kidney	-
Feeding difficulties	+	+	-	+	-	-	-	+	-	-
Heart defects/anomalies	-	ASD	-	AVS	-	-	MVP	PDA,HCM	-	PDA, pulmonary valvular dysplasia without stenosis
Lymphedema	nLE, nCT	nLE	-	-	-	-	-	-	-	-
Height SDS	-2.44	-2.69	0.17	-1.43	-3.60	-1.35	-1.47	-0.80	1.03	-1.05
Developmental delay	-	MD, ID(s)	MD	-	-	-	MD, ID(m)	MD	-	-
Cryptorchidism	NA	NA	NA	+	-	-	NA	NA	-	-
Hair and skin	-	SH, HA	KP	KP, HA	MN	-	KP, MN	SH, MN	MN, CalS	SH, CalS
Skeletal	-	TH, SN	TH, SN	SN	SN	SN	SN	TH, SN	SN	SN
Bleeding diathesis	-	-	Willebrand disease	-	-	-	-	-	ND	Thrombo-cytopenia
Ocular abnormalities	PT	RE, ST, optic nerve pallor, gaze deviation	PT, RE	ST	PT, RE	-	PT, RE, ST	PT	PT	PT
Additional	mildly dilated ventricles and extra-axial spaces	1.24 Mb gain from 22q11.23; hydronephrosis with duplex collecting system			Right clubfoot	Bilateral clubfoot	hydrocephalus; perinatal complications with asphyxia, sepsis, and portal vein thrombosis	upper airway obstruction requiring tracheostomy; hyperinsulinemic hypoglycaemia; hypothalamic tumor	minor renal anomalies, JMML, external hydrocephalus	left renal duplication

Table 6.3: Clinical Data from the *NRAS* cohort. *NRAS* variants are described in the three-letter code according to the isoform NP_002515.1. Abbreviations: -: absent; +: present; ASD: atrial septal defect; AVS: atrial valve stenosis; CalS: Café-au-lait spots; CFCS: Cardio-Facio-Cutaneous syndrome; CH: curly hair; CS: Costello syndrome; f: female; FA: fetal ascites; HA: hemangioma; HCM: hypertrophic cardiomyopathy; HD: prenatal heart defect; HF: hydrops fetalis; ID: intellectual disability; IUFD: intrauterine fetal death; JMML: juvenile myelomonocytic leukemia; KP: keratosis pilaris; m: male; mo: month(s); MD: motor delay; ML: multiple lentigines; MN: multiple nevi; MVP: mitral valve prolapse; NA: not applicable; nCT: neonatal chylothorax; ND: no data; NE: fetal nuchal edema; nLE: neonatal lymphatic edema; NS: Noonan syndrome; PDA: persistent ductus arteriosus; PE: fetal pleural effusions; PH: polyhydramnios; PST: pulmonary stenosis; PT: ocular ptosis; RE: refractive error; SE: sparse eyebrows; SH: sparse hair; SN: short neck /webbed neck; ST: strabismus; TH: thorax anomaly; VSD: ventricular septal defect; VM: ventriculomegaly; WH: woolly hair; y: year(s)

6.1.4. SOS2

Patient ID	G19	G19-2	G21	G22	G24-1	G24-2	G25	G26	G27
Age at last follow-up	13	34	4	2 mo	30	6	6	24	42
Gender	m	f	f	M	f	f	f	m	m
Genotype	p.(Thr376Ser)	p.(Thr376Ser)	p.(Met267Lys)	p.(Met267Lys)	p.(Thr376Ser)	p.(Thr376Ser)	p.(Met267Arg)	p.(Thr264Lys)	p.(Met267Arg)
Segregation	Inherited from mother	<i>De novo</i>	Unknown	Unknown	<i>De novo</i>	Inherited from mother	unknown	<i>De novo</i>	unknown
Prenatal findings	PH	ND	ND	HF, NE, PE, PH	ND	PH	NE	ND	ND
Feeding difficulties	+	+	ND	ND	-	-	+	ND	ND
Heart defects/anomalies	VSD	-	PST, ASD	ND	ASD	-	Septal hypertrophy, ASD	-	PST, HCM
Lymphedema	-	+	+	+	-	-	+	+	-
Height SDS	-2.53	-0.50	-2.5	ND	-0.82	-0.99	-0.97	0.44	-1.65
Developmental delay	ID (mild)	-	MD(mild), ID(mild)	ND	-	-	-	-	-
Cryptorchidism	+	NA	NA	ND	NA	NA	NA	+	+
Hair and skin	SE, SH	SE, CH	HK, CH, SE	ND	SE, KP, SH, UO, CH	SE, KP, SH, UO, CH	SE, KP, UO	SE, KP, SH, UO, CH, ML	SE, CH
Skeletal	SN, TH	SN	-	ND	SN, TH	SN, TH	SN, TH	TH	TH
Bleeding diathesis	-	-	-	ND	-	-	NA	+	-
Ocular abnormalities	PT, RE		PT	ND	PT	PT	PT		PT
Additional		Gastric malrotation	-	ND			Rhabdomyoma of right ventricle (spontaneously resolved), right eye: posterior embryotoxin, left eye: enlarged corneal nerves	Bilateral uretero-pelvic junction stenosis	Charcot-Marie-Tooth disease type 2 (onset in infancy, unidentified gene), hyper eosinophilia

Table 6.4: Clinical Data from the *SOS2* cohort. *SOS2* variants are described in the three-letter code according to the isoform NP_008870.2. Abbreviations: -: absent; +: present; ASD: atrial septal defect; CH: curly hair; f: female; HCM: hypertrophic cardiomyopathy; HF: hydrops fetalis; HK: hyperkeratosis; ID: intellectual disability; KP: keratosis pilaris; m: male; MD: motor delay; ML: multiple lentigines; mo: month(s); NA: not applicable; ND: no data; NE: nuchal edema; PE: pleural effusions; PH: polyhydramnios; PST: pulmonary stenosis; PT: ptosis; RE: refractive error; SE: sparse eyebrows; SH: sparse hair; SN: short neck; TH: thorax anomalies; UO: ulerythema ophryogenes; y: year(s).

6.2. List of primers

Name	Forward Sequence	Reverse Sequence	Size (bp)
PTPN11_E02_HRM	tgcgtcttagctgtgtgttg	ggatcctctcttttcattccaa	231
PTPN11_E03_HRM	cctccctttccaatggacta	tctgacactcagggcacaag	279
PTPN11_E04_HRM	tgaacccatagtagagctaaattcttt	accatttttcaactggagatttac	266
PTPN11_E07_HRM	ttttctgtgactctttgacacg	gggtctaggaatcaaaatctcc	208
PTPN11_E08_HRM	gctggggagtaactgatttga	tcagaaaactgtgaaaagcaa	189
PTPN11_E11_HRM	tggtttttcttgctctactcc	gacagggacaggctgtgg	223
PTPN11_E12_HRM	cctgcttttgcctctctgc	cgtgagcactttccttccat	160
PTPN11_E13_HRM	cctggctctgcagtttctct	cgtatccaagaggcctagca	258
PTPN11_E14_HRM	cctcacatgtgcactcttcc	ccaccatgaccaggtaaaaaag	185
SOS1_E03_HRM	agttgttattttcctattttccaag	ttcccttaaaggcaagaagg	195
SOS1_E04_HRM	catgcttttctttaattttgcag	agaaaagctcagtttctacttt	209
SOS1_E05_HRM	catcaaattctacgaaagcttca	tgcaaatttcacacacattca	321
SOS1_E06_HRM	atgtgttttccccaaacag	ggcttttatgcagacttttctg	207
SOS1_E07_HRM	gcatagtctgccccataat	ttttcagacattgtacatcttcat	231
SOS1_E08_HRM	gggcagcactttatttgcag	aaattcacacttgaatatgttcaaaa	246
SOS1_E09_HRM	tggttcagatttgcattttgg	caccacaatattcagggaaaaa	209
SOS1_E10a_HRM	catgagctctaggtttctgtca	tcatgtttggctctctacacg	229
SOS1_E10b_HRM	gacattggacagtggttaatagaa	gcatgctgtattcattgggtg	233
SOS1_E10c_HRM	tgcgaaaggtaacaattaatga	ctaggcagcctcatctgtctc	226
SOS1_E10d_HRM	ccggagtacactggaaagga	aaagtgacaggcaactgcataa	250
SOS1_E11_HRM	tgcaaaaacattttggaactt	gctcatctaacatttctgaaaagga	290
SOS1_E13_HRM	ttcccatgtaattcaattctgtgt	ttactgagcccaatgacatc	227
SOS1_E14_HRM	aatgtattgcaggtaagcaatg	tcaacttgaatgttaaattacataccg	260
SOS1_E16_HRM	ccitttagttcactttttttattcccag	tctaatttttctaatagggaatgaaagtt	249
RAF1_E07_HRM	agcctaagtgccaatcatgg	ctgacattaccacccccaaag	226
RAF1_E12_HRM	acctccctgagcactttct	gtcccagagaggcatcagac	261
RAF1_E14_HRM	tgaaccagagtccttaacaagc	ttgccctataccagagactgc	191
RAF1_E17_HRM	tgagagcattcttgggcttt	agcctgaagacaggtgcaaa	196
SHOC2_E02_HRM	tgtccaggcttgagtcacc	tccatctttggcatctttcc	178
KRAS_E02_HRM	ggtagtttgattaaaaggtactgg	ggctctgcaccagtaatatgc	265
KRAS_E03_HRM	ccagactgtgtttctcccttc	tgcattggcattagcaaaagac	286
KRAS_E05_HRM	ctgtacacatgaagccatcg	agtctgcatggagcaggaaa	293
PTPN11_E01	agcggagcctgagcaag	ggaggcaggaatgaatgg	283
PTPN11_E02	ttccatgtgctcagcttg	aaatgcaggcagcaagctat	529
PTPN11_E03	aaaatccgacgtggaagatg	ggaatggtatgcaaccctta	525
PTPN11_E04	gatcaatcccttgagggaatg	tcctcttcagcagaaaaatcacc	552
PTPN11_E05	ctgcagtgaacatgagagtgcttg	gttgaagctgcaatgggtacatg	329
PTPN11_E06	tttgattaacaccgttttct	atttgcccaccagtccaaac	448
PTPN11_E07	gcctgaccagatgaacatt	aaccacagacaaagccacct	484
PTPN11_E08+09	tggactaggctggggagtaa	tcctaaacatggccaatctg	526
PTPN11_E10	gcctttctctcccacttct	gagtaacggcaagaccctga	420
PTPN11_E11	cgaagaggacctttcagtg	atggcagtgctgtaggtct	482
PTPN11_E12	caaagccctatgctttttgc	gccacaacatcaccctac	527
PTPN11_E13	ctctatccagccactgacc	cctgtctctctgctcaaaag	505
PTPN11_E14	tccccttaaaataaccattgtcc	ccagtgaaggcatgtgcta	273
PTPN11_E15	accatatctggtgcccaag	agaggaaaaaggagcctggt	345

Name	Forward Sequence	Reverse Sequence	Size (bp)
SOS1_E03	ggatgtgatattccccctaga	gcacccttctcaccacataa	522
SOS1_E04	gtaagcacaggcctcaggaa	ccctagtgtcaacagcacag	519
SOS1_E05	agagaagctgtggagggatg	tgatcatgaattaagtcccacaa	508
SOS1_E06	tgaaggagtcctgagaccaga	tgaccctatgaaaaaggagca	530
SOS1_E07+08_PCR	attgtgctcgcatagtcgtg	ttccatttgcttcttactgg	519
SOS1_E07+08_SEQ	attgtgctcgcatagtcgtg	aaattcacactgaaatgttacaaa	426
SOS1_E09	tccccatttctttcagtgg	tggtttgatgtcacttctctc	562
SOS1_E10a	catgagctctaggttttctgtca	ctaggcagcctcatctgctc	568
SOS1_E10b	cgtgtaggagccaaacatga	aacctatgcaggaaagaaaa	575
SOS1_E11	tgcaaaacattttggaactt	ttgttactgacaagttccatttt	559
SOS1_E13	aggacctttccaaacaagg	cagggtgacttgagccattt	526
SOS1_E14	aagattaggattggggaccg	gcctgcctggccttattact	546
SOS1_E16	tatgcctgactggaggcact	cttaggctgggacctgtgaa	552
RAF1_E07	ggtagagtttgccttaagca	tgatcagatttgaacccaaaa	350
RAF1_E12	gcttctcttctgctcagaatgc	aggcttttctgatcctgggt	442
RAF1_E14	ggctgtgacagaggtaagggtg	cggggaaatgtacagaaacg	330
RAF1_E17	gatggcaatataaggtgggag	taaggccctgtgagcagtct	426
SHOC2_E02a	tcagaaatgggcatagtgtt	gataagtcaaacgcattga	502
SHOC2_E02b	aaaatccagcaatgcagagg	aggcaagtatcaggcattttt	548
KRAS_E02	cttaagcgtcgtggaggag	ttgaaaccaaggtaacattca	490
KRAS_E03	tcactttggagcaggaaca	tgcattggcattagcaaagac	403
KRAS_E04	ttgtggacaggttttgaaaga	agaaaccaagccaaaagca	420
KRAS_E05	cttcttgacatggctttcc	tctaaagtgggtgccacctgt	280
NRAS_E02	tccttccatttggctcctac	tgggtaaagatgatccgaca	557
NRAS_E03	caaaccagataggcagaaatgg	ggtaacctcatttcccataaag	286
RIT1_E01+02	taggagggagggtgaagatg	ttcatccatgcttctctgtca	373
RIT1_E01_HRM	taggagggagggtgaagatg	cgaggaaaagccacctagaa	199
RIT1_E02_HRM	aagcatttctctctcttttc	ttcatccatgcttctctgtca	212
RIT1_E03	tgggtcacctttgtgaggat	ccaactgctgatacccttgtt	245
RIT1_E04	gcatttcttccggcatttat	cccctcccctttgctagagt	185
RIT1_E05	tcaggatagcaggtaatcgaca	aagccaagccaagaatctgt	389
RIT1_E05a_HRM	tcaggatagcaggtaatcgaca	cgtcggactcgataaataagc	243
RIT1_E05b_HRM	gggcaggagaagggtttatc	aagccaagccaagaatctgt	243
RIT1_E06	tgcattcaggtttttggaca	tgcaggttactggactgcttt	364
RIT1_E06a_HRM	tgcattcaggtttttggaca	ggccagtactgcctcctttt	215
RIT1_E06b_HRM	catctgtgcataaccgctac	tgcaggttactggactgcttt	238
RRAS_E01	gtagcgaaggcagcagcag	ccccagggtcagttct	239
RRAS_E02	actgagagaggcatccaag	ctcagccccactgacac	222
RRAS_E03	gtgtcagtggggctgag	agctgcagagcccaggtc	247
RRAS_E04	gagcagtgggtgggtgtg	gacaggtgtgctggaaggag	249
RRAS_E05	ctcttggctgcggtcac	aaacgccagtgtggtggag	247
RRAS_E06	caagtccccttctgtcgt	ctagtcccagagcttggg	195
BRAF_E06	aacccccggttttcatttta	ccagcattacaatttgggaga	496
BRAF_E11	tttctgttggcttgacttga	cctggagggaattccccttta	404
BRAF_E12	catggaacaacaaggttg	ctaccactgggaaccaggag	404
BRAF_E13	gcaacctctagtgcctgtca	tccaaaagaatagcagccaaa	493
BRAF_E14	ggcttgactggagtgaaagg	ccaaaagcaggctgtggtat	508
BRAF_E15	ctgcagcatcttattccaa	agtaactcagcagcatctcagg	551
BRAF_E16	tcatgggaagaattcatctgg	ttcacgcttaccaggagtt	572

Name	Forward Sequence	Reverse Sequence	Size (bp)
BRAF_E17	ctttgccacagtccaaggat	ctagggtgcccactgctcaa	530
MEK1_E02	cccagacctggagctttctt	tggccccaggcttctaagt	370
MEK1_E03	tctgagctccaaagcctctc	tagctggtcacctcccagac	513
MEK1_E06	aagggccttgggtgtacagtg	ccctaccagcacaagactc	393
MEK1_E07	caggaggccaaattcaagag	aacaacaccacctggagac	512
MEK2_E02	tgcaggaatccagctctgtgt	aacctgacctctgtttccag	392
MEK2_E03	ttggtcttgaccactgttgg	gtgaggggggtcttctctc	330
MEK2_E05+06	gggctcggtcaggagctaag	agagcttgggggagagcag	385
MEK2_E07	ttagccatggagagggtgac	tcactgcttcagctctgtc	503
HRAS_E02	caggagacctgtaggagga	gcctctcctggtacctctc	362
HRAS_E03	caggacacagccaggatagg	tgatctgctcctgagaggt	561
HRAS_E04+05	ctgtcctctctgcgcatgtc	gtccgggagacttacagc	428
HRAS_E06	ccagacctggagttcaggag	cctccatgtcctgagcttgt	504

Table 6.5: List of all primers used in this thesis project.

6.3. List of genes analyzed on the NGS panel

Gene	Transcript Number	Reason for Inclusion
PTPN11	NM_002834.3	Reported as causative
SOS1	NM_005633.3	Reported as causative
RAF1 (CRAF)	NM_002880.3	Reported as causative
KRAS	NM_004985.3	Reported as causative
NRAS	NM_002524.4	Reported as causative
SHOC2	NM_007373.3	Reported as causative
CBL	NM_005188.3	Reported as causative
RIT1	NM_014949.2	Reported as causative
RRAS	NM_006270.3	Reported as causative
RASA2	NM_006506.2	Reported as causative
SOS2	NM_006939.2	Reported as causative
LZTR1	NM_006767.3	Reported as causative
BRAF	NM_004333.4	Reported as causative
MAP2K1 (MEK1)	NM_002755.3	Reported as causative
MAP2K2 (MEK2)	NM_030662.3	Reported as causative
HRAS	NM_005343.2	Reported as causative
NF1	NM_001042492.2	Reported as causative
SPRED1	NM_152594.2	Reported as causative
A2ML1	NM_144670.4	Reported as causative
SPRY1	NM_001258038.1	Reported as possible candidate gene
MAP3K8	NM_005204.3	Reported as possible candidate gene
CDC42	NM_001791.3	Unpublished: variant found in RASopathy patient
RRAS2	NM_012250.5	Unpublished: variant found in RASopathy patient
SPRED2	NM_181784.2	Unpublished: variant found in RASopathy patient
SON	NM_138927.2	Unpublished: variant found in RASopathy patient
NBAS	NM_015909.3	Unpublished: variant found in RASopathy patient
MRAS	NM_012219.4	Reported as causative
RASGRP2	NM_001098671.1	Unpublished: variant found in RASopathy patient
PIK3CB	NM_006219.2	Unpublished: variant found in RASopathy patient
PTPRN	NM_002846.3	Unpublished: variant found in RASopathy patient
ITPR2	NM_002223.3	Unpublished: variant found in RASopathy patient
PLCG1	NM_002660.2	Unpublished: variant found in RASopathy patient
PRKCA	NM_002737.2	Unpublished: variant found in RASopathy patient
ZNF641	NM_152320.2	Unpublished: variant found in RASopathy patient
CABIN1	NM_012295.3	Reported as possible candidate gene
ERAS	NM_181532.3	Functional candidate gene
MAPK3 (ERK1)	NM_002746.2	Functional candidate gene

MAPK1 (ERK2)	NM_002745.4	Functional candidate gene
ARAF	NM_001256196.1	Functional candidate gene
SHC1	NM_183001.4	Functional candidate gene
SHC2	NM_012435.2	Functional candidate gene
GAB1	NM_207123.2	Functional candidate gene
GRB2	NM_002086.4	Functional candidate gene
RT2	NM_002930.3	Functional candidate gene
RIN1	NM_004292.2	Functional candidate gene
FGD1	NM_004463.2	Differential Diagnosis: Aarskog syndrome
RPS6KA3	NM_004586.2	Differential Diagnosis: Coffin-Lowry
KAT6B	NM_012330.3	Differential Diagnosis: Ohdo, GPS
SMARCA2	NM_003070.4	Differential Diagnosis: Nicolaides-Baraitser
RIN2	NM_001242581.1	Differential Diagnosis: MACS-syndrom
ACTB	NM_001101.3	Differential Diagnosis: Baraitser-Winter
ACTG1	NM_001614.3	Differential Diagnosis: Baraitser-Winter

Table 6.6: List of genes analyzed using the Nextera Rapid Capture Enrichment on a MiSeq (Illumina).

6.4. Patient list

Patient ID	Result	Gene	Variant(s)	Methods			Classification first variant	Classification second variant
C2	variant found	CBL	c.1096-1G>T		Sanger		likely pathogenic	
C3	variant found	CBL	p.Gln367Pro		Sanger		pathogenic	
C4	variant found	CBL	c.1096-4_1096-1 delAAAG		Sanger		likely pathogenic	
C5	variant found	CBL	c.1096-1G>C		Sanger	NGS	pathogenic	
C6	variant found	CBL	p.Gly838Val		Sanger	NGS	VUS	
C7	variant found	CBL	p.Ala758Val		Sanger	NGS	VUS	
G01	variant found	LZTR1	p.Arg284Cys		Sanger	NGS	pathogenic	
G02	variant found	LZTR1	p.Arg688Gly		Sanger	NGS	likely pathogenic	
G03	variant found	LZTR1	p.Arg283Gln		Sanger	NGS	VUS	
G04	variant found	LZTR1	p.Arg170Gln	HRM	Sanger	NGS	VUS	
G05	variant found	LZTR1	p.His121Asp/ p.Arg755Gln		Sanger	NGS	VUS	VUS
G06	variant found	LZTR1	p.Arg170Trp		Sanger	NGS	VUS	
G07	variant found	LZTR1	p.Ile205Thr(hom)/ p.Arg170Trp(hom)		Sanger	NGS	VUS	VUS
G08	variant found	LZTR1	p.Arg284Cys		Sanger	NGS	pathogenic	
G09	variant found	LZTR1	p.Met91Val			NGS	VUS	
G10	variant found	LZTR1	p.Arg697Glu/ c.2407-2A>G		Sanger	NGS	VUS	VUS
G11	variant found	LZTR1	p.Gln832Arg		Sanger	NGS	VUS	
G12	variant found	LZTR1	p.Arg283Gln		Sanger	NGS	VUS	
G13	variant found	RASA2	p.Ser12Thr	HRM	Sanger	NGS	VUS	
G14	variant found	RASA2	p.Arg511His		Sanger	NGS	VUS	
G16	variant found	SOS2	p.Asn310Ser	HRM	Sanger	NGS	VUS	
G17	variant found	SOS2	p.Asn1229Tyr	HRM	Sanger	NGS	VUS	
G18	variant found	SOS2	p.Pro1318Ser		Sanger	NGS	VUS	
G19	variant found	SOS2	p.Thr376Ser	HRM	Sanger	NGS	pathogenic	
G20	variant found	SOS2	p.Pro404Thr		Sanger	NGS	VUS	
G21	variant found	SOS2	p.Met267Lys/ p.Glu266Asp		Sanger	NGS	pathogenic	
G22	variant found	SOS2	p.Met267Lys		Sanger	NGS	pathogenic	
G23	variant found	SOS2/ LZTR1	p.Lys739Asn/ p.Arg619His (hom)		Sanger	NGS	VUS	VUS
N04-1	variant found	NRAS	p.Thr50Ile		Sanger		pathogenic	
N04-2	variant found	NRAS	p.Thr50Ile		Sanger		pathogenic	

N06	variant found	NRAS	p.Gly60Glu		Sanger		pathogenic	
N14	variant found	NRAS	p.Gly60Glu		Sanger	NGS	pathogenic	
P001	variant found	BRAF	p.Ala246Pro		Sanger		pathogenic	
P002	variant found	BRAF	p.Asn236Lys	HRM	Sanger	NGS	likely pathogenic	
P003	variant found	BRAF	p.Asn580Asp		Sanger		pathogenic	
P004	variant found	BRAF	p.Asn581Asp		Sanger		pathogenic	
P005	variant found	BRAF	p.Asp638Glu		Sanger		pathogenic	
P006	variant found	BRAF	p.Cys532_Ser535 delinsTyrSerTrp		Sanger		likely pathogenic	
P007	variant found	BRAF	p.Gln257Arg	HRM	Sanger		pathogenic	
P008	variant found	BRAF	p.Gln257Arg		Sanger		pathogenic	
P009	variant found	BRAF	p.Gln257Arg		Sanger		pathogenic	
P010	variant found	BRAF	p.Gln257Arg	HRM	Sanger	NGS	pathogenic	
P011	variant found	BRAF	p.Gln257Arg		Sanger		pathogenic	
P012	variant found	BRAF	p.Gln257Arg	HRM	Sanger	NGS	pathogenic	
P013	variant found	BRAF	p.Gln257Arg		Sanger		pathogenic	
P014	variant found	BRAF	p.Gln262Pro	HRM	Sanger	NGS	pathogenic	
P015	variant found	BRAF	p.Gln262Pro		Sanger		pathogenic	
P016	variant found	BRAF	p.Gly464Ala		Sanger		pathogenic	
P017	variant found	BRAF	p.Gly466_Phe468del		Sanger		likely pathogenic	
P018	variant found	BRAF	p.Gly466Ser		Sanger		likely pathogenic	
P019	variant found	BRAF	p.Gly469Glu		Sanger		pathogenic	
P020	variant found	BRAF	p.Gly596Val		Sanger		pathogenic	
P021	variant found	BRAF	p.Leu245Phe		Sanger		pathogenic	
P022	variant found	BRAF	p.Leu485Phe		Sanger		pathogenic	
P023	variant found	BRAF	p.Lys499Glu		Sanger		pathogenic	
P024	variant found	BRAF	p.Phe468Ser		Sanger		pathogenic	
P025	variant found	BRAF	p.Phe595Leu		Sanger		pathogenic	
P026	variant found	BRAF	p.Val600Leu	HRM	Sanger		likely pathogenic	
P027	variant found	FGD1	p.Glu668Lys		Sanger	NGS	VUS	
P028	variant found	HRAS	p.Glu63_Asp69 dup	HRM	Sanger		likely pathogenic	
P029	variant found	HRAS	p.Gly12Ala		Sanger		pathogenic	
P030	variant found	HRAS	p.Gly12Ala		Sanger		pathogenic	
P031	variant found	HRAS	p.Gly12Ser		Sanger		pathogenic	
P032	variant found	HRAS	p.Gly12Ser		Sanger		pathogenic	
P033	variant found	HRAS	p.Gly12Ser		Sanger		pathogenic	
P034	variant found	HRAS	p.Gly12Ser		Sanger		pathogenic	
P035	variant found	HRAS	p.Gly12Ser		Sanger	NGS	pathogenic	
P036	variant found	HRAS	p.Gly13Cys		Sanger		pathogenic	
P037	variant found	HRAS	p.Lys117Arg	HRM	Sanger		pathogenic	
P038	variant found	HRAS	p.Thr58Ile		Sanger	NGS	pathogenic	
P039	variant found	KRAS	p.Asp153Val	HRM			pathogenic	
P040	variant found	KRAS	p.Asp153Val		Sanger		pathogenic	
P041	variant found	KRAS	p.Asp153Val		Sanger	NGS	pathogenic	
P042	variant found	KRAS	p.Gln22Leu	HRM			pathogenic	
P043	variant found	KRAS	p.Glu22Arg			NGS	pathogenic	
P044	variant found	KRAS	p.Ile36Met	HRM	Sanger	NGS	pathogenic	
P045	variant found	KRAS	p.Phe156Leu			NGS	pathogenic	
P046	variant found	KRAS	p.Pro34Arg		Sanger		pathogenic	
P047	variant found	KRAS	p.Thr58Ile	HRM	Sanger	NGS	pathogenic	
P048	variant found	KRAS	p.Val14Ile		Sanger		pathogenic	
P049	variant found	MEK1	p.Asp67Asn		Sanger		pathogenic	
P050	variant found	MEK1	p.Asp67Asn		Sanger	NGS	pathogenic	
P051	variant found	MEK1	p.Asp67Asn		Sanger		pathogenic	
P052	variant found	MEK1	p.Gly128Val		Sanger		pathogenic	
P053	variant found	MEK1	p.Lys59del		Sanger		pathogenic	
P054	variant found	MEK1	p.Tyr130Cys	HRM	Sanger		pathogenic	
P055	variant found	MEK1	p.Tyr130Cys		Sanger		pathogenic	
P056	variant found	MEK1	p.Tyr130Cys	HRM	Sanger		pathogenic	
P057	variant found	MEK2	p.Asn126Asp		Sanger		VUS	

P058	variant found	MEK2	p.Gly132Asp		Sanger		pathogenic	
P059	variant found	MEK2	p.Phe57Cys	HRM	Sanger		pathogenic	
P060	variant found	MEK2	p.Phe57Cys		Sanger		pathogenic	
P061	variant found	MEK2	p.Phe57Ile		Sanger		pathogenic	
P062	variant found	NF1	p.Arg1276Gln	HRM	Sanger	NGS	pathogenic	
P063	variant found	NF1	p.Arg1846Trp		Sanger	NGS	VUS	
P064	variant found	NF1	p.Arg2517X		Sanger		pathogenic	
P065	variant found	NF1	p.Gly1890Val			NGS	VUS	
P066	variant found	NF1	p.Gly1681Valfs *8/ p.Glu1415Lys		Sanger	NGS	pathogenic	VUS
P067	variant found	NF1	p.Tyr1594Cys		Sanger	NGS	likely pathogenic	
P068	variant found	PTPN11	p.Ala461Ser		Sanger		pathogenic	
P069	variant found	PTPN11	p.Ala461Thr		Sanger		pathogenic	
P070	variant found	PTPN11	p.Ala72Ser	HRM			pathogenic	
P071	variant found	PTPN11	p.Ala72Ser		Sanger	NGS	pathogenic	
P072	variant found	PTPN11	p.Arg265Gln	HRM			pathogenic	
P073	variant found	PTPN11	p.Asn308Asp	HRM			pathogenic	
P074	variant found	PTPN11	p.Asn308Asp	HRM			pathogenic	
P075	variant found	PTPN11	p.Asn308Asp	HRM			pathogenic	
P076	variant found	PTPN11	p.Asn308Asp	HRM			pathogenic	
P077	variant found	PTPN11	p.Asn308Asp	HRM			pathogenic	
P078	variant found	PTPN11	p.Asn308Asp	HRM			pathogenic	
P079	variant found	PTPN11	p.Asn308Asp		Sanger	NGS	pathogenic	
P080	variant found	PTPN11	p.Asn308Asp	HRM			pathogenic	
P081	variant found	PTPN11	p.Asn308Asp	HRM			pathogenic	
P082	variant found	PTPN11	p.Asn308Asp	HRM			pathogenic	
P083	variant found	PTPN11	p.Asn308Asp		Sanger		pathogenic	
P084	variant found	PTPN11	p.Asn308Asp			NGS	pathogenic	
P085	variant found	PTPN11	p.Asn308Asp	HRM			pathogenic	
P086	variant found	PTPN11	p.Asn308Ser	HRM			pathogenic	
P087	variant found	PTPN11	p.Asn308Ser	HRM			pathogenic	
P088	variant found	PTPN11	p.Asn308Ser	HRM			pathogenic	
P089	variant found	PTPN11	p.Asn308Ser	HRM			pathogenic	
P090	variant found	PTPN11	p.Asn308Ser	HRM			pathogenic	
P091	variant found	PTPN11	p.Asn308Ser		Sanger		pathogenic	
P092	variant found	PTPN11	p.Asn308Ser	HRM			pathogenic	
P093	variant found	PTPN11	p.Asn308Ser	HRM			pathogenic	
P094	variant found	PTPN11	p.Asn308Ser	HRM			pathogenic	
P095	variant found	PTPN11	p.Asn308Ser	HRM			pathogenic	
P096	variant found	PTPN11	p.Asn308Ser	HRM			pathogenic	
P097	variant found	PTPN11	p.Asn308Ser	HRM			pathogenic	
P098	variant found	PTPN11	p.Asn308Ser	HRM			pathogenic	
P099	variant found	PTPN11	p.Asn308Ser	HRM			pathogenic	
P100	variant found	PTPN11	p.Asn58Asp	HRM			pathogenic	
P101	variant found	PTPN11	p.Asn58Asp	HRM			pathogenic	
P102	variant found	PTPN11	p.Asn58Asp	HRM			pathogenic	
P103	variant found	PTPN11	p.Asn58Lys	HRM			pathogenic	
P104	variant found	PTPN11	p.Asp106Ala	HRM			pathogenic	
P105	variant found	PTPN11	p.Asp106Ala	HRM			pathogenic	
P106	variant found	PTPN11	p.Asp61Asn	HRM			pathogenic	
P107	variant found	PTPN11	p.Asp61Asn	HRM			pathogenic	
P108	variant found	PTPN11	p.Asp61Asn	HRM			pathogenic	
P109	variant found	PTPN11	p.Asp61Asn		Sanger		pathogenic	
P110	variant found	PTPN11	p.Asp61Asn	HRM			pathogenic	
P111	variant found	PTPN11	p.Asp61Gly	HRM			pathogenic	
P112	variant found	PTPN11	p.Asp61Gly	HRM			pathogenic	
P113	variant found	PTPN11	p.Asp61Gly	HRM			pathogenic	
P114	variant found	PTPN11	p.Asp61Gly	HRM			pathogenic	
P115	variant found	PTPN11	p.Asp61Gly	HRM			pathogenic	
P116	variant found	PTPN11	p.Asp61Gly	HRM			pathogenic	
P117	variant found	PTPN11	p.Asp61Gly	HRM			pathogenic	
P118	variant found	PTPN11	p.Asp61Gly	HRM			pathogenic	
P119	variant found	PTPN11	p.Asp61Gly	HRM			pathogenic	
P120	variant found	PTPN11	p.Asp61Gly		Sanger		pathogenic	

P121	variant found	PTPN11	p.Gln256Arg	HRM			pathogenic	
P122	variant found	PTPN11	p.Gln256Arg	HRM			pathogenic	
P123	variant found	PTPN11	p.Gln256Arg		Sanger		pathogenic	
P124	variant found	PTPN11	p.Gln257dup		Sanger		likely pathogenic	
P125	variant found	PTPN11	p.Gln257dup		Sanger		likely pathogenic	
P126	variant found	PTPN11	p.Gln510Glu		Sanger		pathogenic	
P127	variant found	PTPN11	p.Gln510Pro		Sanger		pathogenic	
P128	variant found	PTPN11	p.Gln79Arg	HRM			pathogenic	
P129	variant found	PTPN11	p.Gln79Arg	HRM			pathogenic	
P130	variant found	PTPN11	p.Gln79Arg	HRM			pathogenic	
P131	variant found	PTPN11	p.Gln79Arg	HRM			pathogenic	
P132	variant found	PTPN11	p.Glu110Lys	HRM			pathogenic	
P133	variant found	PTPN11	p.Glu139Asp	HRM			pathogenic	
P134	variant found	PTPN11	p.Glu139Asp	HRM			pathogenic	
P135	variant found	PTPN11	p.Glu139Asp	HRM			pathogenic	
P136	variant found	PTPN11	p.Glu139Asp		Sanger		pathogenic	
P137	variant found	PTPN11	p.Glu139Asp	HRM			pathogenic	
P138	variant found	PTPN11	p.Glu139Asp	HRM			pathogenic	
P139	variant found	PTPN11	p.Glu76Asp		Sanger		pathogenic	
P140	variant found	PTPN11	p.Gly503Arg	HRM			pathogenic	
P141	variant found	PTPN11	p.Gly503Arg	HRM			pathogenic	
P142	variant found	PTPN11	p.Gly503Arg	HRM			pathogenic	
P143	variant found	PTPN11	p.Gly503Arg	HRM			pathogenic	
P144	variant found	PTPN11	p.Gly503Arg	HRM			pathogenic	
P145	variant found	PTPN11	p.Gly503Arg		Sanger		pathogenic	
P146	variant found	PTPN11	p.Gly60Ala	HRM			pathogenic	
P147	variant found	PTPN11	p.Gly60Ala		Sanger		pathogenic	
P148	variant found	PTPN11	p.Gly60del	HRM			pathogenic	
P149	variant found	PTPN11	p.Ile282Met	HRM			pathogenic	
P150	variant found	PTPN11	p.Ile282Met	HRM			pathogenic	
P151	variant found	PTPN11	p.Ile282Val	HRM			pathogenic	
P152	variant found	PTPN11	p.Ile282Val	HRM			pathogenic	
P153	variant found	PTPN11	p.Leu261Phe	HRM			pathogenic	
P154	variant found	PTPN11	p.Leu261Phe	HRM			pathogenic	
P155	variant found	PTPN11	p.Met504Val	HRM			pathogenic	
P156	variant found	PTPN11	p.Met504Val	HRM			pathogenic	
P157	variant found	PTPN11	p.Met504Val	HRM			pathogenic	
P158	variant found	PTPN11	p.Met504Val	HRM			pathogenic	
P159	variant found	PTPN11	p.Met504Val	HRM			pathogenic	
P160	variant found	PTPN11	p.Met504Val	HRM			pathogenic	
P161	variant found	PTPN11	p.Met504Val		Sanger		pathogenic	
P162	variant found	PTPN11	p.Met504Val	HRM			pathogenic	
P163	variant found	PTPN11	p.Phe285Cys	HRM			pathogenic	
P164	variant found	PTPN11	p.Phe285Leu	HRM			pathogenic	
P165	variant found	PTPN11	p.Phe285Ser	HRM			pathogenic	
P166	variant found	PTPN11	p.Phe285Ser		Sanger		pathogenic	
P167	variant found	PTPN11	p.Phe285Ser		Sanger		pathogenic	
P168	variant found	PTPN11	p.Phe285Ser			NGS	pathogenic	
P169	variant found	PTPN11	p.Phe285Ser	HRM			pathogenic	
P170	variant found	PTPN11	p.Phe285Ser	HRM			pathogenic	
P171	variant found	PTPN11	p.Pro491Ala/ Arg498Trp	HRM			likely pathogenic	pathogenic
P172	variant found	PTPN11	p.Pro491Ser	HRM			pathogenic	
P173	variant found	PTPN11	p.Ser502Leu	HRM			pathogenic	
P174	variant found	PTPN11	p.Ser502Leu		Sanger		pathogenic	
P175	variant found	PTPN11	p.Ser502Thr	HRM			pathogenic	
P176	variant found	PTPN11	p.Thr2Ile			NGS	pathogenic	
P177	variant found	PTPN11	p.Thr468Met		Sanger		pathogenic	
P178	variant found	PTPN11	p.Thr468Met		Sanger		pathogenic	
P179	variant found	PTPN11	p.Thr468Met		Sanger	NGS	pathogenic	
P180	variant found	PTPN11	p.Thr468Met		Sanger		pathogenic	
P181	variant found	PTPN11	p.Thr468Met		Sanger		pathogenic	
P182	variant found	PTPN11	p.Thr468Met		Sanger		pathogenic	
P183	variant found	PTPN11	p.Thr468Met	HRM			pathogenic	

P184	variant found	PTPN11	p.Thr468Met		Sanger		pathogenic	
P185	variant found	PTPN11	p.Thr52Ile		Sanger		pathogenic	
P186	variant found	PTPN11	p.Thr73Ile	HRM			pathogenic	
P187	variant found	PTPN11	p.Tyr279Cys		Sanger		pathogenic	
P188	variant found	PTPN11	p.Tyr279Cys	HRM			pathogenic	
P189	variant found	PTPN11	p.Tyr62Asp	HRM			pathogenic	
P190	variant found	PTPN11	p.Tyr62Asp	HRM			pathogenic	
P191	variant found	PTPN11	p.Tyr62Asp		Sanger		pathogenic	
P192	variant found	PTPN11	p.Tyr62Asp	HRM			pathogenic	
P193	variant found	PTPN11	p.Tyr62Asp	HRM			pathogenic	
P194	variant found	PTPN11	p.Tyr62Asp	HRM			pathogenic	
P195	variant found	PTPN11	p.Tyr62Asp	HRM			pathogenic	
P196	variant found	PTPN11	p.Tyr63Cys	HRM			pathogenic	
P197	variant found	PTPN11	p.Tyr63Cys	HRM			pathogenic	
P198	variant found	PTPN11	p.Tyr63Cys	HRM			pathogenic	
P199	variant found	PTPN11	p.Tyr63Cys	HRM			pathogenic	
P200	variant found	PTPN11	p.Tyr63Cys	HRM			pathogenic	
P201	variant found	PTPN11	p.Tyr63Cys	HRM			pathogenic	
P202	variant found	PTPN11	p.Val428Met	HRM			likely pathogenic	
P203	variant found	PTPN11 / CBL	p.Glu139Asp/ p.Gly475Ser		Sanger		pathogenic	
P204	variant found	RAF1	p.Gly361Ala	HRM		NGS	likely pathogenic	
P205	variant found	RAF1	p.Leu613Val		Sanger		pathogenic	
P206	variant found	RAF1	p.Pro261Ala	HRM			pathogenic	
P207	variant found	RAF1	p.Pro261Ser	HRM			pathogenic	
P208	variant found	RAF1	p.Pro261Ser		Sanger		pathogenic	
P209	variant found	RAF1	p.Pro261Thr	HRM			pathogenic	
P210	variant found	RAF1	p.Pro261Thr	HRM			pathogenic	
P211	variant found	RAF1	p.Ser257Leu	HRM			pathogenic	
P212	variant found	RAF1	p.Ser257Leu		Sanger		pathogenic	
P213	variant found	RAF1	p.Ser257Leu	HRM			pathogenic	
P214	variant found	RAF1	p.Ser257Leu		Sanger		pathogenic	
P215	variant found	RAF1	p.Ser257Leu	HRM			pathogenic	
P216	variant found	RAF1	p.Ser257Leu		Sanger		pathogenic	
P217	variant found	RAF1	p.Ser257Leu	HRM			pathogenic	
P218	variant found	RAF1	p.Ser257Leu	HRM			pathogenic	
P219	variant found	RAF1	p.Ser257Leu	HRM			pathogenic	
P220	variant found	RAF1	p.Ser257Leu		Sanger		pathogenic	
P221	variant found	RAF1	p.Ser257Leu		Sanger	NGS	pathogenic	
P222	variant found	RAF1	p.Ser257Leu		Sanger	NGS	pathogenic	
P223	variant found	RAF1	p.Ser257Leu		Sanger		pathogenic	
P224	variant found	RAF1	p.Ser259Pro	HRM			pathogenic	
P225	variant found	RAF1	p.Ser259Tyr	HRM			pathogenic	
P226	variant found	RAF1	p.Thr491Ile		Sanger		pathogenic	
P227	variant found	RAF1	p.Val263Gly		Sanger		pathogenic	
P228	variant found	RRAS	p.Gln87Leu		Sanger	NGS	likely pathogenic	
P229	variant found	SOS1	p.Arg552Gly	HRM			pathogenic	
P230	variant found	SOS1	p.Arg552Gly		Sanger		pathogenic	
P231	variant found	SOS1	p.Arg552Gly	HRM			pathogenic	
P232	variant found	SOS1	p.Arg552Gly	HRM			pathogenic	
P233	variant found	SOS1	p.Arg552Gly		Sanger		pathogenic	
P234	variant found	SOS1	p.Arg552Gly	HRM			pathogenic	
P235	variant found	SOS1	p.Arg552Gly		Sanger	NGS	pathogenic	
P236	variant found	SOS1	p.Arg552Lys	HRM			pathogenic	
P237	variant found	SOS1	p.Arg552Lys	HRM			pathogenic	
P238	variant found	SOS1	p.Arg552Ser	HRM			pathogenic	
P239	variant found	SOS1	p.Arg552Thr		Sanger		pathogenic	
P240	variant found	SOS1	p.Arg552Thr		Sanger	NGS	pathogenic	
P241	variant found	SOS1	p.Cys441Tyr		Sanger		pathogenic	
P242	variant found	SOS1	p.Cys441Tyr	HRM			pathogenic	
P243	variant found	SOS1	p.E551_L554 delinsG		Sanger		pathogenic	

P244	variant found	SOS1	p.E551_L554 delinsG		Sanger		pathogenic	
P245	variant found	SOS1	p.Gln125His	HRM			VUS	
P246	variant found	SOS1	p.Glu191Lys	HRM			likely pathogenic	
P247	variant found	SOS1	p.Glu433Lys	HRM			pathogenic	
P248	variant found	SOS1	p.Glu433Lys		Sanger		pathogenic	
P249	variant found	SOS1	p.Glu433Lys	HRM			pathogenic	
P250	variant found	SOS1	p.Glu846Lys			NGS	pathogenic	
P251	variant found	SOS1	p.Glu846Lys	HRM	Sanger	NGS	pathogenic	
P252	variant found	SOS1	p.Glu95Lys		Sanger		likely pathogenic	
P253	variant found	SOS1	p.Gly434Arg	HRM			pathogenic	
P254	variant found	SOS1	p.Gly434Arg	HRM			pathogenic	
P255	variant found	SOS1	p.Gly434Arg		Sanger		pathogenic	
P256	variant found	SOS1	p.Ile733Phe	HRM			pathogenic	
P257	variant found	SOS1	p.Lys170Glu		Sanger		pathogenic	
P258	variant found	SOS1	p.Met269Ala		Sanger	NGS	pathogenic	
P259	variant found	SOS1	p.Met269Arg	HRM			pathogenic	
P260	variant found	SOS1	p.Met269Arg	HRM			pathogenic	
P261	variant found	SOS1	p.Met269Arg		Sanger		pathogenic	
P262	variant found	SOS1	p.Met269Arg	HRM			pathogenic	
P263	variant found	SOS1	p.Met269Arg	HRM			pathogenic	
P264	variant found	SOS1	p.Met269Arg	HRM			pathogenic	
P265	variant found	SOS1	p.Met269Arg	HRM			pathogenic	
P266	variant found	SOS1	p.Met269Thr	HRM			pathogenic	
P267	variant found	SOS1	p.Ser548Arg	HRM			pathogenic	
P268	variant found	SOS1	p.Thr266Lys	HRM			pathogenic	
P269	variant found	SOS1	p.Thr266Lys	HRM			pathogenic	
P270	variant found	SOS1	p.Thr266Lys	HRM			pathogenic	
P271	variant found	SOS1	p.Thr266Lys	HRM			pathogenic	
P272	variant found	SOS1	p.Trp432Arg			NGS	pathogenic	
P273	variant found	SOS1	p.Tyr702His	HRM			pathogenic	
P274	variant found	SOS1	p.Val1120Ile	HRM	Sanger	NGS	VUS	
P275	variant found	SOS1	p.Val171Gly	HRM			likely pathogenic	
P276	no variant found				Sanger			
P277	no variant found				Sanger			
P278	no variant found				Sanger			
P279	no variant found				Sanger			
P280	no variant found			HRM	Sanger			
P281	no variant found			HRM	Sanger			
P282	no variant found			HRM	Sanger			
P283	no variant found			HRM	Sanger			
P284	no variant found			HRM	Sanger			
P285	no variant found			HRM	Sanger			
P286	no variant found			HRM	Sanger			
P287	no variant found			HRM	Sanger			
P288	no variant found			HRM	Sanger			
P289	no variant found			HRM	Sanger			
P290	no variant found			HRM	Sanger			
P291	no variant found			HRM	Sanger			
P292	no variant found			HRM	Sanger			
P293	no variant found			HRM	Sanger			
P294	no variant found			HRM	Sanger			
P295	no variant found			HRM	Sanger			
P296	no variant found				Sanger			
P297	no variant found				Sanger			
P298	no variant found			HRM	Sanger			
P299	no variant found			HRM	Sanger			
P300	no variant found				Sanger			
P301	no variant found			HRM	Sanger			
P302	no variant found			HRM	Sanger	NGS		
P303	no variant found			HRM	Sanger			
P304	no variant found			HRM	Sanger			
P305	no variant found			HRM	Sanger			

P306	no variant found				Sanger			
P307	no variant found			HRM	Sanger			
P308	no variant found			HRM	Sanger			
P309	no variant found			HRM	Sanger			
P310	no variant found			HRM	Sanger	NGS		
P311	no variant found				Sanger			
P312	no variant found				Sanger			
P313	no variant found				Sanger	NGS		
P314	no variant found			HRM	Sanger			
P315	no variant found				Sanger			
P316	no variant found			HRM	Sanger			
P317	no variant found			HRM	Sanger			
P318	no variant found			HRM	Sanger			
P319	no variant found				Sanger			
P320	no variant found			HRM	Sanger			
P321	no variant found				Sanger			
P322	no variant found			HRM	Sanger			
P323	no variant found				Sanger			
P324	no variant found			HRM	Sanger			
P325	no variant found			HRM	Sanger			
P326	no variant found			HRM	Sanger			
P327	no variant found			HRM	Sanger			
P328	no variant found			HRM	Sanger			
P329	no variant found				Sanger			
P330	no variant found				Sanger			
P331	no variant found			HRM	Sanger			
P332	no variant found			HRM	Sanger			
P333	no variant found			HRM	Sanger			
P334	no variant found			HRM	Sanger	NGS		
P335	no variant found			HRM	Sanger			
P336	no variant found			HRM	Sanger			
P337	no variant found			HRM	Sanger			
P338	no variant found			HRM	Sanger			
P339	no variant found			HRM	Sanger			
P340	no variant found			HRM	Sanger			
P341	no variant found			HRM	Sanger			
P342	no variant found				Sanger			
P343	no variant found				Sanger			
P344	no variant found				Sanger	NGS		
P345	no variant found			HRM	Sanger			
P346	no variant found				Sanger			
P347	no variant found					NGS		
P348	no variant found			HRM	Sanger			
P349	no variant found			HRM	Sanger			
P350	no variant found			HRM	Sanger			
P351	no variant found			HRM	Sanger			
P352	no variant found				Sanger			
P353	no variant found				Sanger			
P354	no variant found				Sanger			
P355	no variant found				Sanger			
P356	no variant found			HRM	Sanger			
P357	no variant found			HRM	Sanger			
P358	no variant found				Sanger			
P359	no variant found				Sanger	NGS		
P360	no variant found			HRM	Sanger			
P361	no variant found			HRM	Sanger	NGS		
P362	no variant found			HRM	Sanger			
P363	no variant found			HRM	Sanger	NGS		
P364	no variant found			HRM	Sanger			
P365	no variant found			HRM	Sanger			
P366	no variant found				Sanger			
P367	no variant found				Sanger			
P368	no variant found				Sanger	NGS		
P369	no variant found			HRM	Sanger			
P370	no variant found			HRM	Sanger			
P371	no variant found			HRM	Sanger			

P372	no variant found				Sanger			
P373	no variant found			HRM	Sanger			
P374	no variant found				Sanger			
P375	no variant found				Sanger	NGS		
P376	no variant found			HRM	Sanger			
P377	no variant found				Sanger	NGS		
P378	no variant found				Sanger			
P379	no variant found			HRM	Sanger	NGS		
P380	no variant found				Sanger	NGS		
P381	no variant found				Sanger	NGS		
P382	no variant found			HRM	Sanger			
P383	no variant found			HRM	Sanger			
P384	no variant found			HRM	Sanger			
P385	no variant found			HRM	Sanger			
P386	no variant found			HRM	Sanger			
P387	no variant found			HRM	Sanger			
P388	no variant found			HRM	Sanger	NGS		
P389	no variant found			HRM	Sanger			
P390	no variant found			HRM	Sanger			
P391	no variant found			HRM	Sanger			
P392	no variant found			HRM	Sanger			
P393	no variant found			HRM	Sanger			
P394	no variant found			HRM	Sanger			
P395	no variant found			HRM	Sanger			
P396	no variant found			HRM	Sanger			
P397	no variant found			HRM	Sanger			
P398	no variant found			HRM	Sanger			
P399	no variant found			HRM	Sanger			
P400	no variant found			HRM	Sanger			
P401	no variant found			HRM	Sanger			
P402	no variant found				Sanger			
P403	no variant found			HRM	Sanger			
P404	no variant found				Sanger			
P405	no variant found			HRM	Sanger			
P406	no variant found			HRM	Sanger			
P407	no variant found			HRM	Sanger			
P408	no variant found			HRM	Sanger			
P409	no variant found				Sanger			
P410	no variant found				Sanger			
P411	no variant found				Sanger			
P412	no variant found			HRM	Sanger			
P413	no variant found			HRM	Sanger			
P414	no variant found				Sanger			
P415	no variant found			HRM	Sanger			
P416	no variant found			HRM	Sanger			
P417	no variant found				Sanger			
P418	no variant found			HRM	Sanger			
P419	no variant found				Sanger	NGS		
P420	no variant found				Sanger	NGS		
P421	no variant found				Sanger			
P422	no variant found			HRM	Sanger	NGS		
P423	no variant found			HRM	Sanger	NGS		
P424	no variant found			HRM	Sanger			
P425	no variant found			HRM	Sanger	NGS		
P426	no variant found			HRM	Sanger	NGS		
P427	no variant found				Sanger			
P428	no variant found				Sanger			
P429	no variant found			HRM	Sanger			
P430	no variant found			HRM	Sanger			
P431	no variant found				Sanger			
P432	no variant found			HRM	Sanger	NGS		
P433	no variant found			HRM	Sanger			
P434	no variant found				Sanger			
P435	no variant found				Sanger			
P436	no variant found				Sanger	NGS		
P437	no variant found			HRM	Sanger	NGS		

P438	no variant found			HRM	Sanger	NGS		
P439	no variant found				Sanger			
P440	no variant found				Sanger			
P441	no variant found			HRM	Sanger	NGS		
P442	no variant found				Sanger	NGS		
P443	no variant found			HRM	Sanger	NGS		
P444	no variant found			HRM	Sanger	NGS		
P445	no variant found			HRM	Sanger	NGS		
P446	no variant found			HRM	Sanger	NGS		
P447	no variant found			HRM	Sanger			
P448	no variant found			HRM	Sanger			
P449	no variant found			HRM	Sanger			
P450	no variant found				Sanger			
P451	no variant found				Sanger	NGS		
P452	no variant found				Sanger	NGS		
P453	no variant found			HRM	Sanger			
P454	no variant found				Sanger	NGS		
P455	no variant found					NGS		
P456	no variant found				Sanger			
P457	no variant found			HRM	Sanger			
P458	no variant found			HRM	Sanger	NGS		
P459	no variant found			HRM	Sanger			
P460	no variant found					NGS		
P461	no variant found				Sanger	NGS		
P462	no variant found				Sanger	NGS		
P463	no variant found				Sanger	NGS		
P464	no variant found				Sanger	NGS		
P465	no variant found				Sanger	NGS		
P466	no variant found				Sanger	NGS		
P467	no variant found				Sanger	NGS		
P468	no variant found				Sanger	NGS		
P469	no variant found				Sanger	NGS		
P470	no variant found					NGS		
P471	no variant found					NGS		
P472	no variant found				Sanger	NGS		
P473	no variant found				Sanger	NGS		
P474	no variant found				Sanger	NGS		
P475	no variant found				Sanger	NGS		
P476	no variant found				Sanger	NGS		
P477	no variant found				Sanger	NGS		
P478	no variant found				Sanger	NGS		
P479	no variant found			HRM	Sanger			
P480	no variant found			HRM	Sanger			
P481	no variant found			HRM	Sanger			
P482	no variant found			HRM	Sanger			
P483	no variant found			HRM	Sanger			
P484	no variant found			HRM	Sanger	NGS		
P485	no variant found			HRM	Sanger			
P486	no variant found			HRM	Sanger	NGS		
P487	no variant found				Sanger			
P488	no variant found				Sanger			
P489	no variant found				Sanger			
P490	no variant found			HRM	Sanger			
P491	no variant found				Sanger			
P492	no variant found			HRM	Sanger			
P493	no variant found			HRM	Sanger			
P494	no variant found			HRM	Sanger			
P495	no variant found			HRM	Sanger			
P496	no variant found			HRM	Sanger	NGS		
P497	no variant found			HRM	Sanger			
P498	no variant found			HRM	Sanger			
P499	no variant found				Sanger	NGS		
P500	no variant found				Sanger			
P501	no variant found				Sanger			
P502	no variant found			HRM	Sanger	NGS		
P503	no variant found				Sanger			

P504	no variant found			HRM	Sanger			
P505	no variant found			HRM	Sanger			
P506	no variant found			HRM	Sanger			
P507	no variant found			HRM	Sanger	NGS		
P508	no variant found			HRM	Sanger			
P509	no variant found			HRM	Sanger			
P510	no variant found			HRM	Sanger	NGS		
P511	no variant found			HRM	Sanger			
P512	no variant found			HRM	Sanger			
P513	no variant found				Sanger			
P514	no variant found				Sanger			
P515	no variant found			HRM	Sanger			
P516	no variant found				Sanger	NGS		
P517	no variant found				Sanger			
P518	no variant found				Sanger			
P519	no variant found				Sanger			
P520	no variant found				Sanger	NGS		
P521	no variant found				Sanger			
P522	no variant found				Sanger	NGS		
P523	no variant found				Sanger	NGS		
P524	no variant found				Sanger	NGS		
P525	no variant found				Sanger	NGS		
P526	no variant found				Sanger	NGS		
P527	no variant found				Sanger	NGS		
R10	variant found	RIT1	p.Thr83Pro		Sanger		pathogenic	
R12	variant found	RIT1	p.Ser35Thr		Sanger		pathogenic	
R14	variant found	RIT1	p.Phe82Leu		Sanger		pathogenic	
R15	variant found	RIT1	p.Gly95Ala	HRM	Sanger		pathogenic	
R16	variant found	RIT1	p.Ser35Thr	HRM	Sanger		pathogenic	
R17	variant found	RIT1	p.Phe82Leu		Sanger		pathogenic	
R19	variant found	RIT1	p.Ala57Gly		Sanger		pathogenic	
R22	variant found	RIT1	p.Ala57Gly		Sanger		pathogenic	
R29	variant found	RIT1	p.Phe82Ile	HRM		NGS	pathogenic	
R30	variant found	RIT1	p.Ala77Thr	HRM	Sanger	NGS	pathogenic	
R31	variant found	RIT1	p.Ala57Gly		Sanger	NGS	pathogenic	
R32	variant found	RIT1	p.Tyr89His		Sanger	NGS	pathogenic	
R33	variant found	RIT1	p.Ala57Gly		Sanger	NGS	pathogenic	
R34	variant found	RIT1	p.Ala77Ser	HRM		NGS	pathogenic	
R35	variant found	RIT1	p.Phe82Leu		Sanger	NGS	pathogenic	
R36	variant found	RIT1	p.Lys23Gln	HRM	Sanger	NGS	pathogenic	
R37	variant found	RIT1	p.Glu81Gly		Sanger	NGS	pathogenic	
R38	variant found	RIT1	p.Ala57Gly	HRM		NGS	pathogenic	
R4-2	variant found	RIT1	p.Gly95Ala		Sanger		pathogenic	
R8	variant found	RIT1	p.Phe82Leu		Sanger		pathogenic	
S19	variant found	SHOC2	p.Ser2Gly		Sanger		pathogenic	
S20	variant found	SHOC2	p.Ser2Gly		Sanger		pathogenic	
S21	variant found	SHOC2	p.Ser2Gly		Sanger		pathogenic	
S22	variant found	SHOC2	p.Ser2Gly	HRM			pathogenic	
S23	variant found	SHOC2	p.Ser2Gly		Sanger		pathogenic	
S24	variant found	SHOC2	p.Ser2Gly		Sanger		pathogenic	
S26	variant found	SHOC2	p.Ser2Gly		Sanger		pathogenic	
S28	variant found	SHOC2	p.Ser2Gly		Sanger		pathogenic	
S29	variant found	SHOC2	p.Ser2Gly		Sanger		pathogenic	
S47	variant found	SHOC2	p.Ser2Gly		Sanger		pathogenic	
S48	variant found	SHOC2	p.Ser2Gly		Sanger		pathogenic	
S50	variant found	SHOC2	p.Ser2Gly		Sanger		pathogenic	
S51	variant found	SHOC2	p.Ser2Gly		Sanger		pathogenic	
S52	variant found	SHOC2	p.Ser2Gly	HRM			pathogenic	
S56	variant found	SHOC2	p.Ser2Gly		Sanger		pathogenic	
S57	variant found	SHOC2	p.Ser2Gly		Sanger		pathogenic	
S60	variant found	SHOC2	p.Ser2Gly	HRM			pathogenic	
S63	variant found	SHOC2	p.Ser2Gly	HRM			pathogenic	
S64	variant found	SHOC2	p.Ser2Gly		Sanger		pathogenic	
S66	variant found	SHOC2	p.Ser2Gly		Sanger		pathogenic	
S69	variant found	SHOC2	p.Ser2Gly		Sanger		pathogenic	
S71	variant found	SHOC2	p.Ser2Gly		Sanger	NGS	pathogenic	

S72	variant found	SHOC2	p.Ser2Gly			NGS	pathogenic	
S73	variant found	SHOC2	p.Ser2Gly		Sanger		pathogenic	
S74	variant found	SHOC2	p.Ser2Gly		Sanger		pathogenic	
S75	variant found	SHOC2	p.Ser2Gly		Sanger		pathogenic	
S76	variant found	SHOC2	p.Ser2Gly		Sanger		pathogenic	

Table 6.7: List of all patients included in this cohort. The cohort included 606 patients and they are shown here with the ID used in this thesis. Abbreviations: C: CBL; G: Novel Genes; HRM: High resolution melting; N: NRAS; R: RIT1; S: SHOC2.

6.5. List of Abbreviations

µl: microliter

A: adenine

A2ML1: alpha-2-macroglobulin like 1

ACMG: American College of Medical Genetics and Genomics

ADHD: attention deficit and hyperactivity disorder

Ala: alanine

ALPS: autoimmune lymphoproliferative syndrome

Arg: arginine

Asn: asparagine

Asp: aspartic acid

bp: basepairs

BRAF: v-raf murine sarcoma viral oncogene homolog B

C: cytosine

c.: position in the coding sequence of the gene

CBL: Cas-Br-M (murine) ecotropic retroviral transforming sequence

CDC: Center for Disease Control

CFCS: Cardio-Facio-Cutaneous syndrome

CGH: comparative genome hybridization

CHD: congenital heart disease

ClinVar: Clinical Variation

CM-AVM: capillary malformation – arteriovenous malformation

CNV: copy number variant

COSMIC: Catalogue of Somatic Mutations in Cancer

CS: Costello syndrome

Cys: cysteine

ddNTPs: dideoxyadenosine, -cytidine, -guanosine, - thymidine triphosphate

dHPLC: denaturing high performance liquid chromatography

DMSO: dimethyl sulfoxide

DNA: Deoxyribonucleic acid

dNTPs: deoxyadenosine, -cytidine, -guanosine, - thymidine triphosphate

dup: duplication

ECG: electrocardiography

EGF: epidermal growth factor

ERMS: embryonal rhabdomyosarcoma

EtOH: ethanol

ExAC: Exome Aggregation Consortium

FGF: fibroblast growth factor

G: guanine

g: grams

GAP: GTPase-activating protein

GCCR: German Childhood Cancer Registry

GDP: guanosine diphosphate

GEF(s): guanine nucleotide exchange factor(s)

GH: growth hormone

Gln: glutamine

Glu: glutamic acid

Gly: glycine

GTP: guanosine triphosphate

H₂O: water

HCM: hypertrophic cardiomyopathy

HGF: hepatocyte growth factor

HGF: hereditary gingival fibromatosis

HGMD: Human Gene Mutation Database

His: histidine

HRAS: Harvey rat sarcoma viral oncogene homolog

HRM: high resolution melting

IL: interleukin

Ile: isoleucine

Indels: insertion deletion

IQ: intelligence quotient

JMML: juvenile myelomonocytic leukemia

kb: kilobases

KRAS: Kirsten rat sarcoma viral oncogene homolog

LCR: low copy repeats

Leu: leucine

LOVD: The Leiden Open Variation Database

Lys: lysine

LZTR1: leucine zipper like transcription regulator 1
M: molar mass
MAP/ERK: mitogen-activated protein/extracellular-signal regulated
MAP3K8: mitogen-activated protein kinase kinase kinase 8
Mb: megabases
MEK1: mitogen-activated protein kinase kinase 1
MEK2: mitogen-activated protein kinase kinase 2
Met: methionine
MgCl: magnesium Chloride
MGCL: multiple giant cell lesions
min: minutes
ml: milliliter
MLPA: multiple ligand probe amplification
mM: millimolar
mm: millimeter
mmol: millimol
MPD: myeloproliferative disorder
MRAS: muscle RAS oncogene homolog
MRI: magnetic resonance imaging
n: number
NBL: neuroblastoma
NCBI: national center for biotechnology information
NCFC: Neuro-Cardio-Facio-Cutaneous
NF1: Neurofibromatosis type 1 or Neurofibromin
NF-kappaB: nuclear factor kappa-light-chain-enhancer of activated B cells
ng: nanograms
NGS: Next Generation Sequencing
NIH: national institutes of health
nm: nanometer
nM: nanomol
NRAS: neuroblastoma RAS viral (v-ras) oncogene homolog
NS: Noonan syndrome
NSLAH: Noonan syndrome with loose anagen hair
NSML: Noonan syndrome with multiple lentigines
OFC: occipitofrontal circumference
OMIM: Online Mendelian Inheritance in Man
p.: position of the amino acid in the protein sequence
PCR: polymerase chain reaction
Phe: phenylalanine

PI3K-AKT: phosphatidylinositol-3-kinase - Protein kinase B
pM: picomolar
pmol: picomol
PPP1CB: protein phosphatase 1 catalytic subunit beta
Pro: proline
Pst: pulmonary valve stenosis
PTP: Protein tyrosine phosphatase
PTPN11: protein tyrosine phosphatase, non-receptor type 11
RAF1: v-raf-1 murine leukemia viral oncogene homolog 1
RAS/MAPK: Rat sarcoma / mitogen activated protein kinase
RASA2: RAS p21 protein activator 2
RIT1: Ras like without CAAX 1
RRAS: related RAS viral (r-ras) oncogene homolog
SBS: sequencing by synthesis
SD: standard deviation
Ser: serine
SH2: Src Homology 2
SHOC2: soc-2 suppressor of clear homolog
SNP: single nucleotide polymorphism
SOS1: son of sevenless homolog 1
SOS2: son of sevenless homolog 2
SPRY1: sprouty RTK signaling antagonist 1
SRC family kinase: cellular sarcoma family kinase
T: thymine
TBE: TRIS-Borat-EDTA
Thr: threonine
TNF: tumor necrosis factor
Trp: tryptophan
Tyr: tyrosine
UV: ultraviolet
V: volt
Val: valine
VSD: ventricular septal defect
VUS: variant of unknown significance
WES: whole exome sequencing
WHO: world health organization

6.6. Funding sources

The work in this thesis has been funded by E-Rare (NSEuroNet), the Bundesministerium für Bildung und Forschung (NSEuroNet and GeNeRARE), and the Deutsche Forschungsgemeinschaft (ZE 524/10-1).

6.7. Publications

Parts of this thesis were published in the following articles

Altmüller F*, Lissewski C*, Bertola D, Flex E, Stark Z, Spranger S, Baynam G, Buscarilli M, Dyack S, Gillis J, Yntema HG, Pantaleoni F, van Loon RLE, MacKay S, Mina K, Schanze I, Tan TY, Walsh M, White SM, Niewisch MR, García-Miñaur S, Plaza D, Ahmadian MR, Cavé H, Tartaglia M* and Martin Zenker M*. 2017. Genotype and phenotype spectrum of NRAS germline variants. *Eur J Hum Genet* 25(7):823-831.

*authors contributed equally to this work

Bülow L*, Lissewski C*, Bressel R, Rauch A, Stark Z, Zenker M, Bartsch O. 2015. Hydrops, fetal pleural effusions and chylothorax in three patients with *CBL* mutations. *Am J Med Genet A* 167(2):394-399.

*authors contributed equally to this work

Kouz K*, Lissewski C*, Spranger S, Mitter D, Riess A, Lopez-Gonzalez V, Lüttgen S, Aydin H, von Deimling F, Evers C, Hahn A, Hempel M, Issa U, Kahlert AK, Lieb A, Villavicencio-Lorini P, Ballesta-Martinez MJ, Nampoothiri S, Ovens-Raeder A, Puchmajerová A, Satanovskij R, Seidel H, Unkelbach S, Zabel B, Kutsche K*, Zenker M*. 2016. Genotype and phenotype in patients with Noonan syndrome and a RIT1 mutation. *Genet Med* 18(12):1226-1234.

*authors contributed equally to this work

Lissewski C, Kant SG, Stark Z, Schanze I, Zenker M. 2015. Copy number variants including RAS pathway genes-How much RASopathy is in the phenotype? *Am J Med Genet A* 167A(11):2658-2690.

Other publications

Binder G, Grathwol S, von Loeper K, Blumenstock G, Kaulitz R, Freiberg C, Webel M, Lissewski C, Zenker M, Paul T. 2012. Health and quality of life in adults with Noonan syndrome. *J Pediatr* 161(3):501-505.

Boppudi S, Bögershausen N, Hove HB, Percin EF, Aslan D, Dvorsky R, Kayhan G, Li Y, Cursiefen C, Tantcheva-Poor I, Toft PB, Bartsch O, Lissewski C, Wieland I, Jakubiczka S, Wollnik B, Ahmadian MR, Heindl LM, Zenker M. 2016. Specific mosaic KRAS mutations

affecting codon 146 cause oculocutaneous syndrome and encephalocraniocutaneous lipomatosis. *Clin Genet* 90(4):334-342.

Ceremsak JJ, Yu A, Esquivel E, Lissewski C, Zenker M, Loh ML, Stieglitz E. 2016. Germline RRAS2 mutations are not associated with Noonan syndrome. *J Med Genet* doi: 10.1136/jmedgenet-2016-103889. [Epub ahead of print]

Cordeddu V, Yin JC, Gunnarsson C, Virtanen C, Drunat S, Lepri F, De Luca A, Rossi C, Ciolfi A, Pugh TJ, Bruselles A, Priest JR, Pennacchio LA, Lu Z, Danesh A, Quevedo R, Hamid A, Martinelli S, Pantaleoni F, Gnazzo M, Daniele P, Lissewski C, Bocchinfuso G, Stella L, Odent S, Philip N, Faivre L, Vlckova M, Seemanova E, Digilio C, Zenker M, Zampino G, Verloes A, Dallapiccola B, Roberts AE, Cavé H, Gelb BD, Neel BG, Tartaglia M. 2015. Activating Mutations Affecting the Dbl Homology Domain of SOS2 Cause Noonan Syndrome. *Hum Mutat* 36(11):1080-7

Jung AM, Zenker M, LiBewski C, Schanze D, Wagenpfeil S, Rohrer TR. 2017. Genetic Polymorphisms as Predictive Markers of Response to Growth Hormone Therapy in Children with Growth Hormone Deficiency. *Klin Padiatr*. doi: 10.1055/s-0043-115223 [Epub ahead of print]

Karaer K, Lissewski C, Zenker M. 2015 Familial cardiofaciocutaneous syndrome in a father and a son with a novel MEK2 mutation. *Am J Med Genet A* 167(2):385-388.

Kratz CP, Franke L, Peters H, Kohlschmidt N, Kazmierczak B, Finckh U, Bier A, Eichhorn B, Blank C, Kraus C, Kohlhase J, Pauli S, Wildhardt G, Kutsche K, Auber B, Christmann A, Bachmann N, Mitter D, Cremer FW, Mayer K, Daumer-Haas C, Nevinsky-Stickel-Hinzpeter C, Oeffner F, Schlüter G, Gencik M, Überlacker B, Lissewski C, Schanze I, Greene MH, Spix C, Zenker M. 2015 Cancer spectrum and frequency among children with Noonan, Costello, and cardio-facio-cutaneous syndromes. *Br J Cancer*. 112(8):1392-1397.

Lorenz S, Lissewski C, Simsek-Kiper PO, Alanay Y, Boduroglu K, Zenker M, Rosenberger G. 2013 Functional analysis of a duplication (p.E63_D69dup) in the switch II region of HRAS: new aspects of the molecular pathogenesis underlying Costello syndrome. *Hum Mol Genet* 22(8):1643-53.

Louati R, Abdelmoula NB, Trabelsi I, Abid D, Lissewski C, Kharrat N, Kamoun S, Zenker M, Rebai T. 2014 Clinical and Molecular Findings of Tunisian Patients with RASopathies. *Mol Syndromol* 5(5):212-7.

Martinelli S, Stellacci E, Pannone L, D'Agostino D, Consoli F, Lissewski C, Silvano M, Cencelli G, Lepri F, Maitz S, Pauli S, Rauch A, Zampino G, Selicorni A, Melançon S, Digilio MC, Gelb BD, De Luca A, Dallapiccola B, Zenker M, Tartaglia M. 2015 Molecular Diversity and Associated Phenotypic Spectrum of Germline CBL Mutations. *Hum Mutat* 36(8):787-796.

Pannone L, Bocchinfuso G, Flex E, Rossi C, Baldassarre G, Lissewski C, Pantaleoni F, Consoli F, Lepri F, Magliozzi M, Anselmi M, Delle Vigne S, Sorge G, Karaer K, Cuturilo G, Sartorio A, Tinschert S, Accadia M, Digilio MC, Zampino G, De Luca A, Cavé H, Zenker M, Gelb BD, Dallapiccola B, Stella L, Ferrero GB, Martinelli S, Tartaglia M. 2017 Structural, Functional, and Clinical Characterization of a Novel PTPN11 Mutation Cluster Underlying Noonan Syndrome. *Hum Mutat* 38(4):451-459.

Simşek-Kiper P, Alanay Y, Gülhan B, Lissewski C, Türkyılmaz D, Alehan D, Cetin M, Utine G, Zenker M, Boduroğlu K. 2013. Clinical and molecular analysis of RASopathies in a group of Turkish patients. *Clin Genet* 83:181-186.

6.8. Erklärung

Hiermit erkläre ich, dass ich die von mir eingereichte Dissertation mit dem Thema „The RASopathies: Molecular Genetics and Genotype-Phenotype Correlations“ selbständig verfasst, nicht schon als Dissertation verwendet habe und die benutzten Hilfsmittel und Quellen vollständig angegeben wurden.

Weiterhin erkläre ich, dass ich weder diese noch eine andere Arbeit zur Erlangung des akademischen Grades doctor rerum naturalium (Dr. rer. nat.) an anderen Einrichtungen eingereicht habe.

Erklärung über Promotionsversuche

Ich erkläre, dass ich keine früheren Promotionsversuche unternommen habe und an keiner anderen Fakultät oder Universität ein Promotionsverfahren anhängig ist.

Magdeburg, den _____

M. Sc. Christina Antonia Lißewski